

ELEVENTH
INTERNATIONAL
SYMPOSIUM
ON
GAS
KINETICS

6445-CH-01

BOOK
OF
ABSTRACTS

(1)

AD-A229 885

DTIC
ELECTE
NOV 16 1990
S D CS D

DTIC FILE COPY

DISTRIBUTION STATEMENT A

Approved for public release
Distribution Unlimited

laudo si magni
p fīe ueto. 7 paere 7 nubilo 7 sereno 7 omne
tēpo. ploquale ale tue creature tu susten
tānto.

Praise be to Thee my Lord for Brother Wind,
for air and clouds, clear sky and all the weathers
through which Thou sustainest all Thy creatures.

*From the Canticle of the Creatures
San Francesco di Assisi, XII Century.*

ELEVENTH INTERNATIONAL SYMPOSIUM ON
GAS KINETICS

ASSISI (Perugia), Italy
2-7 September 1990

Program Committee

V.Aquilanti (Perugia), R.J.Donovan (Edinburgh),
G.Hancock (Oxford), G.G.Volpi (Perugia),
J.P.T.Wilkinson (Shell, U.K.)

Organising Committee

V.Aquilanti, L.Beneventi, B.Brunetti, R.Candori,
S.Cavalli, P.Casavecchia, G.Grossi, A.Laganà,
G.Liuti, F.Pirani, F.Vecchiocattivi, G.G.Volpi.

Sponsors

Regione dell'Umbria; Università di Perugia; Azienda
di Promozione Turistica di Perugia; Consiglio
Nazionale delle Ricerche; U.S.Army European
Research Office; ICI plc; British Gas plc; Shell
Research Ltd; British Petroleum plc; Coherent
(U.K.) Ltd; Spectra Physics Ltd; Laser Lines Ltd.

FOREWORD

This book, prepared by F. Vecchiocattivi and F. Pirani, contains the abstracts of the papers (invited talks, oral presentations, poster contributions) presented at the Eleventh International Symposium on Gas Kinetics. The Symposium is held at La Cittadella, Assisi, Italy, organised by the Gas Kinetics Group of the Royal Society of Chemistry, London, and the Molecular Beams and Dynamics Group of the Department of Chemistry of the University of Perugia. The programme includes contributions on new, as well as traditional, themes in Gas Phase Kinetics. Highlighted topics include: A) Atmospheric Chemistry; B) Theory of Reactive, Inelastic, and Photodissociative Processes; C) Combustion Chemistry; D) Elementary Reactions of Neutral and Ionic Species; E) Reaction Dynamics and State-to-State Chemistry; F) Photodissociation Dynamics; G) Gas-Surface Interactions.

People from more than 27 countries are coming to La Cittadella, within the medieval walls of the town of Assisi, St. Francis' birthplace and for centuries an attraction to travellers (pilgrims, scholars, tourists). Following a suggestion of Dr. G. Agozzino, of the Azienda di Promozione Turistica di Perugia, we took lines from St. Francis' Canticle of the Creatures as the logo of the Symposium. St. Francis' philosophy marked the transition from the Middle Ages to Humanism by proposing a new awareness of nature: I think all those who are converging to Assisi for this Symposium will find particularly appropriate to remember his message in times where progress in Gas Kinetics appears to be crucial in modifying and protecting the environment.

Vincenzo Aquilanti

Accession For	
NTIS Grant	<input checked="" type="checkbox"/>
DTIC TAB	<input type="checkbox"/>
Unannounced	<input type="checkbox"/>
Justification	
By <i>perform 50</i>	
Dt. 1/1/81	
Availability Codes	
Dist	Avail. a. o. or special
A-1	



*(25) ... reactivity,
 combustion chemistry
 ...*

USARDSG (UK)

INVITED TALKS

- I-1 J.J.Valentini (New York, New York, USA)
STATE-TO-STATE REACTION DYNAMICS: A SELECTIVE OVERVIEW
- I-2 F.S.Rowland (Irvine, California, USA)
CHEMICAL REACTIONS OF CHLOROCARBONS AND HYDROCARBONS IN
THE EARTH'S ATMOSPHERE
- I-3 J.Wolfrum (Bielefeld, W.Germany)
FROM SIMPLE TO COMPLEX COMBUSTION KINETICS: EXPERIMENTS
AND MODELS
- I-4 M.Alexander and P.F.Vohralik (College Park, Maryland,
USA)
ROTATIONAL ENERGY TRANSFER BETWEEN POLAR MOLECULES: AN
EXACT QUANTUM STUDY
- I-5 I.W.M.Smith (Birmingham, UK)
RADICAL-RADICAL REACTIONS: KINETICS, DYNAMICS, AND
MECHANISM
- I-6 G.Liuti (Perugia, Italy)
INTERMOLECULAR POTENTIALS IN REACTIVE SYSTEMS
- I-7 S.T.Ceyer (Cambridge, Massachusetts, USA)
BRIDGING THE GAP BETWEEN UHV SURFACE SCIENCE AND THE
KINETICS OF HIGH PRESSURE HETEROGENEOUS CATALYSIS: THE
ACTIVATION AND REACTIONS OF CH_4 ON $\text{Ni}(111)$
- I-8 P.L.Houston (Ithaca, New York, USA)
THE DYNAMICS OF PHOTODISSOCIATIONS PRODUCING THREE
FRAGMENTS: DECIDING BETWEEN STEPWISE AND CONCERTED
MECHANISMS

- I-9 V.L.Talrose (Moscow, USSR)
CONCLUDING REMARKS: OZONE, FREONS AND GREENHOUSE EFFECT

ORAL CONTRIBUTIONS

- O-1 N.Balucani, L.Beneventi, P.Casavecchia, D.Stranges, and
G.G.Volpi (Perugia, Italy)
CROSSED BEAM STUDIES OF THE REACTION DYNAMICS OF O(¹D)
ATOMS WITH SIMPLE MOLECULES
- O-2 J.J.Sloan (Waterloo, Ontario, Canada)
REACTION DYNAMICS AND BRANCHING RATIOS OF O(¹D₂)
REACTIONS WITH HALOGENATED METHANES
- O-3 M.F.Frost, Y.Gu, I.R.Sims, I.W.M.Smith, and
R.Spencer-Smith (Birmingham, UK)
EFFECTS OF REAGENT VIBRATIONAL EXCITATION IN THE
REACTION: CN(v_1) + HCl(v_2) → HCN + Cl
- O-4 L.Copeland, F.Mohammad, M.Zahedi, and W.M.Jackson
(Davis, California, USA)
VIBRATIONAL PRODUCT STATE DISTRIBUTION OF HCN PRODUCED
IN THE REACTION OF CN RADICALS WITH SATURATED
HYDROCARBONS
- O-5 H.Heydtmann, K.Dehe, and U.Schwanke (Frankfurt/Main,
W.Germany)
IR-CHEMILUMINESCENCE FOR REACTIONS OF F-ATOMS WITH SOME
STABLE ORGANIC MOLECULES AND SOME ORGANIC RADICAL
SPECIES
- O-6 L.Bañares, and A.González Ureña (Madrid, Spain)
CHEMI-IONIZATION STUDIES UNDER CROSSED-BEAM CONDITIONS

- O-7 J.N.Crowley, J.P.Burrows, G.K.Moortgat (Mainz, W.Germany), A.Mellouki, G.Poulet, and G.LeBras (Orleans, France)
LABORATORY STUDIES OF THE GAS PHASE REACTIONS BETWEEN NO_3 AND SIMPLE PEROXY RADICALS
- O-8 G.S.Tyndall, C.A.Cantrell, J.J.Orlando, R.E.Shetter, and J.G.Calvert (Boulder, Colorado, USA)
KINETICS OF THE REACTION $\text{NO}_3 + \text{NO}_2 \rightarrow \text{N}_2\text{O}_5$
- O-9 J.F.Gleason, F.L.Nesbitt, and L.J.Stief (Greenbelt, Maryland, USA)
KINETIC STUDIES OF OClo
- O-10 A.D.Parr, M.E.Jenkin, and G.D.Hayman (Oxon, UK)
KINETICS AND SPECTROSCOPIC STUDIES OF ClO RADICAL REACTIONS IMPORTANT IN POLAR OZONE CHEMISTRY
- O-11 A.R.Ravishankara (Boulder, Colorado, USA)
ATMOSPHERIC CHEMISTRY OF BROMINE COMPOUNDS
- O-12 R.Atkinson, D.Hasegawa, and S.M.Aschmann (Riverside, California, USA)
KINETICS OF THE GAS-PHASE REACTIONS WITH A SERIES OF MONOTERPENES WITH O_3
- O-13 J.M.C.Plane and C.-F.Ni  n (Miami, Florida, USA)
THE MISTERY OF CALCIUM IN THE UPPER ATMOSPHERE
- O-14 J.P.Sawersyn (Villeneuve d'Ascq, France), D.Hartmann, J.Karth  user (G  ttingen, W.Germany), and R.Zellner (Hannover, W.Germany)
KINETICS AND HO_2 PRODUCT YIELD OF THE REACTION $\text{C}_2\text{H}_5\text{O} + \text{O}_2$ BETWEEN 295 AND 411 K
- O-15 C.Anastasi (York, UK), T.Ellermann, P.Pagsberg

(Roskilde, Denmark), and S.Pollak (York, UK)
REACTION BETWEEN HYDROXYL AND METHYL RADICALS AT ROOM
TEMPERATURE

- O-16 A.Chakir, M.Bellimam, M.Cathonnet, J.C.Boettner, and
F.Gaillard (Orléans, France)
KINETIC STUDY OF N-PENTANE OXIDATION
- O-17 N.J.B.Green, A.R.de A.Pereira, M.J.Pilling, and
S.H.Robertson (Leeds and Oxford, UK)
KINETIC MODELS OF MULTI-CHANNEL REACTIONS
- O-18 C.Chevalier, U.Maas, and J.Warnaz (Stuttgart,
W.Germany)
SIMULATION OF THE COMBUSTION OF HYDROCARBONS AND OF
OXYGENATED COMPOUNDS UP TO C_2 : LAMINAR FLAME
STRUCTURES, FLAME VELOCITIES, AND IGNITION PROCESSES
- O-19 I.Bar, T.Ben-Porat, A.Ben-Tov, D.Heflinger, Y.Kaufman,
G.Miron, M.Sapir, Y.Tzuk, and S.Rosenwaks (Beer-Sheva,
Israel)
KINETICS AND SPECTROSCOPY OF EXCITED SPECIES OBTAINED
VIA DETONATION OF LEAD AZIDE
- O-20 C.Nyeland (Copenhagen, Denmark)
COLLISION THEORY OF "FALL-OF" IN RECOMBINATION
REACTIONS
- O-21 E.E.Nikitin and J.Troe (Göttingen, W.Germany)
ACCURATE ADIABATIC CHANNEL CALCULATIONS FOR SACM
TREATMENTS
- O-22 A.Degli Esposti (Bologna, Italy) and H.J.Werner
(Bielefeld, W.Germany)
AB INITIO CALCULATION OF $OH(X^2\Pi, A^2\Sigma^+) + Ar$ POTENTIAL
ENERGY SURFACES AND QUANTUM SCATTERING STUDIES OF

ROTATIONAL ENERGY TRANSFER IN THE OH($A^2\Sigma^+$) STATE

- O-23 T.Stoecklin, J.C.Rayez, and B.Duguay (Bordeaux, France)
THEORETICAL STUDY OF THE DYNAMICS AND THE KINETICS OF
THE REACTION $C(^3P) + SH(X^2\Pi) \rightarrow CS(X^1\Sigma^+) + H(^2S)$
- O-24 A.F.Wagner, M.Aoyagi, and R.Shepard (Argonne, Illinois,
USA)
THEORETICAL STUDIES OF THE THERMAL REACTION DYNAMICS OF
 $CH + H_2 \rightleftharpoons CH_3 \rightleftharpoons C^mH_2 + H$
- O-25 J.M.Bowman, Q.Sun (Atlanta, Georgia, USA), J.R.Fisher,
and J.V.Michael (Argonne, Illinois, USA)
THEORETICAL TO EXPERIMENTAL RATE CONSTANT COMPARISON FOR
TWO ISOTOPIC MODIFICATIONS OF THE SIMPLEST CHEMICAL
REACTION, $H + H_2$
- O-26 V.Aquilanti, S.Cavalli, G.Grossi, V.Pellizzari, M.Rosi,
A.Sgamellotti, F.Tarantelli (Perugia, Italy)
POTENTIAL ENERGY SURFACES FOR OXYGEN ATOM REACTIONS FROM
THE HYPERSPHERICAL PERSPECTIVE
- O-27 G.Hancock and D.E.Heard (Oxford, UK)
TIME RESOLVED FTIR STUDIES OF THE $O + CHF$ REACTION
- O-28 J.Peeters, J.Van Hoeymissen, and S.Vanhaelemeersch
(Leuven, Belgium)
ABSOLUTE RATE CONSTANT MEASUREMENTS OF THE REACTION OF
THE $CF(X^2\Pi)$ RADICAL WITH O_2 , F_2 , Cl_2 , AND NO
- O-29 R.Timonen, J.Seetula (Helsinki, Finland), and D.Gutman
(Washington D.C., USA)
KINETICS OF THE REACTIONS OF POLYATOMIC RADICALS WITH
MOLECULAR BROMINE IN THE GAS PHASE
- O-30 O.Dobis and S.W.Benson (Los Angeles, California, USA)

TEMPERATURE COEFFICIENTS OF THE RATES OF Cl ATOM
REACTIONS WITH C_2H_6 , C_2H_5 , AND C_2H_4 . THE RATES OF
DISPROPORTIONATION AND RECOMBINATION OF ETHYL RADICALS

- O-31 M.Damm, F.Deckert, R.Fröchtenicht, H.Hippler, and
P.J.Toennies (Göttingen, W.Germany)
SPECIFIC RATE CONSTANTS FOR UNIMOLECULAR REACTIONS OF
VIBRATIONALLY HIGHLY EXCITED LARGE POLYATOMIC MOLECULES
FROM BULK AND MOLECULAR BEAM EXPERIMENTS
- O-32 H.M.Frey, B.Mason, R.Walsh, and I.M.Watts (Reading, UK)
TIME-RESOLVED KINETIC STUDIES OF THE REACTIONS OF
GAS-PHASE METHYLSILYLENE
- O-33 P.Tosi, F.Boldo, F.Eccher, M.Filippi, and D.Bassi
(Trento, Italy)
HIGH RESOLUTION MEASUREMENTS OF INTEGRAL CROSS SECTIONS
FOR ION-MOLECULE REACTIONS AS A FUNCTION OF THE
COLLISION ENERGY
- O-34 K.H.Becker, B.Engelhardt, R.Kurtenbach, and P.Wiesen
(Wuppertal, W.Germany)
KINETIC INVESTIGATION OF THE PRESSURE AND TEMPERATURE
DEPENDENCE OF THE REACTIONS OF $CH(X^2\Pi)$ RADICALS WITH N_2O
AND H_2
- O-35 P.D.Lightfood, P.Roussel, F.Caralp, V.Catoire and
R.Lesclaux (Bordeaux, France)
A FLASH PHOTOLYSIS STUDY OF THE UV SPECTRA AND
SELF-RECOMBINATION REACTIONS OF CH_2Cl AND $CHCl_2$
- O-36 U.Hold, K.Luther, and A.Symonds (Göttingen, W.Germany)
EXPERIMENTAL PROBABILITY DISTRIBUTIONS OF COLLISIONAL
ENERGY TRANSFER FROM HIGHLY VIBRATIONALLY EXCITED
AZULENE AND TOLUENE

- O-37 A.J.Hynes and P.H.Wine (Atlanta, Georgia, USA)
KINETICS AND MECHANISM OF ACETONITRILE OXIDATION UNDER
ATMOSPHERIC CONDITIONS
- O-38 T.Bérces, S.Dóbbé, and I.Szilágyi (Budapest, Hungary)
THE TEMPERATURE DEPENDENCE OF THE OVERALL REACTION
 $\text{CH}_3\text{O} + \text{H}$ AND THE RATES OF PRODUCT FORMATION
- O-39 S.A.Mitchell, J.M.Parnis, C.E.Brown, and P.A.Hackett
(Ottawa, Ontario, Canada)
ELEMENTARY REACTIONS OF NEUTRAL TRANSITION METAL ATOMS
- O-40 E.A.Ogryzlo and Z.H.Walker (Vancouver, British
Coloumbia, Canada)
KINETICS OF THE REACTIONS OF HALOGEN ATOMS AND MOLECULES
WITH SILICON AND GALLIUM ARSENIDE
- O-41 W.Müller-Markgraf and M.J.Rossi (Menlo Park, California,
USA)
KINETIC STUDIES OF THE INTERACTION OF Cl AND Br ATOMS
WITH POLYCRYSTALLINE Ni AND Si (100) SURFACES
- O-42 I.P.Ipatova, Yu.V.Zhiljaev, A.Yu.Kulikov, Yu.N.Makarov,
and O.P.Chilova-Lusina (Leningrad, USSR)
THE STUDY OF THE REACTION KINETICS AT GaAs GAS-PHASE
EPITAXY BY IN SITU ABSORPTION SPECTROSCOPY
- O-43 M.T.Leu, S.B.Moore, L.F.Keyser, and R.H.Smith (Pasadena,
California, USA)
LABORATORY STUDY OF THE HETEROGENEOUS REACTIONS OF
CHLORINE NITRATE AND HYDROGEN CHLORIDE ON NITRIC ACID
ICE
- O-44 J.M.Van Doren, L.R.Watson, P.Davidovits (Chestnut Hill,
Massachusets, USA) D.R.Worsnop, M.S.Zahniser, and
C.E.Kolb (Billerica, Massachusets, USA)

HETEROGENEOUS INTERACTIONS OF GAS PHASE HCl , HNO_3 AND N_2O_5 ON AQUEOUS DROPLETS AS A FUNCTION OF TEMPERATURE AND SULFURIC ACID CONCENTRATION

- O-45 M.A.Tolbert, C.M.Reihs, A.M.Middlebrook and D.M.Golden
(Menlo Park, California, USA)
HETEROGENEOUS PROCESSES IN THE STRATOSPHERE
- O-46 Yu.M.Gershenson, S.G.Zvenigorodsky, E.V.Antzupov,
V.B.Rozenshtein, and S.P.Smyshlyaev (Moscow, USSR)
THE SINK OF OH AND HO_2 RADICALS ON AEROSOLS
- O-47 A.Pearson and R.Anderson (Santa Cruz, California, USA)
ELECTRON DIFFRACTION STUDIES OF CLUSTER GROWTH MECHANISM
- O-48 J.F.Black, J.R.Waldeck, and R.N.Zare (Stanford,
California, USA)
STUDIES OF NONADIABATIC PHENOMENA IN THE
PHOTODISSOCIATION OF ICN AT 249 nm
- O-49 D.W.Chandler, (Livermore, California, USA),
M.H.M.Janssen (Pasadena, California, USA), S.Stolte
(Amsterdam, The Netherlands) D.H.Parker (Santa Cruz,
California, USA), J.W.Thoman, Jr. (Williamstown,
Massachusetts, USA), and G.O.Sitz (Austin, Texas, USA)
THE 266-nm PHOTOLYSIS OF CD_3I
- O-50 A.J.Yencha, D.K.Kela (Albany, New York, USA),
R.J.Donovan (Edinburgh, UK), A.Hopkirk (Warrington, UK),
and A.Kvaran (Reykjavik, Iceland)
ION PAIR ($\text{Br}^+ + \text{Br}^-$) FORMATION FROM PHOTODISSOCIATION OF
 Br_2 NEAR THE FIRST IONISATION LIMIT
- O-51 F.Stuhl (Bochum, W.Germany)
THE PHOTODISSOCIATION $\text{HN}_3 \rightarrow \text{NH}^* + \text{N}_2$ AND THE REVERSE
PROCESS

- O-52 A.Geers, J.Kappert, F.Temps, and J.W.Wiebrecht
(Göttingen, W.Germany)
SPECTROSCOPY AND DYNAMICS OF HIGHLY VIBRATIONALLY
EXCITED CH_3O AT THE DISSOCIATION LIMIT

A - ATMOSPHERIC CHEMISTRY

- A-1 F.-G.Simon, W.Schneider, G.K.Moortgat, and J.P.Burrows
(Mainz, W.Germany)
A STUDY OF THE ClO ABSORPTION SPECTRUM AND KINETICS OF
THE SELF-REACTION AT 298 K
- A-2 O.J.Nielsen (Roskilde, Denmark), M.Donlon,
H.W.Sidebottom, and J.Treacy (Dublin, Ireland)
KINETICS AND MECHANISMS FOR THE RECTIONS OF THE HYDROXYL
RADICALS WITH ALKYL NITRATES AND NITROALKANES
- A-3 F.Kirchner, G.Libuda, and F.Zabel (Wuppertal, W.Germany)
THERMAL STABILITY OF SELECTED PEROXYNITRATES
- A-4 T.J.Wallington and S.M.Japar (Dearborn, Michigan, USA)
PRODUCT STUDY OF THE REACTION OF CH_3O_2 AND $\text{C}_2\text{H}_5\text{O}_2$ WITH
 HO_2 IN AIR AT 295 K
- A-5 V.P.Bulatov, I.A.Dubinsky, V.N.Khabarov, V.A.Losovsky,
and O.M.Sarkisov (Moscow, USSR)
THE MECHANISM OF AMMONIA OXIDATION IN THE ATMOSPHERE
- A-6 M.E.Jenkin, T.P.Murrells, and G.D.Hayman (Oxon, UK)
KINETICS OF REACTIONS OF ORGANIC PEROXY RADICALS WITH
 HO_2 AND NO
- A-7 J.Arey, S.M.Aschmann, and R.Atkinson (Riverside,

California, USA)

PRODUCTS OF THE GAS-PHASE REACTIONS OF MONOTERPENES WITH
THE OH RADICAL IN THE PRESENCE OF NO_x

- A-8 D.L.Baulch, H.Black, and P.K.Louie (Leeds, UK)
THE REACTIONS OF HYDROXYL RADICALS WITH SOME AROMATIC
AND HETEROCYCLIC COMPOUNDS
- A-9 L.F.Phillips (Canterbury, New Zealand)
PREDICTION OF RATE CONSTANTS FOR REACTIONS OF
ATMOSPHERIC RADICALS
- A-10 C.A.Cantrell, R.E.Shetter, J.G.Calvert, G.S.Tyndall, and
J.J.Orlando (Boulder, Colorado, USA)
UNIMOLECULAR DECOMPOSITION OF N₂O₅
- A-11 P.Biggs, A.A.Boyd, C.E.Canosa-Mas, M.R.Wilson, and
R.P.Wayne (Oxford, UK)
SLOW REACTIONS OF THE NO₃ RADICAL
- A-12 A.C.Brown, C.E.Canosa-Mas, A.D.Parr, K.Rothwell, and
R.P.Wayne (Oxford, UK)
A KINETIC STUDY OF THE REACTIONS OF THE HYDROXYL RADICAL
WITH SIXTEEN HYDROHALOCARBONS: ATMOSPHERIC IMPLICATIONS
- A-13 R.W.S.Aird, C.E.Canosa-Mas, D.J.Cook, P.S.Monks,
R.P.Wayne (Oxford, UK), E.L.Ljungström (Göteborg,
Sweden)
THE TEMPERATURE DEPENDENCE OF THE REACTION OF THE NO₃
RADICAL WITH A SERIES OF HALOBUTENES AND 1-BUTENE
- A-14 H.Hippler, R.Rahn, and J.Troe (Göttingen, W.Germany)
PRESSURE DEPENDENCE OF THE OZONE RECOMBINATION REACTION
O(³P) + O₂ + M → O₃ + M BETWEEN 1 AND 1000 BAR AT
TEMPERATURES FROM 90 TO 370 K

- A-15 R.Forster, H.Hippler, and J.Troe (Göttingen, W.Germany)
 REMPI-SPECTROSCOPY UNDER HIGH PRESSURE CONDITIONS:
 APPLICATION TO THE RECOMBINATION REACTION
 $O(^3P) + NO + M \rightarrow NO_2 + M$
- A-16 A.Heiss, J.Tardieu de Maleissye, K.A.Sahetchian (Paris, France), and I.G.Pitt (Sidney, Australia)
 REACTIONS OF PRIMARY AND SECONDARY BUTOXY RADICALS IN OXYGEN AT ATMOSPHERIC PRESSURE
- A-17 P.Devolder, A.Goumri, J-F.Pauwels, J-P.Sawerysyn (Villeneuve d'Ascq, France)
 REACTION RATES OF SOME BENZYL TYPE RADICALS WITH O_2 , NO, NO_2 BY DISCHARGE FLOW LASER INDUCED FLUORESCENCE
- A-18 I.Seres and L.Seres (Szeged, Hungary)
 THERMAL DECOMPOSITION OF DIALKYL ETHERS
- A-19 Th.Papenbrock and F.Stuhl (Bochum, W.Germany)
 MEASUREMENT OF GASEOUS NITRIC ACID IN EUROPE AND ON THE ATLANTIC OCEAN
- A-20 F.Danis, F.Caralp, J.Masanet, and R.Lesclaux (Bordeaux, France)
 KINETICS OF THE REACTION $BrO + NO_2 + M \rightarrow BrONO_2 + M$
 IN THE TEMPERATURE RANGE 263-343 K
- A-21 E.P.Daykin, J.M.Nicovich, K.D.Kreutter, M.Chin, and P.H.Wine (Atlanta, Georgia, USA)
 KINETICS STUDIES RELEVANT TO UNDERSTANDING THE HALOGEN-INITIATED OXIDATION OF ATMOSPHERIC DIMETHYLSULFIDE
- A-22 S.N.Buben, I.K.Larin, N.A.Missineva, and E.M.Trophimova (Moscow, USSR)
 KINETIC STUDY OF THE REACTIONS ESSENTIAL FOR THE IODINE

DESTRUCTION CYCLE OF THE ATMOSPHERIC OZONE

- A-23 V.L.Orkin, V.G.Khamaganov, and E.E.Kasimovskaya (Moscow, USSR)
INVESTIGATION OF THE ELEMENTARY PROCESSES WHICH
DETERMINE OZONE DEPLETION POTENTIALS OF SOME HALOGENATED
HYDROCARBONS
- A-24 J.Chamboux-Crosnier, F.Jorand, V.Viossat, K.A.Sahetchian
(Paris, France), C.Chachaty (Saclay, France), S.Lunell,
M.-B.Euang (Uppsala, Sweden), and F.Zabell (Wuppertal,
W.Germany)
EXPERIMENTAL AND THEORETICAL STUDIES OF RADICAL
INTERMEDIATES IN THE ATMOSPHERIC OXIDATION OF CS₂
- A-25 C.Anastasi, M.Broomfield, O-J.Nielsen, and P.Pagsberg
(Roskilde, Denmark)
ULTRAVIOLET ABSORPTION SPECTRUM AND KINETICS OF CH₃S AND
CH₂SH RADICALS
- A-26 R.Koch, M.Siese, and C.Zetzsch (Hannover, W.Germany)
ATMOSPHERIC TRANSFORMATION OF BENZENE, TOLUENE AND
PHENOL BY OH: CONSECUTIVE REACTIONS OF THE ADDUCTS WITH
NO_x AND O₂
- A-27 E.V.Belousova, A.V.Polyakova, A.P.Purmal, A.P.
Shvedchikov, and S.O.Travin (Moscow, USSR)
KINETICS AND MECHANISM OF NO_x AND SO₂ OXIDATION IN WET
AIR BY ELECTRON BEAM IRRADIATION
- A-28 A.Fahr, A.Laufer, R.Klein, and W.Braun (Gaithersburg,
Maryland, USA)
A STUDY OF THE REACTION KINETICS OF THE VINYL RADICAL
WITH METHYL AND HYDROGEN ATOMS
- A-29 M.Hippler, A.J.Yates, and J.Pfab (Edinburgh, UK)

ULTRA-TRACE ANALYSIS OF NO BY HIGH RESOLUTION LASER
FLUORESCENCE AND IONIZATION SPECTROSCOPY

- A-30 D.Maric, J.P.Burrows, and G.K.Moortgat (Mainz,
W.Germany)
POSSIBLE ABIOTIC SOURCES OF N_2O

B - THEORY OF REACTIVE, INELASTIC, AND
PHODISSOCIATIVE PROCESSES

- B-1 C.Godoy and G.J.Vazquez (Morelos, MEXICO)
AN AB-INITIO STUDY OF THE PHOTOCHEMISTRY OF NO_2
- B-2 W.Stiller (Leipzig, E.Germany)
RATE COEFFICIENTS CALCULATIONS FOR ION-(POLAR)MOLECULE
REACTIONS IN DILUTE GASES
- B-3 C.E.Klots (Oak Ridge, Tennessee, USA)
THERMAL KINETICS IN A FINITE HEAT BATH
- B-4 T.Körtvélyesi and L.Seres (Szeged, Hungary)
AM1 AND "BOND-STRENGTH-BOND-LENGTH"-STUDIES ON H-ATOM
TRANSFER REACTIONS
- B-5 N.Cohen (Los Angeles, California, USA)
A REVISED MODEL FOR TRANSITION STATE THEORY CALCULATIONS
FOR RATE COEFFICIENTS OF OH WITH ALKANES
- B-6 A.M.Kosmas (Ioannina, Greece)
THEORETICAL STUDIES ON THE $O(^3P) + I_2$ REACTION
- B-7 W.Forst (Bordeaux, France)
MICROCANONICAL VARIATIONAL RRKM THEORY BY INVERSION OF
PARTITION FUNCTION

- B-8 L.B.Harding and R.J.Harrison (Argonne, Illinois, USA)
THEORETICAL STUDIES OF POTENTIAL SURFACES FOR BOND
DISSOCIATION
- B-9 A.Laganà (Perugia, Italy), P.Palmieri (Bologna, Italy),
E.Garcia (Bilbao, Spain), and J.M.Alvariño (Salamanca,
Spain)
CALCULATED VERSUS MEASURED SCATTERING AND KINETIC DATA
FOR THE $\text{Li} + \text{HCl}$ REACTION
- B-10 A.Palma, E.Semprini, and F.Stefani (Monterotondo, Italy)
AB INITIO POTENTIAL ENERGY SURFACE FOR UNIMOLECULAR
REACTION AND KINETICS
- B-11 N.Balakrishnan and N.Sathyamurthy (Kanpur, India)
A COMPARATIVE STUDY OF DIFFERENT METHODS FOR THE
CALCULATION OF REACTION PROBABILITIES USING
TIME-DEPENDENT WAVEPACKET METHOD
- B-12 A.E.Bodrov and F.I.Dalidchik (Moscow, USSR)
ROVIBRATIONAL TRANSITIONS AND DISSOCIATIVE CAPTURE
PROCESSES IN SLOW ELECTRON SCATTERING BY DIATOMIC
MOLECULES AND POSITIVE IONS
- B-13 A.A.Zembekov (Moscow, USSR)
CLASSICAL PHASE SPACE STRUCTURE AND TRANSPORT PROPERTIES
OF THE TWO-MODE COUPLED MORSE OSCILLATOR SYSTEM
- B-14 D.V.Shalashilin and S.Ya.Umanskii (Moscow, USSR)
THE VIBRATIONAL ENERGY EXCHANGE IN COLLISIONS OF OH AND
OD RADICALS WITH N_2 , O_2 , AND CH_4
- B-15 R.I.Asadullina, I.N.Bebelin, N.N.Bezuglov, E.L.Duman,
A.N.Klucharev, E.V.Nosov, V.A.Sheverev, I.P.Shmatov
(Moscow, USSR)

THE PLASMA CONDUCTION, CONTAINING THE VAPORIZING ALKALI METAL DROPS

- B-16 R.I.Asadullina, I.N.Bebelin, N.N.Bezuglov, E.L.Duman, A.N.Klucharev, E.V.Nosov, V.A.Sheverev, I.P.Shmatov (Moscow, USSR)
THE PLASMA NEAR AN ISOLATED VAPORIZING ALKALI METAL DROP
- B-17 B.V.Potapkin, V.D.Rusanov, and A.A.Fridman (Moscow, USSR)
VIBRATIONAL KINETICS AND REACTIONS OF POLYATOMIC MOLECULES IN NONEQUILIBRIUM SYSTEMS
- B-18 E.Garcia (Bilbao, Spain), J.Mateos (Salamanca, Spain), and A.Laganà (Perugia, Italy)
TEMPERATURE DEPENDENCE OF THE $H + H_2$ AND $D + D_2$ RATE CONSTANTS
- B-19 X.Gimenez (Barcelona, Spain) and A.Laganà (Perugia, Italy)
APPROXIMATE QUANTUM CROSS SECTIONS FOR THE $Li + HCl$ REACTION

C - COMBUSTION CHEMISTRY

- C-1 R.W.Walker (N.Humberside, UK)
THE OXIDATION CHEMISTRY OF 'STABLE' ELECTRON-DELOCALIZED RADICALS
- C-2 J.Vandooren (Louvain-La-Neuve, Belgium)
EXPERIMENTAL INVESTIGATION OF THE AMMONIA CONVERSION TO NO_x IN A RICH NH_3 SEEDED $H_2/O_2/Ar$ FLAME
- C-3 M.A.Teitel'boim, V.I.Vedeneev, M.Ya.Goldenberg, and

- A.A.Karnaikh (Moscow, USSR)
ON THE REACTION $\text{CH}_3 + \text{O}_2 \rightarrow \text{CH}_2\text{O} + \text{OH}$ IN PROBLEM OF
MODELLING METHANE OXIDATION
- C-4 R.I.Moshkina, S.S.Polyak, L.B.Romanovich, and
V.I.Vedeneev (Moscow, USSR)
EFFECT OF METHANE-OXYGEN MIXTURES CONTENT AND OF ETHANE
ADDITION ON METHANOL FORMATION
- C-5 Z.A.Mansurov, D.U.Bodikov, S.S.Abilgasinova, and
G.I.Ksandopulo (Alma-Ata, USSR)
ON HEXANE OXIDATION IN THE OSCILLATION REGIME
- C-6 P.Cederbalk, K.J.Hughes, M.J.Pilling, and V.K.Proudler
(Leeds, UK)
BUTANE OXIDATION IN A JET STIRRED REACTOR
- C-7 S.Etemad-Rad and E.Metcalfe (London, UK)
THE THERMAL DECOMPOSITION OF TOLUENE ISOCYANATES
- C-8 Ph.Rocteur and P.J.Van Tiggelen (Louvain-La-Neuve,
Belgium)
CHEMI-IONIZATION INDUCED BY FLUOROCARBON ADDITIVES IN
 $\text{H}_2/\text{CO}/\text{O}_2$ FLAMES
- C-9 H.V.Linnert and J.M.Riveros (Sao Paulo, Brazil)
THE UNIMOLECULAR DECOMPOSITION OF ETHANOL
- C-10 A.B.McEwen and D.M.Golden (Menlo Park, California, USA)
TWO OLD PROBLEMS REVISITED: $\text{CH}_3 + \text{O}_2$ AND $\text{OH} + \text{CO}$
- C-11 Ph.Dagaut, B.Aboussi, M.Cathonnet, and J.C.Boettner
(Orléans, France)
DETAILED KINETIC MODELING OF PROPYNE AND ALLENE
OXIDATION

- C-12 C.Hao, M.Schneider, and J.Wolfrum (Heidelberg,
W.Germany)
OXIDATION OF LARGE HYDROCARBON RADICALS PRODUCED BY
UV-LASER PHOTOLYSIS
- C-13 R.Buth, J.Edelbüttel-Einhaus, and K.Hoyeremann
(Göttingen, W.Germany)
THE DETECTION OF THE BUTINYL RADICAL BY MULTIPHOTON
IONIZATION/MASS SPECTROMETRY AND THE APPLICATION TO THE
STUDY OF THE REACTIONS WITH DEUTERIUM AND OXYGEN ATOMS
- C-14 A.A.Konnov and G.I.Ksandopulo (Alma-Ata, USSR)
OH DISTRIBUTION IN PRE-FLAME ZONE OF C_3H_8 /AIR FLAME
- C-15 F.Billaud, K.Elyahyaoui, and F.Baronnet (Nancy, France)
KINETICS OF THE THERMAL DECOMPOSITION OF
CYCLOEXANE-DECANE BINARY MIXTURE AT CA 720°C
- C-16 F.Billaud, K.Elyahyaoui, and F.Baronnet (Nancy, France)
THERMAL DECOMPOSITION OF CYCLOEXANE AT 720°C
- C-17 F.Billaud, C.Guéret, F.Baronnet (Nancy, France), and
J.Weill (Vernaison, France)
DEVELOPMENT OF METHANE INTO HIGHER HYDROCARBONS
- C-18 M.Braun-Unkhoff, Th.Just, and P.Frank (Stuttgart,
W.Germany)
HIGH TEMPERATURE PYROLYSIS OF BENZYL RADICALS
- C-19 V.S.Arutuynov, V.D.Knyazev, and V.I.Vedeneev (Moscow,
USSR)
THE REACTION OF $O(^3P)$ ATOMS WITH ETHYLENE AT LOW
PRESSURES
- C-20 V.S.Arutuynov, V.Ya.Basevich, A.V.Chernyshova,
V.A.Ushakov, and V.I.Vedeneev (Moscow, USSR)

STUDY OF THE $\text{SO}_2 + \text{CO}$ REACTION

- C-21 A.Seydi, R.Rigny, K.A.Sahetchian (Paris, France), and
L.Batt (Aberdeen, UK)
THE PYROLYSIS OF PERACETIC ACID
- C-22 F.Battin, P.M.Marquaire, F.Baronnet, and G.M.Côme
(Nancy, France)
GAS PHASE REACTIONS OF 1,4-DIOXANE WITH CHLORINE
- C-23 R.Le Bec, P.M.Marquaire, and G.M.Côme (Nancy, France)
KINETIC MODELING $\text{CH}_4\text{-O}_2\text{-Cl}_2$ FLAME REACTION
- C-24 P.Biggs, G.Hancock, M.R.Heal, D.J.McGarvey, and A.D.Parr
(Oxford, UK)
TEMPERATURE DEPENDENCIES OF $\text{CH}_2(\tilde{\text{a}}^1\text{A}_1)$ REMOVAL RATES
- C-25 A.J.Hynes (Atlanta, Georgia, USA)
LASER INDUCED FLUORESCENCE OF SILICON AND SILICON
MONOXIDE IN A GLOW DISCHARGE AND AN ATMOSPHERIC PRESSURE
FLAME
- C-26 P.D.Lightfood, P.Roussel, B.Veyret and R.Lesclaux
(Bordeaux, France)
A FLASH PHOTOLYSIS STUDY OF THE SELF-REACTIONS AND UV
SPECTRA OF THE NEOPENTYLPEROXY AND T-BUTYLPEROXY
RADICALS
- C-27 C.F.Melius, N.Bergan (Livermore, California, USA), and
J.E.Shepherd (Troy, New York, USA)
HIGH PRESSURE EFFECTS OF WATER ON COMBUSTION KINETICS
- C-28 M.Carlier, R.Minetti, J.F.Pauwels, M.Ribaucour, and
L.R.Sochet (Villeneuve d'Ascq, France)
EXPERIMENTAL AND MODELLING INVESTIGATION OF BUTANE
AUTOIGNITION IN A RAPID COMPRESSION MACHINE

C-29 J.F.Pauwels, M.Carlier, P.Devolder, and L.R.Sochet
(Villeneuve d'Ascq, France)
A REDUCED CHEMICAL KINETIC MECHANISM FOR THE SULPHUR
INHIBITION IN FLAMES

C-30 C.Anastasi (York, UK), C.Morley (Chester, UK), D.Muir
(York, UK), and J.Andarez-Alvarez (Merida, Venezuela)
BRANCHING RATIO OF OH-ALKENE REACTIONS

C-31 C.Lalo, J.Masanet, J.Deson, R.Ben-Aim, and J.Rostas
(Paris, France)
TEMPERATURE MEASUREMENT IN A CW CO₂ LASER BEAM BY
LASER-INDUCED FLUORESCENCE OF O₂

D - ELEMENTARY REACTIONS OF NEUTRAL AND IONIC SPECIES

D-1 C.Vinckier and P.Christiaens (Leuven, Belgium)
A KINETIC STUDY OF THE REACTION BETWEEN MAGNESIUM ATOMS
AND NITROUS OXIDE

D-2 V.P.Bulatov, S.I.Vershuk, V.N.Khabarov, and O.M.Sarkisov
(Moscow, USSR)
REACTION OF HO₂ RADICAL WITH HYDROGEN SULFIDE

D-3 A.A.Manthashyan, S.D.Arsentiev, R.R.Grigoryan,
E.A.Arkelyan, A.N.Korcharyan (Armenian, USSR)
NEW NOTION ON THE MECHANISM OF GAS-PHASE OXIDATION OF
UNSATURATED HYDROCARBONS

D-4 J.A.Manion (Menlo Park, California, USA) and R.Louw
(Leiden, The Netherlands)
RATES AND MECHANISMS OF GAS-PHASE DESUBSTITUTION OF
BENZENE DERIVATIVES BY HYDROGEN ATOMS NEAR 1000 K

- D-5 P.E.Dyer, K.A.Holbrook, M.Matthews, and G.A.Oldershaw
(Hull, UK)
COMPARISON OF THERMAL AND LASER-INDUCED DECOMPOSITION OF
1,2-DICHLOROETHANE
- D-6 L.Seres and A.Nacsa (Szeged, Hungary)
RATE CONSTANTS OF H-ATOM ABSTRACTION BY THE CH_3^\cdot AND
 $(\text{CH}_3)_2\text{CHCHCH}_3$ RADICALS FROM AN ADDITION OF THE CH_3^\cdot
RADICAL TO CIS- $\text{CH}_3\text{CH}=\text{CHCH}_3$
- D-7 V.M.Akimov, L.V.Lenin, and L.Yu.Rusin (Moscow, USSR)
EXCITATION FUNCTION FOR THE COMPLEX FORMATION REACTION
 $\text{Hg} + \text{CsBr} \rightarrow \text{HgCs}^+ + \text{Br}^-$
- D-8 R.Zellner (Hannover, W.Germany), J.Karthäuser, and
D.Hartmann (Göttingen, W.Germany)
KINETICS OF $\text{CH}_3\text{O}_x + \text{HO}_x$ INTERACTIONS: A COMBINED
PHOTOFRAGMENT EMISSION/LIF STUDY
- D-9 M.J.MacDonald and J.M.Roscoe (Wolfville, Nova Scotia,
Canada)
THE KINETICS OF REACTION OF CH_3 WITH PROPENE
- D-10 Z.Pytel (Warsaw, Poland) and W.Korneta (Radom, Poland)
THE EFFECT OF INTERPARTICLE INTERACTIONS ON GAS KINETICS
- D-11 F.Castaño, F.Beitia, and M.N.Sanchez Rayo (Bilbao,
Spain)
REACTIONS OF $\text{Ca}(^3\text{P})$ HALOMETHANES AT $T=600-1000$ K
- D-12 F.Castaño, A.Ortiz de Zárate, and M.N.Sanchez Rayo
(Bilbao, Spain)
REACTIONS OF RADICAL $\text{CHF}(\text{X})$ WITH UNSATURATED
HYDROCARBONS AT ROOM TEMPERATURE

- D-13 W.D.Breshears, H.A.Fry, and C.W.Wilson (Los Alamos, New Mexico, USA)
KINETICS OF REACTIVE $D_2-F_2-O_2-CO_2$ MIXTURES
- D-14 L.J.Stief, F.L.Nesbitt, and J.F.Gleason (Greenbelt, Maryland, USA)
TEMPERATURE DEPENDENCE OF THE RATE CONSTANT FOR THE REACTION $HCO + O_2 \rightarrow HO_2 + CO$
- D-15 W.S.Staker and K.D.King (Adelaide, Australia),
G.J.Gutsche, and W.D.Lawrance (Bedford Park, Australia)
DIRECT MEASUREMENT OF METHYLENE REMOVAL RATES BY SPECIES CONTAINING THE OH FUNCTIONAL GROUP
- D-16 W.Hack (Göttingen, W.Germany)
ELEMENTARY REACTIONS OF ELECTRONICALLY EXCITED RADICALS AND MOLECULES
- D-17 A.R.Bossard and M.H.Back (Ottawa, Ontario, Canada)
THE HOMOGENEOUS, THERMAL CONVERSION OF METHANE TO HIGHER HYDROCARBONS IN THE PRESENCE OF ETHYLENE
- D-18 T.Körtvélyesi, A.Tóth, and L.Seres (Szeged, Hungary)
THERMAL DECOMPOSITION OF AZOISOPROPANE IN THE PRESENCE OF 2,3-DIMETHYL-2-BUTENE
- D-19 M.Görgényi (Szeged, Hungary), R.Fischer (Leuna-Merseburg, E.Germany), and L.Seres (Szeged, Hungary)
THE THERMAL DECOMPOSITION OF AZO-ISOPROPANE IN THE PRESENCE OF $TRANS-CH_3-CH=CH-CH_3$
- D-20 J.S.Bertram, R.Becerra, R.Walsh, and I.M.Watts (Reading, UK)
THE THERMAL DECOMPOSITION REACTION OF PENTAMETHYLDISILANE AND ITS REVERSE INSERTION REACTION

- D-21 S.W.Benson and C.Chanmugatas (Los Angeles, California, USA)
FREE RADICAL PROCESSES IN ACETYLENE CHEMISTRY
- D-22 V.B.Rozenshtein, Yu.R.Bedjanian, E.M.Markin, and Yu.M.Gershenzon (Moscow, USSR)
STUDY OF ELEMENTARY REACTIONS OF FO RADICALS
- D-23 R.Becerra (Madrid, Spain) and H.M.Frey (Reading, UK)
THE PHOTOLYSIS OF ACETALDEHYDE
- D-24 S.Dóbé, T.Turányi, T.Bérces, and F.Márta (Budapest, Hungary)
THE KINETICS OF HYDROXYL RADICAL REACTIONS WITH CYCLOPROPANE AND CYCLOBUTANE
- D-25 L.Zalotai, T.Turányi, T.Bérces, and F.Márta (Budapest, Hungary)
DECOMPOSITION OF TETRAFLUOROCYCLOBUTANES. GAS/GAS AND GAS/WALL ACTIVATION
- D-26 D.L.Singleton, G.Paraskevopoulos, and R.S.Irwin (Ottawa, Ontario, Canada)
KINETIC STUDY OF THE REACTION $OD + DNO_3 \rightarrow D_2O + NO_3$.
TEMPERATURE AND PRESSURE DEPENDENCE OF THE RATE CONSTANT
- D-27 H.Frerichs, R.Koch, M.Tappe, and H.Thiesemann (Göttingen, W.Germany)
REACTIONS OF $O(^3P)$ WITH AROMATIC HYDROCARBONS IN THE GAS PHASE
- D-28 A.V.Bulgakov, A.G.Zborovsky, D.V.Muratov, Yu.P.Petrov, S.A.Smirnov, and S.V.Turetsky (Moscow, USSR)
THE HIGH TEMPERATURE DECOMPOSITION OF $(CH_3)_2N_2$, CH_4 AND CH_3 -RADICALS REACTIONS IN SHOCK WAVES

- D-29 A.V.Bulgakov, A.G.Zborovsky, D.V.Muratov, Yu.P.Petrov,
S.A.Smirnov, and S.V.Turetsky (Moscow, USSR)
THE HIGH TEMPERATURE REDUCTION OF SO_2 IN SHOCK WAVES
- D-30 P.M.Marquaire and Ph.D.Pacey (Halifax, Nova Scotia,
Canada)
THE REACTION OF HYDROGEN ATOMS WITH METHANE
- D-31 I.T.Lancar, G.Lavardet, G.Le Bras, and G.Poulet
(Orleans, France)
KINETICS AND PRODUCTS OF SELF AND CROSS COMBINATION
REACTIONS OF HALOGEN OXIDE RADICALS
- D-32 R.Walsh (Reading, UK)
EXPERIMENTAL STUDIES AND THEORETICAL MODELLING OF THE
DYNAMICS OF SiMe_2 INSERTION REACTIONS
- D-33 H.Teitelbaum (Ottawa, Ontario, Canada)
NON-EQUILIBRIUM KINETICS OF THE $\text{OH} + \text{Cl} \rightarrow \text{HCl} + \text{O}$
REACTION
- D-34 I.W.M.Smith and J.F.Warr (Birmingham, UK)
RATES OF VIBRATIONAL ENERGY TRANSFER IN COLLISIONS
BETWEEN HCN, DCN AND LIGHT GASES
- D-35 M.J.Frost and I.W.M.Smith (Birmingham, UK)
RATE CONSTANTS FOR THE REACTIONS OF METHOXY AND ETHOXY
RADICALS WITH NO_2 AND WITH NO OVER A RANGE OF
TEMPERATURE AND TOTAL PRESSURE
- D-36 P.W.Seakins (Oxford, UK) and M.J.Pilling (Leeds, UK)
ALKYL RADICAL HEATS OF FORMATION
- D-37 L.Yu.Rusin and A.A.Sidorenko (Moscow, USSR)
MECHANISM OF IONS Ti^+ FORMATION IN VACUUM ARC IN

PRESENCE OF ARGON

- D-38 V.L.Orkin (Moscow, USSR)
APPLICATION OF THE THERMOMETRIC SYSTEM FOR INVESTIGATION
OF VIBRATIONAL RELAXATION PROCESSES AND REACTIONS IN
GASES
- D-39 V.L.Orkin (Moscow, USSR)
ATOMS PRODUCTION IN REACTION OF VIBRATIONALLY EXCITED
HYDROGEN WITH MOLECULAR FLUORINE AND KINETIC
INVESTIGATION OF $H_2 + F_2 + O_2$
- D-40 V.L.Orkin and V.G.Khamaganov (Moscow, USSR)
IN SITU DETERMINATION OF HETEROGENEOUS PROCESSES
CONTRIBUTION IN FLOW TECHNIQUE INVESTIGATIONS OF
HOMOGENEOUS REACTIONS
- D-41 A.Jowko, M.Forys, and E.Bartkiewicz (Siedlce, Poland)
MECHANISM AND KINETICS OF THE $XeCl^*$ FORMATION IN Xe- RCI
GAS SYSTEMS
- D-42 K.Scherzer, J.Gebhardt, and M.Olzmann (Leuna-Merseburg,
E.Germany)
CHEMICAL ACTIVATION OF CYCLOALKENES BY HYDROGEN ATOMS
- D-43 M.Albertí, R.Sayós, A.Solé, and A.Aguilar (Barcelona,
Spain)
THE $B(^2P) + H_2O(X^1A_1)$ REACTION: POTENTIAL ENERGY SURFACE
AND QUASICLASSICAL 3D TRAJECTORY CALCULATION
- D-44 L.Beneventi, P.Casavecchia, and G.G.Volpi (Perugia,
Italy)
HIGH RESOLUTION CROSSED BEAM STUDIES OF INTERMOLECULAR
FORCES: POTENTIAL ENERGY SURFACES FOR O_2 , N_2 , NO,
 Cl_2 -RARE GASES

- D-45 A.Aguilar, B.Brunetti, M.Gonzalez, F.Vecchiocattivi, and G.G.Volpi (Perugia, Italy)
CROSSED BEAM STUDY OF THE IONIZATION PROCESSES IN THERMAL ENERGY COLLISIONS BETWEEN $\text{Ne}^*(^3\text{P}_{2,0})$ AND HCl
- D-46 G.Vassilev, F.Perales, Ch.Miniatura, J.Robert, J.Reinhardt, F.Vecchiocattivi, and J.Baudon (Paris, France)
MOLECULAR BEAM STUDIES OF COLLISIONAL PROCESSES OF METASTABLE HYDROGEN ATOMS
- D-47 J.Baudon, P.Feron, Ch.Miniatura, F.Perales, J.Reinhardt, J.Robert (Paris, France), H.Haberland (Freiburg, W.Germany), B.Brunetti, and F.Vecchiocattivi (Perugia, Italy)
OPTICAL POTENTIAL FOR $\text{Ne}^*(^3\text{P}_{2,0})$ -Ar, N_2 SYSTEMS
- D-48 W.G.Mallard and J.T.Herron (Gaithersburg, Maryland, USA)
THE NIST GAS-PHASE CHEMICAL KINETICS DATABASE: PROGRESS AND PLANS
- D-49 D.W.Schwenke (Moffet Field, California, USA)
THEORETICAL STUDIES OF THREE-BODY HYDROGEN RECOMBINATION
- D-50 F.Wu and R.W.Carr (Minneapolis, Minnesota, USA)
AN INVESTIGATION OF TEMPERATURE AND PRESSURE DEPENDENCE OF THE REACTION OF CF_2ClO_2 RADICALS WITH NITROGEN DIOXYDE BY FLASH PHOTOLYSIS AND TIME RESOLVED MASS SPECTROMETRY
- D-51 P.M.Guyon, J.B.Ozenne, O.Dutuit, C.Metayer, T.Weng, G.Bellec (Orsay, France), D.Gerlich, M.Schweiser (Freiburg, W.Germany), and J.Hepburn (Waterloo, Canada)
LOW ENERGY STATE SELECTED ION MOLECULE REACTIONS
- D-52 J.Habdas (Katowice, Poland) and D.W.Setser (Manhattan,

Kansas, USA)

THE GENERATION OF NF(a) RADICALS

- D-53 B.V.Potapkin, M.I.Strelkova, V.D.Rusanov, and
A.A.Fridman (Moscow, USSR)
KINETICS OF HYDROGEN SULPHIDE DISSOCIATION IN ELECTRIC
DISCHARGES
- D-54 C.T.Stanton and N.L.Garland (Washington, D.C., USA)
TEMPERATURE DEPENDENCE OF THE REACTION OF CH(CD) + D₂
- D-55 V.Aquilanti, R.Candori, D.Cappelletti, V.Lorent,
E.Luzzatti, and F.Pirani (Perugia, Italy)
MOLECULAR BEAM MEASUREMENT OF THE INTERATOMIC FORCES
BETWEEN CHLORINE ATOMS AND RARE GASES
- E - REACTION DYNAMICS AND STATE-TO-STATE CHEMISTRY
- E-1 J.D.Kettleborough and K.G.McKendrick (Edinburgh, UK)
ALIGNMENT EFFECTS IN BEAM GAS DYNAMICS EXPERIMENTS
- E-2 E.Martínez (Ciudad Real, Spain), P.Puyuelo (Bilbao,
Spain), and B.Cabañas (Ciudad Real, Spain)
LASER INDUCED FLUORESCENCE STUDY OF Se₂
- E-3 E.Martínez (Ciudad Real, Spain), F.Basterrechea,
F.Castaño (Bilbao, Spain), and J.Albaladejo (Ciudad
Real, Spain)
KINETICS OF THE PREDISSOCIATED LEVELS V' > 12 OF THE
B³Π(O_u⁺) STATE OF Cl₂ USING LASER INDUCED FLUORESCENCE
- E-4 S.G.Cheskis, A.A.Iogansen, P.V.Kulakov, I.Yu.Razuvaev,
O.M.Sarkisov, and A.A.Titov (Moscow, USSR)
OH VIBRATIONAL ENERGY DISTRIBUTION IN REACTIONS OF O(¹D)

ATOMS

- E-5 M.Jordan, S.C.Smith, and R.G.Gilbert (Sidney, Australia)
VARIATIONAL TRANSITION STATE THEORY: A SIMPLE MODEL FOR
DISSOCIATION AND RECOMBINATION REACTIONS OF SMALL
SPECIES

- E-6 S.A.Barts, K.V.Pinnex, and J.B.Halpern (Washington D.C.,
USA)
EMISSION OF THE C_2N_2 MOLECULE AND NEW VALUE FOR THE HEAT
OF FORMATION OF CN

- E-7 A.Jacobs, F.M.Schuler, H.R.Volpp, M.Wahl, and J.Wolfrum
(Heidelberg, W.Germany)
ABSOLUTE REACTIVE CROSS SECTIONS AND PRODUCT STATE
DISTRIBUTIONS FOR THE REACTIONS OF HOT H-ATOMS

- E-8 M.Castillejo, A.Costela, J.M.Figuera, and J.M.Muñoz
(Madrid, Spain)
KINETIC STUDIES OF ROVIBRATIONAL LEVELS OF $CO(A^1\Pi)$ BY
VUV LASER INDUCED FLUORESCENCE

- E-9 W.Gardiner and I.Oref (Haifa, Israel, and Austin, Texas,
USA)
PARAMETRIC REPRESENTATION OF UNIMOLECULAR REACTION
FALLOFF BEHAVIOR

- E-10 M.R.Levy (Newcastle-upon-Tyne, UK)
CHEMILUMINESCENCE AND ENERGY TRANSFER IN COLLISIONS OF
Mn ATOMS WITH D_2 AND HYDROCARBONS

- E-11 M.Castillejo, J.M.Figuera, I.Garcia-Moreno,
J.C.Rodriguez and H.A.Zeaiter (Madrid, Spain)
QUENCHING OF DIFFERENT METHYLENE 1B_1 ROVIBRATIONAL
OVERTONES BY SEVERAL GASES AND VAPOURS

- E-12 G.Hancock and A.J.Orr-Ewing (Oxford, UK)
PRODUCT ROTATIONAL DISTRIBUTIONS AND ALIGNMENT FOR THE
REACTION $O(^3P) + CS(X^1\Sigma^+) \rightarrow CO(X^1\Sigma^+) + S(^3P)$
- E-13 T.Griffin, A.Jörg, U.Meier, and K.Kohse-Höinghaus
(Stuttgart, W.Germany)
DETERMINATION OF STATE-TO-STATE ROTATIONAL ENERGY
TRANSFER COEFFICIENTS FOR $OH(A^2\Sigma^+, v'=0)$
- E-14 S.Aragon and R.Anderson (Santa Cruz, California, USA)
INELASTIC COLLISIONS OF STATE SELECTED $NH(A^3\Pi)$
- E-15 L.F.Phillips, I.W.M.Smith, R.P.Tuckett, and C.Whithman
(Birmingham, UK)
THE INTERNAL STATE DISTRIBUTION OF NCO FORMED IN THE
RADICAL-RADICAL REACTION: $CN + O_2 \rightarrow NCO(X^2\Pi, v', j') + O$
- E-16 L.Bañares, G.Muga, and A.González Ureña (Madrid, Spain)
COLLISION DYNAMICS OF ALKALI ATOMS WITH ORGANIC
MOLECULES. ABSOLUTE DETERMINATION OF THE REACTION
CROSS-SECTION

F - PHOTODISSOCIATION DYNAMICS

- F-1 Y.Lazarou (Crete, Greece), K.D.King (Adelaide,
Australia) and P.Papagiannakopoulos (Crete, Greece)
UNIMOLECULAR DISSOCIATION OF DIETHYLNITRAMINE
- F-2 A.W.Simpson, J.A.Dyet, M.R.S.McCoustra, and J.Pfab
(Edinburgh, UK)
STATE-SELECTED PREDISSOCIATION DYNAMICS OF PERHALOGEN
NITROSOMETHANES
- F-3 G.E.Gadd and T.G.Slanger (Menlo Park, California, USA)

ENERGY FLOW AND ENERGY POOLING IN NO FOLLOWING NO₂
PHOTODISSOCIATION

- F-4 K.Luther, T.Rech, A.Schmoltner, K.-M.Weitzel, and J.Troe
(Göttingen, W.Germany)
MULTIPHOTON IONIZATION STUDIES OF THE COMPETING C-C AND
C-H BOND FISSIONS IN HIGHLY VIBRATIONALLY EXCITED
ALKYLBENZENES
- F-5 R.A.Bach (Sussex Drive, Ottawa, Canada) and J.M.Roscoe
(Wolfville, Nova Scotia, Canada)
MINOR PRODUCTS IN THE PHOTOLYSIS OF AZOMETHANE AT LOW
PRESSURE: ALTERNATIVE DECOMPOSITION CHANNELS OF
VIBRATIONALLY EXCITED ETHANE
- F-6 C.Rinaldi, S.I.Lane, V.E.Oexler, J.C.Ferrero, and
E.H.Staricco (Córdoba, Argentina)
THE IR MULTIPHOTON DISSOCIATION OF CF₃I. EFFECT OF
PRESSURE AND OF VISIBLE LIGHT
- F-7 A.M.Schmoltner, D.S.Anex, and Y.T.Lee (Berkely,
California, USA)
DYNAMICS OF ANISOLE PHOTODISSOCIATION
- F-8 A.J.Bell, P.R.Pardon, Ch.Hickman, and J.G.Frey
(Southampton, UK)
PHOTOCHEMICAL DYNAMICS OF HOCl
- F-9 A.J.Bell and J.G.Frey (Southampton, UK)
RESONANCE RAMAN SPECTRA OF NOCl: PHOTOCHEMICAL DYNAMICS
- F-10 W.Braun, R.Klein, A.Fahr, H.Okabe (Gaithersburg,
Maryland, USA), and A.Mele (Rome, Italy)
PHOTODECOMPOSITION OF GROUP III AND V ORGANOMETALLIC
COMPOUNDS AT 193 nm

- F-11 S.Bish and R.Walsh (Reading, UK)
INVESTIGATION OF NOVEL SOURCES OF VINYLIC RADICALS
- F-12 R.Fantoni, M.Giorgi, W.C.M.Berden, V.Barbarossa,
S.Mercuri, and R.Tomaciello (Frascati, Italy)
C.A.R.S. DIAGNOSTIC OF SMALL HYDROCARBON DECOMPOSITION
IN A RADIOFREQUENCY PLASMA REACTOR FOR CARBON FILM
DEPOSITION
- F-13 M.Hande, P.McLoughlin, and I.Shanahan (Dublin, Ireland)
PHOTOOXIDATION OF HALOGENATED ANAESTHETIC AGENTS
- F-14 I.Bar, Y.Cohen, D.David, S.Rosenwaks (Beer-Sheva,
Israel), and J.J.Valentini (Irvine, California, USA)
DIRECT OBSERVATION OF PREFERENTIAL BOND FISSION BY
EXCITATION OF A VIBRATIONAL FUNDAMENTAL:
PHOTODISSOCIATION OF HOD(0,0,1)
- F-15 A.E.Croce de Cobos, C.J.Cobos, and E.Castellano (La
Plata, Argentina)
LASER PHOTODISSOCIATION OF $F_2S_2O_6$ AT 193 nm: COLLISIONAL
DEACTIVATION OF HIGHLY EXCITED FSO_3 RADICALS

G - GAS-SURFACE INTERACTIONS

- G-1 J.L.Brisset, A.Doubla, and J.Amouroux (Paris, France)
A NUCLEOPHILIC SUBSTITUTION REALIZED IN SOLUTION BY
MEANS OF A GASEOUS PLASMA TREATMENT: THE SYNTHESIS OF
 $[Fe(CN)_5CO]^{3-}$
- G-2 G.Petriella (Bari, Italy)
He SCATTERING FROM ORDERED STRUCTURES OF ADSORBATES ON
SURFACE

- G-3 P.Cadman and R.J.Denning (Aberystwyth, UK)
THE OXIDATION OF SOOT PARTICULATES IN SHOCK WAVES
- G-4 I.A.Vardanyan and R.H.Bakhchadjyan (Yerevan, USSR)
THE ROLE OF THE SURFACE IN THE CHAIN OXIDATION PROCESS
- G-5 S.L.Lee and F.Y.Li (Taipei, Taiwan, Republic of China)
EFFECT OF LATERAL INTERACTIONS BEYOND NEAREST-NEIGHBORS
ON SIZE AND SHAPE OF NON-EQUILIBRIUM ISLAND ON SURFACES
- G-6 P.Barbe, P.M.Marquaire, G.M.Côme, and F.Baronnet (Nancy,
France)
REACTION MODELING FOR OXIDATIVE COUPLING OF METHANE OVER
METAL OXIDES
- G-7 I.A.Kirillov, V.D.Rusanov, and A.A.Fridman (Moscow,
USSR)
MECHANISM OF BREAKAWAY ZIRCONIUM OXIDATION AT HIGH
TEMPERATURES AND UNDER IRRADIATION CONDITIONS

STATE-TO-STATE REACTION DYNAMICS: A SELECTIVE OVERVIEW

**James J. Valentini
Department of Chemistry
Columbia University
New York, New York USA**

This talk will present an overview of recent work on the state-to-state dynamics of "simple" atom transfer reactions. The discussion will focus on the dynamics of hydrogen atom transfer reactions like $\text{H} + \text{H}_2 \rightarrow \text{H}_2 + \text{H}$, $\text{H} + \text{HI} \rightarrow \text{H}_2 + \text{I}$, and $\text{H} + \text{CH}_4 \rightarrow \text{H}_2 + \text{CH}_3$ that have been recently investigated experimentally in our laboratory. Comparison of the experimental results with ab initio theoretical descriptions will be made.

**"CHEMICAL REACTIONS OF CHLOROCARBONS AND HYDROCARBONS
IN THE EARTH'S ATMOSPHERE"**

F.S.Rowland (Irvine, California, U.S.A.)

The measured concentrations of methane and several chlorofluorocarbons have increased steadily throughout the 1980s and carry implications for three general atmospheric problems: (1) stratospheric ozone depletion; (2) "greenhouse" retention of infrared radiation; and (3) the oxidative potential of the global atmosphere.

The most abundant chlorofluorocarbon (CFC) gases in the atmosphere are CCl_2F_2 (CFC-12), CCl_3F (CFC-11) and $\text{CCl}_2\text{FCClF}_2$ (CFC-113), with concentrations now approaching 500, 300 and 100 parts per trillion by volume (pptv), respectively. These compounds have atmospheric lifetimes of 75 years (CFC-11) or longer, and their only important sink is ultraviolet photolysis in the stratosphere. This decomposition releases chlorine atoms which initiate ClO_x chain reactions which catalytically deplete stratospheric ozone. The ClO_x chain chemistry consists of homogeneous gas phase reactions in the stratosphere, greatly assisted in polar regions by heterogeneous reactions on the surfaces of polar stratospheric clouds (PSCs) which transform chlorine reservoir molecules (HCl , ClONO_2) into photosensitive species such as Cl_2 and HOCl . The ozone losses during the Antarctic spring have been as large as 60% in total column and >98% in individual air masses. Significant ozone losses have also been observed in all latitudes, with losses over the temperate regions of the northern hemisphere more severe in winter than in summer. Carbon tetrachloride (CCl_4) is another molecule with stratospheric properties closely analogous to those of the CFCs. The current concentration of CCl_4 is approaching 150 pptv, and both it and the three major CFCs increase monotonically in their observed concentrations.

Molecules such as methylchloroform (CH_3CCl_3), CHClF_2 (HCFC-22) and CH_2FCF_3 (HFC-134A) have shorter atmospheric lifetimes because they react with hydroxyl (HO) radicals in the troposphere. Most of the alternative compounds under study for replacements for CFCs fall into the HCFC or HFC classes. The atmospheric lifetimes of such molecules can be estimated from the measured atmospheric lifetime of methylchloroform as $6.5 \text{ years} \pm 20\%$, in combination with the inverse of the reaction rate constants with hydroxyl radical measured in the laboratory.

In the natural atmosphere, the triatomic species CO_2 , H_2O and O_3 retain infrared emission from the Earth's surface, warming it by about 35°C above the calculated black-body temperature for an IR-transparent atmosphere equilibrated with the steady input of solar energy. Growth in the concentrations of CO_2 , CH_4 , N_2O and the CFCs is increasing the IR-trapping capability of the atmosphere, tending to warm the Earth still more. The per-molecule IR absorptive capabilities in the

existing atmosphere (i.e., with 350 ppmv CO_2 , etc.) for incremental additions of CFCs are about 20,000 times that for added CO_2 , while CH_4 is about 30 times that for CO_2 . The predicted growths in atmospheric concentrations of these compounds during the next few decades indicate that the summed "greenhouse" contributions from these other trace species would be about equal to that from CO_2 alone, barring major changes in emission patterns. The Montreal protocol of 1987 and its 1990 modifications will substantially reduce future emissions of CFCs and CCl_4 .

The primary removal processes for CO and CH_4 in the atmosphere are also reaction with HO radical; at the same time, the primary removal for HO is through its reactions with CO and CH_4 . The kinetics of this situation imply a finite oxidative capacity for the Earth's atmosphere (i.e., equal to total HO production) unless subsequent further reactions cause the regeneration of the HO radical. The noted increase of CH_4 implies the possibility of faster removal of HO, with a lower steady state concentration of HO and a consequent longer lifetime for CH_4 , and also for CO. The growth in CH_4 concentrations also will introduce more H into the stratosphere and, after oxidation, more H_2O . This new source of stratospheric H_2O can exert a positive feedback onto the mass and area of PSCs, which can in turn more readily catalyze the heterogeneous chlorine chemistry which depletes polar ozone.

The HO regeneration pathway normally involves nitrogen oxides, which are frequently present in ppbv levels in many urban regions but only 5-20 pptv in some remote regions. For example, the products from HO reaction with CO are CO_2 and H, with the latter immediately converted to HO_2 . Competitive reaction can then occur for HO_2 between NO to form NO_2 and HO, and another HO_2 to form H_2O_2 . The major source of CO in the Southern hemisphere is through the follow-on steps initiated by HO reaction with CH_4 . In the northern hemisphere, atmospheric CO also has important sources in incomplete combustion of fossil fuels and from the oxidation of non-methane hydrocarbons (NMHC).

From simple to complex combustion kinetics:

Experiments and Models

J. Wolfrum

Physikalisch-Chemisches Institut

Universität Heidelberg

D-6900 Heidelberg, F.R.G

Starting from detailed investigations of elementary reactions new experimental and theoretical results for the quantitative description of the complex interaction of chemical and transport processes in oxidation and combustion reactions will be described.

Sensitivity analysis shows, that the elementary steps $H + O_2 \rightarrow OH + O$ and $CO + OH \rightarrow CO_2 + H$ play the most important role in hydrocarbon combustion systems. Experiments on the microscopic dynamic and the determination of absolute cross sections for these reactions using tunable UV-laser for excitation and detection are described.

Laminar premixed and non premixed counterflow diffusion flames constitute an important basis set for the simulation of more complicated turbulent combustion processes. Detailed calculations on pure and partially premixed CH_4 /air counterflow diffusion flames are compared with results of LDA flow determinations and temperature, CH_4 , O_2 and OH radical concentration measurements using CARS and laser absorption spectroscopy for various strain rates of such flames.

For the unsteady case as a simple test system the ignition of O_3/O_2 and CH_3OH/O_2 mixtures by irradiation with a CO_2 -laser along the axis of a cylindrical vessel is described. Mathematical simulation of the ignition process in two dimensions is done by solving the corresponding system of conservation equations. Experimental data are presented for flame temperatures using IR-IR double resonance and 2D LIF experiments for time- and spatially resolved flame front detection.

The last part describes experimental results on 2D-imaging of laminar and turbulent flame fronts, flame quenching processes, concentration and temperature fields using acetaldehyde, OH and O_2 fluorescence excited by tunable UV-laser systems in laboratory laminar flames and industrial OTTO- and DIESEL-engines.

Rotational Energy Transfer between Polar Molecules. An Exact Quantum Study

Millard Alexander, Department of Chemistry, University of Maryland, College Park,
MD 20742, USA

Peter F. Vohralik^{a)}, Department of Chemistry, University of Washington, Seattle, WA
98195

The collisional transfer of rotational energy between polar molecules has been the subject of numerous investigations. The long range of the dipole-dipole interaction is responsible for the large cross sections which have been measured and calculated for this process. The prototypical system has been the self-relaxation of HF. Recently, Vohralik, Miller, and Watts^{1, 2} have used molecular beam techniques to study collisions between HF molecules in $v=0$. They found large cross sections associated with resonant exchange transitions ($J_1=0, J_2=1 \rightarrow J_1=1, J_2=0$). The cell studies of overtone pumped HF molecules by Copeland and Crim^{3, 4} suggest that transitions with $|\Delta J| = 1$ are dominant, in particular the nearly resonant processes ($v=0, j; v, j \pm 1 \rightarrow v=0, j \pm 1; v, j$). Quantum close-coupled studies of rotationally inelastic collisions between HF-HF have been reported by Alexander and DePristo^{5, 6, 7} as well as Schwenke and Truhlar.^{8, 9}

We shall describe the results^{2, 10} of converged, fully quantum, close-coupled determinations of integral and differential rotationally inelastic cross sections between two HF molecules. The potentials of Alexander and DePristo⁵ were used. Calculations were carried out at a number of collision energies, ranging from 240 to 3900 cm^{-1} . Particular attention was paid to the energetically resonant processes ($J, J' \rightarrow J', J$). The cross sections for these transitions were found to increase as the total energy decreased, in contrast to those for all other processes. This is particularly dramatic for the transitions which are dipole coupled to first order ($J, J+1 \rightarrow J+1, J$). At thermal energies these resonant exchange processes dominate the total inelastic energy transfer. Our calculations on nonidentical HF molecules in different vibrational states show that these first-order exchange processes underly the relaxation observed by Copeland and Crim.^{3, 4}

At a total energy of 1480 cm^{-1} , comparable to that used in the experiments of Vohralik, Miller, and Watts,^{1, 2} the differential cross sections for transitions involving the resonant exchange of one rotational quantum ($J, J+1 \rightarrow J+1, J$) are extremely large at small angles, comparable, in fact, to the elastic ($J, J+1 \rightarrow J, J+1$) differential cross sections. At long range (large impact parameters) the resonant rotational exchange transitions dominate the scattering. In modelling the experiments of Vohralik and Miller¹ we predict scattering cross sections of $229-332 \text{ \AA}^2$ and $5-50 \text{ \AA}^2$ for, respectively the $01 \rightarrow 10$ and $02 \rightarrow 20$ cross sections. This compares extremely well with the values

of 320 and 40 Å² extracted from the experimental data.

We wish to acknowledge the support of the National Science Foundation under grant CHE-8917543

a) Present address: CSIRO Division of Applied Physics, P. O. Box 218, Lindfield, NSW 2070, Sydney, Australia

1. P. F. Vohralík and R. E. Miller, J. Chem. Phys. **83**, 1609 (1985).
2. P. F. Vohralík, R. O. Watts, and M. H. Alexander, J. Chem. Phys. submitted.
3. R. A. Copeland and F. F. Crim, J. Chem. Phys. **81**, 5819 (1984).
4. R. A. Copeland and F. F. Crim, J. Chem. Phys. **78**, 5551 (1983).
5. M. H. Alexander and A. E. DePristo, J. Chem. Phys. **65**, 5009 (1976).
6. A. E. DePristo and M. H. Alexander, J. Chem. Phys. **66**, 1334 (1977).
7. M. H. Alexander, J. Chem. Phys. **73**, 5135 (1980).
8. D. W. Schwenke and D. G. Truhlar in *Supercomputer Research in Chemistry and Chemical Engineering*, edited by K. F. Jensen and D. G. Truhlar (American Chemical Society, Washington, D. C., 1987) p. 176.
9. D. W. Schwenke and D. G. Truhlar, J. Comp. Chem. **8**, 282 (1987).
10. P. F. Vohralík, R. O. Watts, and M. H. Alexander, J. Chem. Phys. **91**, 7563 (1989).

Radical-Radical Reactions: Kinetics, Dynamics and Mechanism

Ian W.M. Smith

School of Chemistry
University of Birmingham
Edgbaston
Birmingham B15 2TT

Reactions between free radicals are, in several fundamental respects, different from reactions between a free radical and a molecule (in which all the electrons are 'paired'). Radical-radical reactions usually proceed via a potential energy surface or surfaces which are characterised by potential minima and no potential barriers at least in the entrance channel. Furthermore, such reactions can frequently yield more than one set of products.

In this lecture, I shall attempt to review the present state of our knowledge of radical-radical reactions using as reference points a number of recent or current experiments in my laboratory. These will include investigations of rate constants over very wide ranges of temperature, studies of product state distributions carried out in order to establish the influence of potential energy minima on the reaction dynamics in radical-radical reactions, and finally the results of experiments designed to establish branching ratios.

INTERMOLECULAR POTENTIALS IN REACTIVE SYSTEMS

Giorgio Liuti

Dipartimento di Chimica dell'Università, Perugia (Italy)

The knowledge of the intermolecular interaction features, especially regarding collisions involving open shell species, finds important applications in the analysis of the kinetics of complex chemical processes such as those occurring in combustion, flames, lasers, plasmas, atmospheric and astrophysical phenomena.

The interactions between oxygen atoms and various atoms and molecules and between halogen atoms and various atoms, studied by measuring the integral collision cross section as a function of particles velocity and selecting the open shell atom m_j state during the collision by a deflecting inhomogeneous magnetic field, will be presented and discussed together with the relevant potential energy curves obtained.

Also in view of the importance of a sufficiently accurate information on the potential parameters of as many systems as possible of different nature and considering the scarce information available for cases of interest in many applications, it would be desirable to develop a general correlation capable of yielding the potential parameters expressed in terms of fundamental physical properties.

The usefulness of such a general analysis is enhanced if the results allow to obtain reasonable estimates of the interaction parameters for those pairs difficult to study experimentally and theoretically.

Recently a correlation between the potential parameters and the polarizability of the interacting partners has been

given and tested on many closed shell-closed shell pairs and on some open shell-closed shell pairs.

It will be shown that the correlation can be expressed in simpler and at the same time more general form than before. This generalization widens the applicability of the correlation to any type of interaction, including those involving ions.

Bridging the Gap between UHV Surface Science and the Kinetics of High Pressure Heterogeneous Catalysis: The Activation and Reactions of CH₄ on Ni(111)

S.T. Ceyer
Department of Chemistry
Massachusetts Institute of Technology
Cambridge, MA 02139

Many chemical reactions occurring on the surfaces of solid materials appear to proceed only under high pressures of the gaseous reactants but not at low pressures ($<10^{-4}$ torr), despite favorable thermodynamics. This lack of reactivity at the low pressures where ultrahigh vacuum (UHV) surface science techniques are operable is known loosely as the pressure gap in the reactivity in heterogeneous catalysis. Our group proposed that an origin of the pressure gap is the presence of a barrier to dissociative chemisorption of at least one of the reactants upon collision with the surface. Since it is the translational or internal energy of the incident molecule that is important in surmounting this barrier and not the surface temperature, the rate of the reaction is limited by the flux of incident molecules with energies above the energy of the barrier. High pressures simply increase the absolute number of high energy molecules, thereby increasing the reaction rate sufficiently for the products to be detected.

To verify this hypothesis, we systematically increased the energy of the incoming molecule while monitoring for the onset of dissociation in an ultrahigh vacuum-molecular beam apparatus which combines high resolution electron energy loss spectroscopy with molecular beam techniques. The molecular beam provides a convenient source of monoenergetic molecules at low pressures and electron energy loss spectroscopy, a vibrational spectroscopy for adsorbed species, is a sensitive and chemically specific detector of the adsorbed products of the dissociative chemisorption event. We probed the dissociative chemisorption of CH₄ on Ni(111). Measurements of the dissociation probability as a function of the CH₄ incident energy showed that there is, indeed, a barrier to the dissociation of CH₄. Our low-pressure, dissociation probability measurements as a function of energy were found to agree very well with the rates of CH₄ decomposition on a Ni(111) crystal measured under high-pressure conditions as a function of reactor temperature. The agreement between the low and high-pressure experiments carried out in different laboratories establishes the presence of a barrier along the reaction coordinate as an origin of the pressure gap in heterogeneous catalysis.

Besides providing a link between UHV surface science and high-pressure catalysis, these studies of the dynamics of the dissociative chemisorption of CH₄ have provided a detailed microscopic picture of the mechanism for the C-H bond breaking process. We have shown that a deformation model explains the role of translational and vibrational energy in promoting dissociative chemisorption and suggests that tunneling is the final step in the C-H bond cleavage. Specifically, the probability for dissociative chemisorption of CH₄ on Ni(111) is observed to scale exponentially with the CH₄ translational energy in the direction normal to the surface. Vibrational energy in the CH₄ bending modes is found to be as effective as translational energy but surface temperature has no effect on the dissociation probability. These results are interpreted in terms of a barrier to CH₄ dissociation largely associated with the energy required to deform CH₄.

Additional corroboration of the deformation model arises from the observation of a new kind of mechanism for dissociative chemisorption, collision induced dissociative chemisorption. If the barrier to dissociation of CH₄ is largely the energy required to distort CH₄, then it should be possible to supply this deformation energy to CH₄ physisorbed on Ni(111) by collision with an inert gas atom. The impact of the inert gas atom is predicted to round the molecularly adsorbed CH₄ into the distorted shape of the transition state that leads to dissociation. We showed that this mechanism does occur by monitoring the dissociation rate of CH₄ physisorbed on Ni(111) at 47 K induced by the impact of an incident Ar or Ne atom beam. The absolute cross section for collision induced dissociation, which is proportional to the dissociation rate, is measured over a wide range of kinetic energies (28-52 kcal/mol) and angles of incidence of a Ne or Ar atom beam. Unlike the

translational activation of CH₄ which exhibits strict normal energy scaling, the collision induced dissociation cross section displays a complex dependence on the energy of the impinging inert gas atoms, uncharacteristic of normal energy scaling.

A two-step, dynamical model for the mechanism of collision induced dissociation is shown to provide excellent agreement with the energy and angular dependence of the cross section for dissociation. The model depicts the initial collision between the Ar or Ne and the physisorbed CH₄ to be impulsive and bimolecular. However, the energy transferred to CH₄ in the normal direction only is important. The magnitude of the normal energy transferred is dictated not only by the energy and incident angle of the impinging atom but by the impact parameter of the collision. It is this dependence of the energy transfer on impact parameter that leads to the breakdown of normal energy scaling in the Ar or Ne kinetic energy. Once this collision and energy transfer occurs, the Ar or Ne no longer participates in the dissociation process. The CH₄ molecule is accelerated into the surface by its newly acquired energy, is deformed upon impact with the surface and dissociates. The probability for CH₄ dissociation at the value of the normal energy acquired by CH₄ after its collision with Ar is given by the previous translational activation results. In this way, the model calculations allow the translational activation data to be mapped onto the cross sections for collision induced dissociation. Therefore, translational activation and collision induced activation are shown to be completely consistent. They are simply different ways to provide the energy to deform the CH₄ molecule but, once deformed, the mechanism for the dissociation is the same.

In competition with collision-induced dissociation, we have observed another process, collision induced desorption. The absolute cross section for desorption increases with the incident angle of the Ar atoms at high total kinetic energy and remains approximately constant at low kinetic energy. Classical trajectory simulations indicate that desorption is predominantly the result of direct collisions of Ar with CH₄. The complex angle and energy dependence is shown to arise from the competition between the decrease in the energy available in the normal direction and the increase in the geometrical cross section for the collision as the incident angle increases.

Having established this link between high-pressure catalysis and UHV surface science, we now know how to bypass the high-pressure requirement simply by raising the energy of the incident molecule (translational activation) or collisionally inducing dissociation (collision induced activation). We have used both methods to synthesize and identify spectroscopically, by high resolution electron energy loss spectroscopy, an adsorbed CH₃ radical under low pressure, ultrahigh vacuum conditions. This was accomplished originally by measuring the vibrational spectrum of methane after deposition on the surface at 140 K with a translational energy of 17 kcal/mol. The crystal temperature is maintained at a low value in order to trap the nascent product of the dissociative chemisorption event.

Once the adsorbed CH₃ species are so synthesized, their reactivity is probed by monitoring the vibrational spectrum as a function of surface temperature. Above 150 K, the CH₃ radicals dissociate to form adsorbed CH and more adsorbed atomic hydrogen. The adsorbed CH then recombines to form adsorbed C₂H₂, an acetylenic type of species, as the surface temperature is raised to 230 K. At 370 K, the adsorbed acetylene trimerizes to form adsorbed C₆H₆ while at 410 K the atomically adsorbed hydrogen recombines and desorbs as H₂. At a slightly higher temperature, 425 K, some of the chemisorbed C₆H₆ dehydrogenates to form gas phase H₂ and partially hydrogenated carbon rings on the surface while some of the C₆H₆ desorbs intact as detected by a quadrupole mass spectrometer in a thermal desorption experiment. Although the maximum desorption yield for C₆H₆ is 1.5%, the gas phase hydrocarbon selectivity of this synthesis for benzene production is 100%. This procedure represents the first synthesis of C₆H₆ from CH₄ over a single catalyst and suggests the use of molecular beams as a synthetic tool. These data also provide mechanistic information useful to the possible extrapolation of this synthesis from UHV environments to more practical conditions.

**The Dynamics of Photodissociations Producing Three Fragments:
Deciding between Stepwise and Concerted Mechanisms**

P. L. Houston
Department of Chemistry
Cornell University
Ithaca, NY 14853-1301

Photodissociations producing three photofragments produce special problems for chemical dynamics. When only two fragments are produced, conservation of linear momentum and energy allow one to determine the internal and translational energy of an unobserved fragment from a measurement of these quantities in an observed fragment. With three photofragments, however, even measurement of the internal and translational energy distributions for each is not necessarily sufficient to completely determine the dissociation mechanism. Of particular interest is whether the two bonds break simultaneously or sequentially. Recent measurements from our group include fragment energy distributions in photodissociations of acetone, C_3O_2 , and CH_3NO_2 , each of which is a dissociation of the form $ABC \rightarrow A+B+C$.

A method has been developed for deciding the degree to which a dissociation of this form is concerted based on measurement of the dynamical properties of the fragments. The method considers the joint probability distribution, P , giving the coincidental occurrence for each possible set of the dynamical variables. Information theory is used to obtain the most probable joint probability distribution which is consistent with the experimental measurements available, each of which is simply a projection of P . Once P is found, it can be used to predict the outcome of measurements that are less experimentally accessible; an important prediction is the angular distribution describing the fragmentation. A "concertedness" parameter is defined, which ranges from a value of zero for the stepwise limit of dissociation to a value of unity for the concerted limit. This parameter can be directly calculated from the angular distribution provided by P and can be used to estimate to what degree a reaction is concerted based on the experimental data used to calculate P . Examples will be given from the data listed above and from other data in the literature.

CONCLUDING REMARKS: OZONE, FREONS AND GREENHOUSE EFFECT

V.L. Talrose

Institute of Energy Problems of Chemical Physics, USSR
Ac. of Sci., Moscow, USSR

Influence of freons on ozone layer is considered to be more or less proved that entailed an adoption of the well-known international agreements on reduction of production of the ozone layer depleting freons and substitution them to ozone frendly ones. Not so much attention was paid till now to the role of freons in climate change though it is known that both freons and ozone are so called greenhouse gases.

According to model estimations a share of freons in the greenhous effect befor 1980's was 8% and now it is 14% that is about 30% of CO_2 effect. Other important greenhouse gases are methane (14%), N_2O (5%) and other freons, ozone and stratospheric water vapor (13% at whole).

From the point of view the problems which are under consideration at symposium on gas kinetics the most interesting question is that on the influence of the elementary chemical and photochemical processes proceeding in the troposphere and stratosphere to greenhouse effect. Such an influence really takes place and is assumed to be connected with the chemical and/or photochemical nature of the greenhouse gases atmospheric life times, which determine the rate of accumulation and steady state atmospheric content of the antropogenic and natural substances coming into the atmosphere and their input to the greenhouse effect.

This concerns the freons as well because they are destroyed in atmosphere exclusively in chemical and photochemical reactions. In this connection much attention in the report is paid to the modern state of the atmospheric freon chemistry and the reliability of the estimations of their share in climate change based on the laboratory measurements and data of the atmospheric models. A consideration comprises the freons which are produced now and will be shortened in according with Montreal Protocol and also the ones which are considered as the substitutes not depleting the ozone layer.

A possibility to diminish a possible global warming owing to an application of the substitutes which would be both ozone and climate safe substances is an important ecological question which is discussed in the report.

CROSSED BEAM STUDIES OF THE REACTION DYNAMICS OF $O(^1D)$ ATOMS
WITH SIMPLE MOLECULES

N. Baluzani, L. Beneventi, P. Casavecchia, D. Stranges, and G.G. Volpi
Dipartimento di Chimica, Università di Perugia
06100 Perugia, Italy

We have undertaken the study of elementary reactions of $O(^1D)$ under single collision conditions by the crossed molecular beam scattering method with mass spectrometric detection. The first reactions we have looked at are $O(^1D) + HCl$ and $O(^1D) + HBr$, which are a group of three atom reactions amenable to both detailed experimental and theoretical investigation. Measurements of the absolute rate constants and product yields at 297 K have been recently reported.¹ The $ClO + H$ channel was found to be about 35% of $OH + Cl$, while, surprisingly, the $BrO + H$ channel was found to be only a minor reaction pathway (<4.5%). The internal state distribution of the OH product has been investigated by laser induced fluorescence (LIF) and time-resolved Fourier transform spectroscopy (FTS) techniques.² No information on the reaction dynamics of the XO ($X=Cl, Br$) channel is available. Since the products of these reactions are catalytically active species in upper atmosphere chemistry, it is important to reach a detailed understanding of the mechanism and dynamics of these processes.

The experiments were carried out in a universal crossed molecular beam machine, which has been described in detail elsewhere.⁴ Briefly, supersonic beams of the two reactants, after two stages of differential pumping, are crossed at 90° in a large scattering chamber kept at 10^{-7} mbar. The reaction products are detected by a rotatable quadrupole mass spectrometer detector kept below 10^{-10} mbar. Product velocity distributions are measured using the pseudo-random time-of-flight method. The oxygen atom beam, containing $O(^1D)$ and ground state $O(^3P)$ atoms, is produced in a high pressure (up to 500 mbar) radio frequency (RF) discharge nozzle beam source, by using dilute O_2/He and O_2/Ne gas mixtures and high RF power (up to 250 watts). $O(^1D)$ atom beams with a wide variable range of translational energies ($0.18 < E < 0.80$ eV) are thus produced. The presence of $O(^1D)$ in the beam is checked by observing the production of OH in the reaction $O(^1D) + H_2$ at $E_c \approx 3$ Kcal/mol.

The center-of-mass frame product flux distributions derived from angular and velocity distribution measurements of the XO product at different collision energies provide detailed information on the dynamics of this channel, which appears to be very different from that of the

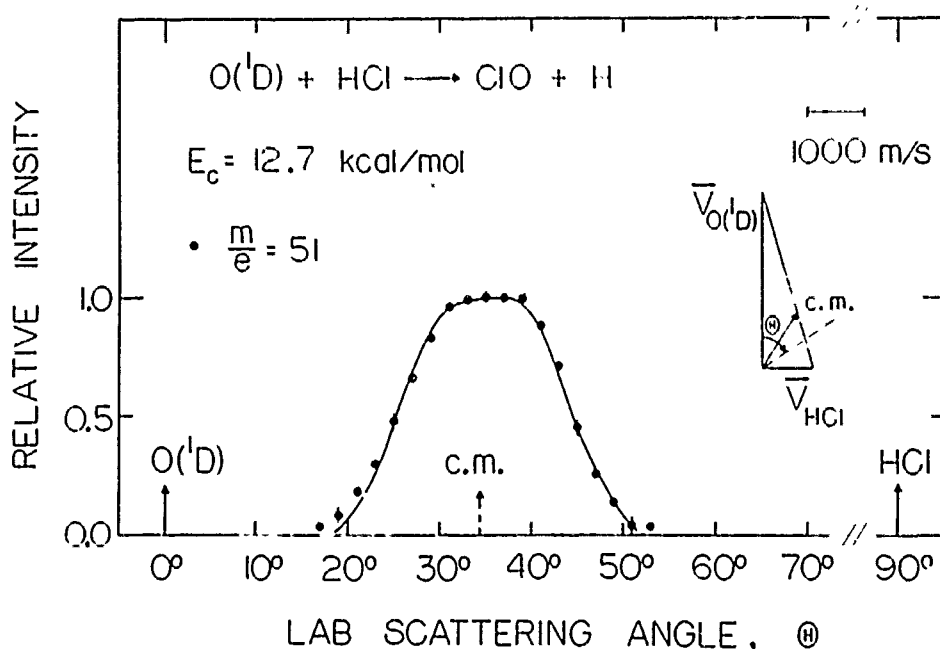


Fig. 1. Laboratory angular distribution of the ClO product from the $O(^1D) + HCl$ reaction. Solid line: calculation with best-fit c.m. angular and translational energy distributions.

OH + X channel. The signal at the kinematically unfavored OH mass is < 0.01 of the signal at the XO mass for both systems. From this the branching ratio between ClO (BrO) and OH formation is estimated to be ≥ 0.34 (≥ 0.25). This differs from what found from absolute rate coefficient measurements¹ at 297 K.

Presently, experiments are being carried out to include reactions with deuterated species, and to extend the investigation also to HF and HI and other simple molecules. Specifically, the four-center system $O(^1D) + H_2S$ is also under study. Information only on the OH + SH channel is available from LIF and IR chemiluminescence studies.⁵ Measurements of angular and velocity distributions for the other two relevant reaction channels, leading to $HSO + H$ and $SO + H_2$ products, are providing detailed information on the reaction mechanism and dynamics. The results will be discussed at the meeting.

REFERENCES

1. P.H.Wine, J.R.Wells, and A.R.Ravishankara, *J.Chem.Phys.* **84**, 1349 (1986)
2. A.C.Luntz, *J.Chem.Phys.* **73**, 5393 (1980); E.J.Kruus, B.I.Niefer, and J.J.Sloan, *J.Chem.Phys.* **88**, 985 (1988)
3. R.Schinke, *J.Chem.Phys.* **80**, 5510 (1984)
4. L.Beneventi, P.Casavecchia, and G.G.Volpi, *J.Chem.Phys.* **85**, 7011 (1986)
5. S.Klee, K.H.Gericke, and F.J.Comes, *Chem.Phys.Lett.* **118**, 530 (1985); P.M.Aker, J.J.A.O'Brien, and J.J.Sloan, *Chem.Phys.* **104**, 421 (1986).

Reaction Dynamics and Branching ratios of $O(^1D_2)$ Reactions with Halogenated Methanes

J.J.Sloan, Waterloo, Ontario, Canada.

Time-resolved Fourier transform spectroscopy (TRFTS) has been used to study the kinetics and dynamics of the reactions of electronically excited oxygen atoms with CH_3X ($X=Cl,F$). The experiments were carried out in a low-pressure chemiluminescence apparatus. Emission spectra of HX, OH and CO were recorded simultaneously from the reaction. Using the fast TRFTS technique, the first observation was made at a time corresponding to less than two gas-kinetic collisions following the reaction, permitting the dynamics of the elementary reactive process to be determined. The subsequent time evolution of the emission spectra gave information about the energy transfer processes and the possible occurrence of subsequent reactions among the radicals created in the initial reaction.

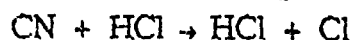
The results indicate that the reactions occur *via* both a direct abstraction channel, and an insertion, followed by HX and/or OH elimination. The predominant path seems to be insertion and HX elimination. The HX is created with substantial rotational excitation in some cases, indicating unusual exit channel dynamics.

Effects of Reagent Vibrational Excitation in the Reaction: $\text{CN}(v_1) + \text{HCl}(v_2) \rightarrow \text{HCN} + \text{Cl}$

M.J. Frost, Y. Gu,* I.R. Sims,† I.W.M. Smith and R. Spencer-Smith

School of Chemistry
University of Birmingham
Edgbaston
Birmingham B15 2TT, U.K.

The dependence on temperature of the rate constant for the reaction



can be fitted to the Arrhenius expression with an A-factor of $7.8 \times 10^{-12} \text{ cm}^3 \text{ molecule}^{-1} \text{ s}^{-1}$ and an activation energy of 18.8 kJ mol^{-1} . Experiments employing time-resolved laser-induced fluorescence following pulsed laser photolysis of NCNO enable one to observe independent decays of $\text{CN}(v=1)$ and $\text{CN}(v=0)$. Such experiments show that the rate of reaction is scarcely affected by CN excitation.

Our present measurements seek to establish the enhancement of the reaction rate which results from excitation of the vibration of HCl. A pulsed HCl chemical laser is used to excite HCl, the fraction excited being estimated by comparing traces of infrared fluorescence in the presence and absence of a 'cold gas' filter.

Our experimental results will be compared with transition state theory predictions which use a scaled ab initio potential energy surface.

* permanent address: Dalian Institute for Chemical Physics, Chinese Academy of Sciences, Dalian, China.

† present address: Department of Chemistry, California Institute of Technology, Pasadena, Calif. 91125, U.S.A.

Vibrational Product State Distribution of HCN Produced in
the Reaction of CN Radicals with Saturated Hydrocarbons.

Leon Copeland, Fida Mohamnad, Mansour Zahedi

and

William M. Jackson

Department of Chemistry

University of California

Davis, CA 95616

Time resolved infra-red emission studies have been used to study the formation of vibrationally excited HCN molecules produced in the reaction of CN radicals with saturated hydrocarbons. A kinetic model is used to fit the observed IR time response for HCN molecules in the $v''=2$ and $v''=1$ levels of the ν_3 mode. The rate coefficients for quenching of the $v''=2 \rightarrow v''=1$ and $v''=1 \rightarrow v''=0$ were determined from the data using a kinetic for this homologous series hydrocarbons. These rate coefficients are collected in Table 1 and they are all very fast, indicating that the reaction takes place on nearly every collision. This is to be expected because of the near resonance between the C-H frequencies in the molecules.

The branching ratio for the production of $v''=2$ relative to $v''=1$ could also be determined from the time resolved spectra because the resolution was high enough to clearly resolve the R branch of the $v''=1$ transition from the P branch of the $v''=2$ transition. The branching ratio at time $t = 0$ was then gotten by taking the ratio of the appropriate integrated band intensities. Table 2 gives the % of $v''=2$ for the molecules that were studied. More HCN molecules are formed in the $v''=2$ level than in the $v''=1$ level for each of the reactants indicating there is an early barrier on the potential energy surface for these reactions and that this reaction produces a population inversion in HCN. This agrees with our prior expectation since the system is a heavy-light-heavy system. The presence of a population inversion from the chemical reaction suggests that it is possible to make a HCN chemical laser at approximately 3208 cm^{-1} .

Table 1.

Rate Coefficients for Vibrational Quenching.

GAS	P(RH)	$k_{21}(\text{s}^{-1} \text{ Torr}^{-1})$	$k_{10}(\text{s}^{-1} \text{ Torr}^{-1})$
CH ₄	0.37 Torr	6.76E5	2.16E5
C ₂ H ₆	0.05 Torr	1.24E6	2.91E5
C ₃ H ₈	0.10 Torr	7.22E5	1.54E5
n-C ₄ H ₁₀	0.13 Torr	5.62E5	1.81E5
i-C ₄ H ₁₀	0.18 Torr	5.53E5	1.28E5
neo-C ₅ H ₁₂	0.11 Torr	6.63E5	1.93E5

Table 2.

Percentage of HCN(2) Produced in the Reaction.

GAS	HCN(1)/HCN(2)	%HCN(2)
METHANE	1.2141	45
ETHANE	0.1712	85
PROPANE	0.1728	85
n-BUTANE	0.4164	71
i-BUTANE	0.4089	71
neo-PENTANE	0.4934	67
c-PROPANE	1.5980	38

The authors gratefully acknowledge support from the DOE Basic Energy Sciences Combustion Program under grant # DE-FG05-84ER13213 and the conversation with G. Hancock about this project.

IR-chemiluminescence from reactions of F-atoms with some stable organic molecules and some organic radical species

Horst Heydtmann, Kathrin Dehe, Ulrich Schwanke

Institut für Physikalische und Theoretische Chemie
Johann Wolfgang Goethe-Universität
Niederurseler Hang
D-6000 Frankfurt/Main

HF chemiluminescence has been measured and analysed for a number of reactions $F + RH$ under arrested relaxation conditions [1]. Fluorine atoms are prepared by microwave dissociation of F_2 or CF_4 . The primary vibrational and rotational distributions are given for the hydrogen atom abstraction from azomethane, 2,2'-azobisisobutane, azodicarbonic acid dimethylester, t-butylisonitrile and butyne-2 [2-4]. The different ensuing vibrational distributions are presented in the table below and will be discussed. $F + CH_4$ and $F + C_2H_6$ yield vibrational/rotational distributions for $HF(v \leq 3)$ which are independent for the molecular components at room temperature or at elevated temperatures (1200 - 1600K). In the systems $F +$ ethyne and $F +$ butyne-2 with high excess of F-atoms secondary processes must occur which populate higher vibrational levels of HF. Under these conditions in the former system HF ($v = 1-7$) has been observed whereas in the latter system HF ($v = 1-6$) was detected. In the case $F +$ ethyne IR-chemiluminescence is entirely caused by secondary processes; the following vibrational distribution was found: $N_{v=1} : N_{v=2} : N_{v=3} : N_{v=4} : N_{v=5} : N_{v=6} : N_{v=7} = 16 : 20 : 15 : 19 : 21 : 10 : 1$. This distribution indicates that at least two F-atom reactions with radicals occur.

- [1] B. Dill, H. Heydtmann; Chem. Phys. 35; 161, (1978)
- [2] U. Schwanke, H. Heydtmann, J. J. Sloan; Chem. Phys. 132; 413; (1989)
- [3] K. Dehe, H. Heydtmann, U. Schwanke; Chem. Phys. Letters; in press
- [4] U. Schwanke, H. Heydtmann; to be published in Ber. Bunsenges. Phys. Chem.

Table: HF vibrational distribution from the reactions of $F + RH$

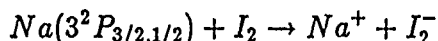
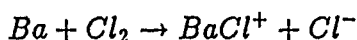
RH	v=1	v=2	v=3	v=4
$CH_3-N=N-CH_3$	50	33	16	2
$(CH_3)_3C-N=N-C(CH_3)_3$	46	49	5	-
$CH_2OOC-N=N-COOCH_3$	43	47	10	-
$(CH_3)_3C-NC$	46	51	3	-
$CH_3-C \equiv C-CH_3$	26	36	32	7

CHEMI-IONIZATION STUDIES UNDER CROSSED-BEAM CONDITIONS

L. Bañares and A. González Ureña

Departamento de Química Física. Facultad de Química.
Universidad Complutense de Madrid. 28040-Madrid, SPAIN.

Using one of our molecular beam machines, supersonic beams of Cl_2 and I_2 diluted in H_2/He were crossed with Ba and electronic excited Na beams. A study of the following charge transfer processes:



was carried out as a function of collision energy, electronic excitation and spin-orbit effects. The collision energy was changed by the seeding technique as well as using the time-of-flight method under crossed-beam conditions (1). On the other hand, a modulated dye laser pumped by an Ar^+ laser was used to excite the Na atom to its $^2P_{3/2}, ^2P_{1/2}$ states right at the scattering center. Both the laser induced fluorescence of the Na^* beam and the chemiionization signal from the title reaction were measured as a function of the laser excitation wavelength and collision energy. Chemiionization spectra were collected changing the collision energy to obtain energy thresholds and post-threshold laws for both spin-orbit states.

Figure 1 displays a typical laser excited chemiionization spectrum at 0.77 eV of collision energy. Excitation function data for both spin-orbit states over a significant range of collision energy will be presented and discussed at the Symposium in the light of collision dynamics effects of the $Na^+ \dots I_2^-$ transition state.

This work received financial support from CICYT grant PB88/146 and EEC grant SC1-0006C

(1) E. Verdasco and A. González Ureña, *J. Chem. Phys.*, in press

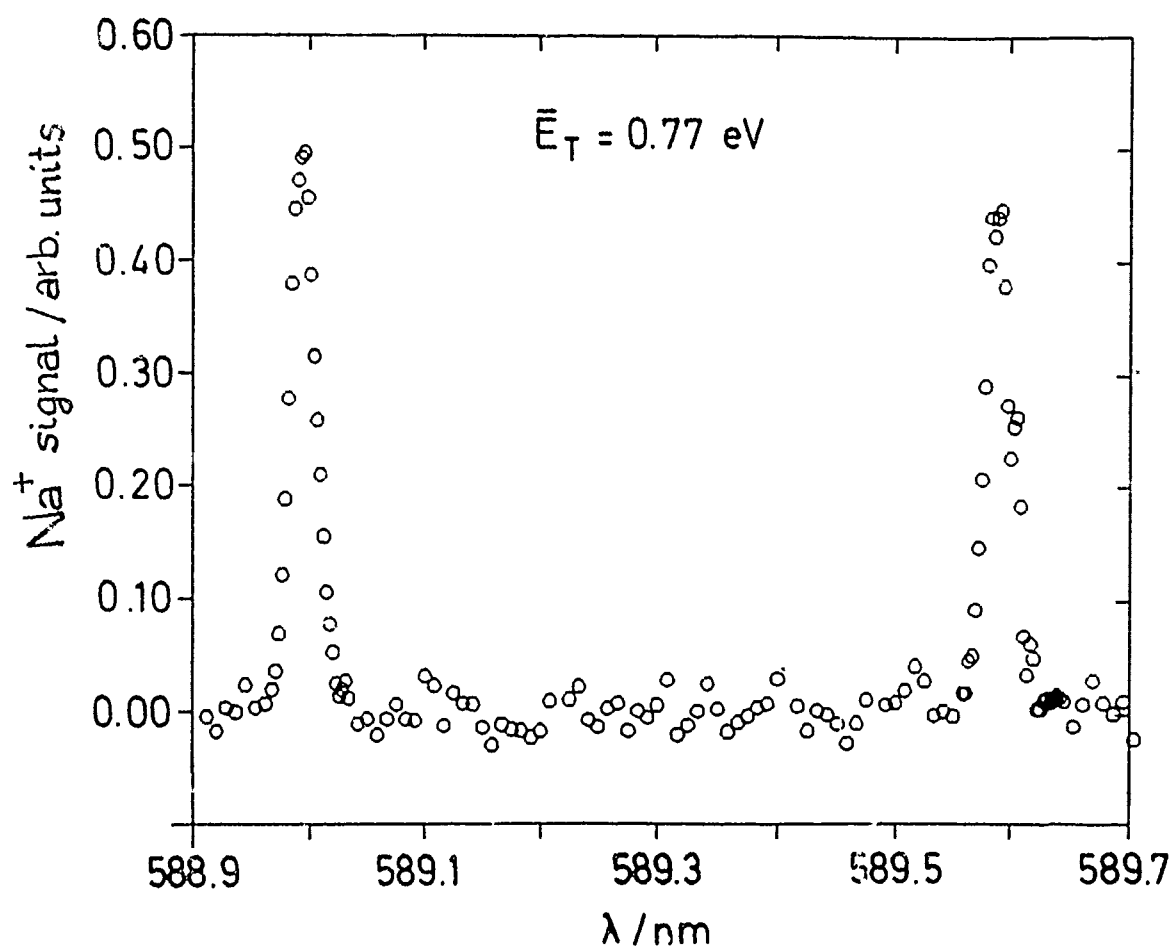


Figure 1. Positive ion signal as a function of laser wavelength for the $\text{Na} + \text{I}_2$ crossed-beam experiment at the indicated collision energy.

Laboratory Studies of the Gas Phase Reaction Between NO₃ and Simple Peroxy Radicals.

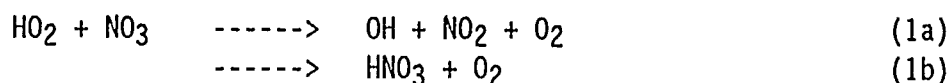
J.N. Crowley¹, J.P. Burrows¹, G.K. Moortgat¹,
L. Mellouki², G. Poulet² and G. LeBras².

¹Max-Planck-Institut Für Chemie, 6500 Mainz, F.R.G.

²Centre de Recherches sur la Combustion et des Hautes Températures,
C.N.R.S., 45071 Orléans-Cedex 2, France.

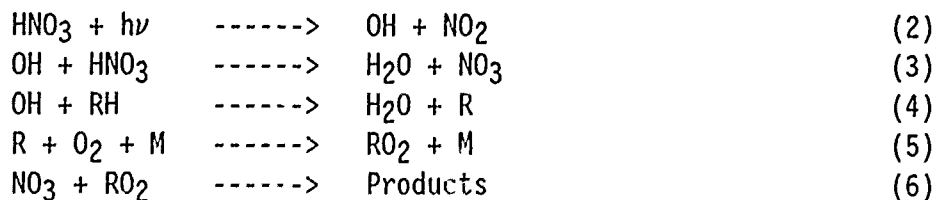
The ozonolysis of organic unsaturated compounds^[1] and the reactions of NO₃ with hydrocarbons are believed to produce organic peroxy radicals, RO₂^[2-4]. The peroxy radicals thus formed in the nighttime in the troposphere are likely to react with NO₃. The analysis of laboratory measurements of reactions between NO₃ and organic molecules also requires a full understanding of the subsequent reaction between NO₃ and the peroxy radical product. Rate coefficients for reaction between NO₃ and three simple peroxy radicals are presented here.

The simplest peroxy radical is HO₂, and the rate constant and products of its reaction with NO₃ have been measured by the discharge flow technique ^[5] (Orléans):



With k_{1a} and k_{1b} equal to 36 and $9.2 \times 10^{-13} \text{ cm}^3 \text{ molecule}^{-1} \text{ s}^{-1}$ respectively at room temperature.

The reaction between NO₃ and either methylperoxy or ethylperoxy radicals was studied by the modulated photolysis technique (Mainz). Here, the modulated photolysis (253.7 nm) of HNO₃ in the presence of RH and O₂ results in a reaction sequence producing both RO₂ and NO₃ as shown below:



The modulated absorption profile of NO₃ was monitored by absorption of light from a tungsten lamp at either 623 nm over a 131 cm path length, or at 628 nm over a 975 cm path length provided by internal white optics.

A typical modulated absorption profile along with computer fits of the data in a $\text{CH}_3\text{O}_2 + \text{NO}_3$ experiment is presented in Figure 1.

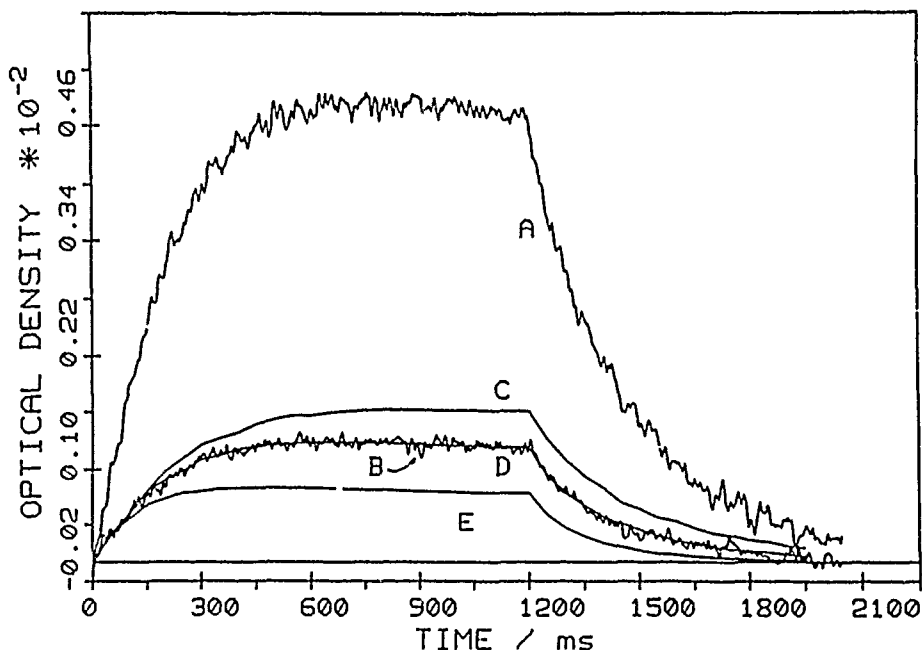


Figure 1. NO_3 absorption profiles (623 nm) and computer simulations: A. Experimental curve, no methane. B. Experimental curve, 2.1×10^{17} molecules cm^{-3} methane. C, D, E, simulations with $k(\text{NO}_3 + \text{CH}_3\text{O}_2) = 1 \times 10^{-13}$, 1.51×10^{-12} and 1×10^{-11} $\text{cm}^3 \text{ molecule}^{-1} \text{ s}^{-1}$ respectively.

Analysis of NO_3 concentration curves thus obtained enabled a rate constant of $(2.3 \pm 0.7) \times 10^{-12}$ $\text{cm}^3 \text{ molecule}^{-1} \text{ s}^{-1}$ to be obtained for the reaction between CH_3O_2 and NO_3 and 298 K and 20 Torr.

The reaction between $\text{C}_2\text{H}_5\text{O}_2$ and NO_3 proved to be slower, and early results indicate a room temperature rate coefficient of about $(4 \pm 2) \times 10^{-13}$ $\text{cm}^3 \text{ molecule}^{-1} \text{ s}^{-1}$.

References.

1. O. Horie, G.K. Moortgat, *Chm. Phys. Lett.*, **156**, (1989),
2. H. Bandow, M. Okuda, H. Akimodo, *J. Phys. Chem.*, **84**, (1980),
3. C.A. Cantrell, J.A. Davidson, W.P.L. Carter, J.C. Calvert, *J. Geophys. Res.*, **91**, (1986), 5347.
4. J. Hjorth, F. Cappellani, C. Lohse, C. Nielsen, G. Restelli, H. Skov, Proceedings to the COST-EUROTRAC meeting "Mechanisms of gas phase and liquid phase chemical transformations in tropospheric chemistry", held in UEA, Norwich, England (1988).
5. A Mellouki, G. Le Bras, G. Poulet, *J. Phys. Chem.*, **92**, (1988), 2229.

KINETICS OF THE REACTION $\text{NO}_3 + \text{NO}_2 \rightarrow \text{N}_2\text{O}_5$

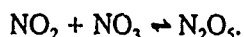
G.S. Tyndall, C.A. Cantrell, J.J. Orlando, R.E. Shetter and J.G. Calvert.

National Center For Atmospheric Research

Atmospheric Chemistry Division

P.O. Box 3000, Boulder, CO 80307, USA.

The chemistry of the nitrate radical, NO_3 , is important in determining the levels of active nitrogen in both the troposphere and the stratosphere. Through its equilibrium with NO_2 and N_2O_5 it controls the partitioning of NO_x species:



Measurements of NO_3 in the atmosphere have not been successfully reconciled with attempts to model its concentration, suggesting that some fundamental parameters are not known with sufficient accuracy.

We have used a discharge-flow system to measure the rate coefficient for the addition reaction with NO_2 from 236 to 355 K:



The kinetics of this reaction have never been measured at low temperature and low pressure. The rate coefficients derived have been combined with previous measurements made over a limited range of temperature.¹⁻³ The overall fit to the data is in good agreement with previous evaluations, but with a greatly reduced uncertainty on both the magnitude of the limiting low pressure rate coefficient, and its temperature dependence.

The rate coefficients can also be combined with new measurements from our laboratory on the thermal decomposition of N_2O_5 (C.A. Cantrell et al., Poster A10, this Symposium). This will provide a complete set of data on the fall-off characteristics of this reaction pair for use in atmospheric modeling, and place constraints on the equilibrium constant for this system.

References

- 1.) C.C. Kircher, J.J. Margitan and S.P. Sander, J. Phys. Chem., 88, 4370 (1984).
- 2.) A.E. Croce de Cobos, H. Hippler and J. Tropea, J. Phys. Chem., 88, 5083 (1984).
- 3.) C.A. Smith, A.R. Ravishankara and P.H. Wine, J. Phys. Chem., 89, 1423, (1985).

Kinetic Studies of OC10

J. F. Gleason, F. L. Nesbitt, and L. J. Stief

Laboratory for Extraterrestrial Physics,

NASA/Goddard Space Flight Center

Greenbelt, MD 20771, U.S.A.

The observation of elevated quantities of OC10 in the Antarctic stratosphere has renewed interest in the chemistry of this molecule. Although photolysis is expected to be the dominant loss process for OC10, potential chemical loss processes have not been thoroughly investigated. We will describe our recent experiments, using a discharge flow system with mass spectrometry/resonance fluorescence detection, on the reactions of OC10 with stratospherically important atoms and radicals.

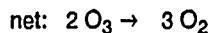
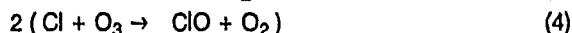
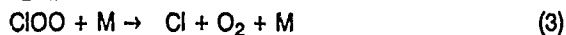
Kinetics and Spectroscopic Studies of ClO Radical Reactions Important in Polar Ozone Chemistry

by

A.D.Parr*, M.E.Jenkin and G.D.Hayman

The Harwell Laboratory, Didcot, Oxon, OX11 0RA

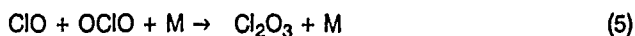
ClO and higher chlorine oxides such as ClOO, Cl₂O₂, OClO, play a major rôle in the destruction of stratospheric ozone observed over the Antarctic in recent years. It is now recognised that catalytic cycles involving ClO radicals, present in elevated concentrations in the dehydrated and denitrified conditions existing at these times, account for the ozone loss, eg:



Studies at the Harwell Laboratory have previously addressed aspects of this cycle: the UV spectroscopy, photochemistry and thermochemistry as well as the room temperature kinetics of the dimerisation reaction (1). The kinetics of this reaction are important as it is the rate-limiting step in the above cycle. The measurements have now been extended to lower temperatures (down to 200K) to define the rate parameter more precisely for atmospheric models.

The results of these studies and those obtained by other workers appear to agree at the lowest temperatures used but deviate significantly at room temperature. The origin of this discrepancy is not clear but may indicate the presence of a second dimer - a highly unstable asymmetric dimer, ClOClO. This hypothesis is currently being tested.

Elevated concentrations of OClO are also present in the polar stratospheres. An association reaction (5) between ClO and OClO has recently been observed in this laboratory and the UV spectrum of the adduct recorded.



The kinetics of the association reaction (5) have been the subject of recent work so that the importance of the adduct for polar ozone chemistry can be assessed.

* Present address: Physical Chemistry Laboratory, South Parks Road, Oxford, OX1 3QZ, UK.

ATMOSPHERIC CHEMISTRY OF BROMINE COMPOUNDS

A.R. Ravishankara

Aeronomy Laboratory, National Oceanic and Atmospheric Administration, 325
Broadway, Boulder CO 80303 USA

Bromine can destroy stratospheric ozone more efficiently than chlorine and its action is synergistic with that of chlorine because of the coupling between the ClO_x and BrO_x cycles. The reaction between ClO and BrO is believed to contribute significantly to the Antarctic ozone loss. BrO radical has been measured in the atmosphere at concentrations which are reasonably consistent with the known sources of bromine. A large fraction of the atmospheric bromine comes from the man-made halogenated compounds, such as those used in fire extinguishers. Therefore, understanding atmospheric bromine chemistry is of great current interest. The atmospheric chemistry of brominated methanes and ethanes and stratospheric chemistry of bromine are being investigated in our laboratory. The tropospheric studies include the reactions of OH with the brominated compounds, their absorption cross sections, and the quantum yields for the formation of Br in the photolysis of these compounds. The stratospheric studies deal with the reactions of BrO using a pulsed photolysis - time resolved diode array spectrometry. Some the recent results from these studies will be presented.

KINETICS OF THE GAS-PHASE REACTIONS OF A SERIES OF MONOTERPENES WITH O_3

Roger Atkinson, David Hasegawa and Sara M. Aschmann

Statewide Air Pollution Research Center, University of California,
Riverside, California 92521, U.S.A.

Rate constants for the gas-phase reactions of O_3 with a series of monoterpenes and related compounds have been determined at 296 ± 2 K and 740 Torr total pressure of air or O_2 using a combination of absolute and relative rate techniques. Good agreement between the absolute and relative rate data was observed, and the rate constants obtained (in units of 10^{-17} cm³ molecule⁻¹ s⁻¹) were: α -pinene, 8.7; β -pinene, 1.5; Δ^3 -carene, 3.8; 2-carene, 24; sabinene, 8.8; d-limonene, 21; γ -terpinene, 14; terpinolene, 140; α -phellandrene, 190; α -terpinene, 870; myrcene, 49; trans-ocimene, 56; p-cymene, <0.005; and 1,8-cineole, <0.015. While these rate constants for α - and β -pinene and sabinene are in good agreement with recent absolute and relative rate determinations, those for the other monoterpenes are generally lower than the literature data by factors of ~2-10. The measured rate constants for the monoterpenes are reasonably consistent with predictions based upon the number and positions of the substituent groups around the $>C=C<$ bond(s).

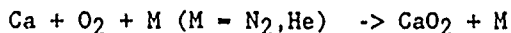
THE MYSTERY OF CALCIUM IN THE UPPER ATMOSPHERE

J.M.C. Plane and C.-F. Nien
 Rosenstiel School of Marine and Atmospheric Science
 Division of Marine and Atmospheric Chemistry
 4600 Rickenbacker Causeway
 Miami, Florida 33149-1098.

A number of metals - Na, K, Li, Ca and Fe - are known to be present as thin layers of free atoms at about 90 km in the atmosphere. Although the alkali atoms have been observed for many years, Ca was only first observed by the lidar technique in 1985. There is very strong evidence that the major source of these metals is meteoric ablation. Since Ca and Na have similar abundances in meteoritic minerals, the observation that the atomic Ca density in the mesosphere is lower than that of Na by a factor of 120 is extremely puzzling.

In order to understand this phenomenon, we have embarked on a series of studies of reactions of $\text{Ca}(^1\text{S})$ atoms and the calcium oxides. The reaction $\text{Ca}(^1\text{S}) + \text{N}_2\text{O}$ was studied over the temperature range 250 - 898 K.¹ Ca atoms were produced in an excess of N_2O and He bath gas by the pulsed 2-photon (193.3 nm) dissociation of CaI_2 , and then monitored by time-resolved laser induced fluorescence spectroscopy at $\lambda = 422.7$ nm ($\text{Ca}(^4\text{P}_1 - ^4\text{S})$). Above 500 K there is a clear upward curvature in the Arrhenius plot as shown in Figure 1, and the best description of the temperature dependence of the rate constant over the experimental temperature range is given by $k(T) = (2.43 \pm 0.29) \times 10^{-11} \exp[-(6.84 \pm 0.27) \text{ kJmol}^{-1}/RT] + (9.70 \pm 1.39) \times 10^{-10} \exp[-(24.58 \pm 1.09) \text{ kJmol}^{-1}/RT]$ $\text{cm}^3 \text{molecule}^{-1} \text{s}^{-1}$. This behaviour is explained by vibrationally excited N_2O enhancing the reaction at high temperatures. The 2-photon (193.3 nm) dissociation of CaO , produced by mixing a flow of Ca atoms and N_2O , is shown to yield $\text{Ca}(^1\text{P})$, and this process is then used to study the reaction $\text{CaO} + \text{O} \rightarrow \text{Ca} + \text{O}_2$, which proceeds at $(6 \pm 2) \times 10^{-10} \text{ cm}^3 \text{molecule}^{-1} \text{s}^{-1}$ at 805 K.

In addition, we have recently studied the reaction



from 215 - 1100 K, using both CaI_2 and Ca acetyl acetonate as Ca atom precursors. This is a special type of recombination reaction because $\text{Ca}(^1\text{S})$ is a *closed-shell* atom. Such reactions have been rarely studied, and the kinetics of this reaction exhibits an unusual temperature dependence, as shown in Figure 2. The slight positive temperature dependence below 400 K may be explained by a small barrier of about 8 kJmol^{-1} in the entrance channel of the triplet surface, probably at the avoided crossing between the covalent and the ionic diabats. The rate coefficients have been fitted to the following expressions (uncertainty of about 20% over the experimental temperature range):

$$k(\text{M}=\text{N}_2) = 2.26 \times 10^{-28} \cdot \exp(-1400/T) \cdot (T/300)^{-2.85} \text{ cm}^6 \text{molecule}^{-2} \text{s}^{-1}$$

$$k(\text{M}=\text{He}) = 1.01 \times 10^{-28} \cdot \exp(-1340/T) \cdot (T/300)^{-3.10} \text{ cm}^6 \text{molecule}^{-2} \text{s}^{-1}$$

The rates of these reactions are quite similar to the analogous Na reactions^{2,3} This accords with the observation that profiles of the Na and Ca layers measured simultaneously in the mesosphere are very similar, implying nearly identical atmospheric chemistries.⁴ Possible explanations for the missing atomic Ca will be explored.

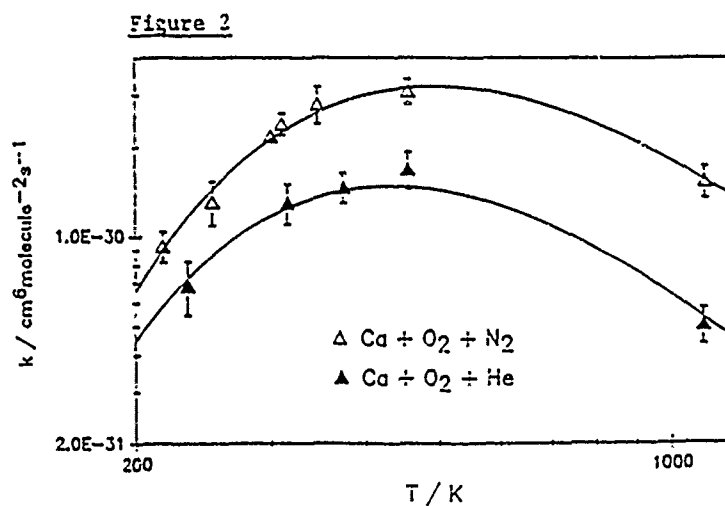
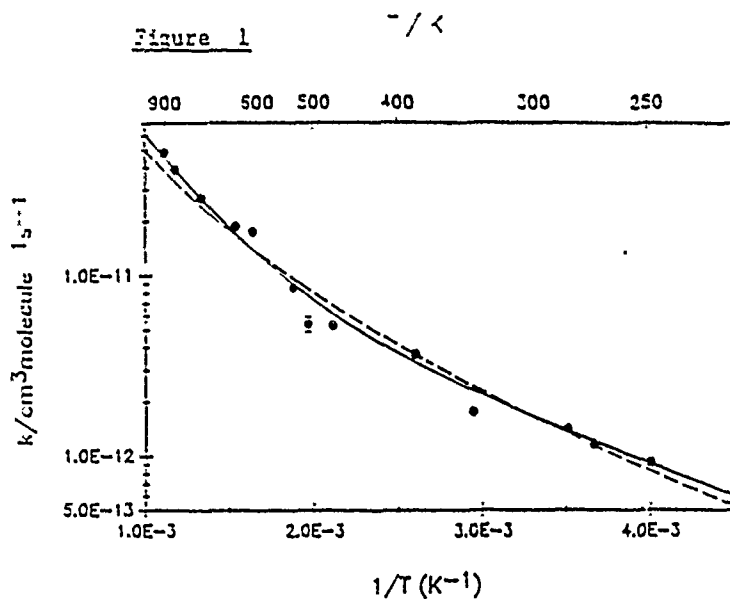


Figure 1 Arrhenius plot ($\ln(k)$ against $1/T$) over the temperature range 200 - 1000 K for the reaction $\text{Ca} + \text{N}_2\text{O}$. The broken line is a best fit through the experimental data of the functional form $A.T^{-n}.\exp(-B/T)$; the solid line is a best fit of the form $A.\exp(-B/T) + C.\exp(-D/T)$.

Figure 2 Plot of $\ln(k)$ against $\ln(T)$ for the reaction $\text{Ca} + \text{O}_2 + \text{M}$. The solid lines are the fitted expressions given above.

- 1 Plane, John M.C. and C.-F. Nien, *J. Phys. Chem.*, in press.
- 2 Plane, John M.C. and B. Rajasekhar, *J. Phys. Chem.*, (1989), **93**, 3135.
- 3 Plane, J.M.C. and D. Husain, *J. Chem. Soc., Faraday Trans. 2*, (1986), **82**, 2047.
- 4 Plane, J.M.C., *Int. Rev. Phys. Chem.*, in press.

KINETICS AND HO₂ PRODUCT YIELD OF THE REACTION C₂H₅O + O₂ BETWEEN 295 AND 411 K.

Jean-Pierre Sawerysyn*, Dietmar Hartmann**, Joachim Karthäuser**, Reinhardt Zellner***

* Laboratoire de Cinétique et Chimie de la Combustion. UA CNRS 876
Université de Lille I. 59655 Villeneuve d'Ascq. France

** Institut für Physikalische Chemie. Universität Göttingen 3400 Göttingen.
Federal Republic of Germany

*** Institut für Physikalische Chemie and Elektrochemie. Universität Hannover
3000 Hannover. Federal Republic of Germany.

Alkoxy radicals play an important role as intermediate species in the tropospheric photo-oxidation of hydrocarbons and in combustion. Under tropospheric conditions, the reactions of small alkoxy radicals with O₂ are preponderant by comparison with their isomerization and decomposition reactions [1]. In contrast of the reaction of methoxy radicals with O₂ which has been studied extensively, only two experimental studies [2,3] have been devoted to the reaction of ethoxy radicals with O₂, viz



In the present work we report measurements of k_1 between 295 and 411 K and HO₂ product yield for this reaction.

The rate coefficient k_1 has been directly determined using a combined Laser Photolysis/Laser Induced Fluorescence (LP/LIF) technique. Ethoxy radicals have been generated by the 248 nm (KrF exciplex) laser flash photolysis of ethyl nitrite in C₂H₅ONO/O₂ mixtures diluted in He. All experiments were performed at total pressures of 34 mbar under pseudo-first order conditions with O₂ in large excess. The reaction was primarily followed by monitoring the temporal decay of the fluorescence intensity of C₂H₅O radicals excited at 328.8 nm by the probe laser pulse. In order to determine the branching ratio for product HO₂ formation, experiments were performed in the presence of additional NO in concentration large enough to allow rapid conversion of HO₂ to OH. The time resolved profiles of OH were determined by quantitative LIF, then compared with computed OH profiles.

The results for k_1 at different temperatures are shown in fig.1 in Arrhenius form. From measurements in the range 295 to 411 K we obtain :

$$k_1 = (7.1 \pm 0.7) \cdot 10^{-14} [(-552 \pm 64) \text{K/T}] \text{ cm}^3/\text{s}$$

Product investigations using a chemical titration of HO₂ by NO and subsequent quantitative detection of OH by LIF indicate the dominance of the formation

channel with $\phi_{\text{HO}_2} = 0,89 \left(\begin{smallmatrix} + 0,22 \\ - 0,12 \end{smallmatrix} \right)$.

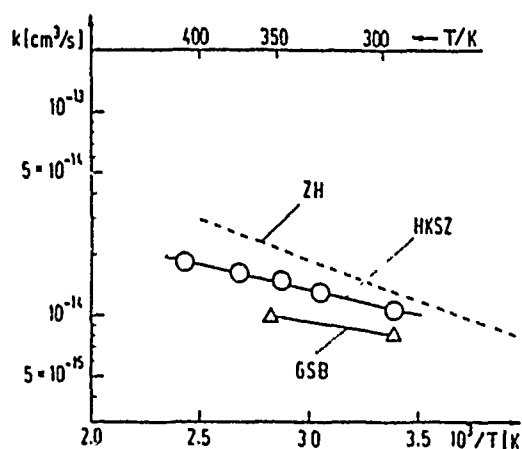


Fig.1 : Arrhenius representation of the rate coefficients for $\text{C}_2\text{H}_4\text{O} + \text{O}_2 \rightarrow \text{products}$.

GSB = Gutman et al (2)

ZH = Zabarnick, Heiklen (3)

HKSZ = this work (4)

References

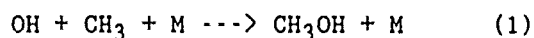
- 1 - R. Atkinson and A.C. Llyod. J. Phys. Chem. Ref. Data 13, 315, 1984
- 2 - D. Gutman, M. Sanders and J.E. Butler. J. Phys. Chem. 86, 66, 1982
- 3 - S. Zabarnick and J. Heiklen, J. Chem. Kinet. 17, 455, 1985
- 4 - D. Hartmann, J. Karthäuser, J-P. Sawerysyn, R. Zellner. Ber. Bunsenges Phys. Chem. 1990 in press.

Reaction between hydroxyl and methyl radicals at room temperatureC Anastasi⁺, T Ellermann⁺, P Pagsberg⁺ and S Pollak^{*}.

⁺ Department of Chemistry, Riso National Laboratory, DK-4000, Roskilde, Denmark.

^{*} Department of Chemistry, University of York, Heslington, York, YO1 5DD, England.

Radical-radical reactions play a very important role both in atmospheric and combustion chemistry. The reaction between methyl and hydroxyl radicals is of particular interest since it involves the reaction of a diatomic radical with an organic polyatomic species, a class of reactions rarely studied.



There have been several indirect measurements⁽¹⁾⁽²⁾ and a theoretical study⁽³⁾ of the rate constant for this reaction but no previous direct measurements have been reported.

Recently, we have used the pulse radiolysis kinetic absorption technique⁽⁴⁾ to obtain the first direct study of the reaction at room temperature and pressure. The CH_3 radical was monitored by its characteristic absorption at 216nm while the OH radical was monitored at 303nm. Computer modelling was employed to analyse the experimental decay curves and extract the required rate constant.

References

- (1) T W Sworski, C J Hochanadel and P Ogren, *J. Phys. Chem.*, **84** 19 (1980).
- (2) K A Bhaskaran, P Frank and Th Just, *Proc 12th Symp. on Shock Tubes and Waves*, The Magnes Press, 503 (1979).
- (3) A M Dean and P R Westmoreland, *Int. J. Chem. Kin.*, **19** 207 (1987).
- (4) P B Pagsberg, J Eriksen and H C Christensen, *J. Phys. Chem.*, **83** 582 (1979).

KINETIC STUDY OF N-PENTANE OXIDATION

A. CHAKIR, M. BELLIMAM, M.CATHONNET, J.C. BOETTNER and F. GAILLARD

*Centre de Recherches sur la Chimie de la Combustion
et des Hautes Températures - C.N.R.S
1C, Avenue de la Recherche Scientifique
45071 Orléans Cédex 2, France*

The oxidation of n-pentane has been studied in a jet stirred flow reactor at atmospheric pressure in the temperature range 900 - 1100K for a wide range of fuel - oxygen equivalence ratios (0.2 to 2). The initial n-pentane concentration is 0.2% to 0.3%, the diluent being nitrogen. The experimental procedure is similar to those used in previous studies¹. The major products determined by gas-chromatography were carbon monoxide, carbon dioxide, ethylene, propene, methane, 1-butene and ethane. The minor products were 1,3-butadiene, 1-pentene, 2-pentene and acetylene. In addition, some C₃, C₄ and C₅ olefins and diolefins were also found at trace level.

An earlier mechanism developed for the oxidation of 1-butene and n-butane was extended to include the oxidation and pyrolysis of C₅ chemical species. The resulting mechanism involves 479 reactions among 65 species. The model gives a good prediction of the measured concentrations of the molecular species in the entire experimental range (Fig.1).

Sensitivity and reaction path analysis studies were performed to identify the major reaction steps for n-pentane consumption and for the formation of the main products.

The main reactions consuming n-pentane are in lean mixtures H abstraction by OH radicals and in rich mixtures H abstraction by H atoms, methyl radicals and OH radicals. These reactions form 1, 2 and 3 - pentyl radicals which decompose to form the main hydrocarbon intermediates : ethylene, propene and 1-butene.

The same mechanism can correctly reproduce the jet stirred reactor data of Thornton et al.² (Fig. 2) and the ignition delays measured by Burcat et al.³ behind a in a shock tube (Fig. 3).

This work is supported by Groupement Scientifique Moteurs and Ministère de la Recherche et de la Technologie.

1. A. Chakir, M. Cathonnet, J.C. Boettner and F. Gaillard : Comb. Sci. Tech., 65, 207 (1989).
2. M.M. Thornton, P.C. Malte, W.J. Pitz and C.K. Westbrook : Comb. Flame, 72, 45 (1988).
3. A. Burcat, K. Scheller and A. Lifshitz : Comb. Flame, 16, 29 (1971).

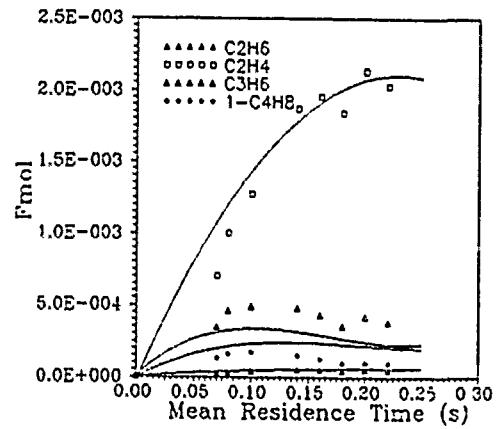
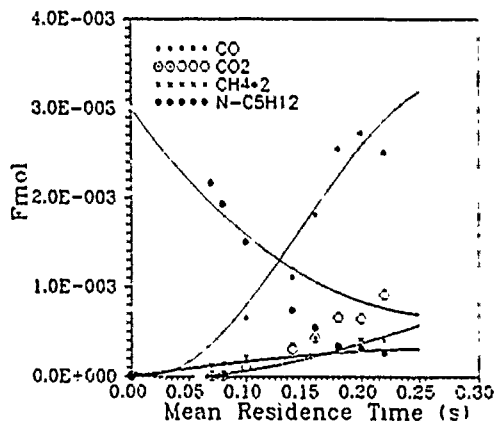


Figure 1 : Initial temperature = 980K ; Equivalence ratio = 0.5
Points : experiments ; Lines : computation

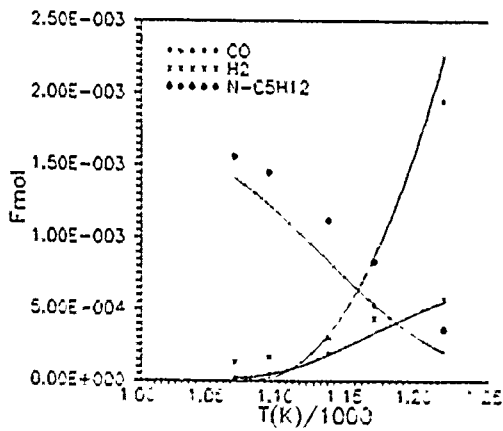


Figure 2 : Comparaision between computation (lines) and experiments of Ref. 2 (points).

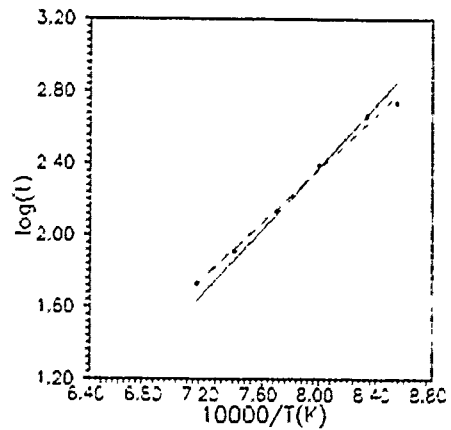


Figure 3 : Comparaision between computation (dashed line) and experiments of Ref. 3 (solid line).

Kinetic models of multi-channel reactions

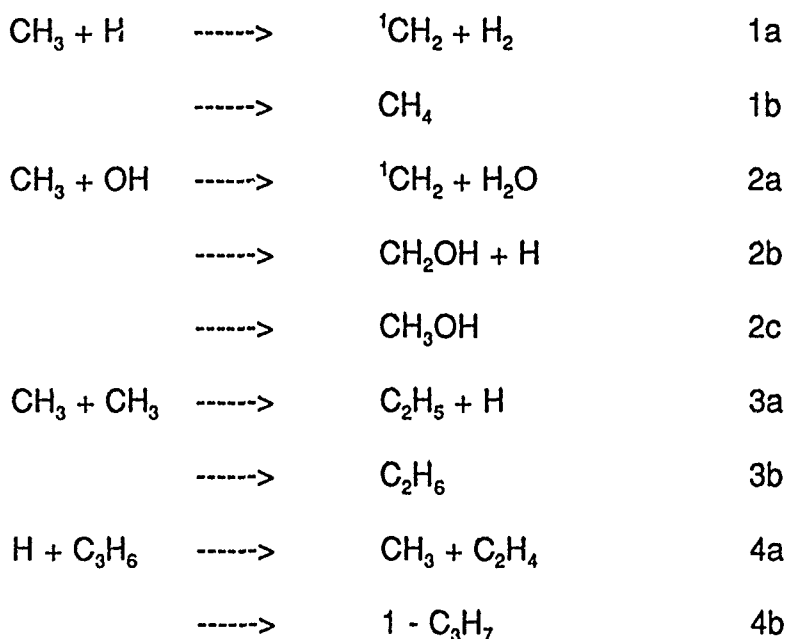
Nicholas J B Green, A Richard de A Pereira,
Michael J Pilling and Struan H Robertson.

Physical Chemistry Laboratory, South Parks Road,
Oxford, OX1 3QZ, United Kingdom

and

School of Chemistry, University of Leeds
Leeds, LS2 9JT

Several reactions of significance in combustion proceed through a stable intermediate, which can fragment to form radical products or can be collisionally stabilised. Examples include:-



Experimental data are fragmentary and often refer only to low temperatures. The problems of extrapolation to flame temperatures are compounded by the difficulty of constructing realistic models for association reactions proceeding on Type II potential energy surfaces (i.e. those without a potential barrier).

A realistic, yet easily implemented technique, preferably based on experimental measurements, is required to simulate the behaviour of these systems under the extreme conditions found in flames and detonations.

We have developed a technique based on a master equation analysis in which the single channel microcanonical rate coefficients for dissociation are generated by inverse Laplace transformation of the appropriate canonical association rate coefficient. The validity of the approach has been tested for a wide range of pressure conditions using model calculations on reaction 3b. The technique has been applied to reactions 1 - 4 and demonstrates the complex P,T behaviour that can result with channels of similar energy

SIMULATION OF THE COMBUSTION OF HYDROCARBONS AND OF
OXYGENATED COMPOUNDS UP TO C₂: LAMINAR FLAME STRUCTURES,
FLAME VELOCITIES, AND IGNITION PROCESSES.

C. Chevalier, U. Maas, J. Warnatz

Institut für Technische Verbrennung, Universität Stuttgart

Pfaffenwaldring 12, 7000 Stuttgart 80, W.Germany.

Using the kinetic values recommended by the CEC /1/, and recently developed mechanisms for iso-octane /2/ and H₂-O₂ /3/, a detailed mechanism describing the combustion of saturated and unsaturated hydrocarbons, alcohols, and aldehydes (360 reactions, 45 species) has been developed for temperatures above 1100 K .

For lean and rich mixtures, at pressures between 0.3 and 20 bar, a sufficient agreement with experimental results from the literature is observed, for ignition delay times, laminar burning velocities, as well as flame structures. One common mechanism is used to explain those phenomena. It has only been necessary to slightly vary the coefficients of some rate limiting reactions within experimental uncertainties. Particularly, the reaction $\text{CH}_3 + \text{OH} \rightarrow \text{CH}_3\text{O} + \text{H}$ and most of the reactions involving C₂H₃ (especially the decomposition into C₂H₂ + H) had to be reevaluated in detail.

/1/ Evaluation of kinetic data for combustion modelling.

Proposals of the 2nd CEC Comb. Program (D. BAULCH, Leeds).

/2/ C. ESSER, W.J. PITZ, J. WARNATZ, K.C. WESTBROOK, 22nd Int. Symp. Comb. pp. 893-901 (1988).

/3/ U. MAAS, J. WARNATZ, Comb & Flame 74, pp. 53-69 (1988).

KINETICS AND SPECTROSCOPY OF EXCITED SPECIES OBTAINED VIA DETONATION OF LEAD AZIDE

I. Bar, T. Ben-Porat, A. Ben-Tov, D. Heflinger, Y. Kaufman,
G. Miron, M. Sapir, Y. Tzuk and S. Rosenwaks

Department of Physics, Ben-Gurion University of the Negev,
Beer-Sheva, Israel.

Results of an ongoing research aimed at achieving preferential population, inversion and lasing in electronically excited species following the detonation of lead azide ($\text{Pb}(\text{N}_3)_2$) are presented. Studies of the spectroscopy, kinetics and hydrodynamics of the species produced in the gas phase during the first microseconds after the initiation are described. It is shown that population inversion is achieved in the $\text{Pb}(^3\text{P}_1^0 - ^1\text{D}_2)$ transition due to preferential energy transfer from electronically excited N_2 combined with the effect of self-trapping of the emission from the $^3\text{P}_1^0$ state to the $^3\text{P}_{2,1,0}$ states. Also, optical homogeneity of the medium is obtained by shining a pulsed laser beam through the medium following the detonation or by expanding the detonation products via a supersonic nozzle. The implications of the results are discussed in the context of the current approaches to short-wavelength chemical lasers.

COLLISION THEORY OF "FALL-OFF" IN RECOMBINATION REACTIONS.

Carl Nyeland, University of Copenhagen, Denmark.

By a treatment of three body interactions in recombination reactions following a random multiple collisions statistic, a formal theory of the "fall-off" behaviour is considered. A general "fall-off" function is obtained for the transition from third order reaction at low pressure to second order reaction at high pressure including redissociation and deactivation to final states. Comparisons are presented for results from the "fall-off" behaviour of the Lindemann type mechanism, and of the method of Troe et al. based on the RRKM theory, together with some recent experimental results at low and intermediate pressures.

Accurate Adiabatic Channel Calculations for SACM
Treatments

E. E. Nikitin and J. Troe

(Institute of Chemical Physics, Academy of Sciences,
Moscow, USSR and Institut für Physikalische Chemie,
Universität Göttingen, FRG)

Adiabatic channel potential curves for atom + linear molecule, atom + symmetric top and linear molecule + linear molecule collisions have been calculated including Coriolis effects, angular momentum couplings, symmetry rules and avoided channel crossings. The effects of the anisotropy of the potential energy surface on statistical adiabatic channel calculations of various rate processes are illustrated. Also, the extent of non-adiabatic dynamical effects at avoided channel crossings are estimated. The relevance of details of the potential energy surface for highly state-resolved processes and the decreasing importance of these details in highly averaged situations are illustrated.

Ab Initio Calculation of the OH ($X^2\Pi$, $A^2\Sigma^+$) + Ar Potential Energy Surfaces and Quantum Scattering Studies of Rotational Energy Transfer in the OH ($A^2\Sigma^+$) State

Alessandra Degli Esposti

Istituto di Spettroscopia Molecolare - C.N.R., Bologna (Italy)

and

Hans-Joachim Werner

Fakultät für Chemie - Universität Bielefeld (Federal Republic of Germany)

The potential energy surfaces of OH + Ar, which correlate asymptotically with OH($X^2\Pi$) + Ar($1S$) and OH($A^2\Sigma^+$) + Ar($1S$), have been calculated using the coupled electron pair approximation (CEPA) and a very large basis set. The OH-Ar van der Waals complex is found to be bound by about 100 cm^{-1} in the electronic ground state. In agreement with several recent experimental studies the first excited state is found to be much more stable. The A state potential energy surface has two minima at collinear geometries which correspond to isomeric OH-Ar and Ar-OH structures. The dissociation energies D_e are calculated to be 1100 cm^{-1} and 1000 cm^{-1} respectively; both forms are separated by a barrier of about 1000 cm^{-1} . The equilibrium distances for OH-Ar and Ar-OH are calculated to be 2.9 \AA and 2.2 \AA , respectively, relative to the center of mass of OH. In order to investigate the nature of the strong binding in the A state we have calculated accurate dipole and quadrupole moments as well as dipole and quadrupole polarizabilities for the X and A states of the OH radical and for the Ar atom. These data are used to estimate the contributions of induction and dispersion forces to the long-range OH-Ar potential. The calculated potential energy surfaces have been fitted to an analytical function and used in quantum scattering calculations for collision induced rotational energy transfer in the A state of OH. From the integral cross sections rate constants have been evaluated as a function of the temperature. The theoretical rate constants are considerably larger than the corresponding experimental values of Lengel and Crosley (J. Chem. Phys. 67, 2085 (1977)), but in good agreement with recent measurements of Jörg et al. (J. Chem. Phys., to be published). The

calculated rate constants at 300° K are listed in the table.

Table: Rate constants (in 10^{-11} cm³s⁻¹) for rotationally inelastic transitions in OH($A^2\Sigma^+$) in collisions with Ar at a temperature of 300° K.

Final state		Initial state											
		$N = 0$		$N = 1$		$N = 2$		$N = 3$		$N = 4$		$N = 5$	
		F_1	F_2	F_1	F_2	F_1	F_2	F_1	F_2	F_1	F_2	F_1	F_2
$N = 0$	F_1		7.07	6.93	1.64	1.62	0.72	0.71	0.32	0.32	0.06	0.06	
$N = 1$	F_2	6.00		6.76	5.06	2.05	1.22	0.89	0.50	0.63	0.25	0.17	
	F_1	11.78	13.50		4.81	7.72	1.90	2.18	1.23	1.08	0.37	0.44	
$N = 2$	F_2	2.03	7.32	3.47		6.98	1.61	2.31	1.30	0.90	0.19	0.20	
	F_1	3.00	4.45	8.37	10.37		3.70	5.93	1.41	1.79	0.29	0.29	
$N = 3$	F_2	0.82	1.64	1.28	4.28	2.22		6.65	3.58	2.70	1.29	0.70	
	F_1	1.08	1.59	1.96	2.85	4.89	8.80		3.67	4.52	0.96	1.55	
$N = 4$	F_2	0.26	0.46	0.57	0.84	0.61	2.50	1.70		7.92	1.39	1.31	
	F_1	0.32	0.73	0.63	0.72	0.96	2.34	2.95	9.87		1.67	1.71	
$N = 5$	F_2	0.03	0.13	0.10	0.07	0.07	0.50	0.28	0.78	0.70		9.77	
	F_1	0.03	0.11	0.14	0.09	0.08	0.33	0.54	0.88	0.92	11.69		
$N = 6$	F_2	0.02	0.00	0.01	0.06	0.04	0.01	0.01	0.34	0.16	0.37	0.22	
	F_1	0.02	0.01	0.01	0.04	0.06	0.01	0.02	0.17	0.36	0.25	0.41	

Theoretical study of the dynamics and the kinetics of the reaction



T. STOECKLIN, J. C. RAYEZ et B. DUGUAY

Laboratoire de Physicochimie Théorique URA 503 - CNRS

Université Bordeaux I - 33405 TALENCE Cedex

The determination of some points of the potential energy surfaces (PES) which play a role in this exothermic reaction ($\Delta E_0 = -3.82$ eV) by means of the *ab initio* MCSCF 6-31G** method leads to the following main conclusions :

- i) Only one PES of symmetry $^2A'$ is concerned.
- ii) No significant barrier occurs along the entrance valley.
- iii) This PES exhibits two wells. These two wells correspond to two bent intermediates CSH (angle CSH = 103°) and SCH (angle SCH = 129°). The CSH well is accessible directly by the reactants, but the SCH well is only accessible from the CSH well.
- iv) The minimum of the SCH well is 40 kcal/mole deeper than the minimum of the CSH well. The CSH well is separated from the products by a col of 0.7 eV above the minimum and is roughly at the same energy level as the products.
- v) An isomerisation col 1 eV above the minimum of the CSH well links these two wells.

An analytical description of this PES allows us to perform a study of the dynamics of this reaction at 300K using the Quasi Classical Trajectory (QCT) method. The important result of this QCT study is the appearance of a bimodal vibrational distribution of CS highly inverted around $\nu_{\text{CS}} = 22$ and less highly inverted around $\nu_{\text{CS}} = 10$. A detailed analysis shows that there are only two sets of reactive trajectories :

- i) the set T_1 (associated with the formation of highly vibrationally excited CS molecules) which corresponds to reactive trajectories passing through the CSH well only before going out towards the products and
- ii) the set T_2 (associated with more vibrationally relaxed CS molecules) which corresponds to reactive trajectories moving back and forth through both wells before going to the product valley.

The partition of the energy disposal (3.82 eV) is 64% (CS vibration), 4% (CS rotation) and 32% (relative recoil energy).

Moreover, this study allows us to propose a reasonable value of the rate constant of this reaction (without any barrier) at 300K : $k(300) = 3.1 \cdot 10^{-11} \text{ cm}^3/\text{molecule} \cdot \text{s}$.

Theoretical Studies of the Thermal Reaction Dynamics
of
 $\text{CH} + \text{H}_2 \rightleftharpoons \text{CH}_3 \rightleftharpoons \text{CH}_2 + \text{H}^a$

Albert F. Wagner, Mutsumi Aoyagi, and Ron Shepard
Theoretical Chemistry Group
Argonne National Laboratory, Argonne, IL 60439

Theoretical studies of the thermal reaction dynamics on the ground state potential energy surface of CH_3 will be reported. The reaction path on the potential energy surface connecting dissociation product asymptotes with the CH_3 minimum is being determined by *ab initio* electronic structure calculations involving a relatively large basis set and a relatively high degree of correlation. The calculations indicate: (1) no addition barrier to forming CH_3 from either the $\text{CH}+\text{H}_2$ or CH_2+H asymptotes; (2) an unusual reaction path for CH adding to H_2 where C follows the perpendicular bisector of H_2 but the CH and H_2 bond axes are *parallel* to each other (the "usual" C_{2v} insertion is energetically highly unfavorable); and (3) the $\text{CH}+\text{H}_2$ asymptote is lower in energy than the CH_2+H asymptote (in agreement with experimental thermodynamic estimates). Variational RRKM calculations on the calculated reaction path will be used to determine the temperature and pressure dependent thermal addition and dissociation rate constants. The calculated thermal addition rate constants from both asymptotes will be compared to available measurements. The thermal dissociation rate constants will also be determined, including the branching ratio between bond-fission and molecular elimination.

- a. Work performed under the auspices of the Office of Basic Energy Sciences, Division of Chemical Sciences, U.S. Department of Energy, under Contract W-31-109-Eng-38.

The submitted manuscript has been authored by a contractor of the U.S. Government under contract No. W-31-109-ENG-38. Accordingly, the U.S. Government retains a nonexclusive, royalty-free license to publish or reproduce the published form of this contribution, or allow others to do so, for U.S. Government purposes.

Theoretical to Experimental Rate Constant Comparisons for Two Isotopic Modifications of the Simplest Chemical Reaction, $H + H_2$.

by

Joel M. Bowman and Qiyan Sun, Department of Chemistry, Emory University, Atlanta, GA 30322, USA.

and

J. Robert Fisher and Joe V. Michael, Chemistry Division, Argonne National Laboratory, Argonne, IL 60439

ABSTRACT

Theoretical rate constants for two isotopic modifications of the simplest possible chemical reaction, $H + D_2 \rightarrow HD + D$ and $D + H_2 \rightarrow HD + H$, are presented. The basis of these new calculations is the accurate DMBE potential energy surface, and the rate constants are calculated with the CEQB method. With this new calculation it is now possible to judge the accuracy of the ab initio potential energy surface and to assess theoretical chemical kinetic methods since new experimental results have recently been obtained in the higher temperature regime by the Flash Photolysis-Shock Tube (FP-ST) technique. This technique combines reflected shock wave heating with flash photolysis of a suitable source molecule in order to produce a transient species (either H- or D-atoms in this case) that subsequently react with the added reactant. The transient atomic species are monitored by atomic resonance absorption spectroscopy (aras). These new results are combined with lower temperature results giving an experimental understanding of the rate behavior over a very large temperature range, ~200 to 2000 K, and the agreement between theory and experiment is outstanding over the entire temperature range.

This work was supported by the U. S. Department of Energy, Office of Basic Energy Sciences, Division of Chemical Sciences, under Contracts No. W-31-109-Eng-38 (Argonne National Laboratory) and No. DE-FG05-86ER13568 (Emory University).

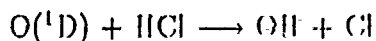
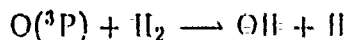
POTENTIAL ENERGY SURFACES FOR OXYGEN ATOM REACTIONS FROM THE HYPERSPHERICAL PERSPECTIVE.

V. Aquilanti, S. Cavalli, G. Grossi, V. Pellizzari, M. Rosi,
A. Sgamellotti and F. Tarantelli

Dipartimento di Chimica dell'Università, 06100 Perugia, Italy.

In the theory of elementary chemical reactions, the hyperspherical coordinate approach[1] is providing an important alternative to the more conventional treatments based on the reaction path concept both for the qualitative understanding of the dynamics from features of the potential energy surfaces and for the quantitative implementation of advanced quantum mechanical treatments. The description of potential energy surfaces directly in hyperspherical coordinates (the hyperradius r and the two angles Θ and Φ) allows to represent most accurately those features which are more relevant from an hyperspherical approach to the dynamics: these features include [2] *kinetic paths*, i.e. extremal points as a function of the hyperradius and can be distinguished as *valley bottom* lines and *ridge* lines.

Ab initio calculations of the potential energy surfaces have been performed for the following reactions:



Complete Active Space SCF (CASSCF) methods including analytic gradient calculations are found to be useful only for localizing the saddle point of the surface and the characteristics of the *valleys* of reactants and products. Multi-reference state configuration interaction calculations were subsequently performed on the saddle point, the reagents, and the products, in order to improve the determination of the barrier height and the exoergicity. Multi-reference configuration interaction calculations have been performed also along the kinetic paths; the results have shown that the energy dependence of valley bottoms and ridges as a function of the kinetic radius is essentially the same of that obtained at CASSCF level. These calculations, which include single and double excitations from the active orbitals, have been performed by using the direct-CI method. Davidson's correction was added to include the effect of unlinked clusters. All computations were performed by using vectorized program packages, implemented on IBM 3090 and CRAY YMP computers.

The results show that both reactions are essentially collinear. For the $\text{O} + \text{H}_2$ reaction [3,4] the information on the collinear configuration have been complemented by a characterization of the surface as the area angle Θ , varies around the values

corresponding to the collinearity. This essentially amounts to study the bending degree of freedom as it varies along the kinetic paths. For the O+HCl reaction the bending of the system give rise to $^1A'$ and $^1A''$ surfaces. Only the second one is relevant for the study of the above reaction, while the first one correlates with HOCl ground state.

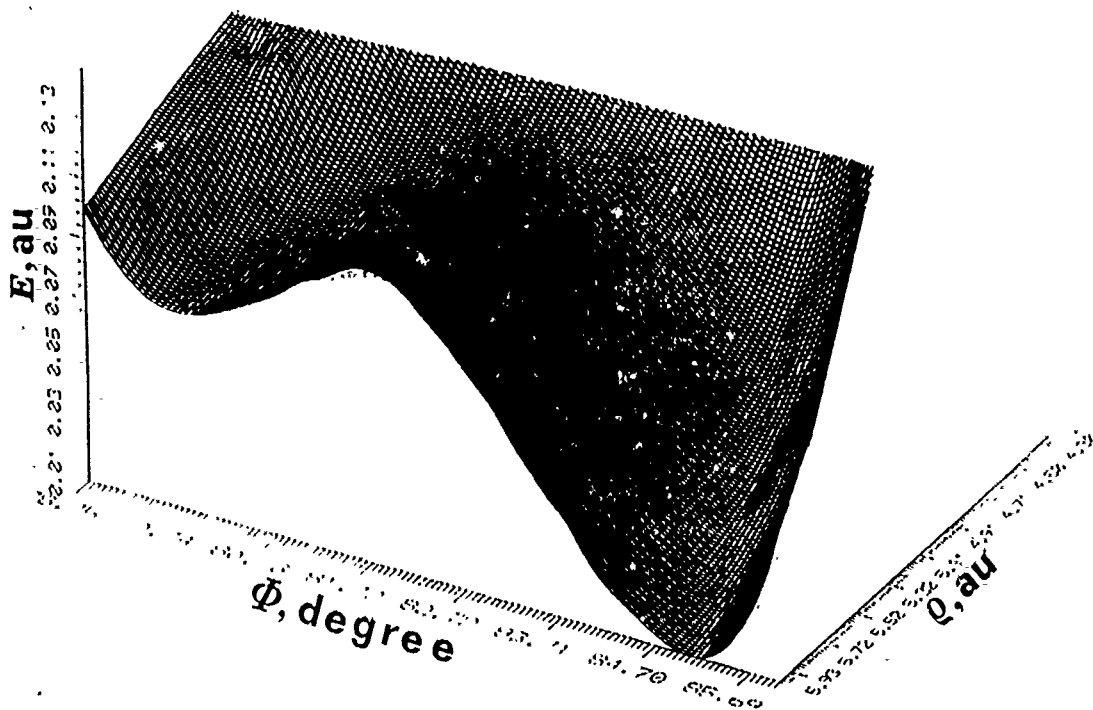


Fig.1 - Potential energy surface for $O(^1D) + HCl \rightarrow OH + Cl$ reaction as a function of the hyperradius ρ and the kinematic angle Φ for the collinear configuration ($\Theta=0$). The energy is measured from the $OH + Cl$ asymptote.

References

- [1] V. Aquilanti and S. Cavalli, *J. Chem. Phys.* **85** (1986) 1355; V. Aquilanti, S. Cavalli and G. Grossi, *J. Chem. Phys.*, **85** (1986) 1362.
- [2] V. Aquilanti and S. Cavalli, *Chem. Phys. Lett.*, **141** (1987) 309.
- [3] V. Aquilanti, S. Cavalli, G. Grossi, M. Rosi, A. Sgamellotti and F. Tarantelli, in *Supercomputer Algorithms for Reactivity, Dynamics and kinetics of Small Molecules*, A. Lagana Ed., Kluwer, Dordrecht 1989, pp. 95-104.
- [4] V. Aquilanti, S. Cavalli, G. Grossi, M. Rosi, V. Pellizzari, A. Sgamellotti and F. Tarantelli, *Chem. Phys. Lett.*, **162** (1989) 179.

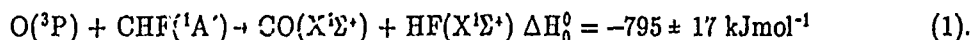
Time resolved FTIR studies of the O + CHF reaction

G. Hancock and D.E. Heard

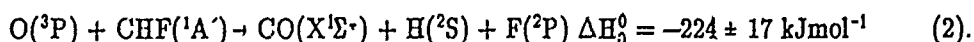
Physical Chemistry Laboratory, South Parks Road,

Oxford, OX1 3QZ, U.K.

Time resolved Fourier Transform Infrared (FTIR) emission spectroscopy has been used to observe the nascent $\text{CO}(\text{X}^1\Sigma^+)$ and $\text{HF}(\text{X}^1\Sigma^+)$ vibrational energy distributions in the reaction of ground state oxygen atoms (^3P) and $\text{CHF}(\text{A}')$ radicals. The radicals were generated by pulsed infrared multiple photon dissociation (IRMPD) of CH_2F_2 diluted in a flowing mixture of Ar and oxygen atoms, the latter produced in a microwave discharge. Time and wavenumber resolved emissions were observed in a variety of spectral regions, with the emission between $1800\text{--}4500\text{ cm}^{-1}$, shown in Fig. 1, easily identifiable as arising from the $\Delta\nu = -1$ fundamental bands of $\text{CO}(\text{near } 2000\text{ cm}^{-1})$ and $\text{HF}(\text{near } 4000\text{ cm}^{-1})$. HF emission appeared both in the absence and presence of O atoms, and was shown to originate from both vibrationally excited photofragments of the IRMPD of CH_2F_2 , and HF formed in the reaction



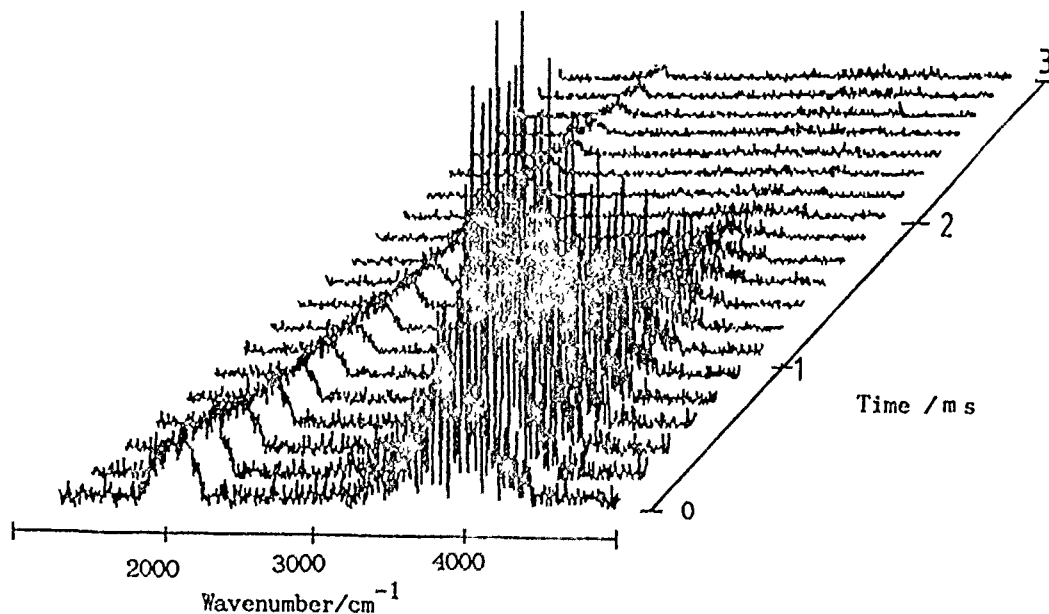
The nascent vibrational distributions in both these processes are listed in Table 1 and, for the reaction (1) are seen to be in good agreement with previous studies [1,2]. Vibrationally excited CO can be formed from process (1) and from the reaction



The nascent distribution was found to be a monotonically decreasing function of ν , and appears to be broadly similar to, but slightly hotter than, that obtained by laser absorption measurements at considerably higher reagent pressures [1]. Emission in the $6000\text{--}14000\text{ cm}^{-1}$ region was also observed, and attributed to d-a Triplet and a'-a Asundi band systems of CO, indicating that considerable internal excitation can reside in the CO product of the O + CHF reaction.

On addition of D_2 to reaction mixture, emission from vibrationally excited DF was observed with a nascent distribution indicating its formation from the $\text{F} + \text{D}_2$ reaction, with F atoms being produced by reaction (2). The branching ratio into the channels (1) and (2) will be reported, and comparisons of the HF + CO vibrational distributions will be made between the present results and those for the closely related $\text{F} + \text{HCO}$ reaction [3].

Three-dimensional representation of the time evolution of the infrared chemiluminescence spectra following the IRMPD of CH_2F_2 in the presence of O atoms. Conditions used were 28.5 mTorr CH_2F_2 , 12.0 mTorr O atoms, 5.09 Torr total pressure, unapodised FWHM resolution 6.04 cm^{-1} , Nyquist wavenumber 7901.4 cm^{-1} with the signal obtained for 1 shot per sampling point. The data were digitised at $30\text{ }\mu\text{s}$ resolution but are shown here with $150\text{ }\mu\text{s}$ between spectra and have been corrected for the instrument response function. Emission from two spectral regions with differing temporal behaviour is evident.



- [1] D.S. Hsu, R.G. Shortridge and M.C. Lin, Chem. Phys., 38, 285 (1979).
- [2]. D. Klenerman and I.W.M. Smith, J. Chem. Soc., Faraday Trans., 2, 83, 243 (1987).
- [3]. D.J. Donaldson and J.J. Sloan, J. Chem. Phys., 82, 1873 (1985).

Table 1

Nascent HF vibrational distributions

	$v = 1$	$v = 2$	$v = 3$
a) IRMPD of CH_2F_2	$0.72 \pm .05$	$0.20 \pm .05$	$0.08 \pm .02$
b) O + CHF reaction:			
This work	$0.58 \pm .05$	$0.30 \pm .02$	$0.12 \pm .04$
Ref. [1]	$0.50 \pm .02$	$0.38 \pm .02$	$0.13 \pm .03$
Ref. [2]	$0.59 \pm .06$	$0.23 \pm .03$	$0.18 \pm .02$

ABSOLUTE RATE CONSTANT MEASUREMENTS OF THE REACTION OF THE CF($X^2\Pi$) RADICAL WITH O₂, F₂, Cl₂ AND NO

J. Peeters, J. Van Hoeymissen and S. Vanhaelemeersch

Department of Chemistry, K.U. Leuven

Celestijnenlaan 200F, B-3030 Leuven, Belgium

Free fluorocarbon radicals are, besides their significance in atmospheric chemistry, of major importance in the chemistry of plasmas used for semiconductor etching in electronic device processing. Determination of the kinetic coefficients of the elementary reactions and elucidation of the mechanisms is a basic requirement to the quantitative understanding of plasma etching processes. In the present study, rate constants of the reactions of CF($X^2\Pi$, $v=0$) with O₂, F₂, Cl₂ and NO at $T = 294$ K and $p = 2$ to 10 torr (He or Ar bath gas) have been determined, using the LPD-LIF technique.

Ground state CF radicals were generated by photodissociation of CF₂Br₂ at 248 nm using a focussed KrF excimer laser. After a controlled delay, they are probed by a pulsed dye-laser, tuned to the P₁₁ band head of the $A^2\Sigma^+ - X^2\Pi$ (1,0) transition at 223.88 nm. The exponential decays of [CF] were recorded by monitoring the laser-induced fluorescence at increasing delay between the photolysis and probe laser pulses. Concentrations of coreactants – at least in a thousandfold excess over CF – ranged from 10^{14} to $3 \cdot 10^{16}$ molecules cm⁻³; in each case they were varied over about an order of magnitude. In all experiments, the decay at larger reaction times (where vibrational relaxation is complete) closely obeys an exponential law, usually over more than three 1/e-lifetimes. Pseudo first-order rate constants, k_{obs} , were derived from the slopes of plots of $\ln(\text{CF signal})$ versus reaction time, using a weighted least-square routine. For a series of experiments, the k_{obs} -values are plotted versus reactant concentrations to obtain the second order rate coefficients. Figure 1 shows a typical example of such a plot.

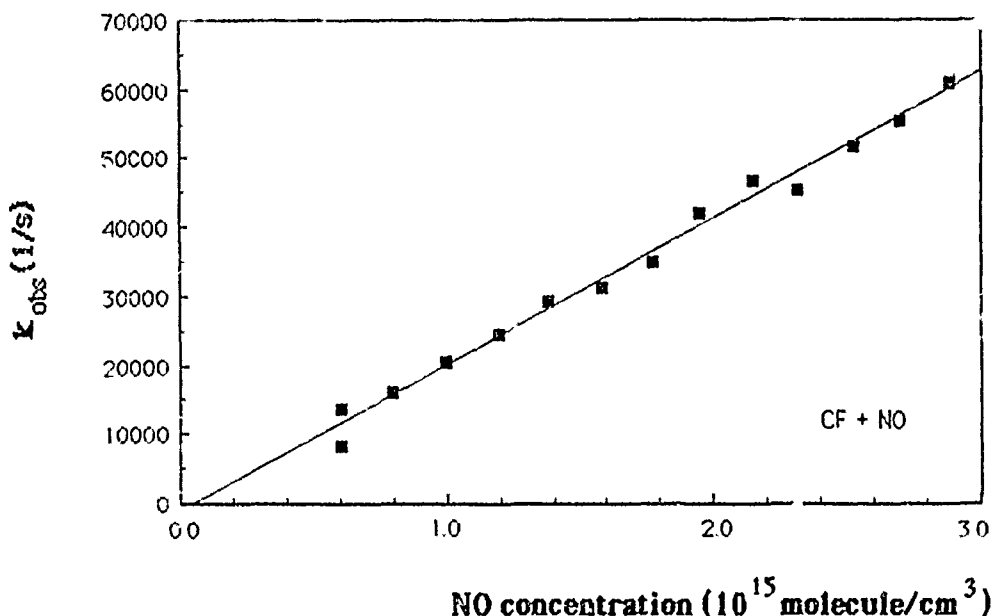


Figure 1. Pseudo first-order rate constants plotted versus $[NO]$ for the reaction of $CF + NO$, at a total pressure of 2 Torr and Ar as bath gas. The solid line is a weighted linear least squares fit.

The rate constant for each of the title reactions was found to be independent of pressure (2 to 10 torr range) and of the nature of the diluent gas : $k(O_2) = 1.6 \pm 0.15 \cdot 10^{-12}$; $k(F_2) = 3.9 \pm 0.4 \cdot 10^{-12}$; $k(Cl_2) = 1.7 \pm 0.2 \cdot 10^{-11}$ and $k(NO) = 2.1 \pm 0.2 \cdot 10^{-11} \text{ cm}^3 \text{ molecule}^{-1} \text{ s}^{-1}$.

Besides, an upper limit $k < 10^{-14}$ was established for the reactions of $CF(X)$ with H_2 , CH_4 , CF_4 , C_2H_2 and CO_2 .

All the investigated $CF(X)$ reactions are markedly slower than the $CH(X^2\Pi)$ analogues. The low reactivity of CF towards closed-shell molecules is explained in terms of the high stability of this species which in turn is ascribed to the high electronegativity of the fluorine atom causing a displacement of the carbon lone pair towards the C-F bond region. In regard to insertion processes, the effect can also be understood as a reduction of the availability of the lone pair for forming a new σ bond.

KINETICS OF THE REACTIONS OF POLYATOMIC RADICALS WITH MOLECULAR BROMINE IN THE GAS PHASE

Raimo Timonen*, Jorma Seetula*, and David Gutman*

* DEPARTMENT OF PHYSICAL CHEMISTRY. UNIVERSITY OF HELSINKI,
MERITULLINKATU 1C, SF-00170 HELSINKI, FINLAND

* DEPARTMENT OF CHEMISTRY, THE CATHOLIC UNIVERSITY OF AMERICA,
WASHINGTON D.C. 20064, U.S.A.

Kinetics of the reactions of molecular bromine with 14 different polyatomic carbon-centered free radicals have been studied over temperature ranges of 296-532 K. The free radicals were generated by the pulsed 193 or 248 nm photolysis of suitable precursors in a tubular flow reactor coupled to a photoionization mass spectrometer. For these measurements reactors were coated by halocarbon waxes or teflon. Most of these reactions have been studied previously in a boric acid coated reactor.¹ The apparatus has also been described previously.^{1,2} Kinetics of the reactions of alkyl radicals with molecular bromine has already been published.³

The total pressure in the reactor was typically 1 - 4 torr consisting of over 99 percent He (the collider gas) and molecular reactants in excess compared to radicals. Radical decay profiles were monitored as a function of concentrations of molecular reactants in real-time experiments to obtain the rate constants for the reactions. The rate constants were measured as a function of temperature to obtain Arrhenius parameters for these reactions.

Arrhenius rate constant parameters for the bromine reactions varied for $-\log(A/\text{cm}^3 \text{ molecule}^{-1} \text{ s}^{-1})$ from 10.6 to 12.5 and for $E_a/\text{kJ mole}^{-1}$ from -4 to 6. Our results are compared with the results of the other measurements. Also the measurements of the reactions of other halogens with free radicals and the correlation between the pre-exponential factors (A) of these reactions and ionization potentials of radicals will be discussed as well as the negative activation energy obtained for a considerable number of these fast reactions. The measured rate constants of the reactions are given in the following table.

TABLE: The Reactions of Free Radicals with Molecular Bromine

Radical	Rate constant
$t\text{-C}_4\text{H}_9$	$k = 2.0 \times 10^{-11} \exp(+4.1 \text{ kJ/mol /RT})$
$i\text{-C}_3\text{H}_7$	$k = 2.4 \times 10^{-11} \exp(+4.5 \text{ kJ/mol /RT})$
C_2H_5	$k = 2.6 \times 10^{-11} \exp(+3.4 \text{ kJ/mol /RT})$
CH_3	$k = 2.0 \times 10^{-11} \exp(+1.6 \text{ kJ/mol /RT})$
CH_2Cl	$k = 4.8 \times 10^{-12} \exp(+2.8 \text{ kJ/mol /RT})$
CHCl_2	$k = 9.8 \times 10^{-13} \exp(+1.6 \text{ kJ/mol /RT})$
CCl_3	$k = 3.0 \times 10^{-13} \exp(-6.0 \text{ kJ/mol /RT})$
CF_3	$k = 1.2 \times 10^{-12}$
CF_2Cl	$k = 1.3 \times 10^{-12} \exp(+0.5 \text{ kJ/mol /RT})$
CFCl_2	$k = 6.4 \times 10^{-13} \exp(+0.4 \text{ kJ/mol /RT})$
C_2H_3	$k = 4.0 \times 10^{-11} \exp(+2.4 \text{ kJ/mol /RT})$
C_3H_5	$k = 4.8 \times 10^{-12} \exp(+1.6 \text{ kJ/mol /RT})$
C_3H_3	$k = 2.8 \times 10^{-12} \exp(-2.3 \text{ kJ/mol /RT})$

The units of rate equations are $\text{cm}^3 \text{ molecule}^{-1} \text{ s}^{-1}$ and the reactions were studied from room temperature to 532 K (the temperature range for $\text{CF}_3 + \text{Br}_2$ was only from 296 K to 399 K). The error limits are typically ± 20 percent and exceptionally for $t\text{-C}_4\text{H}_9$, $i\text{-C}_3\text{H}_7$ and C_2H_5 radicals ± 30 percent. All reactions were studied in a halocarbon wax or a teflon coated reactor.

REFERENCES

1. R. Timonen, *Annales Academiae Scientiarum Fennicae Ser. A II. Chemica*, **218**, 1988.
2. R. Timonen and D. Gutman, *J. Phys. Chem.* **90**, 1986, 2987.
3. R. Timonen, J. Seetula, and D. Gutman, *J. Phys. Chem.* **94**, 1990, 3005.

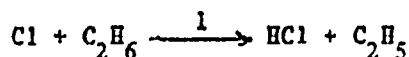
TEMPERATURE COEFFICIENTS OF THE RATES OF Cl ATOM REACTIONS WITH
 C_2H_6 , C_2H_5 , and C_2H_4 . THE RATES OF DISPROPORTIONATION AND
RECOMBINATION OF ETHYL RADICALS.

Otto Dobis* and Sidney W. Benson

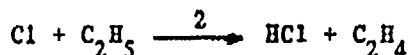
Distinguished Professor of Chemistry and
Scientific Co-Director, Emeritus
Loker Hydrocarbon Research Institute
University of Southern California
University Park
Los Angeles, California 90089-1661

*Technical University
H-1521 Budapest
HUNGARY

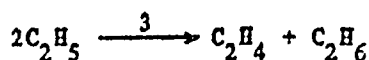
Using the Very Low Pressure Reactor (VLPR) with recent improvements we have been able to measure the following rate constants over the range 203-343°K:



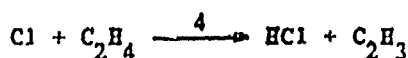
$$k_1 = (8.20 \pm 0.12) \times 10^{-11} \exp \{(-170 \pm 20)/RT\}$$



$$k_2 = (1.20 \pm 0.08) \times 10^{-11}$$



$$k_3 = (2.13 \pm 0.18) \times 10^{-12}$$



$$k_4 = (1.15 \pm 0.13) \times 10^{-10} \exp \{(-3200 \pm 140)/RT\}$$

All rate constants are in units of $\text{cm}^3/\text{molecule}\cdot\text{sec}$ and energies are in cal/mole. Reactions 2 and 3 have no observable temperature dependence over the range measured.

Combining k_3 with the experimentally measured value of the ratio of recombination to disproportionation of 0.14 ± 0.01 , also independent of temperature, yields for the rate of recombination of ethyl radicals:

$$k_r = (1.81 \pm 0.23) \times 10^{-11}$$

Combining the values of k_4 with the previously measured values of the equilibrium constant K_4 and 3rd Law corrected values of ΔH_4 and ΔS_4 gives for the back reaction:

$$k_{-4} = (9.5 \pm 0.3) \times 10^{-13} \exp \{(-200 \pm 200)/RT\}$$

and hence $\text{DH}_{298}^{\circ}(\text{C}_2\text{H}_3\text{-H}) = 106.0 \pm 0.3 \text{ kcal/mole}$.

Specific Rate Constants for Unimolecular Reactions of
Vibrationally Highly Excited Large Polyatomic Molecules
from Bulk and Molecular Beam Experiments.

M.Damm, F.Deckert, R.Fröchtenicht*, H.Hippler, and P.J.Toennies*,
Institut für Physikalische Chemie der Universität Göttingen,
Tammannstr.6, D-3400 Göttingen

* Max-Planck-Institut für Stömungsforschung,
Bunsenstraße 10, D-3400 Göttingen

Specific rate constants $k(E)$ for unimolecular reactions of vibrationally highly excited polyatomic molecules are of particular interest for a prediction of thermal rate constants under pyrolysis and combustion conditions. For this purpose the exact knowledge of $k(E)$ for a large domaine of internal excitation energies is essential. This is especially true when reaction threshold energies are not known with sufficient precision. In bulk experiments specific life-times ($\tau = k(E)^{-1}$) of excited molecules can only be observed when they are greater than the pulse-length of the excitation laser (≈ 20 ns for excimer lasers) and shorter than the diffusion time of the reacting molecules out of the observation volume (typically $\approx 20\mu\text{s}$). Three orders of magnitude for the specific rate constants are accessible which represents only a small part of the interesting range of excitation energies. Lifetimes up to about 10 ms can be detected by performing experiments in a molecular beam. Combining both techniques a rang of 6 orders of magnitude for $k(E)$ can be covered which allows for a reasonably well characterization of the energy dependence of the reaction dynamics.

Vibrationally highly excited azulene molecules in the electronic ground state have been prepared by UV-laser absorption followed by fast internal conversion. 193 nm radiation from an ArF excimer laser has been used in bulk experiments and 351 nm from an Ar⁺-laser in the molecular beam experiments. The measured specific rate constants for the isomerisation of azulene to naphtalene are $k(E) \approx 5 \cdot 10^5 \text{ s}^{-1}$ and $\approx 6 \cdot 10^2 \text{ s}^{-1}$ for excitation energies of $\langle E \rangle_{\text{ac}} = 52700 \text{ cm}^{-1}$ and 33000 cm^{-1} , respectively. These rate constants are directly compared with results from RRKM theory using parameters obtained from fitting thermal isomerisation rate constants from shock-wave experiments.

TIME-RESOLVED KINETIC STUDIES OF THE REACTIONS
OF GAS-PHASE METHYLSILYLENE

by H M Frey, B Mason, R Walsh and I M Watts,
Department of Chemistry, University of Reading, Whiteknights,
Reading RG6 2AD, U.K.

This paper will describe new measurements of rates of reaction of methylsilylene, MeSiH using the method of time-resolved laser flash photolysis. MeSiH , detected directly for the first time, is monitored via its $\tilde{X} \rightarrow \tilde{A}$ absorption at 458 nm. Si-H insertion rate constants for reactions with the various methylsilanes will be compared with those of SiH_2 and SiMe_2 . Temperature dependence studies are underway and we hope to be able to report the values of activation energies at the meeting. These studies provide further insight into the nature of the silylene insertion process.

High Resolution Measurements of Integral Cross Sections for Ion-Molecule Reactions as a Function of the Collision Energy.

P. Tosi, F. Boldo, F. Eccher, M. Filippi and D. Bassi

Dipartimento di Fisica e Unità INFM di Trento

Università degli Studi di Trento

I-38050 Povo, Italy

In recent years a major experimental effort has been made in the attempt to study ion-molecule reactions at very low energies.

Among the different techniques, beam experiments are particularly interesting because they permit to study the single collision and to measure directly the reactive cross section for each channel. This is usually done allowing a mass and energy selected beam to react with neutral molecules in a reaction cell. All ionic products are then collected and analyzed.

Unfortunately the applications of beam techniques at energies below a few eV is limited by severe experimental difficulties.

A powerful approach for dealing with low-energy ion beams is based on the use of radio-frequency octopole guides. They consist of eight parallel rods connected to opposite phases of a r.f. oscillator. The effect of the r.f. field is to confine ions in the transverse direction [1]. Octopoles are ideal for integral cross-section measurements because of the high efficiency in guiding low-energy primary ions and in collecting scattered ions. Guided ion beam tandem mass spectrometers have allowed measurements of integral reactive cross-sections down to a nominal collision energy of 5 meV [2].

Unfortunately, because of the fact that the observed cross-section is actually the convolution of the true cross-section with the relative energy distribution of the reactants, at very low energies the thermal motion of the target gas obscures the behaviour of the true cross-section. As noted by Armentrout [2] the observed cross-section tends toward $\sigma_{eff} \propto E^{-0.5}$ as $E \rightarrow 0$ regardless of the low energy behaviour of the true cross-section. In other words for nominal collision energies $E \ll K_B T$, where T is the scattering cell temperature, because of the Doppler broadening, beam-cell experiments will always yield a cross-section which behaves as $E^{-0.5}$. For energies comparable with $K_B T$ (let's say energies below ≈ 100 meV) the Doppler broadening hides any sharp features of the cross-section. As an example at a nominal collision energy of 50 meV a beam-cell measurement has an energy spread characterized by a FWHM of about 130 meV [2].

This problem may be overcome replacing the static reaction cell with a kinematically well defined beam of reactant molecules in such a way to reduce Doppler broadening effects. The main problem of this approach is the much lower density of molecules in a beam with respect to a static cell. A partial solution is to use a pulsed neutral beam that is much more intense

of a continuous beam [3]. Because of the fact that the kinetic energy of the neutral beam is of the order of a few $K_B T_0$, the temperature of the source T_0 will set the kinetic energy of the neutral beam. For this reason very low energies can be reached only by cooled beams. Unfortunately the temperature of a pulsed source cannot be precisely controlled. Therefore in our apparatus we use a continuous supersonic beam which, although less intense than a pulsed beam, can be easily cooled down to liquid nitrogen temperature. The price paid in terms of intensity is compensated by the possibility to reach a lower collision energy.

The cooled beam is crossed at the center of an octopole guide with an ion beam. This crossed beams configuration enable us to reach a much better energy resolution with respect to experiments using a room-temperature scattering cell and to investigate the detailed structure of the integral reactive cross-section as a function of the collision energy [4].

In particular we will present some new measurements on the reaction $Ar^+ + H_2 \rightarrow ArH^+ + H$ and its isotopic variant $Ar^+ + D_2 \rightarrow ArD^+ + D$. These results show the importance of both spin-orbit and non-adiabatic effects in these systems.

References

- [1] P.Tosi, G.Fontana, S.Longano and D.Bassi, Int. J. Mass Spectr. and Ion Processes, 93 (1989) 95.
- [2] K.M.Ervin and P.B.Armentrout, J. Chem. Phys. 83 (1985) 166.
- [3] D.Gerlich, R.Disch, S.Scherbart, J. Chem. Phys. 87 (1987) 350 .
- [4] P.Tosi, F.Boldo, F.Eccher, M.Filippi and D.Bassi, Chem. Phys. Letters 164 (1989) 471.

Kinetic Investigation of the Pressure and Temperature Dependence of the Reactions of $\text{CH}(\text{X}^2\Pi)$ Radicals with N_2O and H_2

K.H. Becker, B. Engelhardt, R. Kurtenbach and P. Wiesen

Physikalische Chemie / Fachbereich 9

Bergische Universität - Gesamthochschule Wuppertal

Postfach 100127, D-5600 Wuppertal 1, FRG

The reactions of $\text{CH}(\text{X}^2\Pi)$ radicals with N_2O and H_2 were measured under pseudo-first-order conditions at different total pressures and temperatures.

$\text{CH}(\text{X}^2\Pi)$ radicals, which are of great importance in hydrocarbon combustion, planetary atmospheres and interstellar clouds, were generated by 248 nm photolysis of $\text{CHClBr}_2/\text{Ar}$ mixtures under slow flow conditions and detected by laser induced fluorescence. Kinetic measurements were carried out by following the relative CH concentration from the integrated intensity of the Q-branch of the $\text{A}^2\Delta \longrightarrow \text{X}^2\Pi$ (0,0) transition at 431.5 nm while varying the time delay between the photolysis and the probe dye laser.

$\text{CH} + \text{N}_2\text{O}$:

The reaction of $\text{CH}(\text{X}^2\Pi)$ with N_2O was found to be pressure independent. From the temperature dependence of the rate constant in the range 200 - 485 K, the following Arrhenius expression was derived, $k_{\text{CH}+\text{N}_2\text{O}} = (4.0 \pm 0.6) \cdot 10^{-11} \cdot \exp[(1.6 \pm 0.3)/RT] \text{ cm}^3\text{s}^{-1}$, with E_a in units of $\text{kJ}\cdot\text{mole}^{-1}$.

MNDO calculations show that the reaction, which has several accessible exothermic reaction routes, proceeds via an insertion-addition mechanism similar to the reaction of CH radicals with unsaturated hydrocarbons leading to the formation of N_2 and HCO or in the formation of N_2 , H atoms and CO.

$\text{CH} + \text{H}_2$:

The reaction $\text{CH}(\text{X}^2\Pi) + \text{H}_2$ was studied as a function of temperature in the range 200 - 400 K at 4 Torr total pressure and as a function of total pressure in the range 2 - 591 Torr at 298 K. The reaction proceeds via a vibrationally excited $\text{CH}_3^\#$ adduct resulting in two product channels. Under our experimental conditions, an abstraction channel leading to the formation of $\text{CH}_2 + \text{H}$ dominates the reaction above 300 K with an activation energy of

$(13.82 \pm 4.19) \text{ kJ}\cdot\text{mole}^{-1}$, whereas below 300 K the formation of the CH_3 adduct becomes more important. In the temperature range below 300 K the rate constants exhibit a negative temperature dependence with an activation energy of $(-6.12 \pm 1.93) \text{ kJ}\cdot\text{mole}^{-1}$ consistent with an addition followed by collisional stabilization of the adduct.

The addition channel led to a pressure dependent rate constant which was investigated in the pressure range 2- 591 Torr. A fit of the rate constants to Troe's semiempirical equation yielded limiting rate constants $k_0 = (9.0 \pm 3.0) \cdot 10^{-30} \text{ cm}^6 \cdot \text{s}^{-1}$ and $k_\infty = (7.3 \pm 2.0) \cdot 10^{-11} \text{ cm}^3 \cdot \text{s}^{-1}$ and a broadening factor $F_C = (0.85 \pm 0.10)$.

A RRKM-TST model based on the reaction mechanism provided good agreement with the observed pressure and temperature dependences.

A Flash Photolysis Study of the UV Spectra and Self-recombination Reactions of CH₂Cl and CHCl₂

P.D. Lightfoot, P. Roussel, F. Caralp, V. Catolre and R. Lesclaux

Laboratoire de Photophysique et Photochimie Moléculaire,
Université de Bordeaux I,
33405 TALENCE Cedex, FRANCE.

The recombination reactions:



and



have been studied using flash photolysis and UV absorption spectroscopy, from 273 to 686 K and from 30 to 760 Torr N₂ total pressure. The radicals were generated by the flash photolysis of Cl₂/(CH₃Cl or CH₂Cl₂)/N₂ mixtures. Both radicals display strong UV absorption spectra in the region 190-230 nm, with peak absorption cross-sections of $\sigma(\text{CH}_2\text{Cl}, 200 \text{ nm})/\text{cm}^2 \text{ molecule}^{-1} = 1.56 \times 10^{-17}$ and $\sigma(\text{CHCl}_2, 215 \text{ nm})/\text{cm}^2 \text{ molecule}^{-1} = 1.53 \times 10^{-17}$, measured relative to that of CH₃O₂ at 240 nm¹. Although some fall-off is evident (maximum 20%) at temperatures above 500 K, the two reactions are essentially at their high pressure limits under most of our experimental conditions, as confirmed by RRKM calculations. Weighted fits to the data give $k_1^\infty/\text{cm}^3 \text{ molecule}^{-1} \text{ s}^{-1} = (3.17 \pm 0.14) \times 10^{-11} (T/298)^{-(0.78 \pm 0.12)}$ and $k_2^\infty/\text{cm}^3 \text{ molecule}^{-1} \text{ s}^{-1} = (1.05 \pm 0.04) \times 10^{-11} (T/298)^{-(0.72 \pm 0.08)}$. Errors are 1 σ . The self-recombination reactions for the series CH₃², CH₂Cl, CHCl₂ and CCl₃³ all display a negative temperature dependence of the limiting high pressure rate constant. The difficulty of modelling such behaviour within the framework of existing statistical theories of reaction rate constants will be discussed.

1. P.D. Lightfoot, R. Lesclaux and B. Veyret, *J. Phys. Chem.*, **94**, 708 (1990).
2. I.R. Slagle, D. Gutman, J.W. Davies and M.J. Pilling, *J. Phys. Chem.*, **92**, 2455, (1988).
3. F. Danis, F. Caralp, B. Veyret, H. Lolrat and R. Lesclaux, *Int. J. Chem. Kin.*, **21**, 715 (1989).

Figure 1.
CH₂Cl and CHCl₂ Spectra

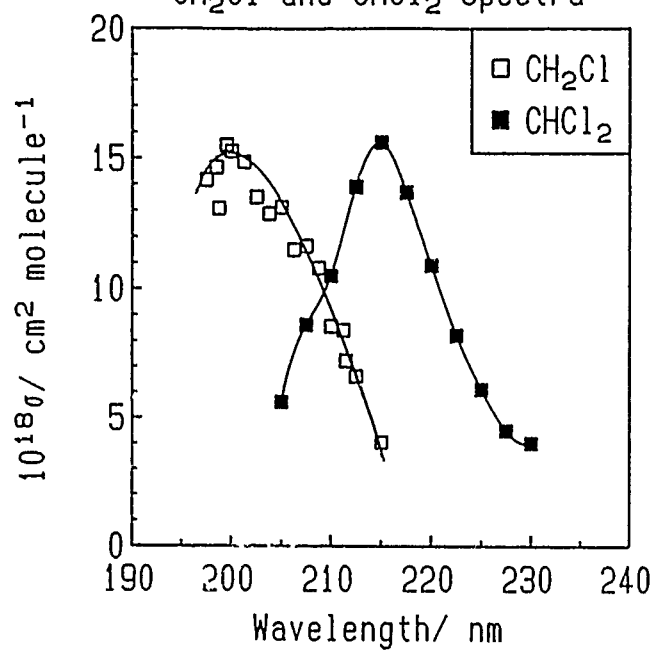
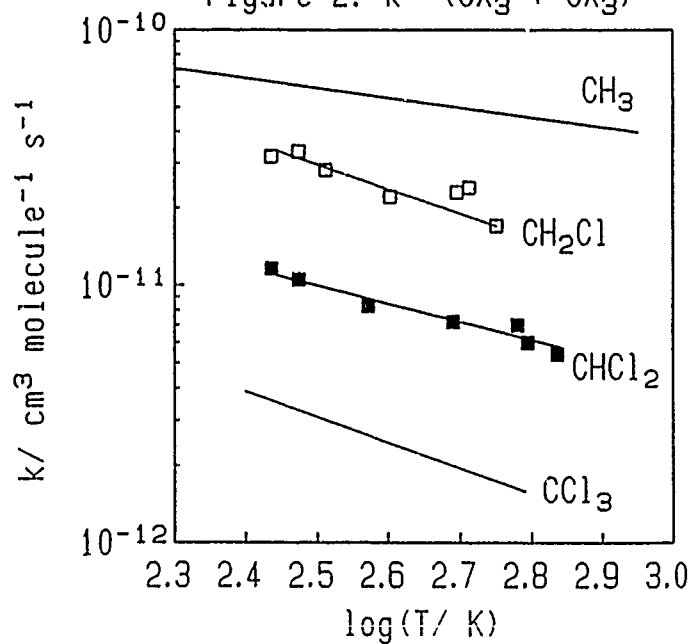


Figure 2. k° (CX₃ + CX₃)



Experimental probability distributions of collisional energy transfer from highly vibrationally excited azulene and toluene.

U. Hold, K. Luther, and A. Symonds

Institut für Physikalische Chemie der Universität Göttingen,
Tammannstraße 6, D-3400 Göttingen, West Germany

Detailed energy transfer parameters of collisional activation and deactivation of vibrationally hot polyatomics - a key process in the course of many chemical reactions - can now be determined in direct experiments (1).

We report our recent results of such experiments with azulene and toluene. The molecules are prepared by laser excitation, followed by fast internal conversion into the electronic ground state. The "kinetically controlled selective ionization" method (KCSI) is used for energy selective detection of vibrationally excited molecules during collisional deactivation. Pump and probe type experiments at several observation energies and for various colliders provide a sensitive picture of the ongoing collisional relaxation. Approximate values and main characteristics of important energy transfer parameters can be deduced very simply. A full master equation analysis of the observed time evolution of molecular energy distributions during the relaxation of a sample even allows to derive the energy dependent transition probability distributions of collisional energy transfer in the high density of states regime. The results for azulene and toluene are compared and discussed with respect to aspects like the magnitudes and energy dependences of the moments $\langle \Delta E \rangle(E)$ and $\langle \Delta E^2 \rangle(E)$ and the relative contributions of observed "strong" collisions.

- (1) H. G. Löhmannsröben and K. Luther, Chem. Phys. Lett. 144, 473 (1988); K. Luther and K. Reihs, Ber. Bunsenges. Phys. Chem. 92, 442 (1988); K. Luther, K. Reihs, and A. Symonds, J. Chem. Phys., to be published.

KINETICS AND MECHANISM OF ACETONITRILE OXIDATION UNDER ATMOSPHERIC CONDITIONS

A.J.Hynes and P.H.Wine

Molecular Sciences Branch, Georgia Tech Research Institute,
Georgia Institute of Technology, Atlanta, Georgia 30332.

The pulsed laser photolysis- pulsed laser induced fluorescence technique has been used to determine absolute rate coefficients for the reaction $\text{OH} + \text{CH}_3\text{CN}$ (1) and its isotopic variants, $\text{OH} + \text{CD}_3\text{CN}$ (2), $\text{OD} + \text{CH}_3\text{CN}$ (3) and $\text{OD} + \text{CD}_3\text{CN}$ (4). Reactions (1) and (2) were studied as a function of pressure and temperature in N_2 , N_2/O_2 , He and Ar buffer gases. In the absence of O_2 , the rate of reaction (1) was found to be independent of pressure over the range 50-700 Torr and well described by the Arrhenius expression $k_1(T) = (1.1 \pm 0.4) \times 10^{12} \exp(-1135 \pm 94 / T) \text{ cm}^3 \text{ molecule}^{-1} \text{ s}^{-1}$. Reaction (2) showed a significant pressure dependence increasing from (1.18 ± 0.11) to $(2.10 \pm 0.10) \times 10^{14} \text{ cm}^3 \text{ molecule}^{-1} \text{ s}^{-1}$ over the pressure range 50-700 Torr of N_2 at 298K. Data at pressures >600 Torr which appear to be at, or close to the high pressure limit give $k_2(T) = (9.4 \pm 5.0) \times 10^{13} \exp(-1181 \pm 250 / T) \text{ cm}^3 \text{ molecule}^{-1} \text{ s}^{-1}$. The rates of reactions (3) and (4) were independent of pressure over the range 50-700 Torr of N_2 with 298K rate coefficients given by $k_3 = (3.10 \pm 0.36) \times 10^{14} \text{ cm}^3 \text{ molecule}^{-1} \text{ s}^{-1}$ and $k_4 = (2.20 \pm 0.30) \times 10^{14} \text{ cm}^3 \text{ molecule}^{-1} \text{ s}^{-1}$.

In the presence of O_2 each reaction showed non-exponential behavior and/or an apparent decrease in the observed rate constant indicating the presence of significant OH or OD regeneration. Observation of regeneration of OH in (2) and OD in (3) provide almost conclusive evidence of a reaction channel which proceeds via addition followed by reaction of the adduct, or one of its decomposition products, with O_2 . The observed OH and OD decay profiles have been modelled using a simple mechanistic scheme to extract branching ratios and rate coefficients for the adduct reaction with O_2 .

THE TEMPERATURE DEPENDENCE OF THE OVERALL REACTION $\text{CH}_3\text{O} + \text{H}$ AND THE RATES OF PRODUCT FORMATION

T.Bérces, S.Dóbbé and I.Szilágyi

Central Research Institute for Chemistry
 Hungarian Academy of Sciences
 Budapest, Hungary

The overall reaction between methoxy radical and hydrogen atom has been studied in an isothermal fast flow reactor under pseudo first order conditions using hydrogen atom excess. Hydrogen atoms were produced by microwave discharge and the absolute H-atom concentration was obtained from titration with NO_2 . Different CH_3O sources were used in order to check the reliability of the results. Reaction $\text{F} + \text{CH}_3\text{OH}$ and reaction $\text{CH}_3 + \text{NO}_2$ as methoxy sources gave practically the same results. Methoxy radical concentration was monitored by LIF using either 292.6 nm or 298.0 nm excitation wavelengths. The overall rate coefficient for the $\text{CH}_3\text{O} + \text{H}$ reaction, extracted from the slope of the plot of pseudo first order rate constant against hydrogen atom concentration, was found to be temperature independent as shown in Fig. 1. In the 298-490 K temperature range a value of $k(\text{overall}) = (3.8 \pm 1.1) \times 10^{-11} \text{ cm}^3 \text{ molec.}^{-1} \text{ s}^{-1}$ is suggested. This value agrees very well with the room temperature rate coefficient determined by Hoyerman et al. using a flow discharge-mass spectrometric technique.

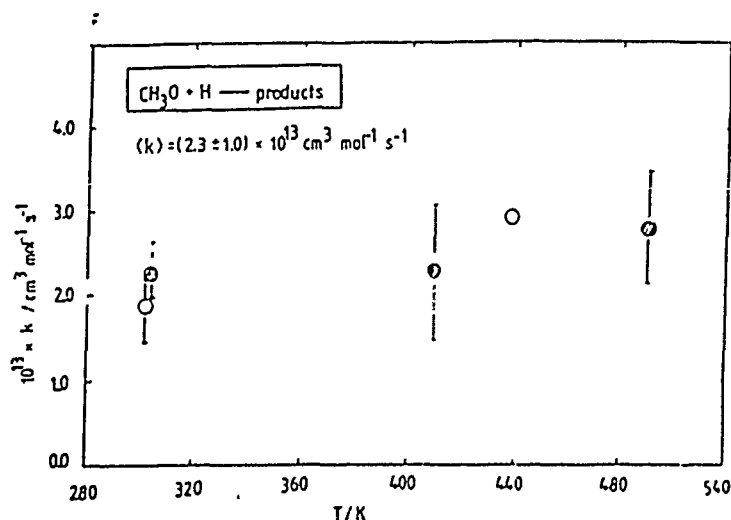


Fig.1. Plot of the overall rate coefficient as a function of temperature

Product formation was also studied in the fast flow system and the following reaction routes were identified:



Methanol formation is small under the conditions of the fast flow experiments. The formation of hydroxy radicals was detected and measured using LIF technique (308.3 nm excitation). Formaldehyde was also identified by LIF (351 nm excitation). The branching fractions for the reaction routes are determined and the mechanism hypotheses of direct reaction and product formation via an energized methanol species are discussed.

ELEMENTARY REACTIONS OF NEUTRAL TRANSITION METAL ATOMS

Steven A. Mitchell, J. Mark Parnis, Carl E. Brown and Peter A. Hackett

Laser Chemistry Group, Division of Chemistry,

National Research Council of Canada, Ottawa, Canada K1A 0R6

We have used a pulsed laser photolysis-laser fluorescence technique for studies of the reaction kinetics of neutral transition metal atoms under static pressure conditions near room temperature. Ground state transition metal atoms including Cr, Fe, Ni and W are produced by visible multiphoton dissociation of a volatile organometallic compound. Their chemical removal by added gases is monitored by resonance fluorescence excitation at variable time delay following the photolysis pulse. The use of relatively low temperatures and total pressures to ~ 1 atm. makes the technique well suited for studies of termolecular association reactions in which adducts are formed between metal atoms and simple ligand molecules. In favorable circumstances, a relaxation to chemical equilibrium may be observed in the adduct formation reactions, which allows for direct measurements of binding energies for mono-ligated metal atoms. The binding energy for $\text{Fe}(\text{NH}_3)$ is found to be 8 ± 1 kcal mol^{-1} . RRKM theory is used to model the temperature and pressure dependence of the association reactions. For $\text{Cr} + \text{O}_2$, the results are consistent with formation of $\text{O}-\text{Cr}-\text{O}$ with negligible activation energy. Atom transfer reactions including O -atom transfer from N_2O , $\text{C}_2\text{H}_4\text{O}$ and O_2 have also been investigated. We will attempt to show how the combination of this approach with matrix-isolation studies and *ab initio* calculations can provide detailed information on the nature of elementary reactions of transition metal atoms.

KINETICS OF THE REACTIONS OF HALOGEN ATOMS AND MOLECULES WITH SILICON AND GALLIUM ARSENIDE

E. A. Ogryzlo and Z. H. Walker, Department of Chemistry, The University of British Columbia, Vancouver, B.C., Canada, V6T 1Y6.

The reaction of a gaseous atom or molecule with a solid surface to produce gaseous products (a process called "gas phase etching") is very poorly understood. Earlier workers have all assumed that the reactions of both atoms and molecules with these surfaces are first order in the pressure of the gas phase etchant. Furthermore, in the $\text{Si} + \text{Br}_2^1$, $\text{Si} + \text{Cl}_2^2$, and $\text{GaAs} + \text{Cl}_2^3$ reactions, these workers have assumed that deviations from first order kinetics at high pressures is a consequence of the saturation of surface sites, resulting ultimately in a pressure-independent etch rate. We have studied the kinetics of the reactions of Cl , Cl_2 , Br , and Br_2 with silicon, and gallium arsenide over a temperature range from 20 to 600°C and a pressure range from 100 mTorr to 50 Torr using laser interferometry and surface profilometry to follow the removal of the semiconductor material. Rate constants and their temperature dependencies have been determined for most combinations of these materials. The activation energies and reaction orders provide evidence for different, but related, mechanisms for the reactions of atoms and molecules.

The reactions of bromine molecules and atoms with silicon has been the subject of our most complete study. The data lead us to propose a mechanism with the following rate determining steps:



The first step is the reversible dissociative adsorption of bromine on the solid surface. To be consistent with our data this must be followed by a rate controlling step which is first order in Br_{ads} . From the variation of the

etch rate with temperature and pressure the following rate constants have been determined:

$$k_1 = 1 \times 10^{11} \text{ nm min}^{-1} \text{ Torr}^{-1} e^{-(146 \pm 3 \text{ kJ/mol})/RT} \quad (3)$$

$$(k_1/k_{-1})^{1/2} k_2 = 7 \times 10^9 \text{ nm min}^{-1} \text{ Torr}^{-1/2} e^{-(127 \pm 7 \text{ kJ/mol})/RT} \quad (4)$$

where: $(k_1/k_{-1})^{1/2} k_2$ is the high-pressure composite half-order rate constant. Combining these experimental activation energies with those which we have obtained for the reaction of Br-atoms with silicon, allows us to draw the potential energy curves for the rate controlling steps in the reaction. This leads us to the conclusion that the step represented by reaction (1) is a novel "dissociative physisorption"

Similar studies of the reactions of Cl_2 with Si, Br_2 with GaAs, and Cl_2 with GaAs suggest that dissociative physisorption may be the most common mechanism for the etching of semiconductors by the halogens. The effects of dopants on the reaction rates have also been studied, and the elementary steps which are affected by the doping have been identified for the $\text{Br}_2/\text{Br}/\text{Si}$ system.

References

1. L.L. Sveshnikova, S.M. Repinskii, and A.B. Posadov, *Poverkhnost. Fiz., Khimiya. Mekh.*, 8, 134 (1982).
2. E. A. Ogryzlo, D. L. Flamm, D. E. Ibbotson, and J. A. Mucha, *J. Appl. Phys.* 64, 6510 (1986).
3. J. H. Ha, E. A. Ogryzlo and S. Polyhronopoulos, *J. Chem. Phys.*, 89, 2844 (1988).

KINETIC STUDIES OF THE INTERACTION OF CL AND BR ATOMS WITH POLYCRYSTALLINE NI AND SI(100) SURFACES

Wolfgang Mueller-Markgraf and Michel J. Rossi
Department of Chemical Kinetics, SRI International, Menlo Park, CA 94025

We report sticking coefficients for the ground and spin-orbit excited states of Cl and Br atoms on several surfaces of interest. The kinetic experiments have been performed in a low pressure reactor in which the atoms have been introduced by means of a pulsed valve downstream from a microwave discharge [1]. $\text{Cl}(^2\text{P}_{3/2})$, $\text{Cl}^*(^2\text{P}_{1/2})$, $\text{Br}(^2\text{P}_{3/2})$ and $\text{Br}^*(^2\text{P}_{1/2})$ have been observed *in situ* and in real time within the low pressure reactor by [3+2] Resonance Enhanced Multiphoton Ionization (REMPI). In addition, effusive beam sampling mass spectrometry has been used to monitor and detect stable reaction products.

In order to enable the kinetic studies on selected test surfaces, the interaction of halogen atoms on an "inert" surface such as PTFE (Teflon) had to be studied first. Table I presents a summary of initial sticking coefficients (γ_0) of Cl and Cl^* on Teflon, where γ_0 is defined as k_s/ω upon initial exposure, with k_s being the surface reaction rate constant for the loss of the halogen and ω the gas-wall collision frequency. According to Table I Teflon is an inert wall material for Cl and Cl^* .

With polycrystalline Ni as a test surface, the decay of Cl^* followed simple first order behavior, whereas the corresponding decays for Cl were found to be complex. A simple kinetic model involving gas-phase and surface elementary steps was used to extract γ_0 (Table I) and to interpret the temperature and dosage dependent kinetic data. Briefly, the kinetics suggest the existence of a shallow precursor well bound by 3.9 kJ mol^{-1} . No barriers in the entrance channel for Cl and Cl^* were found thus leading to a temperature-independent γ_0 from 300 to 750 K. The process of the formation of chemisorbed Cl adatoms from weakly adsorbed (physisorbed) Cl atoms occurs with an activation energy of 6.8 kJ mol^{-1} . This barrier is the cause for the apparent temperature dependence of the adsorption process. The long term saturation behavior of the Ni/Cl system has also been successfully modeled using the simple chemical kinetics model. The value for γ_0 on Ni (Table I) is identical to the estimated reaction probability of Cl on polycrystalline Mo for similar reaction conditions [2] and similar to a value measured on a Mo filament at 300 C [3].

The Cl and Cl^* decays on Si(100) were simple exponentials whose decay rate constants are summarized in Table I. For Cl only a limiting value could be given because the Cl atom decay was given by the effusion of Cl out of the reactor. Despite the low value of γ for the Cl/Si system, the etch product SiCl_2 was observed to desorb from the Si surface. The formation of SiCl_2 rather than

the thermodynamically more stable SiCl_4 [4] is expected as the primary etch product in view of the chlorine deficient environment. No saturation behavior of the etch rate was observed.

In the case of Br and Br^* interacting with a polycrystalline Nickel surface corrections for the interaction with Teflon had to be made because Teflon is apparently not a completely "inert" surface on our time scale of seconds. Table I shows the small but significant sticking coefficient of Br and Br^* with Teflon, which was almost temperature independent in the range 300 to 700 K. The decays for the Br/Ni system were of the simple exponential type and showed a significant temperature dependence. For Br, γ was temperature independent from 300 to 500 K, after which γ rapidly increased from $3 \cdot 10^{-3}$ to $2 \cdot 10^{-2}$ at 700 K. By contrast, γ for Br^* followed an Arrhenius type behavior over the same temperature range with an apparent activation energy of 24 kJ mol^{-1} , which is about half the spin-orbit splitting in Br (44 kJ mol^{-1}). The ordering of the Br, Br^* reactivity in the low temperature range (300 to 500 K) is interesting, in that $\gamma(\text{Br}^*)$ is smaller than $\gamma(\text{Br})$.

[1] W. Mueller-Markgraf and M. J. Rossi, Rev. Sci. Instrum. 61, 1217 (1990)

[2] D. S. Fischl and D. W. Hess, J. Vac. Sci. Technol. B6, 1577 (1988)

[3] D. E. Rosner and H. D. Allendorf, J. Phys. Chem. 69, 4290 (1965)

[4] T. A. Cleland and D. W. Hess, J. Vac. Sci. Technol. B7, 35 (1989)

Table 1: Summary of initial sticking coefficients for chlorine and bromine atoms

	T/° C	Cl ($^2\text{P}_{3/2}$)	Cl* ($^2\text{P}_{1/2}$)
Teflon (PTFE)	25	$\leq 5 \times 10^{-6}$	$\leq 5 \times 10^{-6}$
Ni (H_2 - treated)	25 to 500	$1.6 \pm 0.1 \times 10^{-2}$	$1.5 \pm 0.1 \times 10^{-2}$
Ni (pre-exposed)	25 to 500	$1.5 \pm 0.5 \times 10^{-2}$	$1.0 \pm 0.1 \times 10^{-2}$
Si(100) (n-doped)	31	$\leq 5.0 \times 10^{-5}$	$4.6 \pm 0.6 \times 10^{-4}$

		Br ($^2\text{P}_{3/2}$)	Br ($^2\text{P}_{1/2}$)
Teflon (PTFE)	25	$5.6 \pm 1.5 \times 10^{-5}$	$10.6 \pm 2.3 \times 10^{-5}$

THE STUDY OF REACTION KINETICS AT GaAs GAS-PHASE EPITAXY BY IN SITU ABSORPTION SPECTROSCOPY

I.P.Ipatova, Yu.V.Zhiljaev, A.Yu.Kulikov, Yu.N.Makarov, O.P.Chikalova - Lusina

Ioffe Physical Technical Institute, USSR Academy of Sciences, Leningrad 194021, USSR

Electron molecular spectroscopy constitutes a powerful means for compositional analysis of the epitaxy gas phase. Gas phase composition control is essential for the growth of semiconductor quantum well structures and superlattices, since at low temperatures ($T < 800^{\circ}\text{C}$) the kinetics of the homogeneous and heterogeneous reactions is a major factor in the formation of the gas phase.

The composition of the input gas phase was studied in a $\text{Ga} - \text{As} - \text{AsCl}_3 - \text{HCl} - \text{He} - \text{H}_2$ system by in situ UV optical absorption spectroscopy. Recording molecular absorption spectra at 220-360 nm provided information on the concentration of AsCl_3 , As_4 , GaCl and GaCl_3 molecules.

The principal conclusion from this work is that at temperatures below 800°C and at typical consumption rates for the mixture (the gas flux velocity is c. a. 1 - 5 cm/s), the composition of the input gas phase deviates from thermodynamic equilibrium. So the adequate description of the process requires a knowledge of the kinetical characteristics of the homogeneous and heterogeneous chemical reactions involved.

The reaction rate constants were inferred by comparison of the experimental output concentrations with the corresponding values derived from the calculations of the mass transfer in the source area of the reactor.

The $k(T)$ plot for the homogeneous reaction displays two parts with different activation energies, indicating the complex mechanism of the reaction.

LABORATORY STUDY OF THE HETEROGENEOUS REACTIONS OF CHLORINE
NITRATE AND HYDROGEN CHLORIDE ON NITRIC ACID ICE

Ming-Taun Leu, Steven B. Moore, Leon F. Keyser, and Roland H. Smith

Jet Propulsion Laboratory, California Institute of
Technology, 4800 Oak Grove Drive, Pasadena, CA 91109

Because they release gas-phase products which are photolyzed to produce active chlorine, heterogeneous reactions, such as:



which occur on acid-ice surfaces in polar stratospheric clouds (PSCs) could be important in springtime polar stratospheric ozone depletion. The predominant cloud, Type I PSCs, which is composed of HNO_3 and H_2O in the form of frozen nitric acid trihydrate (NAT), may be particularly important. In this paper we report the first direct measurements of the reaction probabilities at stratospheric temperatures for the above-mentioned reactions on NAT.

Using a fast flow reactor coupled with a mass spectrometer, we have measured the reaction probability of ClONO_2 on nitric acid-ice substrates with compositions near that of NAT at 196 K. We have also measured the reaction probability of ClONO_2 in the presence of small HCl concentrations in the substrates. The substrates were analyzed for total acid by titration versus standard base and for total chloride by using calibrated ion selective electrodes. Separate surface area and pore volume measurements were carried out to determine the effect of the porous ice structure on the rate constant measurements. In addition, separate infrared absorption experiments showed that the substrates contained hydronium and nitrate ions. The kinetic data were corrected for the interaction of flow dynamics and gas-phase diffusion within the gaseous core of the reactor and within the pores of the substrates. These results and their implications for the polar ozone depletion will be presented at the conference.

Acknowledgments. The research described in this paper was performed by the Jet Propulsion laboratory, California Institute of Technology, under a contract with the National Aeronautics and Space Administration.

References:

1. S. B. Moore, L. F. Keyser, M-T. Leu, R. P. Turco, and R. H. Smith, *Nature*, in press (1990).
2. M-T. Leu, *Geophys. Res. Lett.* **15**, 17 (1988); *ibid.*, **15**, 851 (1988).

**Heterogeneous Interactions of Gas Phase HCl, HNO₃
and N₂O₅ on Aqueous Droplets as a Function of
Temperature and Sulfuric Acid Concentration.**

J. M. Van Doren, L. R. Watson and P. Davidovits,
Boston College Chemistry Department, Chestnut Hill, MA 02167,
U.S.A.

D. R. Worsnop, M. S. Zahniser and C. E. Kolb,
Aerodyne Research, Inc.

Billerica, MA 01821 U.S.A.

Heterogeneous reactions of HCl, HNO₃ and N₂O₅ with aerosols in polar stratospheric clouds are important steps in the formation of active chlorine species implicated in the ozone loss mechanism in the Antarctic. In the mid-latitude stratosphere the majority of aerosol particles are composed mainly of aqueous sulfuric acid. In order to assess the importance of these heterogeneous processes on the ozone balance in the mid-latitude stratosphere we measured the uptake coefficients for these species as a function of temperature and sulfuric acid concentration. The experimental method employs a monodisperse train of droplets (~200 μm diameter) in a low pressure flow reactor. Droplet-trace gas interaction times are ~1 ~2 ms.

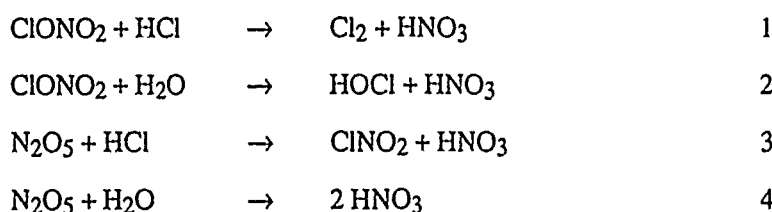
The uptake coefficients for all three species show a significant negative temperature dependence. For example, for HNO₃ the uptake coefficient increases from 0.077 to 0.23 as the temperature drops from 294 to 268K. The dependence of the uptake coefficient on sulfuric acid concentration is different for each species. For HCl the coefficient is 0.15 for pure water, remains constant up to 0.1 mole fraction of H₂SO₄ (40 wt %) and then drops sharply to 10^{-2} at 0.2 mole fraction (60 wt %). The uptake of HNO₃ and N₂O₅ is much less sensitive to sulfuric acid concentration. The production of gas phase HNO₃ arising from the heterogeneous reaction of N₂O₅ with the aqueous surface was also measured. A model which explains the observed results will be presented.

HETEROGENEOUS PROCESSES IN THE STRATOSPHERE

Margaret A. Tolbert, Christa M. Reihs, Ann M. Middlebrook and David M. Golden
SRI International, Menlo Park CA 94025

ABSTRACT

The importance of heterogeneous reactions in the stratosphere has been dramatically illustrated by the central role reactions such as 1 - 4 play in the photochemical mechanism



responsible for the yearly occurrence of the Antarctic 'ozone hole'.¹ These reactions have been shown to occur readily on laboratory ice surfaces that simulate the type II polar stratospheric clouds (PSCs) found over Antarctica in the winter.²⁻⁴ Reactions 1-3 convert the stable chlorine reservoir species (ClONO_2 and HCl) into more active forms (HOCl , Cl_2 , ClNO_2) which photolyze readily to provide Cl for catalytic ozone destruction cycles. All of the above heterogeneous reactions result in the formation of nitric acid. Nitric acid plays a key role in Antarctic ozone depletion because denitrification of the stratosphere is required for efficient ozone destruction.

Just as a coherent explanation of the ozone hole is emerging, new data indicate that ozone loss is not confined to the Antarctic stratosphere. Substantial ozone losses have reportedly occurred recently in the Arctic and throughout the northern hemisphere during the winter.⁵ The global ozone losses reported recently by the Ozone Trends panel are larger than those predicted using current photochemical models containing only homogeneous chemistry. Heterogeneous chemistry may thus be important in the global ozone cycle. In contrast to the situation over Antarctica, temperatures in the global and Arctic stratospheres are rarely low enough to support formation of type II PSCs (ice). Therefore, the particles available for heterogeneous processes in

these areas are likely to be either type I PSCs (nitric acid trihydrate, NAT), or sulfuric acid droplets.⁶ We are currently performing laboratory studies of heterogeneous reactions on surfaces that simulate these types of particles.

A Knudsen cell flow reactor is used to study the heterogeneous reactions 1 - 4 on sulfuric acid surfaces (40-90% H₂SO₄ by weight) in the temperature range 180 to 240 K. The rates of these reactions are determined as a function of sulfuric acid concentration and temperature. In addition to reaction rates, we have measured uptake rates for non-reactive gases such as HCl and HNO₃. The uptake rates are used to determine solubilities of these gases in sulfuric acid solutions under stratospheric conditions.⁷ The present work on liquid sulfuric acid solutions will be presented and the atmospheric implications of the results will be discussed.

Heterogeneous reactions on surfaces representative of type I and type II PSCs are being investigated using a newly constructed apparatus which incorporates *in situ* FTIR detection of the condensed phase during exposure to the trace gases. We have used this apparatus to study the competitive growth and evaporation of ice and NAT films under stratospheric conditions. Briefly, NAT films form in our experiment at temperatures approximately 5-7 degrees higher than ice films, even when water vapor is present in great excess (60-fold). Furthermore, we find that coating ice with a thin layer of NAT prevents evaporation of ice even when the temperature is raised significantly above the frost point. For example, we observe that ice evaporation occurs about 5 degrees higher when ice is coated with 0.02 μ of NAT. The results of our present work on ice and NAT surfaces will be presented and discussed in light of current theories for PSC formation and stratospheric denitrification.

1. Solomon, S., *Rev. Geophys.*, 26, 131-148, 1988.
2. Molina, M. J., T.-L. Tso, L. T. Molina, and F. C.-Y. Wang, *Science*, 238, 1253-1257, 1987.
3. Tolbert, M. A., M. J. Rossi, R. Malhotra, and D. M. Golden, *Science*, 238, 1258-1260, 1987. Tolbert, M. A., M. J. Rossi, and D. M. Golden, *Science*, 240, 1018-1021, 1988a.
4. Leu, M.-T., *Geophys. Res. Lett.*, 15, 17-20, 1988a. Leu, M. -T., *Geophys. Res. Lett.*, 15, 851-854, 1988b.
5. Watson, R. T., et al., *Present State of Knowledge of the Upper Atmosphere 1988: An Assessment Report*, NASA Reference Publications 1208, August, 1988.
6. Turco, R. P., O. B. Toon and P. Hamill, *J. Geophys. Res.*, 94, 16,493-16,510, 1989.
7. Reihs, C.M., D. M. Golden and M. A. Tolbert, *J. Geophys. Res.*, in press.

The Sink of OH - and HO₂ - Radicals on Aerosols.

Yu.M.Gershenzon, S.G.Zvenigorodsky, E.V.Antzupov, V.B.Rozenshtein,
S.P.Smyshlyaev.

EPR and IRLMR techniques were used for measurements of the OH - and HO₂ - radicals loss probabilities γ on many surfaces similar aerosol surfaces / SiO₂ , NaCl , H₂SO₄ , ice , metallic oxides β . Temperature depends γ and its depends on gas composition / presence of H₂O - vapor and hydrocarbons / confirm that $\gamma_{OH} \approx 0,1 \div 1$ and $\gamma_{HO_2} = 10^{-3} - 10^{-2}$ are typical values for many solid aerosol particles.

The results were used for creating 1-D model of aerosol atmosphere. Three scenarios are discussed.

1. Negative correlation between aerosol and ozone was explained by sink of OH - radicals on aerosols. With experimental value $\gamma_{OH} = 1$ for H₂SO₄ we succeeded in quantitative modeling on served ozone deficit after EL Chichon eruption.

2. The influence of OH - and HO₂ - heterogeneous loss processes is extremely effective in urban regions. Model results in more than 3 - 5 times decrease of OH - concentration and therefore in increase of *unhealthful* gases O₃ , CO , NO_x in troposphere.

3. A decrease of tropospheric OH abundance leads to general degradation of self - cleaning properties and reduces the filtering effect with respect to ozone - active pollutants. It is especially important in alternative freons emissions and their influence on stratospheric ozone depletion.

Laboratory measurements and modeling indicate an important role of OH and HO₂ - heterogeneous sink in atmospheric chemistry.

Electron Diffraction Studies of Cluster Growth Mechanisms

Anthony Pearson and Roger Anderson

Department of Chemistry

University of California, Santa Cruz, CA 95064

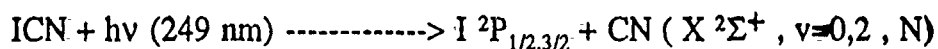
Synthetic electron diffraction spectra are calculated for computer grown random clusters. Two and three dimensional clusters of size to 27000 atoms are generated on square and cubic lattices. The striking conclusion of the work is that the electron diffraction powder patterns of high density (close packed) and low density (diffusion limited aggregation) are so similar to preclude experimental differentiation. To investigate the extent of the similarities in the diffraction patterns, cubic lattice clusters were also grown with restrictions on the valency of an occupied site. The valency of the cubic lattice is 6, and restriction of clusters to 3, 4, and 5 nearest neighbors still yield the same expected pattern. Clusters grown where each atom has only two nearest neighbors (random polymer) have similar but distinct patterns. Fixed orientation and single cluster rotationally averaged patterns will be reported. The implications of this work on the identification of crystalline or noncrystalline clusters will be discussed.

Studies of Nonadiabatic Phenomena in the Photodissociation of ICN at 249 nm

J.E.Black *, J.R.Waldeck ** and R.N.Zare *** , Stanford University ,
Stanford , CA 94305 , USA †

The Born-Oppenheimer approximation provides a useful first-order framework around which we may develop models for electronic transitions and, more specifically for our purposes, molecular photodissociation. It is also a well-known theoretical tenet that this approximation breaks down for all classes of fragmentation which yield open shell products, i.e., fragments possessing non-vanishing electronic angular momentum [1]. This breakdown has its most profound effects in the molecular recoupling region between the Franck-Condon zone accessed in electronic promotion and the asymptotic limit of fragment separation. It has been predicted to produce subtle variations in (i), the populations of the fine structure states in the fragments, (ii), the angular distributions of the photofragments and (iii), the orientation and alignment, corresponding respectively to the first and second moments of the angular momentum distribution.

Using various combinations of linearly and circularly polarized laser light in both the photolysis and probe photon fields, we have obtained a quantum-mechanically complete description of the CN ($X^2\Sigma^+$, $v=0,2$, N) state distribution following photolysis of ICN at 249 nm in the reaction .



In what we believe is the first experimental vindication of the theory, we have identified all but one of the features listed by Band et al. [2], predicted to signify the action of nonadiabatic interactions stemming from the breakdown of the Born-Oppenheimer approximation. These experimental features are particularly evident near the threshold for production of electronically excited iodine atoms, in accord with the general results of the theory.

[1] Williams, Freed, Singer and Band, Farad. Disc. Chem. Soc. **82**, 51 (1986) and refs therein.

[2] Band, Freed and Kouri, Chem. Phys. Letts. **79**, 233 (1981)

* SERC/NATO Postdoctoral Research Fellow 1987 - 1989

Present Address: Continuum, 3150 Central Expressway, Santa Clara, CA 95051 USA

** Present Address: Department of Chemistry, University of Pittsburgh, Pittsburgh, PA 15260, USA

*** Author to whom correspondence should be addressed

† Work supported by NSF PHY 88-05603

The 266-nm Photolysis of $\text{CD}_3\text{I}^\#$

David W. Chandler^(a), Maurice H.M. Janssen^(b), Steven Stolte^(c), David H. Parker^(d),
John W. Thoman Jr^(e), and Greg O. Sitz^(f)

^(a) Combustion Research Facility, Sandia National Laboratories, Livermore CA, 94551

^(b) Chemistry Dept., California Institute of Technology, Pasadena CA, 91125

^(c) Department of Physical and Theoretical Chemistry, Free University, De Boelelaan 1083, 1081 HV Amsterdam, The Netherlands

^(d) Chemistry Department, University of California at Santa Cruz, Santa Cruz CA, 95064

^(e) Chemistry Department, Williams College, Williamstown MA, 01267

^(f) Physics Department, The University of Texas at Austin, Austin Texas, 78712

Internal state populations, velocity distributions and alignment moments of methyl fragments from the 266-nm photodissociation of CD_3I in a supersonic beam are measured using the photofragment imaging technique. Methyl radicals are state-selectively ionized using (2+1) resonance-enhanced multiphoton ionization (REMPI) via the $3p_z$ Rydberg state, and the imaging technique records the velocity distribution of the ions. Using the previously derived $3p_z - X$ Franck-Condon factors a branching ratio for the $v=2/v=0$ levels of the umbrella mode is determined to be 1.15 ± 0.13 . Propensity ratios for forming the selected fragment state via the ground state iodine $\text{I}(^2P_{3/2})$ (I) or excited state iodine $\text{I}(^2P_{1/2})$ (I^*) channel are obtained from the images. I/I^* ratios are obtained while resonant on the 0_0^0 , 2_0^0 , 2_1^1 , 2_2^1 , 2_3^1 and 1_1^1 transitions. The I/I^* branching ratio is found to increase rapidly with increasing vibrational excitation.

A line-by-line rotational analysis of the $3p_z - X$ 0_0^0 band, including conservation of the parent molecule's ortho/para ratio in the planar fragment molecules, indicates that about 85 cm^{-1} of rotational excitation about a C_2 -symmetry axis in CD_3 results from the photolysis. The photodissociation appears to conserve the initial (low) rotational excitation about the C_3 -symmetry axis of the (cold) parent molecule. An analysis of the rotational populations based on bimolecular collision theory allows us to extract from the populations the probability of rotational energy transfer into the CD_3 fragment as a function of the appropriate energy gap. This is shown in Fig. 1.

The alignment of CD_3 fragments created by photodissociation of CD_3I with linearly polarized 266 nm light is characterized using the ion imaging technique. A linearly polarized probe laser is used for resonance-enhanced multi-photon (2+1) ionization of the methyl fragment. By measuring the dependence of the REMPI signal on the angle between the probe laser polarization and the photolysis laser polarization for specific parts of the image and by analyzing REMPI spectra recorded at specific angles, the population, $n(N,K)$, and the alignment moments $A_0^{(2)}$ and $A_0^{(4)}$ of the angular momentum distribution of velocity-selected CD_3 fragments are obtained. A representative spectrum is shown in Figure 2 along with a model spectrum incorporating the alignment moments and populations for each (N,K) state. The alignment moments extracted for single rotational levels (N,K) indicate that the fragments recoiling along the direction of the photolysis transition dipole approach the maximum values expected for a purely axial recoil process, i.e., for a methyl fragment in the N,K rotational state, $|NKM_N| \geq |NKK|$. The alignment measurements will be discussed in detail.

[#] Research Supported by the U.S. Department of Energy, Office of Basic Energy Sciences, Div. of Chemical Sciences.

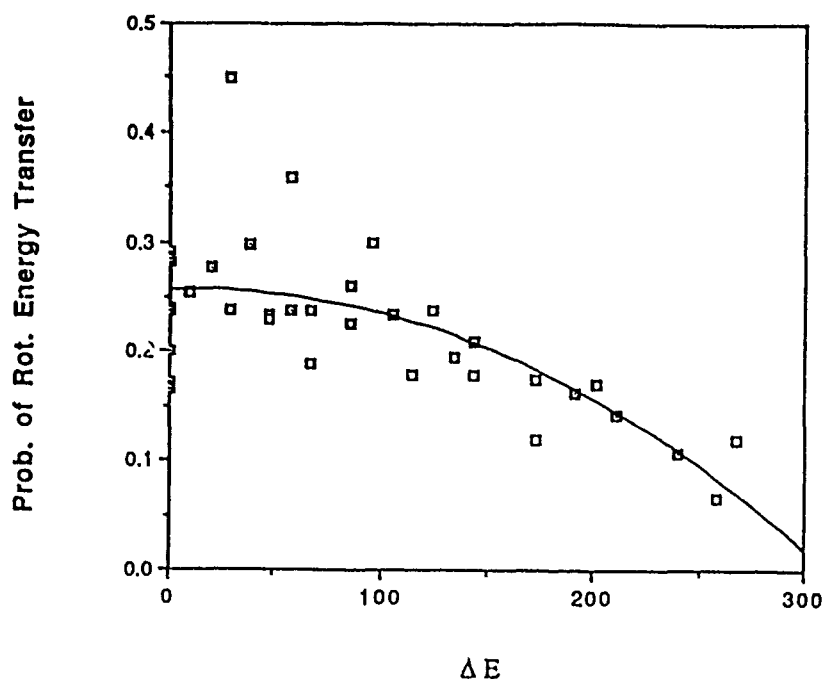


Figure 1: Plot of the probability of CD_3 obtaining an amount of rotational energy upon dissociation as a function of the rotational energy obtained. These probabilities are obtained assuming the populations used to fit the spectrum in Fig. 2.

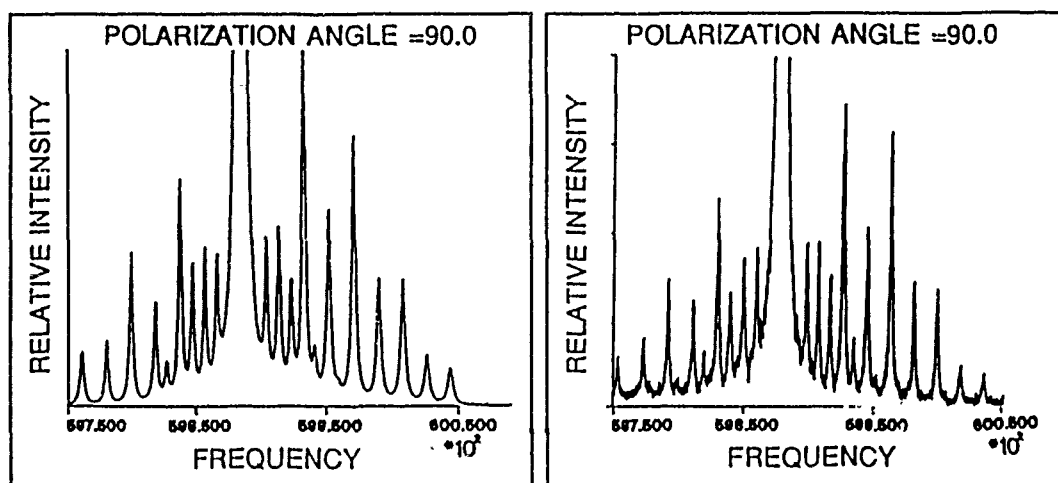


Figure 2: REMPI spectra of CD_3 following the 266-nm photolysis of CD_3I . The spectrum is taken with the angle between the polarization axes of the photolysis and ionization lasers at 90° . Only fragments with recoil velocities parallel to the photolysis laser beams polarization axis are detected.

ION-PAIR ($\text{Br}^+ + \text{Br}^-$) FORMATION FROM PHOTODISSOCIATION OF Br_2
NEAR THE FIRST IONISATION LIMIT

Andrew J. Yencha* and Devinder K. Kela

Department of Chemistry, State University of New York at
 Albany, Albany, New York 12222, USA

Robert J. Donovan

Department of Chemistry, University of Edinburgh,
 West Mains Road, Edinburgh EH9 3JJ, UK

Andrew Hopkirk

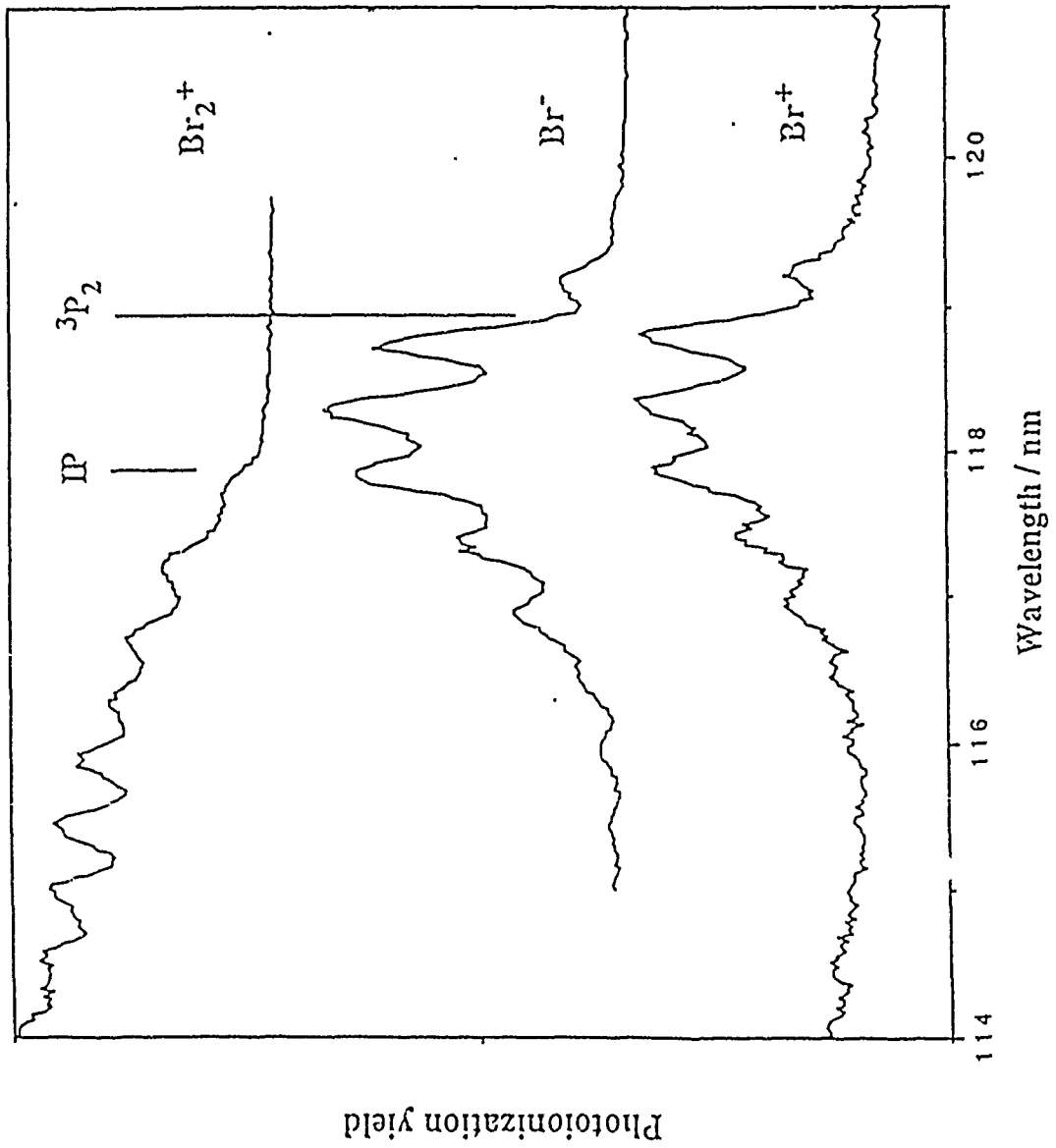
SERC Daresbury Laboratory, Daresbury,
 Warrington WA4 4AD, UK

Agust Kvaran

Science Institute, University of Iceland,
 107 Reykjavik, Iceland

Excitation functions for Br^- and Br^+ formation from jet-cooled Br_2 , in the region 120-114 nm (ie. from threshold to above the ionisation limit of Br_2), are reported. The mechanism for ion-pair formation is discussed in terms of homogeneous coupling between the $8p\pi$ Rydberg state and the $\text{D}(^1\text{O}_u^+)$ ion-pair state, correlating with $\text{Br}^-(^1\text{S}_0) + \text{Br}^+(^3\text{P}_2)$.

* Also Department of Physics.



Excitation functions for Br⁻ and Br⁺ formation, together with the ionisation function for the parent molecule, Br₂. The threshold for formation of Br⁻(¹S₀) + Br⁺(³P₂) is indicated together with the adiabatic ionisation potential of Br₂.

THE PHOTODISSOCIATION $\text{HN}_3 \rightarrow \text{NH}^* + \text{N}_2$ AND THE REVERSE PROCESS

F. Stuhl

Physikalische Chemie I, Ruhr-Universität, D-4630 Bochum, FRG

ABSTRACT

The dissociation of hydrazoic acid (HN_3) in the photolysis by 248 and 193 nm laser light has been recently studied in our laboratory in detail. In these experiments the formation of electronically excited $\text{NH}(a^1\Delta, b^1\Sigma^+, A^3\Pi, \text{ and } c^1\Pi)$ radicals was clearly established for 193 nm irradiation. In the 248 nm photolysis only $\text{NH}(a)$ radicals were observed. For these four NH states the rotational and vibrational distributions were measured and for the two metastable $\text{NH}(a, b)$ states additionally the translational energy. For the 193 nm photolysis, the quantum yields for the various NH states were roughly estimated.

We have furthermore investigated the kinetics of the quenching of all stable NH states, except $\text{NH}(d)$. Among numerous quenching molecules, we have used N_2 as collision partner. This allows us to comment on the kinetics of the reverse processes of the photodissociation.

With the method of *ab initio* CASSCF calculations, the dissociation of HN_3 has been recently investigated for selected configurations (U. Meier and V. Staemmler, private communication). Variation of the HN-N_2 bond length indicates among other features (a) a barrier upon the approach of $\text{NH}(a) + \text{N}_2$, (b) steep repulsion upon the approach of $\text{NH}(X, b \text{ and } A) + \text{N}_2$ and (c) a nonadiabatic process for $\text{HN}_3 \rightarrow \text{NH}(c) + \text{N}_2$. These calculations will be used here to discuss the photodissociation and quenching processes.

Financial support by the Deutsche Forschungsgemeinschaft is gratefully acknowledged.

Spectroscopy and Dynamics of Highly Vibrationally Excited CH₃O
at the Dissociation Limit.

A. Geers, J. Kappert, F. Temps, and J.W. Wiebrecht
 Max-Planck-Institut f. Strömungsforschung,
 Bunsenstrasse 10, 3400 Göttingen, W.-Germany

We have studied the spectroscopy and dynamics of highly vibrationally excited states of CH₃O radicals in their \tilde{X}^2E electronic ground state at energies around the dissociation limit for their unimolecular decomposition reaction



CH₃O radicals were excited to individual rotation vibration states in the energy range $35 \text{ kJ/mol} \leq E_{\text{vr}} \leq 100 \text{ kJ/mol}$ ($3\,000 \text{ cm}^{-1} \leq E_{\text{vr}} \leq 8\,100 \text{ cm}^{-1}$) using the method of Stimulated Emission Pumping (SEP) spectroscopy. The observed SEP spectra show evidence for strong rovibronic level mixing. At $E_{\text{vr}} = 6\,300 \text{ cm}^{-1}$, where the calculated total harmonic vibrational density of states is $g_{\text{vr,h}} = 0.43/\text{cm}^{-1}$, close to every quantum state of CH₃O at this energy can be observed in the spectrum. The highest excitation energy exceeds the H-CH₂O dissociation energy ($\Delta H_{\text{R,OK}}^0 = 80 \text{ kJ/mol} \approx 6\,700 \text{ cm}^{-1}$). The observation of individual resolved quantum states up to $E_{\text{vr}} = 8\,100 \text{ cm}^{-1}$ supports an experimental lower limit of the dissociation threshold of $E_0 \approx 97 \text{ kJ/mol}$. The investigations provide the basis for the fully rotation vibration quantum state resolved study of the CH₃O unimolecular decomposition.

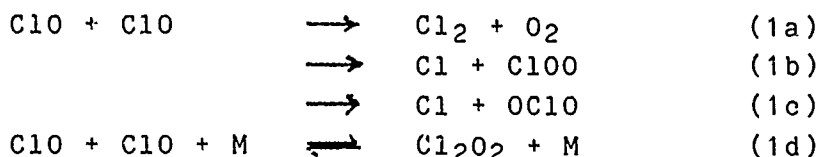
Topics: (E) - Reaction Dynamics or (F) - Photodissociation Dynamics.

A STUDY OF THE ClO ABSORPTION SPECTRUM AND KINETICS OF THE SELF-REACTION AT 298 K.

F.-G. Simon¹, W. Schneider, G.K. Moortgat and J.P. Burrows.

Max-Planck-Institut für Chemie, Air Chemistry Department,
Saarstrasse 23, D-6500 Mainz, FRG.

The ClO radical plays an important role in the active chlorine ClO_x (Cl and ClO) catalyzed destruction of stratospheric ozone. It is known that the self-reaction of ClO produces several product channels:



ClO was generated by the modulated photolysis of Cl₂ in the presence of Cl₂O and O₂. The ClO absorption spectrum was measured in the range 240-310 nm using a diode array camera, and is shown in Figure 1. Also displayed is the spectrum of Cl₂O.

The kinetics of the self-reaction were investigated at 298K using molecular modulation spectroscopy. The temporal behavior of optical density black squares is shown in Figure 2, together with simulations for various combinations for k_{1a}:k_{1b}:k_{1c}. The following bimolecular reaction rate constants were obtained:

$$\begin{array}{l} k_{1a} = (7.3 \pm 1.8) \times 10^{-15} \\ k_{1b} = (7.2 \pm 1.6) \times 10^{-15} \\ k_{1c} = (7.3 \pm 2.6) \times 10^{-15} \text{ cm}^3 \text{ molecule}^{-1} \text{ s}^{-1}. \end{array}$$

The results of this investigation are discussed and compared with previous measurements.

¹ New Address: Asea Brown Boveri AG, Forschungszentrum
CH-5405 Baden-Dättwil.

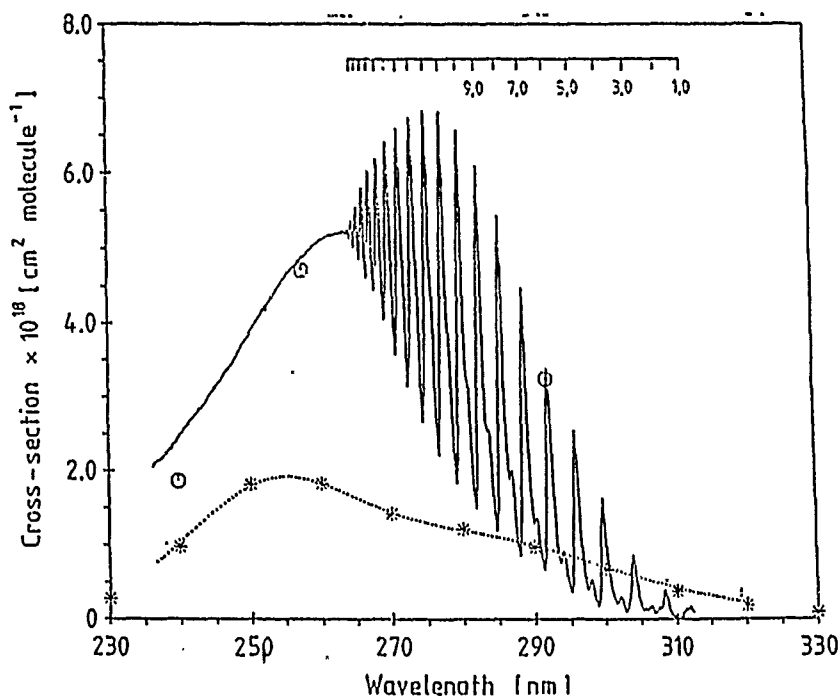


Figure 1. Absorption spectrum of ClO (—) and Cl_2O (.....), taken with the diode array spectrometer, with 0.3 nm resolution. The circles at 240.0, 257.7 and 292 nm represent measurements made by the modulated photolysis technique. The spectral notations relate to the v , v'' progression. The Cl_2O spectrum was scaled to the absorption cross section of Lin , \star (J. Chem. Eng. Data, 21, 41, (1976)).

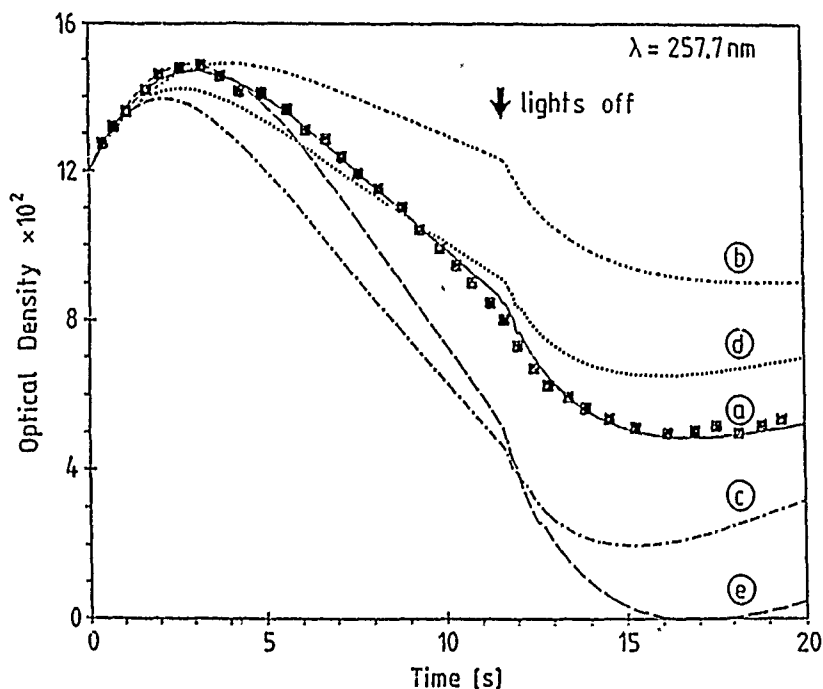


Figure 2. A set of simulations of the temporal behaviour of the absorption trace at 257.7 nm. Black squares are experimental data, simulated with values for $k_1a:k_1b:k_1c$ in units $10^{-15} \text{ cm}^3 \text{ molecule}^{-1} \text{ s}^{-1}$. Curve a: 7.3 : 7.2 : 7.3; curve b: 7.3 : 0 : 3.6; curve c: 7.3 : 14.7 : 10.9; curve d: 14.7 : 3.6 : 7.3; curve e: 3.6 : 14.7 : 7.3.

KINETICS AND MECHANISMS FOR THE REACTIONS OF HYDROXYL RADICALS
WITH ALKYL NITRATES AND NITROALKANES

Ole J. Nielsen
Chemistry Department, Risø National Laboratory, DK-4000 Roskilde,
Denmark.

Michael Donlon and Howard W. Sidebottom
Department of Chemistry, University College Dublin, Dublin
Ireland.

Jack Treacy
Department of Chemistry, Dublin Institute of Technology, Dublin,
Ireland

Abstract:

Alkyl nitrates can be formed in the oxidation of volatile organic compounds in the troposphere, especially when larger peroxy radicals react with NO. These organic nitrates provide temporary reservoirs for nitrogen oxides and are expected to be involved in long range transport of NO_x. Nitroalkanes are employed as propellants and as industrial solvents leading to their potential release into the atmosphere. Reaction of these organonitrogen compounds with hydroxyl radicals is an important factor in determining their atmospheric residence times. However, previously very little information concerning the kinetics and mechanisms for these reactions has been available.

In this work rate constants for the reaction of OH radicals with a series of n-alkyl nitrates and nitroalkanes have been determined at 298 K and 1 atmosphere total pressure using both pulse radiolysis combined with kinetic spectroscopy and a conventional relative rate method. The data indicate that the reaction of OH radicals with alkyl nitrates and nitroalkanes involves both an abstraction and an addition channel. The nitrate and the nitro groups substantially decrease the rate constant for H atom abstraction from groups bonded directly to the functional groups and also decrease those for abstraction in the β position. The addition reaction was studied as a function of temperature and pressure using the pulse radiolysis method. The results show that the addition process is a major reaction pathway for short chain compounds at atmospheric pressure and 298 K.

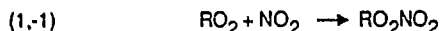
Thermal Stability of Selected Peroxynitrates

F. Kirchner, G. Libuda and F. Zabel

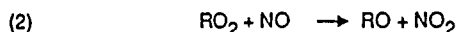
Universität - GH Wuppertal, Physikalische Chemie / FB 9, Gaußstr. 20,

5600 Wuppertal 1, FRG

A common reaction of peroxy radicals in the atmosphere is the addition of NO_2 to form peroxynitrates, RO_2NO_2 . Peroxynitrates are thermally unstable and can act as temporary reservoirs for both NO_x and RO_2 :



RO_2NO_2 radicals are irreversibly destroyed by the reaction with NO .



If the lifetime of RO_2NO_2 is sufficiently high, it may contribute to the long range transport of NO_x or it may carry halogens from the upper troposphere into the stratosphere.

In the present work, thermal lifetimes of RO_2NO_2 are measured as a function of temperature and total pressure for $\text{R} = \text{CH}_3\text{C}(\text{O})\text{CH}_2$, CH_2Cl and CClO , which derive from acetone, methyl chloride and formyl chloride, respectively. For this purpose, effective first order rate constants for the loss of RO_2NO_2 were measured in the presence of an excess of NO in a 420 l reaction chamber from DURAN glass. Under these conditions, $k_{\text{eff}} = k_{-1}$. The concentrations of RO_2NO_2 , NO and NO_2 were measured as a function of time via long-path IR absorption using a built-in White mirror system and a FTIR spectrometer. The measured temperature dependencies of k_{-1} at total pressures of 800 and 10 mbar ($\text{M} = \text{N}_2$) are shown in fig. 1. Each Arrhenius line is based on ca. 10 independent measurements. At one temperature, additional measurements were performed at a total pressure of 100 mbar in order to establish the pressure dependence of k_{-1} . The data sets are represented by the three-parameter formalism of Troe [1], e.g. for the reaction $\text{CH}_2\text{ClO}_2\text{NO}_2 + \text{M} \rightarrow \text{CH}_2\text{ClO}_2 + \text{NO}_2 + \text{M}$.

$$k_0/[\text{N}_2] = 1.6 \times 10^{-3} \exp(-88.5 \text{ kJ mol}^{-1} / RT) \text{ cm}^3 \text{ s}^{-1}$$

$$k_{\infty} = 3.6 \times 10^{16} \exp(-96.1 \text{ kJ mol}^{-1} / RT) \text{ s}^{-1}$$

$$F_c = 0.4$$

By comparison with other results from this laboratory for $\text{R} = \text{alkyl}$ [2], $\text{R} = \text{chloro-fluoromethyl}$ [3] and $\text{R} = \text{acetyl}$ [4] and with literature data for $\text{R} = \text{H}$ [5], the following conclusions are drawn:

- (i) k_{-1} values at 1 atm and 298 K decrease within the series $\text{R} = \text{C}_2\text{H}_5$, $\text{CH}_3\text{C}(\text{O})\text{CH}_2$, CH_3 , CH_2Cl , CCl_3 , H , CCl_2F , CClF_2 , CH_3CO , CClO from 3.4 s^{-1} ($\text{R} = \text{C}_2\text{H}_5$) to 0.00018 s^{-1} ($\text{R} = \text{CClO}$); see table I.
- (ii) The pressure dependence of k_{-1} is well described by the three-parameter fits suggested by Troe [1] (k_0 , k_{∞} , F_c) with F_c values derived from the vibrational frequencies of the respective RO_2NO_2 molecule, proper values of F_c ranging from 0.6 ($\text{R} = \text{H}$ [5]) to 0.22 ($\text{R} = \text{CCl}_3$ [3]).
- (iii) Pre-exponential factors of the limiting high pressure rate constants seem to increase with increasing bond energy, covering a range of a factor of 20 (disregarding $\text{R} = \text{H}$). Partially, this effect may be obscured by the scatter induced by small errors in the activation energies.

- (iv) The very different lifetimes of RO_2NO_2 (~ 0.3 s for $\text{R}=\text{C}_2\text{H}_5$ vs. ~ 1.5 h for $\text{R}=\text{CClO}$ at 298 K, 1013 mbar N_2) are thus mainly due to different $\text{ROO}-\text{NO}_2$ bond energies (see table I).

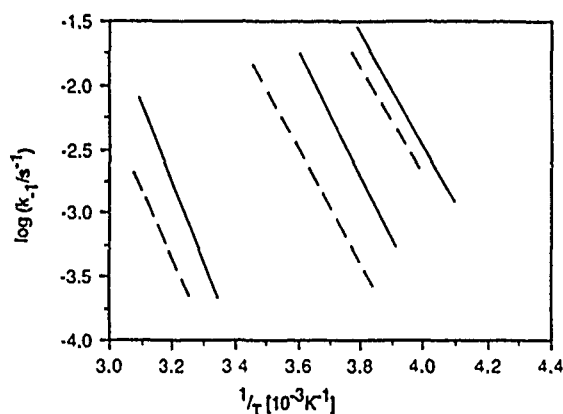
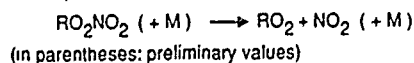


Figure 1 : Temperature dependence of k_1 for $\text{R}=\text{CClO}$, CH_2Cl , and $\text{CH}_3\text{C}(\text{O})\text{CH}_2$ (total pressure 800 mbar (full lines) and 10 mbar (broken lines), $\text{M}=\text{N}_2$)

- (v) The bond energies from table I suggest that -I and -M substituents weaken the $\text{ROO}-\text{NO}_2$ bond, the largest impact being introduced by a carbonyl group adjacent to the peroxy group.
- (vi) In the atmospheric boundary layer, lifetimes of peroxynitrates are determined by thermal decomposition. In the upper troposphere, peroxynitrates with $\text{R}=\text{halo-methyl}$ and $\text{R}=\text{R}'\text{C}(\text{O})$ are thermally stable and their lifetimes are limited by photolysis (photolysis lifetimes in the order of 100 days).

R	k (298K, 1013mbar N_2) [s^{-1}]	E_{bond} [kJ/mol]	A_{pre} [10^{16}s^{-1}]	F_c	Ref.
C_2H_5	3.4	88.8	0.88	0.3	2
$\text{CH}_3\text{C}(\text{O})\text{CH}_2$	2.5	(87)	(0.50)	0.4	this work
CH_3	1.65	87.8	1.1	0.4	2
H	0.19	88.6	0.034	0.6	5
CH_2Cl	0.33	96.1	3.6	0.4	this work
CCl_3	0.20	98.3	4.8	0.22	3
CCl_2F	0.070	101.8	6.6	0.28	3
CClF_2	0.041	99.7	1.6	0.30	3
CH_3CO	0.00046	113.3	3.9	0.3	4
CClO	0.00018	(118)	(12)	-	this work

Table I : Kinetic parameters for thermal decomposition reactions



References

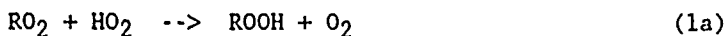
- [1] J. Troe, Ber. Bunsenges. Phys. Chem. 87(1983)161;
J. Troe, J. Chem. Phys. 65(1977)4758
- [2] F. Zabel, A. Reimer, K.H. Becker, and E.H. Fink, J. Phys. Chem. 93(1989)5500
- [3] D. Köppenastrop and F. Zabel, submitted for publication
- [4] I. Brikier, F. Caralp, H. Loirat, R. Lesclaux, B. Veyret, K.H. Becker, A. Reimer, and F. Zabel, submitted for publication
- [5] R.A. Graham, A.M. Winer, and J.N. Pitts, J. Chem. Phys. 68(1978)4505
R. Patrick and D.M. Golden, Int. J. Chem. Kinet. 15(1983)1189

PRODUCT STUDY OF THE REACTIONS OF CH_3O_2 AND $\text{C}_2\text{H}_5\text{O}_2$ WITH HO_2 IN AIR AT 295K.

Timothy J. Wallington and Steven M. Japar

Research Staff
Ford Motor Company
P. O. Box 2053
Dearborn, Michigan 48121

Fourier transform infrared spectroscopy was used to identify and quantify methylhydroperoxide and ethylhydroperoxide as the dominant products of the gas phase reaction of methylperoxy and ethylperoxy radicals with hydroperoxide radicals. From our measurements we are able to establish that over the pressure range 20 - 700 torr, at 295K, within our experimental errors, 100% of these reactions proceed via reaction (1a)

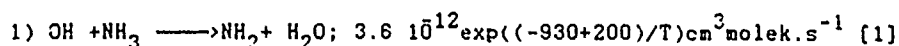


Results are discussed with respect to the previous kinetic and mechanistic studies of peroxy radicals and computer models of atmospheric chemistry.

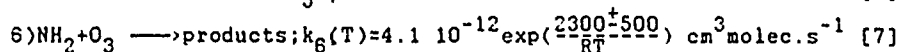
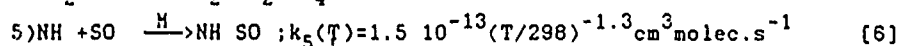
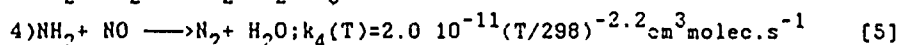
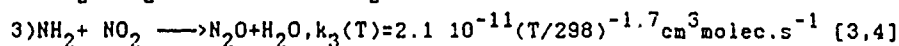
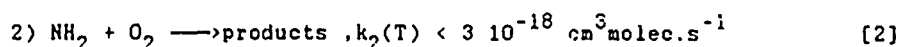
THE MECHANISM OF AMMONIA OXIDATION IN THE ATMOSPHERE

Bulatov V.P., Dubinsky I.A., Khabarov V.N., Losovsky V.A.,
Sarkisov O.M.
Institute of Chemical Physics, USSR Academy of Sciences,
117334 Moscow, USSR.

The ammonia oxidation is known to be initiated by the following reaction:



Lately scientists paid much attention to NH_2 radical reactions with the atmospheric components such as NO , NO_2 , SO_2 , O_2 , O_3 . These elementary reactions were studied in our laboratory and the following rate constants were obtained:

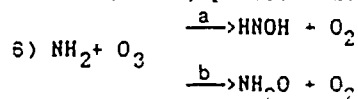


As for reaction 6) it was assumed [7], that its product is NH_2O radical.

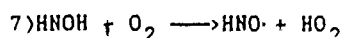
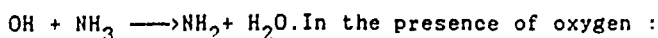
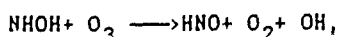
In the present work we studied the NH_2 radical kinetics in the system $\text{NH}_3 + \text{O}_3 + \text{N}_2 + \text{O}_2$. NH_2 radicals were formed by flash photolysis of ammonia ($\text{NH}_3 + h\nu \longrightarrow \text{NH}_2 + \text{H}$) or ozone ($\text{O}_3 + h\nu \longrightarrow \text{O}(^1\text{D}) + \text{O}_2$, $\text{O}(^1\text{D}) + \text{NH}_3 \longrightarrow \text{NH}_2 + \text{OH}$). The registration of NH_2 radical was realized by intracavity laser spectroscopy.

It was shown that in system without oxygen products of reaction 6) participate in the further reactions forming NH_2 radicals. In the presence of oxygen the NH_2 radicals formation was reduced.

We assume that the reaction 6) proceed through channels:



We consider the main product of this reaction to be the HNOH radical which can form the NH_2 radical via two steps:

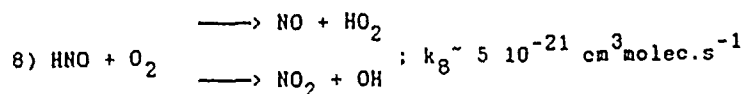


The application of this kinetic model for the processing of the experimental data enabled to determine the rate constants of reactions 6) and 7):

$$k_6 = 1.3 \cdot 10^{-13} \text{ cm}^3 \text{ molec. s}^{-1}$$

$$k_7 \sim 6.0 \cdot 10^{-15} \text{ cm}^3 \text{ molec. s}^{-1}$$

On the basis of the obtained data one can suggest that the mechanism of NH_3 oxidation in the atmosphere includes steps 1) - 7). HNO is likely to interact with oxygen or ozone forming nitrogen oxides. In our laboratory the preliminary data (to be published) were obtained about reaction 8) :



The estimate of rate constant k_2 is not enough to neglect the atmospheric reaction 2) which may produce NO_x . However if we assume that this reaction may be neglected, the removal or formation of NO_x is defined by three reactions 3), 4) and 6). If we take into account the atmospheric concentrations of O_3 , NO_2 and NO , our estimate shows that ammonia removes nitrogen oxides from the atmosphere.

REFERENCES

1. Chemical Kinetics and Photochemical Data for Use in Stratospheric Modeling. Evaluation Number 8 .NASA .1987.
2. V.A.Lofovsky, M.A.Ioffe, O.M.Sarkisov. "On the reaction of the NH_2 Radical with oxygen." - Chem. Phys. Lett., 1984, v. 110, n. 6, pp. 651-654.
3. V.P.Bulatov, A.A.Ioffe, V.A.Lofovsky, O.M.Sarkisov. "On the reaction of the NH_2 radical with NO_2 at 295-620K." - Chem. Phys. Lett., 1989 v. 159, n. 2/3, pp 171-174.
4. V.P.Bulatov, A.A.Ioffe, V.A.Lofovsky, O.M.Sarkisov. On the reaction of the NH_2 radical with NO at 295-620K." - Chem. Phys. Lett., 1989. v. 161, n. 2, pp. 141-146.
5. A.A.Ioffe, V.P.Bulatov, V.A.Lofovsky, M.Ya.Goldenberg, O.M.Sarkisov, S.Y.Umanskiy. "On the reaction of the NH_2 radical with SO_2 at 298-363K." - Chem. Phys. Lett., 1989, v. 156, n. 5, pp. 425-432.
6. Bulatov V.P., Buloyan A.A., Iogansen A.A., Sarkisov O.M., Cheskis S.G. Khim. Fiz. n. 4, 1982, pp. 513-515

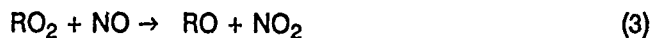
Kinetics of Reactions of Organic Peroxy Radicals with HO₂ and NO

by

M.E.Jenkin, T.P.Murrells and G.D.Hayman

The Harwell Laboratory, Didcot, Oxon, OX11 0RA

Work is currently in progress to investigate the kinetics and product channels of a series of reactions involving substituted-organic peroxy radicals (RO₂) using ultraviolet absorption spectroscopy. Emphasis is placed on the characterisation of the self- and mutual-reactions (1) and (2), and the reactions with NO (3).



The molecular modulation and laser flash photolysis techniques are used to study the kinetics of these reactions, with RO₂ radicals detected in their ultraviolet absorption bands. The pressure and temperature dependences of the kinetics, and also of the product ratios are investigated in order to provide more detailed information on the mechanisms of these reactions.

Organic peroxy radicals are important intermediates in the oxidation mechanisms for hydrocarbons in the atmosphere. Reactions such as (1) and (2) may act as radical sinks whereas reactions of type (3) are propagating, and lead to the production of tropospheric ozone.

PRODUCTS OF THE GAS-PHASE REACTIONS OF MONOTERPENES
WITH THE OH RADICAL IN THE PRESENCE OF NO_x

Janet Arey, Sara M. Aschmann and Roger Atkinson

Statewide Air Pollution Research Center, University of California,
Riverside, California 92521, U.S.A.

Monoterpenes emitted from vegetation react in the troposphere with OH and NO₃ radicals and O₃, with all three of these reaction pathways being calculated to be important as loss processes for the monoterpenes. The products of the gas-phase reactions of the OH radical with a series of monoterpenes have been investigated, in the presence of NO_x, at room temperature and atmospheric pressure of air by gas chromatography and combined gas chromatography-mass spectrometry. For α- and β-pinene and Δ³-carene, only a single significant product was observed, while two significant products were observed from d-limonene and sabinene and none from myrcene. The product from the OH radical reaction with β-pinene has been identified as nopinone (6,6-dimethylbicyclo[3.1.1]heptane-2-one) and its yield determined to be 30 ± 5%. One of the products from d-limonene has been identified as 4-acetyl-1-methylcyclohexene with a 16% formation yield. Further experimental results will be reported from this ongoing study.

The Reactions of Hydroxyl Radicals with some
Aromatic and Heterocyclic Compounds
by D.L. Baulch, H. Black, and P.K. Louie
(School of Chemistry, University of Leeds)

A discharge flow system has been used to study the reaction of hydroxyl radicals with a number of compounds of importance in atmospheric chemistry. The radicals were generated by the reaction of H atoms with NO_2 and the progress of the reaction was followed by monitoring the hydroxyl radical concentration by resonance fluorescence as a function of reaction time.

The compounds investigated in the present work include benzene, indane, indene, furan and tetrahydrofuran. In each case the reaction has been studied at 298 K and over a pressure range of the carrier gas of 0.5 - 10 Torr. The magnitudes of the rate constants and the ways in which they vary with pressure reflect the different reaction channels operating in the various cases.

The relationship between the rate constants and the structures of the compounds is discussed.

Prediction of rate constants for reactions of atmospheric radicals

L.F. Phillips

University of Canterbury, New Zealand

Many free-radical reactions occur with no activation barrier, so that the rate of reaction is controlled by the rate of crossing the centrifugal barrier in the long-range intermolecular potential. For such reactions, provided there is no significant bottleneck in the exit channel leading to products, the reaction rate is equal to the rate of crossing the centrifugal barrier, multiplied by the appropriate electronic degeneracy factor. The present paper gives the results of quasi-classical trajectory calculations for approximately thirty reactions whose rates are relevant to the chemistry of planetary atmospheres, over the temperature range 10-600 K. For the majority of the reactions the calculated rate constants are in excellent accord with experimental results; in all cases the results provide a useful guide to the behaviour of the rate constant at very low temperatures.

Unimolecular Decomposition of N_2O_5

C. A. Cantrell, R. E. Shetter, J. G. Calvert, G. S. Tyndall, and J. J. Orlando
National Center for Atmospheric Research
Atmospheric Chemistry Division
Atmospheric Kinetics and Photochemistry Group
P.O. Box 3000
Boulder, CO 80307, USA

The chemical system involving the reactions which form and destroy dinitrogen pentoxide are important in the partitioning of these species in the atmosphere.



Accurate values for the rate coefficients for these reactions, as functions of temperature and pressure, are required to be able to quantitatively understand the atmospheric distributions of NO_3 and N_2O_5 . We have used Fourier transform infrared spectroscopy to measure the concentration of N_2O_5 in a temperature regulated, long path cell. An excess of nitric oxide was added to an N_2O_5 / N_2 mixture. NO scavenges NO_3 and minimizes the occurrence of reaction 2) in the system. Thus measurement of the loss rate of N_2O_5 is a direct measure of the rate of reaction 1). The data from this reaction can be combined with data from reaction 2), also measured in this laboratory, to yield a data set which can be compared to measured equilibrium data.

Slow Reactions of the NO₃ Radical

P. Biggs, A.A. Boyd, C.E. Canosa-Mas, M.R. Wilson and R.P. Wayne*

Physical Chemistry Laboratory, Oxford University, UK

Many important reactions of the NO₃ radical in the atmosphere are too slow to be measured by conventional laboratory kinetic techniques. This presentation describes the measurement, by two different methods, of the rate parameters of some of these slow reactions.

The techniques used were a gas-phase stopped-flow system and a static laser photolysis setup. The stopped-flow system consists of a conventional discharge-flow system in which the NO₃, generated by the F + HNO₃ reaction, is monitored by its optical absorption at $\lambda=662$ nm. The flow through the absorption cell can be isolated by electromechanical glass valves, and the time-dependant decay of the NO₃ monitored.

The static laser photolysis system also uses the F + HNO₃ reaction to generate NO₃; however, the F atoms are generated in this case by the photolysis of F₂ with the $\lambda=308$ nm radiation from a XeCl excimer laser. If the rate of decay of NO₃ between consecutive laser flashes is slow, then a steady-state concentration of NO₃ builds up in the photolysis cell; on cessation of the photolysis, the NO₃ is seen to decay, and the rate of this decay can be used to derive the rates of the reactions of NO₃ in the cell. The NO₃ concentration was again monitored by optical absorption, but this time by the $\lambda=623$ nm radiation from a cw dye laser.

In both systems, the decay of NO₃ due to its self reaction and wall losses occurs over a period up to 30 seconds. The range of rate constants that has been measured is $10^{-16} - 10^{-19}$ cm³ molecule⁻¹ s⁻¹. Results are presented for the reaction of NO₃ with species that are of importance in the atmosphere, such as CH₄, C₂H₆, C₂H₄, various halocarbons and NO₃ itself.

Listed below are preliminary results from the experiments performed on the stopped-flow system. It should be noted that the values of the rate constants quoted here are those derived directly from the NO_3 decay data and include the contribution to the overall rate from the secondary reactions. Interpretation of the data is still in progress, and the numbers shown in this table will have to be divided by a stoichiometry factor of at least 2.

Species	k^{298} $\text{cm}^3\text{molecule}^{-1}\text{s}^{-1}$
$\text{H}_2\text{C}=\text{CH}_2$	$(4.8 \pm 2.0) \times 10^{-16}$
C_2H_6	$(5.0 \pm 0.9) \times 10^{-17}$
$(\text{CH}_3)_2\text{CHCH}_3$	$(1.1 \pm 0.2) \times 10^{-15}$
CH_4	$< 1 \times 10^{-18}$
CH_2Cl_2	$(9.6 \pm 2.6) \times 10^{-18}$
CF_3CFH_2	$< 5 \times 10^{-19}$
CH_3COCH_3	$(1.7 \pm 1.0) \times 10^{-17}$

A kinetic study of the reactions of the hydroxyl radical with sixteen hydrohalocarbons: atmospheric implications.

A.C.Brown, C.E.Canosa-Mas, A.D.Parr, K.Rothwell and R.P.Wayne*

Physical Chemistry Laboratory, Oxford University, UK

As a consequence of the general concern about the effects of chlorofluorocarbons (CFCs) on stratospheric ozone, a series of hydrohalocarbons have been considered as substitutes for the CFCs. The hydrohalocarbons (RH) have significantly shorter atmospheric lifetimes, and thus much lower probabilities of accumulation in the troposphere, than the halocarbons because they react with the OH radical (1), a daytime tropospheric oxidant



We have measured the absolute rate constants as a function of temperature for the reaction of OH with 16 hydrohalocarbons using a conventional discharge-flow technique with resonance fluorescence detection of the OH radical. Our kinetic data are shown in the table. We have estimated the ozone depletion potentials (ODPs) from rates and spectra measured in the laboratory, and published values of ODPs, which have been determined with atmospheric models, for analogous compounds.¹ We assume that reaction with OH is the main tropospheric sink for RH and estimate tropospheric lifetimes, τ_{RH} , using equation 1 as recommended by Prather²

$$\tau_{\text{RH}} = \tau_{\text{MC}} \times \frac{k_1(\text{MC}, 277\text{K})}{k_1(\text{RH}, 277\text{K})} \quad (1)$$

here MC is methyl chloroform (CH_3CCl_3). A value of 6.3 years for τ_{MC} was used in Prather's work and is the value used here.

The amount of chlorine transported from ground level to the stratosphere is proportional to the emission rate, lifetime and number of chlorine atoms in RH. For the same emission rate of a reference compound (CFC-11), the ozone depletion potential, ODP, is given by

$$\text{ODP}(\text{RH}) = \frac{\tau_{\text{RH}}}{\tau_{\text{CFC-11}}} \times \frac{M_{\text{CFC-11}}}{M_{\text{RH}}} \times \frac{n_{\text{Cl}}}{3} \times \text{CEF}(\text{RH}) \quad (\text{II})$$

where M represents relative molecular mass. The "chlorine effectiveness factor" (CEF) is dependent on the uv absorption cross-sections of RH since they will determine the altitude within the stratosphere at which the molecule is photodissociated. Where a CEF is not available explicitly from model calculations¹ for particular compounds, we estimate a value for the

CEF by comparison of the uv spectrum of RH with uv data for species whose effectiveness factors are known.

The ODPs for brominated compounds (R'H) are calculated relative to a bromine-containing species, halon 1301 (CF_3Br), the ODP of which has been calculated taking into account the chemical behaviour of bromine-containing species in the stratosphere. Our values for the ODPs as estimated by the method described above are given in the table.

Compound	$10^{15}k_2$ (298K) $\text{cm}^3 \text{ molecule}^{-1} \text{ s}^{-1}$	$10^{13}A$	(E \pm AE)/R K	Number of Ts	T-range K	ODP
CF_2HCH_3	59 \pm 9	14.2	1050 \pm 250	6	220-423	0
CF_3CFH_2	6.9 \pm 1.5	5.8	1350 \pm 100	7	231-423	0
$\text{CF}_3\text{CF}_2\text{H}$	2.9 \pm 1.0	2.8	1350 \pm 100	5	257-423	0
CH_3Cl	53 \pm 8					
$\text{CF}_2\text{CClCH}_3$	3.7 \pm 1.4	2.6	1230 \pm 250	6	231-423	0.04
CFCl_2CH_3	13.6 \pm 2.7	5.8	1100 \pm 250	7	238-426	0.05
$\text{CF}_3\text{CCl}_2\text{H}$	59 \pm 6	11.8	900 \pm 150	4	294-441	0.01
$\text{CF}_3\text{CF}_2\text{CCl}_2\text{H}$	3.7 \pm 0.8	2.3	550 \pm 750	3	251-393	0.01
CF_2BrH	1.3 \pm 0.9	4.4	1050 \pm 400	5	275-420	0.50
CF_3CFBrH	1.7 \pm 0.3	11.3	1250 \pm 350	5	279-423	0.35
$\text{CF}_3\text{CCl}_2\text{BrH}$	60 \pm 4				303	0.15
CH_3I	72 \pm 7	28.9	1100 \pm 200	5	271-423	
CF_3I	31 \pm 5				300	
$\text{CF}_2\text{HOCF}_2\text{CFC}_2\text{H}$	17 \pm 5	6.1	1080 \pm 500	2	302&423	0.004
$\text{CF}_2\text{HOCC}_2\text{HCF}_3$	21 \pm 7				298	0.004
$\text{CF}_3\text{CH}(\text{CF}_3)\text{OCH}_2\text{F}$	73 \pm 22	15.3	900 \pm 500	2	302&423	0

References.

1. World Meteorological Organisation Global Ozone Research and Monitoring Project - Report No. 20 Scientific Assessment of Stratospheric Ozone:1989 Volume I, Chapter 4, WMO Geneva 1990.
2. Ibid. AFAS Report Appendix.

The temperature dependence of the reaction of the NO_3 radical with a series of halobutenes and 1-butene

R.W.S.Aird, C.E.Canosa-Mas, D.J.Cook, P.S.Monks and R.P.Wayne*

Physical Chemistry Laboratory, Oxford University, U.K.

E.Ljungstrom

Dept. Of Inorganic Chemistry, Chalmers University of Technology
and University of Goteburg, Goteburg, Sweeden.

The NO_3 radical is the most important oxidant in the night-time troposphere. The variety and abundance of hydrocarbons in the troposphere leads to the need for an understanding of the patterns of reactivity of the NO_3 radical with such compounds.

A conventional discharge-flow technique, with the NO_3 radical detected by optical absorption at $\lambda = 662 \text{ nm}$, has been used to measure rate data for a homologous series of halo-substituted C_4 alkenes. Where pseudo-first order kinetic conditions could not be obtained, because of low reactant volatility, the experimental data were fitted numerically to the integrated second order rate equation. The experimental conditions and rate coefficients are shown in table 1.

The results shown in table 1 can be rationalised by considering two competing factors, which affect the rate of addition to the double bond. The initial electrophilic attack of the the NO_3 radical on the alkene is influenced by the inductive effect of halogen atoms. Halogen atoms reduce electron density on the π -bond causing deactivation towards electrophilic attack. The effect depends on the proximity of the halogen substituent to the π -bond. This primary negative effect on rate is counterbalanced by stabilisation of the radical intermediate; the more stable the radical intermediate, the faster the rate. Halogen atoms have a greater stabilising effect than alkyl groups.

Table 1 The rates of reaction of halobutenes and 1-butene with the NO_3 radical

T K	P(total) Torr	$10^{-14}[\text{NO}_3]$ molecule cm^{-3}	$10^{-14}[\text{X}_0]$ molecule cm^{-3}	$10^{14}k$ $\text{cm}^3\text{molecule}^{-1}\text{s}^{-1}$
1-chloro-2-butene				
298	1.27-1.33	0.31	1.05-3.54	2.0 ± 0.7
373	1.39-1.41	0.29	0.24-1.72	5.0 ± 1.7
473	1.32-1.53	0.27-0.29	0.22-3.30	7.0 ± 5.5
2-chloro-1-butene				
299	1.43-1.54	0.29	0.81-4.18	1.7 ± 0.3
3-chloro-1-butene				
296	1.04-1.12	0.27	1.97-10.0	0.3 ± 0.07
373	1.25-1.42	0.25	1.27-8.75	1.2 ± 1.0
473	1.23-1.37	0.21-0.23	1.85-4.21	3.5 ± 1.2
2-chloro-2-butene				
298	1.34-1.36	0.32-0.40	0.68-1.18	11.0 ± 4.0
1-butene				
299	1.07-2.18	>0.51	1.94-24.1	1.0 ± 0.2
323	1.31-1.36	>0.43	2.66-9.85	1.6 ± 0.5
373	1.34-1.89	>0.39	2.99-8.01	1.8 ± 0.4
423	1.27-1.40	>0.37	1.91-9.39	2.9 ± 1.0
473	1.36-1.45	>0.32	1.80-6.50	3.6 ± 0.8
1-chloromethylpropene				
298	1.15-1.23	0.42-0.62	0.93-3.87	9.0 ± 2.3
3-chloromethylpropene				
298	1.20-1.23	0.48-0.50	1.10-7.56	2.5 ± 0.4
373	1.20-1.23	0.39-0.43	0.71-2.64	4.7 ± 0.5
473	1.16-1.20	0.32-0.34	0.77-2.63	12.3 ± 0.6
3-bromo-1-butene				
298	1.11-1.17	0.40-0.45	0.54-2.27	0.4 ± 0.1
4-bromo-1-butene				
298	1.13-1.19	0.51-0.64	1.36-2.47	0.5 ± 0.1
2-bromo-2-butene				
298	1.18-1.21	0.44-0.48	0.59-2.30	13.4 ± 0.1

The error limits are $\pm 2\sigma$.

Pressure dependence of the ozon recombination reaction

$$\text{O}(^3\text{P}) + \text{O}_2 + \text{M} \rightarrow \text{O}_3 + \text{M}$$
 between 1 and 1000 bar at temperatures from 90 to 370 K.

H.Hippler, R.Rahn und J.Troe,
 Institut für Physikalische Chemie der Universität Göttingen,
 Tammannstr.6, D-3400 Göttingen

The production of ozone from reaction of $\text{O}(^3\text{P})$ with O_2 is responsible for the build-up of the protecting atmospheric ozone-layer. In the low pressure regime the rate constant for this reaction shows an unusually large negative temperature coefficient¹⁾. A high-pressure limit²⁾ of this rate constant has been extrapolated from only a weak fall-off observed at room temperature at pressures around 100 bar. Therefore, we decided not only to extend the pressure range up to 1000 bar but also to vary the temperature between 90 and 370 K. We developed a high-pressure (1000 bar) low temperature (77 K) reaction cell for direct time-resolved UV-absorption spectroscopy. $\text{O}(^3\text{P})$ -atoms were generated by photodissociation of N_2O at 193 nm or of O_3 at 248 nm followed by efficient quenching of $\text{O}(^1\text{D})$ -atoms by N_2 . The formation of ozone was directly monitored via time-resolved UV absorption in the Hartley-continuum at 265 nm. The observed recombination rate constant k_{rec} shows a pressure dependence which significantly differs from typical fall-off behaviour. At low pressures we find a linear pressure-dependence which then levels off at intermediate pressures around 100 bar. At higher pressures however, instead of reaching a high-pressure limit, k_{rec} again increases with pressure. The largest rate coefficient measured lies about a factor of 10 above the previously extrapolated high-pressure limit. From the observed pressure and temperature dependence we conclude that more than one reaction mechanism is operative. Probably reactions on electronically excited state surfaces have to be included.

1. W.T.Rawlins, G.E.Caledonia und R.A.Armstrong,
 J.Chem.Phys.87, 5209, (1987)
2. A.E.Croce de Cobos und J.Troe,
 Int.J.Chem.Kinet.16, 1519, (1984)

REMPI-spectroscopy under high pressure conditions: Application to the recombination reaction $O(^3P) + NO + M \rightarrow NO_2 + M$.

R.Forster, H.Hippler, and J.Troe,
Institut für Physikalische Chemie der Universität Göttingen,
Tammannstr.6, D-3400 Göttingen

A new application of the REMPI-spectroscopy has been developed. In situ measurements of rates of elementary chemical reactions at high overall pressures were by now restricted to non-resonant techniques such as UV-absorption. Resonant methods are both powerful and sensitive at low and moderate pressures. At higher densities, however, severe disadvantages have to be overcome. Linewidths will be spectrally broadened and quenching of excited states will occur. Using REMPI the lifetime of intermediate electronically excited states can be controlled artificially by varying the pump rate of the ionisation step.

We constructed a high-pressure reaction cell for REMPI application. Recommended field strengths for separating the created charges were in the order of $10 - 100 \text{ V}\cdot\text{cm}^{-1}/\text{bar}$. We prepared $O(^3P)$ -atoms by photolysing N_2O at 193 nm followed by efficient quenching of the $O(^1D)$ -atoms by N_2 . The temporal evolution of the concentration of $O(^3P)$ -atoms was monitored using (2+1)-REMPI at 226 nm. With this new method we could for the first time directly measure the pressure dependence of the rate for the reaction $O(^3P) + NO + M \rightarrow NO_2 + M$ at pressures up to 200 atm of N_2 .

REACTIONS OF PRIMARY AND SECONDARY BUTOXY RADICALS IN OXYGEN AT ATMOSPHERIC PRESSURE

Adolphe HEISS, Jean TARDIEU de MALEISSYE, Krikor A. SAHETCHIAN

*Laboratoire de Chimie Générale, Unité de Recherche Associée au
CNRS n°870, Université P. et M. Curie, T. 55 E4, 4, Place Jussieu
75252 Paris cedex 05, France*

and Ian G. PITT

*School of Chemistry, University of Sydney, Sydney, NSW 2006
Australia*

Alkoxy radicals RO are important intermediates in the photo-oxidation and the low temperature oxidation of hydrocarbons, which play a crucial role in both atmospheric pollution and combustion chemistry. For RO radicals generated in the oxidation of hydrocarbon species having a carbon chain length $\geq C_4$, three modes of reactions have been identified : reaction with oxygen, decomposition and isomerization. Reaction mechanisms and kinetics of these pathways have seldom been well established ; much qualitative information exists, but only few reliable experimental data have been obtained.

In light of the discrepancies and complexities observed during the last 15 years, and for experiments performed *always in presence of NO_x species*, we were convinced to use a *NO_x-free system* [Carter et al.(1) found that "photochemical smog models validated against chamber data assuming only initial HONO as the radical source must be reevaluated"] and to study the pathways of RO radicals only in presence of O₂ and N₂.

Butoxy radicals, either n-BuO [$n\text{-CH}_3\text{CH}_2\text{CH}_2\text{CH}_2\text{O}^\bullet$] or s-BuO [$s\text{-C}_2\text{H}_5\text{CH}(\text{O}^\bullet)\text{CH}_3$], are generated in a flow system by the pyrolysis of di-butylperoxide, either n-(C₄H₉O)₂ or s-(C₄H₉O)₂ at concentrations \approx 30 ppm, in an atmosphere of O₂ and N₂ at atmospheric pressure. The studies of n-BuO and s-BuO radicals were performed at temperatures ranging from 393 to 453 K and from 353 to 503 K respectively. The reactions of RO radicals in presence of O₂ were studied by analysing end products formed, particularly peroxides and carbonyl compounds. The peroxides were qualitatively identified by thin-layer chromatography TLC and quantitatively analysed by high pressure liquid chromatography HPLC. Carbonyl compounds were quantitatively converted into the corresponding 2,4-DNPhhydrazones and then analysed by HPLC.

n-butoxy radicals

The peroxides shown and analysed are H₂O₂, C₃H₇O₂H, n-(C₄H₉O)₂ and a complex hydroperoxide which formula we assume to be HO(CH₂)₃CH₂OOH. The carbonyl compounds observed are butyraldehyde and formaldehyde.

s-butoxy radicals

The peroxides analysed are H₂O₂, C₂H₅O₂H and s-(C₄H₉O)₂. The carbonyl compounds are acetaldehyde (MeCHO), methylethylketone (MEK) and traces of propionaldehyde.

The decomposition of di-s-butylperoxide in O₂ is well described by a set of 14 elementary reactions. A good agreement was obtained between experiments and a computer simulation made, according to the Gear method. The reaction of decomposition (3) s-BuO \rightarrow C₂H₅ + MeCHO and the reaction (2) s-BuO + O₂ \rightarrow HO₂ + MEK were studied, in order to determine the ratio k₃/k₂. An investigation of the ratio (MeCHO/MEK), as a function of temperature, gave the Arrhenius plot of fig.1 representing $\ln(k_3/k_2[\text{O}_2])$ versus $1/T$, with 28 experimental points. The

least-squares fit to the data gives a difference of activation energies
 $E_3 - E_2 = 14.8 \pm 0.9 \text{ kcal.mol}^{-1}$; error = $\pm 1 \sigma$

By using the last revised value of Arrhenius parameters (2) for the reaction $s\text{-BuO} + \text{O}_2$ ($A_2 = 2.64 \times 10^{-14} \text{ cm}^3 \text{ molecule}^{-1} \text{ s}^{-1}$; $E_2 = 0.2 \text{ kcal.mol}^{-1}$), the following decomposition rate constant was obtained:

$$k_3 = 10^{13.8 \pm 0.3} \times \exp [(15.0 \pm 0.9 \text{ kcal}) / RT] \text{ s}^{-1}$$

It should be noticed that the ratio k_3/k_2 is independent of the actual value of k_2 . A good agreement is observed between this value of k_3 , obtained from experiments, and that deduced from an appropriate RRKM treatment (fig.2).

Fig.1 Arrhenius plot $\ln (k_3/k_2[\text{O}_2])$

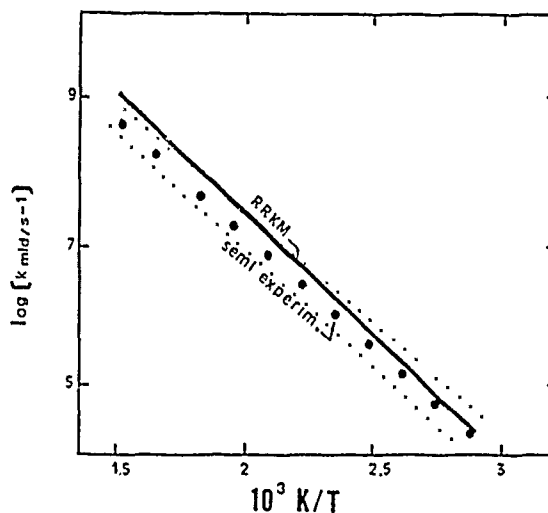
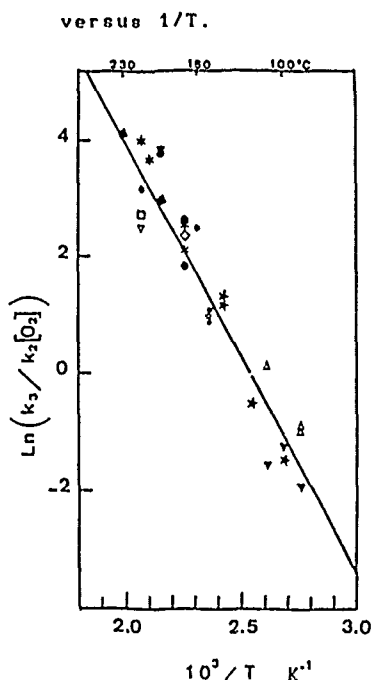


Fig.2 Arrhenius plot of the *s*-butoxy middle bond breaking channel (MBBC) as compared with the RRKM results (solid line).

An extrapolation of our data, to *room temperature under atmospheric conditions*, shows that the reaction of decomposition represents *less than 1% of the reaction $s\text{-BuO} + \text{O}_2$* .

In conclusion, oxygen is a medium well suited to the study of the different reaction pathways of alkoxy radicals. However, the study of *n*-butoxy radicals is much more difficult than that of *s*-butoxy, and this is very likely due to an isomerization reaction.

Under *atmospheric conditions*, the reaction with O_2 , yielding HO_2 and butanal (for *n*-BuO) or MEK (for *s*-BuO) is, by far, the main channel for both *n*-butoxy and *s*-butoxy radicals, at room temperature.

In the *field of combustion*, the reaction of decomposition of *s*BuO, producing C_2H_5 radicals and CH_3CHO , is the main pathway, the channel $s\text{-BuO} + \text{O}_2$ decreasing tremendously in importance as the temperature is increased. The rate constant of the decomposition reaction of *s*-BuO radicals has been determined. An RRKM calculation has been carried out that supports the experimental conclusions.

- 1) W.P.L. CARTER, R. ATKINSON, A.M. WINER, J.N. PITTS, Jr., *Int. J. Chem. Kinet.* 14 (1982) 1071.
- 2) R.J. BALLA, H.H. NELSON, J.R. McDONALD, *Chem. Phys.* 99 (1985) 323.

REACTION RATES OF SOME BENZYL TYPE RADICALS WITH O₂. NO,NO₂ BY
DISCHARGE FLOW LASER INDUCED FLUORESCENCE.

P. Devolder, A. Goumri, J-F. Pauwels, Sawerysyn
Laboratoire de Cinétique et Chimie de la Combustion
URA CNRS 876
Université des Sciences et techniques de Lille
59655 Villeneuve d'Ascq Cedex. FRANCE

The tropospheric oxidation of aromatic hydrocarbon is initiated by an attack by the radical OH. Both ring addition and abstraction are present for every hydrocarbon with variable relative importance. For methyl substituted aromatic hydrocarbons, (for example, toluene), the dominant path of the abstraction route produces a benzyl type radical (see for example R. Atkinson, Chem. Review, 1986, vol.86, p.69). We have investigated the reaction rates of a few benzyl type radicals with O₂ and atmospheric trace gas NO₂ and NO with the discharge flow technique. The radicals are generated by fluorine abstraction from the parent hydrocarbon and probed by Laser Induced Fluorescence in the visible range.

Rate constants with O₂, NO₂ and NO are (in 10⁻¹² cm³ molecule⁻¹ s⁻¹):
For p-fluorobenzyl : O₂:(0.82 ± 0.04); NO₂:(49 ± 2); NO:(10 ± 0.4)
For m-fluorobenzyl : O₂:(0.6 ± 0.05); NO₂:(48 ± 2); NO:(9.0 ± 0.4)
For o-methylbenzyl : O₂:(1.00 ± 0.05); NO₂:(50 ± 2)
For m-methylbenzyl : O₂:(1.10 ± 0.08); NO₂:(49.7 ± 1.4)

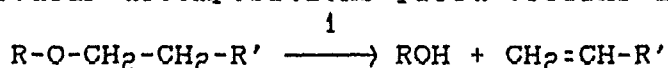
THERMAL DECOMPOSITION OF DIALKYL ETHERS

I. Seres¹ and L. Seres²¹*Institute of Inorganic and Analytical Chemistry,*²*Institute of Physical Chemistry,**Attila József University, Szeged, Hungary*

In an attempt to obtain data for a comparison of the reactivities of different dialkyl ethers, the thermal decompositions of methyl ethyl, diethyl, methyl *n*-propyl, methyl *i*-propyl, and methyl *t*-butyl ethers (MEE, DEE, MNPE, MIPE, MTBE) were studied in a static system at sub-atmospheric pressures and different temperatures. Product analysis was performed by gas-chromatography. Occasionally, C¹⁴-labelling was used to reveal precursor-product relations.

The experimental data obtained support the contribution of radical chain and molecular processes to the decomposition, in agreement with the literature data. Some of the primary products (aldehydes, alcohols and olefins) have similar reactivities to those of the parent compounds, while others (paraffins) are relatively stable. The initial rates of formation of all the products formed in higher than negligible quantities were determined. All the kinetic data derived were calculated from these data.

Molecular decompositions yield olefins and alcohols:



The Arrhenius parameters of reaction (1) have been determined and are shown in Table 1 together with the rate constants calculated for 700 K.

Table 1. Arrhenius parameters of reaction (1) and the calculated $K(700)$ values^a

Ether	E	log A	K(700)
MEE	254	12.2	$1.7 \cdot 10^{-7}$
DEE	256	12.7	$3.6 \cdot 10^{-7}$
MNPE	223	10.8	$1.2 \cdot 10^{-6}$
MIPE	278	15.2	$2.7 \cdot 10^{-6}$
MTBE	-	-	$5.9 \cdot 10^{-5}$

^a Units : kJ mol^{-1} and s^{-1}

The radical chain processes are initiated via C-O bond rupture. The radicals formed in the initiation or in chain steps yield primary products in H-abstractions (β radicals) and in decompositions (μ radicals). If there is a C-O or C-C bond in the β position to the radical centre, a radical is inclined to behave as a μ radical, while if only C-H bonds are present in the β position, the β character predominates. Thus, almost independently of the structure and size of the alkyl groups in the ether molecule, low molecular weight paraffins (CH_4 , C_2H_6 , C_3H_8) and higher molecular weight

olefins are formed as typical products besides the oxygenated compounds (alcohols and aldehydes).

In most of the reactions studied, more than one dominant alkyl radical must be considered as chain carrier, and the decompositions are so complex that even determination of the rate constant ratios becomes rather difficult.

In the case of diethyl ether decomposition, however, the only alkyl radical yielding products in significant amounts is ethyl, which provides an opportunity for determination of the rate constant of H-abstraction from the $-\text{CH}_2\text{-O-}$ group:

$$\log[k/\text{dm}^3 \text{ mol}^{-1} \text{ s}^{-1}] = (9.1 \pm 0.4) - (49.8 \pm 5.5) \text{ kJ mol}^{-1}/\Theta,$$

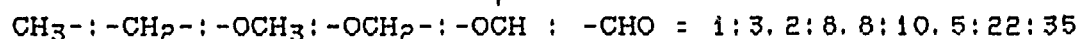
where $\Theta = RT \ln 10$.

For some other ethers, it was possible to estimate the relative rates of H-abstraction from different positions, assuming identical selectivities for the radicals involved (Table 2).

Table 2. Relative rates of H-abstractions from different donor groups at 700 K

Ether	$-\text{OCH}_2-$	$-\text{OCH}_2-$	$-\text{OCH}_2-$	$-\text{OCH}_2-$	$-\text{OCH}_3$	$-\text{OCH}_3$
	$-\text{CH}_3$	$-\text{CH}_2-$	$-\text{OCH}_3$	$-\text{CHO}$	$-\text{CH}_2-$	$-\text{O-H}$
MEE	-	-	1.2	0.3	-	-
DEE	10.5	-	-	0.3	-	-
MNPE	-	3.3	1.2	0.3-0.5	2.7	0.4

The high reactivity of the C-H bonds in the groups adjacent to the ether oxygen is apparent. Finally, the relative donor reactivities of different groups to H-abstractions were calculated from the data given in Table 2:



The relative contributions of molecular and radical processes to the overall decomposition were also calculated (Table 3). The contribution of molecular processes predominates in the decomposition of MTBE, and it is significant in ethers with alkyl groups $\geq \text{C}_3$.

Table 3. Relative contributions of molecular and radical processes to the overall decompositions^a
($T = 700 \text{ K}$, $c = 2.2 \cdot 10^{-3} \text{ mol dm}^{-3}$)

Ether	$v(\text{molecular})$	%	$v(\text{radical})$	%
MEE	$3.7 \cdot 10^{-10}$	2.0	$7.6 \cdot 10^{-8}$	98
DEE	$7.9 \cdot 10^{-10}$	1.2	$6.5 \cdot 10^{-8}$	98.8
MNPE	$2.6 \cdot 10^{-9}$	10	$2.6 \cdot 10^{-8}$	90
MIPE	$5.9 \cdot 10^{-9}$	14	$4.1 \cdot 10^{-8}$	86
MTBE	$1.3 \cdot 10^{-8}$	99.7	$3.7 \cdot 10^{-10}$	0.3

^a Units : $\text{mol dm}^{-3} \text{ s}^{-1}$

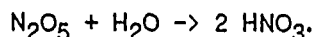
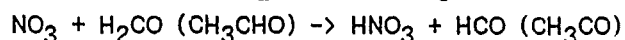
Measurement of Gaseous Nitric Acid in Europe and on the Atlantic Ocean

Th. Papenbrock and F. Stuhl

Physikalische Chemie I, Ruhr-Universität, D-4630 Bochum, FRG

ABSTRACT

Nitric Acid (HNO_3) is a major final product of atmospheric NO_x and HO_x chemistry. It is produced by the following reactions



It is hence indicative for two of the most important cycles (HO_x and NO_x) in clean and polluted atmospheres. It furthermore contributes significantly to the acidity of rain.

We have recently developed a direct, selective, continuous, sensitive and fast method to detect HNO_3 in the atmosphere. This method is based on the sequential two-photon ArF(193nm)-laser photolysis of HNO_3 yielding excited $\text{OH}(\text{A}^2\Sigma^+)$. For the detection of gaseous HNO_3 in ambient air, the $\text{OH}(\text{A} \rightarrow \text{X})$ -fluorescence intensity is taken as a measure of the HNO_3 mixing ratio. At the present time, the detection limit for long integration times is 0.03 ppbv and for short times about 0.2 ppbv. Field measurements were performed in Bochum (RUB), Jülich (KFA), Black Forest (UBA), Petten, Netherlands (ECN) and on the occasion of three trips across the Atlantic Ocean. Whenever possible the data were compared with data measured simultaneously by other methods such as denuders. The basic features of the photolysis method will be summarised and field measurements will be presented and discussed during the presentation.

We gratefully acknowledge financial support by BMFT.

KINETICS OF THE REACTION $\text{BrO} + \text{NO}_2 + \text{M} \longrightarrow \text{BrONO}_2 + \text{M}$ IN THE
TEMPERATURE RANGE 263-343 K.

F. Danis, F. Caralp, J. Masanet and R. Lesclaux

Laboratoire de Photophysique et Photochimie Moléculaire,
Université de Bordeaux I, 33405 TALENCE Cedex, France

The rate constant of the reaction $\text{BrO} + \text{NO}_2 + \text{M} \longrightarrow \text{BrONO}_2 + \text{M}$ ($\text{M} = \text{O}_2$) has been measured at low pressure, $P < 12$ Torr, and as a function of temperature from 263 to 343 K. The rate expression obtained is $k_1(0) = (4.2 \pm 0.8) \times 10^{-31} (T/298)^{-2.0 \pm 0.5}$ with $F_c = \exp(-T/325)$. This expression was obtained by using for $k_1(\infty)$ the rate expression reported in references [4] and [5] : $k_1(\infty) = 2.0 \times 10^{-11} (T/298)^{-1}$. A theoretical analysis of this reaction, using both RRKM and Troe's simplified calculations, accounts correctly for the temperature dependence but not for the absolute value of $k_1(0)$. These results are discussed in connection with previous findings concerning equivalent reactions of halogen oxides.

KINETICS STUDIES RELEVANT TO UNDERSTANDING THE HALOGEN-INITIATED OXIDATION OF ATMOSPHERIC DIMETHYLSULFIDE

E. P. Daykin, J. M. Nicovich, K. D. Kreutter, M. Chin, and P. H. WineMolecular Sciences Branch, Georgia Tech Research Institute,
Georgia Institute of Technology, Atlanta, GA 30332, USA

Since marine emissions of dimethylsulfide (CH_3SCH_3 , DMS) account for about 25% of the global sulfur flux into the atmosphere, a detailed understanding of atmospheric DMS oxidation pathways is central to an assessment of the relative contributions of biogenic and anthropogenic sulfur to such problems as acid rain, visibility reduction, and climate regulation. Recently, it has been suggested that halogen monoxide radicals may be important initiators of DMS oxidation [1]. To further our understanding of the role of halogen species in marine sulfur chemistry, we have initiated a series of direct kinetic studies of the elementary reactions of halogen atoms and halogen monoxide radicals with DMS.

The kinetics of the $\text{IO} + \text{DMS}$ reaction have been investigated at 298K using time-resolved long pathlength absorption spectroscopy to monitor the temporal behavior of IO following 351 nm laser flash photolysis of $\text{NO}_2/\text{I}_2/\text{DMS}/\text{N}_2/\text{O}_2$ mixtures. We obtain an upper limit bimolecular rate constant for the $\text{IO} + \text{DMS}$ reaction of $3.5 \times 10^{-14} \text{ cm}^3 \text{ molecule}^{-1} \text{ s}^{-1}$; this upper limit is nearly three orders of magnitude slower than previously reported measurements [1]. Our results suggest that coupling of the marine sulfur and iodine cycles via the $\text{IO} + \text{DMS}$ reaction is negligible.

The kinetics of the reactions of atomic bromine with DMS have been studied as a function of temperature and pressure using time-resolved resonance fluorescence spectroscopy to monitor the temporal behavior of $\text{Br}(^2\text{P}_{3/2})$ following 266 nm laser flash photolysis of $\text{CF}_2\text{Br}_2/\text{DMS}/\text{N}_2$ mixtures. Evidence for both reversible adduct formation and hydrogen abstraction pathways has been observed. Equilibrium constants for adduct formation and dissociation have been determined as a function of temperature; from these results, the S-Br bond strength in DMS-Br is estimated to be 14 kcal mole⁻¹. The activation energy for the $\text{Br} + \text{DMS}$ hydrogen abstraction reaction is found to be 4.4 kcal mole⁻¹ –

considerably smaller than the value expected based on the literature value for the CH_3SCH_2 heat of formation [2].

A laser flash photolysis-long pathlength absorption technique was employed to search for BrO production from the reaction of the DMS-Br adduct with O_2 . No BrO production was observed, but a strong absorption was observed at 338 nm which, based on its temporal behavior and invariance to substitution of N_2 for O_2 as the bath gas, is attributed to DMS-Br.

This work was supported by the National Science Foundation.

-
1. I. Barnes, K. H. Becker, D. Martin, P. Carlier, G. Mouvier, J. L. Jourdain, G. Laverdet, and G. LeBras, in Biogenic Sulfur in the Environment, E. Saltzman and W. Cooper, editors, ACS Symposium Series No. 393, 1989, pages 464-475, and references therein.
 2. L. G. S. Shum and S. W. Benson, *Int. J. Chem. Kinet.* **17**, 277 (1985).

KINETIC STUDY OF THE REACTIONS ESSENTIAL FOR THE IODINE DESTRUCTION CYCLE OF ATMOSPHERIC OZONE.

Institute of Energy Problems of Chemical Physics, Academy of Sciences of the USSR.

Buben S.N., Larin I.K., Messineva N.A., and Trophimova E.M.

The gas-flow system involving the detection of iodine atoms by resonance fluorescence was used for studying the reactions of I atoms and IO radicals. Concentrations of active particles were low enough for secondary reactions not to be taken into account.

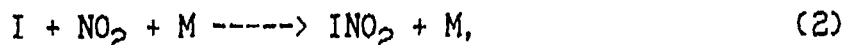
Rate constant and activation energy for reaction



were measured over the temperature range 231-337 K:

$$k = (2,3 \pm 0,2) \cdot 10^{-11} \exp[(-1760 \pm 30) / RT] \text{ cm}^3/\text{sec}.$$

For the reaction



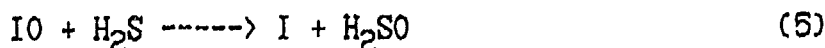
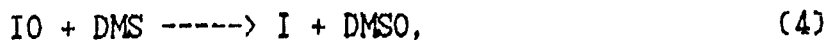
where $M = N_2, O_2, He, Ar$ ($T=298 \text{ K}$), k values were $(3,2 \pm 0,6), (2,7 \pm 0,5), (1,7 \pm 0,3), (2,1 \pm 0,4) \cdot 10^{-31} \text{ cm}^6/\text{sec}$, respectively.

The reaction



was shown to be homogeneous with $k_3 = 2,2 \cdot 10^{-11} \text{ cm}^3/\text{sec}$ at $T=289 \text{ K}$ being in good agreement with [1,2].

Rate constants of reactions IO with dimethylsulfide and H_2S



were also estimated. The value of k_4 differs greatly from that obtained in [3,4].

Accommodation coefficients for iodine atoms and IO radicals on different surfaces were measured also.

Literature.

1. Ray G.W., R.T. Watson, J. Phys. Chem., 1981, v. 85, p. 2955.
2. Inoue Gen, Makoto Sozaki, Nobuaki Washide, J. Chem. Phys., 1983, v. 79, p. 4730.
3. Martine D., J.L. Jourdain, G. Laverdet, G. Le... Int. J. Chem. Kin. 1987, v. 19, p. 503.
4. Barnes J., K.H. Becker, P. Carlier, G. Mouvier, Int. J. Chem. Kin., 1987, v. 19, p. 483.

INVESTIGATION OF THE ELEMENTARY PROCESSES WHICH DETERMINE OZONE DEPLETION POTENTIALS OF THE SOME HALOGENATED HYDROCARBONS.

Orkin V.L., Khamaganov V.G., Kasimovskaya E.E.

Institute of Energy Problems of Chemical Physics,
Academy of Sciences of the USSR, Moscow.

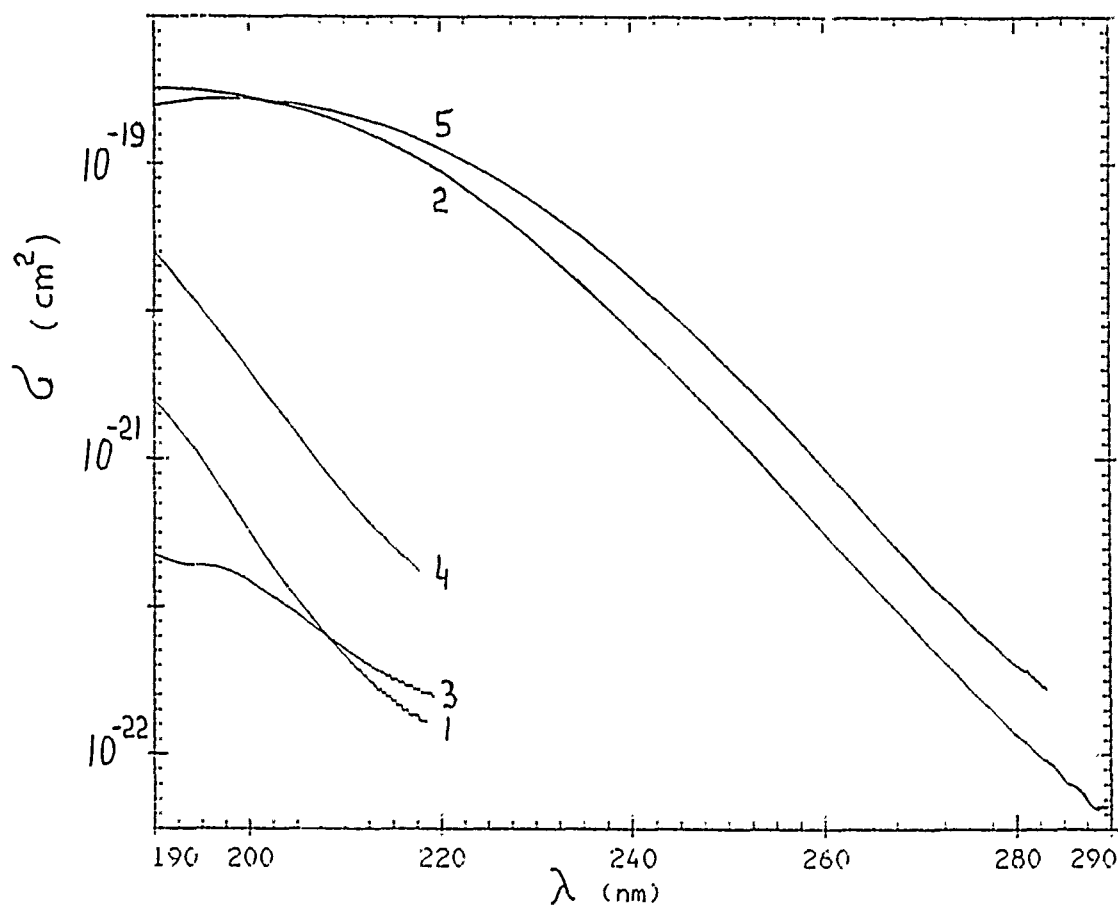
Main processes which determine a danger of halogenated hydrocarbons for Earth's stratospheric ozone are the reactions with atmospheric OH-radicals and photodissociation under UV-solar radiation.

Precision laboratory studies of that processes for a set of halogenated methanes and ethanes, which are considered to be alternative freons or hallons: CHClF_2 , CHBrF_2 , $\text{CH}_2\text{F-CF}_3$, CHClF-CClF_2 , CHBrF-CF_3 , were carried out. Besides this, the rate constants of reactions between OH-radicals and HBr, HI were determined. These reactions result in a regeneration of halogen atoms in the kinetic cycles of ozone depletion. The reaction rate constants of all these substances with OH-radicals determined at temperature range 298-370 K are presented in an Arrhenius form $k(T) = A * \exp\{-E/RT\}$:

molecule	$A * 10^{13}, \text{cm}^3/\text{s}$	$E/R, \text{K}$	$k(298) * 10^{14}, \text{cm}^3/\text{s}$
CHClF_2	7.1	1480 ± 50	0.50 ± 0.04
CHBrF_2	7.7	1270 ± 80	1.12 ± 0.06
$\text{CH}_2\text{F-CF}_3$	9.6	1570 ± 100	0.49 ± 0.04
CHClF-CClF_2	7.2	1200 ± 110	1.25 ± 0.11
CHBrF-CF_3	7.4	1080 ± 50	1.95 ± 0.07
HBr	$2.4 * 10^2$	260 ± 50	$(1.00 \pm 0.08) * 10^3$
HI	$3.0 * 10^2$	0 ± 100	$(3.0 \pm 0.5) * 10^3$

Experiments were done by a precision discharge flow technique with an EPR detection of radicals.

The UV-absorption cross sections in a range of 190-300 nm were obtained at either 212 or 298 K using *Shimadzu UV-3100* spectrophotometer. Figure shows the absorption cross sections obtained (units are cm^2 , base is e , $T = 298 \text{ K}$). Near a center of "stratospheric transparency window" at $\lambda = 200 \text{ nm}$ absorption cross sections are: 0.033, 28, 0.015, 0.38, 27 (units are 10^{-20} cm^2) for CHClF_2 , CHBrF_2 , $\text{CH}_2\text{F-CF}_3$, CHClF-CClF_2 , CHBrF-CF_3 respectively.



1- CHClF_2 ; 2- CHBrF_2 ; 3- $\text{CH}_2\text{F-CF}_3$; 4- CHClF-CClF_2 ; 5- CHBrF-CF_3

EXPERIMENTAL AND THEORETICAL STUDIES OF RADICAL INTERMEDIATES IN THE ATMOSPHERIC OXIDATION OF CS₂

J. CHAMBCUX-CROSNIER, F. JORAND, V. VIOSSAT, K. A. SAHETCHIAN

Laboratoire de Chimie Générale, U. R. A. - C. N. R. S.

Université P. et M. Curie - T. 55 E4,

4 Place Jussieu, F-752 52 PARIS Cedex 05, FRANCE

C. CHACHATY

IRDI/DESICP Département de Physico-Chimie

C. E. N. SACLAY, F-91191 GIF sur YVETTE Cedex, FRANCE

S. LUNELL, M.-B. HUANG

Department of Quantum Chemistry, Uppsala University

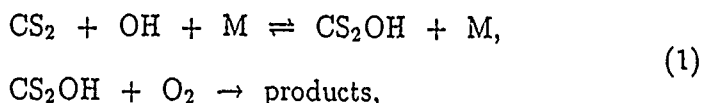
Box 518, S-75120 Uppsala, SWEDEN

F. ZABEL

Physikalische Chemie, Universität-Gesamthochschule Wuppertal

D-56 Wuppertal 1, WEST GERMANY

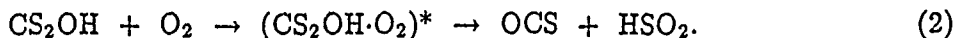
It is now well established that the OH initiated oxidation of CS₂ in the presence of oxygen proceeds via the reactions [1 - 3]:



The mechanism leading to the observed final products COS and SO₂ is, however, unknown. To date, CS₂OH has not been directly observed nor have any other intermediates been identified. In the present work, an attempt is made to identify intermediates in the OH initiated oxidation of CS₂ both by theoretical calculations and by ESR spectrometry.

Quantum chemical calculations [4] show that OH reacts with CS₂ without an energy barrier to form an adduct where OH is bonded to the carbon atom. Direct transfer of the proton from the oxygen atom to one of the sulphur atoms followed by a cleavage of the carbon - sulphur bond could then produce COS, which is one of the observed final products.

The calculations show, however, that such a proton transfer is energetically improbable. It is therefore more likely that O_2 is attached to one of the sulphur atoms prior to the proton transfer, suggesting the following mechanism:



The aim of the experiments is:

- 1) to prepare HS and HSO_2 radicals and to identify their ESR spectra.
- 2) to characterize the free radicals present during the reaction of CS_2 with OH in the presence of O_2 .

Pure solid H_2S free from O_2 is collected in a glass bulb kept in liquid nitrogen. The bulb is sealed, and while still in liquid nitrogen it is lighted by a UV beam and put into the resonant cavity of an ESR spectrometer. The spectrum obtained corresponds to the HS radical.

A similar experiment is performed, but with O_2 added to H_2S . The ESR spectrum obtained corresponds to the superposition of HSO_2 with a small amount of HS.

In order to characterize the radicals issued from the reaction $CS_2 + OH$ in the presence of O_2 , the gaseous mixture $CS_2 + O_2 + H_2O_2$, at a pressure of ≈ 100 mb, is lighted by a UV beam. A small part of the reactant mixture is withdrawn by a microprobe and trapped on the cold finger located in the resonant cavity of the ESR spectrometer.

The ESR spectrum obtained is found to correspond to a superposition of HSO_2 with a small amount of HO_2 .

Both the experimental ESR measurements and the quantum chemical calculations are hence found to support the reaction mechanism proposed in equation (2).

References:

- [1] B. M. R. Jones and S. A. Penkett, *Chem. Phys. Lett.* 88 (1982) 372.
- [2] B. M. R. Jones, R. A. Cox, and S. A. Penkett, *J. Atmos. Chem.* 1 (1983) 65.
- [3] I. Barnes, K. H. Becker, E. H. Fink, A. Reiner, F. Zabel, and H. Niki, *Int. J. Chem. Kinet.* 15 (1983) 631.
- [4] S. Lunell, M.-B. Huang, K. A. Sahetchian, C. Chachaty, and F. Zabel, *J. Chem. Soc., Chem. Commun* (1990) 000.

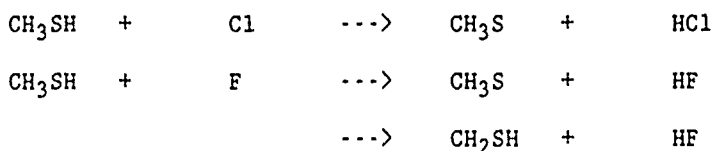
Ultraviolet absorption spectrum and kinetics of CH_3S and CH_2SH radicalC Anastasi*, M Broomfield*, O-J Nielsen⁺ and P Pagsberg⁺⁺ Department of Chemistry, Riso National Laboratory, DK-4000, Roskilde, Denmark

* Department of Chemistry, University of York, Heslington, York, YO1 5DD, England

Reduced sulphur compounds form an important part of the acid precipitation cycle. Most natural sulphur emissions are of this type, and so it is important to have a clear understanding of the oxidation mechanisms of these species. This will enable us to assess the anthropogenic contribution to the atmospheric sulphur burden. The situation at present is unclear with many areas of uncertainty and contradiction.

We have recently studied the ultraviolet spectrum and kinetics of CH_2OH^1 . Tentative observations of CH_2SH , the sulphur analogue of this radical, have also been made^{2,3}. However, it has not been widely considered in spectroscopic or kinetic studies^{4,5}.

We have recently made direct observations of the ultraviolet absorption spectrum in the range 220 - 400 nm of transient species formed by attack of chlorine and fluorine atoms on CH_3SH . The spectra have been assigned predominantly to the CH_3S radical in the case of chlorine atoms, and to both the CH_3S and CH_2SH radicals in the case of F atoms.



The kinetics of these species have been investigated using the pulse radiolysis/kinetic absorption and molecular modulation spectroscopy techniques. Rate constants for the self-reaction of these species and for the reactions with O_2 , NO and NO_2 have been measured at room temperature.

REFERENCES

1. P Pagsberg, J Munk, C Anastasi and V J Simpson; J Phys Chem, 93, 5162 (1989)
2. D J Nesbitt and S R Leone; J Chem Phys, 75, 4949 (1981)
3. M Jacox; Can J Chem, 61, 1036 (1983)
4. A B Callear, D R Dickson; JCS Faraday Trans, 66, 1987 (1970)
5. B J Finlayson-Pitts and J N Pitts; 'Atmospheric Chemistry', Wiley (1986)

ATMOSPHERIC TRANSFORMATION OF BENZENE, TOLUENE AND PHENOL BY OH: CONSECUTIVE REACTIONS OF THE ADDUCTS WITH NO_x AND O₂

Rainald Koch, Manfred Siese and Cornelius Zetzsch

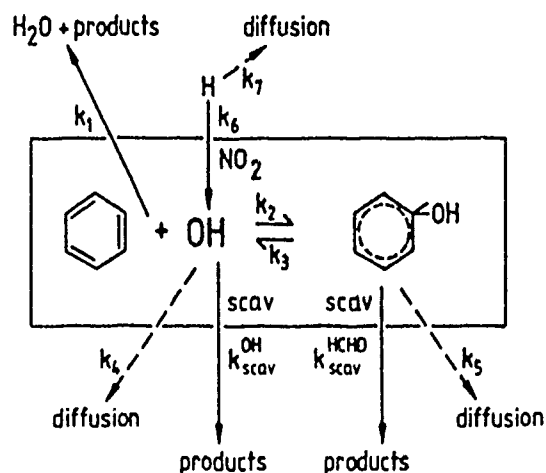
Fraunhofer-Institut für Toxikologie und Aerosolforschung,
Nikolai-Fuchs-Straße 1, D 3000 Hannover 61, FRG

Addition of OH is the main atmospheric reaction path of aromatics, and the abstraction channel is a minor pathway only. Since the formation of the adduct is reversible, further reactions of the adduct (presumably with O₂, NO or NO₂) are required to remove the aromatic pollutant from the atmosphere. The behaviour of the adducts of OH with the aromatics benzene, toluene and phenol is investigated employing the pulsed vuv photolysis/resonance fluorescence method at 130 mbar in Ar in the presence of NO, NO₂ and O₂ at various temperatures from 300 to 350K.

Biexponential decays of OH are observed in the presence of the aromatics as expected from the general solution of the appropriate system of differential equations:

$$\begin{aligned} d[\text{OH}]/dt &= -a [\text{OH}] + b [\text{adduct}]; \\ d[\text{adduct}]/dt &= c [\text{OH}] - d [\text{adduct}], \end{aligned}$$

where the parameters a - d contain k₁-k₅, the elementary reactions and physical processes addition, unimolecular decay and abstraction and diffusive loss of OH and the adduct (1).



In favorable cases, a complete data set of observed amplitude ratios and decay rates of the biexponential decays for a manifold of temperatures and concentrations can be used to separate the different rate constants using a non linear least squares fit routine. The rate constants are treated as adjustable parameters. The minimization is performed by the successive use of a simplex and a gradient function minimization, where the function is built up by the expressions $[(\text{obs}-\text{calc})/\text{error}_{\text{obs}}]^2$ for the amplitude ratios and the experimental decay rates, respectively. The results are Arrhenius expressions for addition, unimolecular decay and abstraction, and T² expressions for the diffusion terms.

The aromatics benzene, toluene and phenol are reinvestigated in order to obtain a consistent data set for the subsequent analysis of the reactions of the adducts with NO, NO₂ and O₂. A simultaneous fit of the amplitude ratios and decay rates of the biexponential decays at several temperatures enables us to observe the very minor abstraction channel even at room temperature. The mathematical procedure, limitations and confidence intervals for the results of the global fit will be discussed for all studied aromatics.

After eliminating NO₂ impurities from the NO sample, the reactivity of the adducts against NO was observed to vanish. Upper limits of $<10^{-14}$, $<3 \cdot 10^{-14}$ and $<7 \cdot 10^{-14} \text{ cm}^3 \text{ s}^{-1}$ are obtained for the reactions of benzene-OH, toluene-OH and phenol-OH with NO.

Preliminary values of $2 \cdot 10^{-16} \text{ cm}^3 \text{ s}^{-1}$ and $5 \cdot 10^{-16} \text{ cm}^3 \text{ s}^{-1}$, respectively, are obtained for the reactions of benzene-OH and toluene-OH with O₂, respectively, at room temperature from a similar quantitative treatment of the biexponential decays of OH. In the case of benzene-OH, the reaction of the adduct is determined from 300 to 350 K, yielding the Arrhenius expression:

$$k_{\text{O}_2} = 6.6 \times 10^{-15} \exp(-1025 \text{ K}/T) \text{ cm}^3 \text{ s}^{-1}.$$

For these measurements, the maximum concentration of O₂ is limited to about 10^{17} cm^{-3} by the quenching of the resonance fluorescence signal and by the absorption of the VUV flash light. The room temperature result for benzene-OH + O₂ has been confirmed in our laboratory at higher concentrations of O₂ using the cw-uv-laser longpath absorption technique.

Triexponential decays of OH are observed in the presence of NO₂ and aromatics that can likewise be evaluated quantitatively with an extended reaction mechanism (2). Rate constants of (2.5 ± 0.6) , (3.7 ± 0.6) and $(3.4 \pm 0.6) \cdot 10^{-11} \text{ cm}^3 \text{ s}^{-1}$ are obtained for the reactions of benzene-OH, toluene-OH and phenol-OH with NO₂, fairly independent of temperature.

Acknowledgement This work was supported by the Bundesminister für Forschung und Technologie in the programme EUROTRAC/LACTOZ (contract 07EU705). Furthermore, the authors thank Dr. Pascal Devolder for participating in the initial phase of the measurements of toluene-OH with NO and Dipl. Phys. R. Knispel for supplying data by the cw-UV-laser absorption technique.

References

1. A. Wahner and C. Zetzsch, J. Phys. Chem. **87**, 4945-4951 (1983)
2. C. Zetzsch, R. Koch, M. Siese and F. Witte in: Physico-Chemical Behaviour of Atmospheric Pollutants, pp. 320-327, Kluwer, Dordrecht, 1990.

KINETICS AND MECHANISM OF NO_x AND SO_2 OXIDATION IN WET AIR BY ELECTRON BEAM IRRADIATION

E.V. Belousova, A.V. Polyakova, A.P. Purmal, A.P. Shvedchikov, S.O. Travin

Institute of Chemical Physics USSR Academy of Sciences
117334 Moscow, V-334, Kosygin st., 4, USSR

A general kinetic mechanism for fast electrons (dose rate 3 KGy/s, dose 0-200 KGy) induced oxidation of NO_x and SO_2 in the mixtures $\text{H}_2\text{-O}_2\text{-H}_2\text{O}$ (2-5 v.%) - NO_x (0.05 v.%) - SO_2 (0.01-5 v.%) is formulated. We have used chemical kinetics modelling as a tool to analyze the SO_2 and NO_x removal processes in exhaust gases by electron-beam irradiation. We used a reaction set with more than 40 measured rate constants for H, N, O, S atoms, OH, HO_2 , HOSO_2 , HOSO_3 , SO, NO_3 radicals and intermediate molecules (O_3 , SO_3 , N_2O , etc.) to fit the available data. The rates of primary species (H, N, O, OH) production have been used from literature^{/1/}.

Dose dependence of NO_x and SO_2 decay and production of intermediates (atoms, radicals, molecules) and final products (H_2SO_4 , S, etc.) at 70-200°C have been calculated. The main oxidizing particles are OH, O and HO_2 , the dominant removal mechanism of SO_2 includes the reactions: $\text{SO}_2 + \text{OH} \longrightarrow \text{HOSO}_2 \xrightarrow{-\text{H}_2\text{O}} \text{HO}_2 + \text{SO}_3 \xrightarrow{-\text{H}_2\text{O}} \text{H}_2\text{SO}_4$ with production of H_2SO_4 as a final product.

At higher concentrations of water vapours radiation-chemical yield $G(-\text{SO}_2)$ increases because in such conditions the concentration of OH radicals increases also. At low concentrations of H_2O and O_2 and at high temperatures the rate of sulfur production increases (reaction $\text{SO} + \text{SO} \longrightarrow \text{S} + \text{SO}_2$). At low concentration of SO_2 $G(-\text{SO}_2)$ diminishes. For example in mixtures containing 0.5 and 0.1 v.% SO_2 and 5 v.% H_2O at 150°C $G(-\text{SO}_2)$ drops from 17 to 6 molecules/100 eV. Additions of H₂O (0.02 - 0.1 v.%) considerably decreases $G(-\text{SO}_2)$. The calculated data correlates with experimental results^{/2,3/}.

1. F. Dusi et al., References:

Radiat. Phys. Chem., 1965, 25, 321-3, pp. 47-55

2. A. P. Shvedchikov et al., Radiat. Phys. Chem., 1983, 31, 321-3, pp. 15-19

3. S. Machi et al., Radiat. Phys. Chem., 1977, 9, pp. 371-383

A Study of the Reaction Kinetics
of the Vinyl Radical with Methyl and Hydrogen Atoms

A. Fahr, A. Laufer, R. Klein and W. Braun

Chemical Kinetic Division
National Institute of Standards and Technology
Gaithersburg, Maryland 20899

The vinyl radical is the simplest unsaturated hydrocarbon radical. Vinyl chemistry is expected to play an important role in high temperature kinetics and in the chemistry of planetary atmospheres.

The combination kinetics of vinyl radicals has been measured previously, using the photochemical dissociation of divinyl mercury (DVM) as the vinyl source and by monitoring a newly identified vinyl vuv absorption band¹. In the present work other sources of vinyl have been investigated through detection of the combination product, butadiene in the far uv.

An important objective of the present work is to characterize photodissociation channels of precursor molecules and the reaction kinetics of vinyl radical reactions with various additives such as methyl and hydrogen.

Using the present method reasonable agreement has been found for the rate constant of vinyl combination and rate constants for vinyl plus methyl and vinyl plus hydrogen have been determined. Quantum yields for the photodissociation of divinyl mercury, vinyl iodide and vinyl bromide have been determined using a new apparatus capable of measuring directly dissociation of parent and the production of transient species (at about the 1% absorption level).

The methodology involves the excimer laser photodecomposition of various vinyl precursor molecules either at 193 nm or 248 nm, employing an excimer laser, and the careful measurement of its percent dissociation. The transient and stable species produced are monitored in the far uv and vacuum uv. Chromatographic end product analysis are used to corroborate and complement the optical results. Real time temporal results coupled with detailed modelling allow for rate constant determinations. Results obtained with and without titrant additives allow sorting out complicating reactions that would otherwise be difficult to identify.

Some quantitative results are given in the following table:

Reaction	Radical Source	$k/\text{cm}^3 \text{ molecule}^{-1} \text{ s}^{-1}$
$\text{C}_2\text{H}_3 + \text{C}_2\text{H}_3$	DVM, (248 nm)	$1.1 * 10^{-10}$
$\text{CH}_3 + \text{CH}_3$	CH_3I , (248 nm)	$5.4 * 10^{-11}$
$\text{C}_2\text{H}_3 + \text{H}$	$\text{C}_2\text{H}_3\text{I}$, (198 nm)	$\sim 1 * 10^{-10}$
$\text{C}_2\text{H}_3 + \text{CH}_3$	$\text{C}_2\text{H}_3\text{I} + \text{AzoMe}$ (198 nm)	$9.5 * 10^{-11}$

Reference:

1. A. Fahr and A. H. Laufer, J. Phys. Chem., 726, 94, (1990).

Ultra-Trace Analysis of NO by High Resolution Laser Fluorescence and Ionisation Spectroscopy

M. Hippler, A.J. Yates and J. Pfab
Heriot-Watt University, Edinburgh

The nitric oxide molecule is of key importance in atmospheric chemistry since its concentration controls the level of ozone and other oxidants in the lower atmosphere. It also acts as a precursor to the formation of nitric acid (HNO_3). There is a lack of reliable measurements of NO in non-urban environments and consequently there is much uncertainty in the estimates of the contribution of NO to the global budget of tropospheric O_3 and HNO_3 .

Measurements of NO in the low ppb range are not very reliable and require expensive and complex instruments, long analysis times and considerable operator experience. The recent state-of-the-art has been summarised in an intercomparison study of chemiluminescence (CL) and laser-induced fluorescence (LIF) instruments¹, which highlighted the difficulty of obtaining reliable measurements of NO mixing ratios in the part per trillion (1 in 10^{12}) range¹.

The main objective of our work is to demonstrate the use of a pulsed jet-LIF instrument for measurements of atmospheric NO in the difficult but important sub-ppb range. Measurements that are not affected by interference from other NO-containing air pollutants and free from artefacts are important for atmospheric modelling studies. A further aim is to provide a viable alternative to the well-developed chemiluminescence instruments. Samples are jet-cooled by pulsed expansion with a rare gas through circular or slit-shaped orifices, and NO is analysed by one- or two-photon LIF utilising the A, C or D state with simple parallel-plate-detection of the ions.

Recent results on detection limits and interference effects will be reported, and a comparison of different laser excitation and detection techniques will be presented.

Reference

1. J.M. Hoell, G. Gregory, D.D. Davies, B.A. Ridley et al. J. Geophys. Res., 92, 1995 (1987).

Possible Abiotic Sources of N₂O

D. Maric, J. P. Burrows and G. K. Moortgat

Max-Planck-Institut für Chemie, D-6500 Mainz F.R.G.

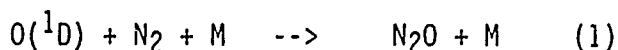
ABSTRACT

Nitrous Oxide, N₂O, plays an important role in the chemistry and physics of the atmosphere. It is thought to be the most important source of stratospheric NO_x (NO+NO₂) and is one of the "greenhouse" gases, whose tropospheric concentration has been found to be increasing.

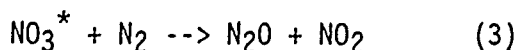
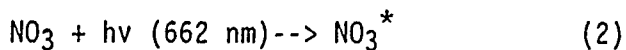
The most important atmospheric source of N₂O is the bacterial decomposition of biomass in soils and possibly in the oceans. As N₂O reacts slowly with OH and is photolysed only at short wavelengths, its lifetime in the troposphere is long and the major loss occurs by transport into the stratosphere, where it can be photolysed or react with O(¹D).

It is of interest to investigate whether there are any other atmospheric sources of N₂O. In this study three possible abiotic sources of N₂O have been investigated and their importance for the global budget of N₂O evaluated:

i) the slow reaction between O(¹D) and N₂:



ii) the proposition that excited NO₃ may react with N₂ (Zellner, private communication):



iii) the irradiation of NO₂ and NO at wavelengths shorter than 260 nm has been shown in this study to lead to the formation of N₂O. The mechanism of this source is at present under investigation.

A schematic of the apparatus used in these studies is shown in figure 1. UV visible absorption spectroscopy was used where appropriate to determine the concentrations of reactants or products. The mixing ratio of N_2O in the system was determined by sampling into a Gas Chromatograph equipped with an electron capture detector. The minimum detectable amount of N_2O in this arrangement was 3 ppbv.

In the study of NO and NO_2 photolysis, relatively small amounts of NO_2 or NO were used. The production of N_2O in the photolysis of NO was observed to be proportional to $[\text{NO}]^{1/2}$. The simplest explanation of the data requires NO dimer formation in agreement with previous suggestions [1, 2].

The results obtained from an experimental study of the three possible sources of N_2O will be described, and their potential relevance for atmospheric chemistry discussed.

References

- [1] D. H. Volman J. Photochem. 25 15-19 (1984)
- [2] D. H. Volman J. Photochem. and Photobio. A: Chemistry 51 1-7 (1990)

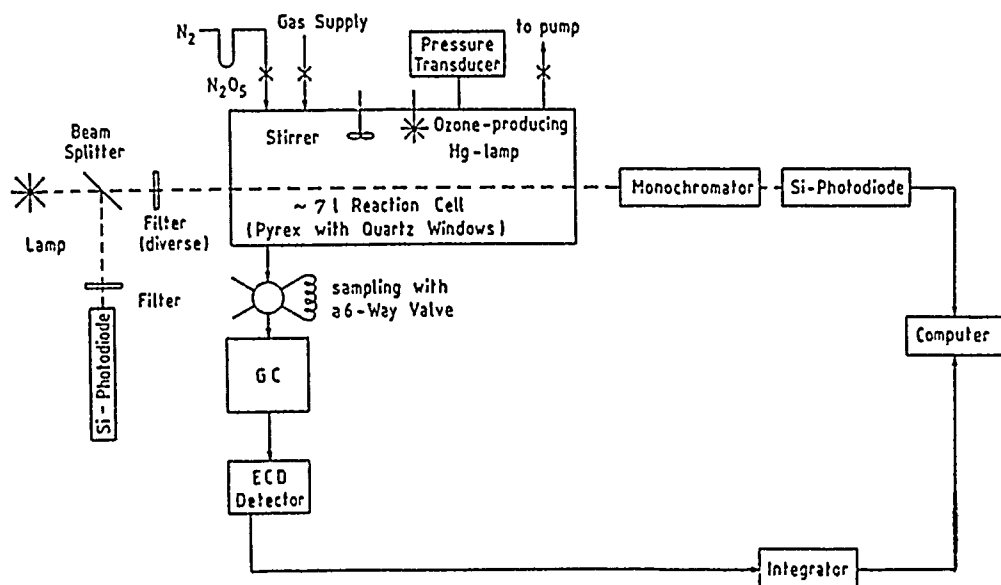


Figure 1. Schematic diagram of the apparatus.

AN AB-INITIO STUDY OF THE PHOTOCHEMISTRY OF NO₂

Carolina Godoy and Gabriel J. Vazquez

Instituto de Física, UNAM

Laboratorio Cuernavaca

62191 Morelos, MEXICO

Ab-initio MRD-CI electronic structure calculations have been carried out on the nitrogen dioxide molecule. An extended basis set of DZ+POL quality augmented with s- and p-type Rydberg functions has been employed. Cuts of the potential energy surfaces along the O-N-O bending and ON-O stretching coordinates are reported for the lowest ten doublet ($5^2A'$, $5^2A''$) and six quartet ($3^4A'$, $3^4A''$) states. Oscillatory strengths for transitions from the X^2A_1 ground state to the excited doublets were calculated as well as the dipole moment functions for the sixteen computed electronic species. Over the past two decades the NO₂ radical has been the subject of numerous theoretical and experimental studies, partly due to its role in the build up of ozone in polluted urban atmosphere, but in spite of this effort the visible absorption spectrum and photodissociation mechanism are still poorly understood. The present ab initio study, the most extensive carried out so far, provides a considerable amount of new information on the excited states which is employed to discuss the spectroscopy and photochemistry of NO₂.

Rate Coefficient Calculations for Ion-(Polar)Molecule
Reactions in Dilute Gases

W. Stiller

(Central Institute of Isotope and Radiation Research,
Leipzig, Academy of Sciences of the GDR)

Rate coefficients for proton transfer with ion-(polar)molecule reactions in diluted rare gases have been calculated on the basis of total reactive cross sections and Maxwellian distribution functions of the translational energies of the reactants. Then the calculations are extended to the peculiar case in which the reaction of a small ion (H^- , D^-) with larger molecules (e. g. CH_3NO_2 , HCN) in a heavy carrier gas (Xe) produces a non-equilibrium effect in the ionic energy distribution function. This leads to corrections of the equilibrium rate coefficient of the reaction. Also the kinetic isotope effect under such conditions is studied.

For all these calculations a comparison with experimental data (flowing afterglow measurements, high pressure mass spectroscopy etc.) is made.

THERMAL KINETICS IN A FINITE HEAT BATH

Cornelius E. Klotz

Chemical Physics Section, Health and Safety Research Division

Oak Ridge National Laboratory, Oak Ridge, Tennessee 37831-6125, U.S.A.

Rate constants in small systems are increasingly being reported as a function of energy. They are considered more fundamental than those measured in an infinite heat bath. Nevertheless, the latter have uses. We have shown how to pass back and forth, from one to the other, in a model-free manner. We may thus use either to obtain estimates of such fundamental parameters as Born-Oppenheimer activation energies, band gaps, and work functions. Illustrations will be given.

"The submitted manuscript has been authored by a contractor of the U.S. Government under contract DE-AC05-84OR21400. Accordingly, the U.S. Government retains a nonexclusive, royalty-free license to publish or reproduce the published form of this contribution, or allow others to do so, for U.S. Government purposes."

*Research sponsored by the Office of Health and Environmental Research, U.S. Department of Energy under contract DE-AC05-84OR21400 with Martin Marietta Energy Systems, Inc.

AM1 AND "BOND-STRENGTH-BOND-LENGTH" STUDIES ON H-ATOM TRANSFER REACTIONS

T. Körtevélyesi and L. Seres

*Institute of Physical Chemistry,
Attila József University, Szeged, Hungary*

The H-atom transfer (H-abstraction and disproportionation) reactions of small alkyl (CH_3 , $\text{2-C}_3\text{H}_7$, $\text{t-C}_4\text{H}_9$) and halogenated alkyl (CH_2F , CHF_2 , CF_3 , CH_2Cl , CHCl_2 , CCl_3) radicals were studied by means of AM1 (Austin Model 1) [1] semiempirical quantum-chemical calculations. The activation energies and the geometries of the transition states were calculated.

The Arrhenius parameters of the same reactions were calculated by means of the "Bond-Strength-Bond-Length" [2] method (BSBL). BSBL was improved by a new potential function [3], which depends on the differences in the group electronegativities. The bond lengths in the transition states and the activation energies of the H-abstraction reactions, and also the character of the calculated (by means of AM1 and BSBL) potential energy surfaces, support the Hammond postulate. The BSBL method was extended to radical disproportionations. The calculated structures in the transition states were compared with the result of AM1 calculations and with the experimental results obtained in gas-kinetic measurements.

References:

- [1] M. J. S. DEWAR, E. G. ZOEBISCH, E. F. HEALY, J. J. P. STEWART,
J. Amer. Chem. Soc. 107, 3902 (1985).
- [2] T. BERCES, J. DOMBI, *Int. J. Chem. Kinet.* 12, 153 (1978).
- [3] A. A. ZAVITSAS, A. L. J. BECKWITH, *J. Phys. Chem.* 93,
5419 (1989).

A REVISED MODEL FOR TRANSITION STATE THEORY CALCULATIONS
FOR RATE COEFFICIENTS OF OH WITH ALKANES.

N. Cohen

Aerophysics Laboratory, Aerospace Corp.,
P. O. Box 92957, Los Angeles, Calif. 90009.

Recent shock tube measurements^{1,2} of the reactions of OH radicals with various hydrocarbons provide the basis for revising an earlier model³ used to carry out thermochemical transition state theory calculations for the reaction rate coefficients of OH with alkanes. In this paper, details of the revised model are presented and calculations are described and compared with experiments. The question is discussed whether there is sufficient experimental evidence to justify distinguishing among different types of primary (or secondary, or tertiary) H atoms, or whether it is adequate to treat them all as equivalent.

¹ J. F. Bott and N. Cohen, *Int. J. Chem. Kinet.* 21, 485 (1989).

² J. F. Bott and N. Cohen, to be published.

³ N. Cohen, *Int. J. Chem. Kinet.* 14, 1339 (1982).

Theoretical studies on the $O(^3P)+I_2$ reaction

A.M.Kosmas

Department of Chemistry

University of Ioannina

Ioannina, Greece 45332

Although extensive studies of classical trajectories on potential surfaces corresponding to direct reactions have been reported, relatively less work has been done on potential well surfaces on which long-lived reactive collisions are expected to take place. Thus, it is hoped that trajectory studies of long-lived reactive collisions will both help correlate special features of the observed dynamics with the potential energy surface and aid the formulation of statistical models with the appropriate approximations and constraints.

Recently we have studied the angular distributions of $O(^3P)+I_2$ reaction at different values of the initial translational energy using the classical trajectory method [1]. The results were compared with the experimental findings of Grice and coworkers [2] from molecular beam experiments. The potential surface employed was a LEPS potential energy function with Sato parameters empirically adjusted as to yield a satisfactory agreement with experiment. It must be noted, however, that there is considerable uncertainty concerning the molecular parameters of the $O(^3P)+I_2 \rightarrow OI+I$ potential energy surface. In view of this we continue the calculations in the

same direction in order to determine a surface which will lead to a thermal rate constant in good agreement with the results of Ray and Watson [3].

Preliminary trajectory calculations show that the scattering results are very sensitive not only to the magnitude of the potential well but the shape as well. Also the initial rotational energy of the reactants plays a significant role as well as the initial angular momentum of the colliding partners. From our results so far we conclude that the $O(^3P)+I_2$ reaction exhibits a potential well of 261 kJmol^{-1} with respect to atomic species and it is satisfactorily represented by a LEPS function with Sato Parameters $S_{OI}=0.14$, $S_{I_2}=0.15$.

REFERENCES

- [1] A.M.Kosmas and R.J.Williams, Chem.Phys. in press.
- [2] N.C.Firth, N.W.Keane, D.J.Smith and R.Grice, Laser Chem. 9 (1988) 277; D.P.Fernie, D.J.Smith, A.Durkin and R.Grice, Mol.Phys. 46(1982) 41 and references therein.
- [3] G.W.Ray and R.T.Watson, J.Phys.Chem. 85(1981) 2955.

MICROCANONICAL VARIATIONAL RRKM THEORY BY INVERSION OF PARTITION FUNCTION

Wendell Forst

Laboratoire de Physicochimie Théorique, URA 503
Université de Bordeaux I, 33405 Talence Cedex, France

An interpolation scheme involving the logarithms of partition functions is used to connect initial and final states in a bond-fission reaction via a switching function. This represents the partition function of the transition state as a function of distance along the reaction coordinate. Inversion of the partition function yields a distance-dependent sum of states, which is then used in a variational routine incorporated into a standard RRKM calculation. In this way, states of so-called transitional modes, in particular, are made to connect smoothly with the proper number of states of fragment rotations. The method requires only a modest computational effort comparable to a canonical calculation. The method is illustrated using the association reaction $\text{CH}_3 + \text{H} \rightarrow \text{CH}_4$ as a test case, with satisfactory results.

Theoretical Studies of Potential Surfaces for Bond Dissociation[†]

Lawrence B. Harding and Robert J. Harrison
Chemistry Division
Argonne National Laboratory
Argonne, IL 60439

There is currently a great deal of controversy of the CH bond strengths of acetylene and ethylene. For acetylene there have been four recent measurements. Two of these (Field et al and Wittig et al) led to an upper limit on the CH bond strength of 127 kcal/mole. The other two measurements (Lee et al and Ellison et al) both yielded bond strengths approximately 5 kcal/mole above this upper limit. For ethylene there is also a disagreement of approximately 5 kcal/mole between a measurement by Gutman et al (105 kcal/mole) and Ellison et al (110 kcal/mole).

In order to calibrate our calculations, the basis set dependence of the bond energies of a number of first-row hydrides has been examined using the correlation consistent basis sets of Dunning and multi-reference, singles and doubles configuration interaction (CI) calculations. With the smallest basis set, (3s,2p,1d/2s,1p) or double-zeta, the root-mean-square error in the calculated bond energies is 10 kcal/mole. With the (4s,3p,2d,1f/3s,2p,1d), triple-zeta, basis set this error is reduced to 3 kcal/mole and with the (5s,4p,3d,2f,1g/4s,3p,2d,1f), quadruple-zeta, basis set the error is further reduced to 1 kcal/mole. Addition of diffuse functions to the quadruple-zeta basis set reduces this error to 0.8 kcal/mole. In all cases, with all basis sets, the calculated bond energies are below the experimental bond energies.

Quadruple-zeta calculations on the CH bond energy of acetylene yield a D_e of 139.05 kcal/mole. Correcting for the expected 1 kcal/mole error in this ab initio bond energy and correcting for zero point effects, leads to a best estimate of 132.0 kcal/mole for the D_0 . This is in good agreement with the measurements of Lee et al, 132.6 ± 1.2 kcal/mole, and Ellison et al, 131.3 ± 0.7 kcal/mole, but is significantly above the results of Field et al, ≤ 126.6 kcal/mole, and Wittig et al, 127 ± 1.5 kcal/mole. To further check these calculations, a selected CI plus perturbation theory estimate of the full-CI bond energy was carried out with the double-zeta basis set and the result compared to the multi-reference, singles and doubles CI method. The two calculations agree to within 0.1 kcal/mole.

Triple-zeta calculations have now been completed on the CH bond energy of ethylene. The ab initio D_e is 117.4 kcal/mole. Correcting for the expected 3 kcal/mole error with this basis set and correcting for zero point effects leads to a best estimate of 111.4 kcal/mole for the D_0 . This is in good agreement with the measurement of Ellison et al, 109.7 ± 0.8 kcal/mole, but significantly above that of Gutman et al, 105.0 ± 0.3 kcal/mole.

[†]*Acknowledgement.* This work was supported by the U.S. Department of Energy, Office of Basic Energy Sciences, Division of Chemical Sciences, under contract W-31-109-ENG-38.

Calculated versus measured scattering and kinetic data for the Li+HCl reaction

A. Lagana, Dipartimento di Chimica, Università di Perugia, Italy,

P. Palmieri, Dipartimento di Chimica Fisica ed Inorganica, Università di Bologna, Italy,

E. Garcia, Departamento de Química Física, Universidad del País Vasco, Bilbao, Spain, and

J.M. Alvarino, Departamento de Química Física, Universidad de Salamanca, Spain.

The Li+HCl reaction has been the subject of recent experimental scattering [1] and kinetic [2] research. On the theoretical side, we have used the Bond Order scheme [3] to fit calculated *ab initio* points and obtain a preliminary (BO2) potential energy surface (PES). Quasiclassical trajectory calculations run on this surface for vibrationally ground HF at a rotational temperature of 60 K compare as follows with the experimental scattering results : a) absolute values of the theoretical cross section are much smaller than experimental ones and, specially, b) the theoretically computed effect of collision energy in the range 2.9-9.2 kcal/mol on the cross section is 7 times larger than the measured effect, but c) in spite of that disagreement, calculated detailed distributions satisfactorily agree with experimental results.

Therefore, when trying to improve the BO2 PES care was given to lessen the discrepancies between calculation and experiment without affecting the overall shape of the BO2 fit which should be reasonable. Thus, using the new surface (BO3), disagreement in point b) above was completely overcome while agreement in point c) was retained. Moreover, although calculated absolute values of the cross section are still lower than experimental data, the computed rate constant variation with temperature lies within error bounds of the kinetic experiment thus confirming the essential adequacy of BO3 as a faithful representation of the reactive interaction of the Li+HCl system.

References

- [1] C.H. Becker, P. Casavecchia, P.W. Tiedemann, J.J. Valentini, and Y.T. Lee, *J. Chem. Phys.*, 73 (1980) 2833.
- [2] J.M.C. Plane and E.S. Saltzman, *ibid.*, 87 (1987) 4606.
- [3] E. García and A. Lagana, *Mol. Phys.*, 56 (1985) 529.

AB INITIO POTENTIAL ENERGY SURFACE FOR UNIMOLECULAR
REACTION AND KINETICS.

A. Palma, E. Scamporrini, F. Stefani
CNR-I.T.S.E., Via Salaria KM 29.5, CP 10
00016 Monterotondo Scalo (RM), Italy

The identification of the reaction mechanism has always been one of the major problems in chemical Kinetics. Because the analysis of highly reactive intermediates is troublesome it has not yet been possible to obtain results confirming the initiation mechanism of the acetylene pyrolysis experimentally.

So confining our attention to the unimolecular mechanism, possible intermediates such as methin CH , vinylidene C-CH_2 and the biradical of acetylene HC=CH are studied at different levels of theory.

In the present study we compute the Potential Energy Surface (PES) for unimolecular reactions by "ab initio" molecular orbital methods with a large basis set. The electron correlation energy is estimated via the Moller-Plesset perturbation theory up to the fourth order. Zero point energies and vibrational frequencies are calculated at HF-SCF level.

We evaluate the stationary points on the PES (reactants, products, saddle points) and the IRC for the reactions under study, at MC-SCF level of theory too.

All the information such as electronic energy, nuclear geometry and force constants, is used in simple statistical approaches (RRKM or TS theory) in order to evaluate the total thermal rate constant $K(T)$ of the reaction.

A COMPARATIVE STUDY OF DIFFERENT METHODS FOR THE CALCULATION OF
REACTION PROBABILITIES USING TIME-DEPENDENT WAVEPACKET METHOD

N. Balakrishnan and N. Sathyamurthy
Department of Chemistry
Indian Institute of technology
Kanpur 208 016 India

In this study we report the quantum reactive scattering results for a collinear $\text{He} + \text{H}_2^+(\nu=0) \longrightarrow \text{HeH}^+ + \text{H}$ reaction in the energy range 0.81-4 eV using time-dependent wavepacket method. The calculations have been carried out with wavepackets of different initial momentum distributions and the translational energy dependence of the state-selected reaction probability (P^R) has been obtained using different approaches. Their relative merits and demerits viz-a-viz their ability to predict P^R accurately and the computational time requirement have been examined. The results thus obtained have also been compared with those resulting from the quasiclassical trajectory method.

ROVIBRATIONAL TRANSITIONS AND DISSOCIATIVE CAPTURE PROCESSES
IN SLOW ELECTRON SCATTERING BY DIATOMIC MOLECULES AND
POSITIVE IONS

A.E. Bodrov and F.I. Dalidchik

Institute of Chemical Physics, Academy of Science, Moscow, USSR

The rovibrational excitation of diatomic molecules and positive ions by slow electrons is investigated within the energy-modified adiabatic approximation. The electronic-vibrational coupling is taken into account by means of the continued fraction method. The account of the rotational degree of freedom can modify substantially the shape of cross section resonant features although the rotational frequency is small with respect to the vibrational one.

The role of a dissociative term in the resonant scattering processes and the dissociative capture processes are investigated by means of the nonlocal optic potential.

CLASSICAL PHASE SPACE STRUCTURE AND TRANSPORT PROPERTIES OF
THE TWO-MODE COUPLED MORSE OSCILLATOR SYSTEM.

A.A.ZEMBEKOV

INSTITUTE OF CHEMICAL PHYSICS, ACADEMY OF SCIENCES OF THE USSR,
KOSYGIN STR.4, V-334, 117334, MOSCOW, USSR

A new method for constructing the PSOS has been proposed which enables us to analyze the phase space structure of two coupled Morse oscillators. The results of the calculations can be summarized as follows:

- The phase space structure appears regular and quite simple. All hyperbolic orbits have at least one configuration point on one of the lines $\phi=0$, $\phi=\pi$ in the (R, ϕ) plane. This feature enables us to make one-dimensional search of the periodic orbits.

- The Farey tree organization of the resonances provides a very useful decomposition of the phase space. The positions R_n of the resonances obey approximately geometric scaling. This empirical property speeds significantly the search of the periodic orbits.

- The pattern of the hyperbolic orbits of the Farey tree sequences exhibits a self-similar (fractal) structure. This in turn results in the self-similar organization of the unstable manifolds. As a consequence, the phase space area entering (or escaping from) the resonance also has a well-defined self-similar structure.

- The homoclinic and heteroclinic orbits provide the most resistance to transport. Furthermore, our numerical results show that due to the Cantorian structure of the unstable manifolds there can be a considerable order in the irregular motion on a time scale shorter than the diffusion time. Moreover the structure of the unstable manifolds must be self-similar on different time scales.

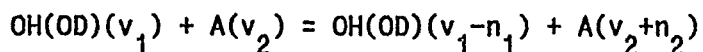
- The pattern of the periodic (or quasiperiodic) hyperbolic, homoclinic and heteroclinic orbits, which densely fill the relevant phase space area, appears to be associated with the weak form of localization of certain eigenstates of classically chaotic Hamiltonian systems.

THE VIBRATIONAL ENERGY EXCHANGE IN COLLISIONS OF OH AND OD
RADICALS WITH N_2 , O_2 AND CH_4 .

D.V. Shalashilin, S.Ya. Umanskiĭ

Institute of Chemical Physics Academy of Sciences of the USSR,
Moscow, USSR

The vibration-to-vibration exchange in collisions of the hydroxyl radical with the almost isotropic partners



is considered.

When A is N_2 or CH_4 three mechanisms of the process have to be taken into account:

- 1) the electronically nonadiabatic one (VVE),
- 2) adiabatic short range forces rotational one (VVR) with the transfer of energy defect into the rotation of hydroxyl,
- 3) adiabatic long range forces mechanism of Sharma and Brau.

The semiclassical model calculations of the rate constants displayed that the principle mechanism is the second one.

In the $OH(DH)-O_2$ system also the relaxation through the long lived intermediate complex should be involved.

The application of the results is the atmospheric kinetics.

THE PLASMA CONDUCTION, CONTAINING THE VAPORIZING ALKALI METAL DROPS.

R.I. Asadullina, I.N. Bebelin, N.N. Bezuglov, E.L. Duman,
A.N. Klucharev, E.V. Nosov, V.A. Sheverev, I.P. Shmatov.

The plasma containing the vaporizing alkali metal drops is considered. The characteristic plasma volume exceeds both drop dimension and average distances between ones considerably (strongly). The disperse phase is modeled by the point stationary sources emitting charge pairs (electrons and ions) to environment.

The expressions for the plasma conductivity are obtained at homogeneous electric field E for the two simple cases: 1) an isolated drop, 2) the drops are in great numbers.

The processes of ionisation and recombination in the volume are taken into account with the constants ν and β accordingly.

The current J between the infinite plane electrodes at a distance d is determined by expression:

$$J = eI \left[1 - \frac{n_- \beta d}{D_+ E} - \frac{I \beta}{4\pi D_- D_+} \frac{1}{E} \right]$$

where e - is an electron charge, n_- - is the concentration of the electrons, $E = \frac{eE}{kT}$; D_+ , D_- - are the diffusion coefficients of the ions and the electrons.

The formulae is correct when $E > \left[\frac{kT}{e} \right] \left[\frac{\beta}{D_+} \right] \left[n_- d + \frac{I}{4\pi D_-} \right]$.

The expressions for the current were obtained in the approximation when there are two the same point sources between the electrodes. The environment conductivity depends on the disposition of the sources one relatively another.

The largest interaction of the charged particles emitted by the different sources takes place when the electric field is directed along the line connecting the sources. This interaction (recombination) results in decrease of the total current through the electrodes.

In the alternative case the drops are distributed in the environment uniformly. The calculation of the plasma conductivity is reduced to solving of the transfer equation for the electrons.

Taking into account the ionisation and the recombination into the plasma the conductivity is given by expression:

$$\sigma = e\mu \left[\frac{\nu}{2\beta} + \sqrt{\left(\frac{\nu}{2\beta} \right)^2 + \frac{In_0}{\beta}} \right]$$

where μ - is the electron mobility.

The expression under the square root determines the additional term of the conductivity connected with the charge emission from the drops.

In the case the sodium drops with the concentration $n_0 = 10^3 \text{ cm}^{-3}$ and radius 15 micron into normal argon atmosphere our calculation gives for the plasma conductivity at the temperature 3000 K value $200 \text{ ohm}^{-1} \text{ cm}^{-1}$.

THE PLASMA NEAR AN ISOLATED VAPORIZING ALKALI METAL DROP.

R.I. Asadullina, I.N. Bebelin, N.N. Bezuglov, E.L. Duman,
A.N. Klucharev, E.V. Nosov, V.A. Sheverev, I.P. Shmatov.

The plasma containing a vaporizing alkali metal drop is investigated theoretically. The drop is surrounded in the noble gas environment. An unhomogeneous density distribution of the alkali metal atoms and noble gas atoms are formed near the drops on account of the alkali metal vaporizing. An unhomogeneous temperature distribution are formed too. The drop temperature approximately is equal the metal boiling temperature near the drop surface. One coincides with the noble gas temperature at a great distance from the drop.

The stationary spatial density distribution of the noble gas atoms, the alkali metal atoms and the temperature field are determined by the vaporizing kinetic of the drop substance. The solution of the kinetic equations for the plasma components (electrons, atoms, atomic and molecular ions) are obtained. The frequency of the electron and ion emission from the plasma is equal $4 \cdot 10^{15} \text{ s}^{-1}$ for the sodium drop into argon at the temperature 3000 K and the drop radius us $15 \mu\text{m}$.

VIBRATIONAL KINETICS AND REACTIONS OF POLYATOMIC MOLECULES
IN NONEQUILIBRIUM SYSTEMS.

B. V. Potapkin, V. D. Rusanov, A. A. Fridman

This work concerns elementary processes and physical kinetics of relaxation and reactions of polyatomic molecules in nonequilibrium conditions. The main emphasis will be on kinetic features caused by the strong interaction of polyatomic molecule modes in the quasi continuum region. The simple semiclassical model was proposed for description of VT and VV relaxation of highly excited polyatomic molecules. It is assumed that during elementary process of polyatomic molecules may be presented as a set of oscillations, with the distribution of the squares of amplitudes given by the vibrational Fourier spectrum of the system. The mean square of the vibrational energy transferred to translational and vibrational degrees of freedom in collision is obtained by averaging the respective formula for diatomic molecules over the vibrational spectrum of the system.

In frame of diffusion approximation the vibrational distribution function for polyatomic molecules in the quasi-continuum region and reaction rate of these molecules were found too. The concrete calculation of reaction rate constants using the proposed model were made for carbon dioxide dissociation stimulated by vibrational excitation of molecules.

One qualitative conclusion of this work should be especially noted. Despite fast mixing of vibrational modes in quasi-continuum the conservation of the modes individuality stimulates an effect for polyatomic molecules like the Treanor effect for diatomic molecules. The overpopulation of the highly excited states connected with the Treanor effect leads to a significant increase in reaction rates of polyatomic molecules under strong vibrational-translational nonequilibrium conditions.

TEMPERATURE DEPENDENCE OF THE $H + H_2$ and $D + D_2$ RATE CONSTANTS

Ernesto Garcia, *Departamento de Quimica Fisica, Facultad de Ciencias, Bilbao (Spain)*

Jesus Mateos, *Departamento de Quimica Fisica, Facultad de Quimica, Salamanca (Spain)*

Antonio Laganà, *Dipartimento di Chimica dell'Università, Perugia (Italy)*

Keywords: *Rate Constants, Temperature Dependence, $H + H_2$*

The production of H^- ions in magnetic multicusp H_2 discharges occurs through a dissociative attachment of electrons onto vibrationally excited hydrogen molecules.¹ Therefore, when modeling such a source competition from processes deexciting vibrationally excited hydrogen molecules has to be considered. Deexcitation of vibrationally excited hydrogen molecules can occur by collision with electrons, hydrogen atoms, hydrogen molecules and walls.

The hydrogen atom hydrogen molecule system has been in the past investigated using a variety of theoretical methods.² Converged quantum three dimensional calculations have been performed only at low energy. To extend the investigation to higher energies calculations were performed by making use of 3D quasiclassical and reduced dimensionality quantum computational procedures implemented on supercomputers. The adopted potential energy surface is the LSTII one.³

The reduced dimensionality quantum rate constants decrease smoothly for deexcitation processes (more smoothly than for collinear results) while those for excitation processes drop dramatically when v' increases. These calculations indicate that deexcitation to the next lower vibrational state is a very efficient process. In agreement with reduced dimensionality quantum results, quasiclassical deexcitation rate constants vary quite smoothly when plotted versus v' . This confirms that an appropriate inclusion of the system rotations (in addition to vibration) makes quite efficient deexcitations to much lower vibrational states. Quasiclassical results indicate also that non reactive deexcitation rate constants are smaller than reactive ones and confirm that reaction is the most effective way for deexciting vibrationally excited H_2 molecules.

A first important question on how the variation of the system parameters alters the dynamical outcome of the $H + H_2$ reaction is about the role of isotopic effects. We have studied this by carrying out quasiclassical calculations of rate constants for the $D + D_2$ reaction. At $T=500$ K rate constant values calculated for the two systems are almost identical once that a scaling for the different reduced mass is performed.

Another question important for practical applications is how the system behaviour changes when the collisional temperature (T_{tr}) differs from the rotational temperature (T_{rot}). For this reason we performed quasiclassical calculations by cooling the rotational temperature down to 500 K while keeping T_{tr} at its highest value (4000 K). At $T_{tr} = T_{rot}=4000$ K and $T_{tr} = T_{rot}=500$ K for the $H + H_2$ system, an increase of the collisional temperature is far more effective than an increase in rotational temperature. In particular, the effect of increasing the translational temperature while keeping the rotational temperature cold leads to rate constants similar to that of processes occurring at $T_{tr} = T_{rot}=4000$ K.

This work has been partially supported by the CNR within the *Progetto finalizzato: Sistemi Informatici e Calcolo Parallelo*

References

1. Topics in Current Physics, *Nonequilibrium Vibrational Kinetics*, M. Capitelli ed., Springer, Berlin (1986); C. Gorse, M. Capitelli, M. Bacal, J. Bretagne, and A. Laganà Chem. Phys. 117, 177 (1987).
2. D.G. Truhlar and R.E. Wyatt, Ann. Rev. Phys. Chem. 27, 1 (1976); G.C. Schatz, *Overview of Reactive Scattering in: Potential energy Surfaces and Dynamics Calculations* D.G. Truhlar ed., Plenum, New York (1981); G.C. Schatz, *Recent Quantum Scattering Calculations on the $H + H_2$ Reaction and its isotopic Counterparts in: Theory of Chemical Reaction Dynamics* D.C. Clary ed., Reidel, Dordrecht (1986).
3. D.G. Truhlar and C.J. Horowitz, J. Chem. Phys. 68, 2466 (1978); 71, 1514(E) (1979)

APPROXIMATE QUANTUM CROSS SECTIONS FOR THE $Li + HCl$ REACTION

Xavier Gimenez, *Departamento de Química Física, Facultad de Ciencias, Barcelona (Spain)*

Antonio Laganà, *Dipartimento di Chimica dell'Università, Perugia (Italy)*

Keywords: *Infinite Order Sudden, Cross Section*

The progress of computer technologies has allowed the extension of high level quantum mechanical treatments to the calculation of detailed reactive properties of atom-diatom systems for three different atoms. Interesting prototypes of these reactive systems are the $M + HY$ (M =alkali atom, Y =halogen atom) reactions. These reactions are characterized by the following features:

- (a) the transition state has a bent configuration;
- (b) the barrier to reaction is located late in the exit channel.

To carry out the calculation we made use of a functional representation of the potential energy surface based on Bond Order coordinates¹ fitted to *ab initio* values² after modifying the transition state region. On this surface, three dimensional quasiclassical calculations have been performed (see abstract B9) starting from the same initial conditions of the experiment to compare calculated and measured cross sections and to test the validity of the adopted empirical corrections to *ab initio* values. Quantum calculations have been carried out using the Reactive Infinite Order Sudden Approximation (RIOSA)³ which has been shown to yield satisfactory results for several atom diatom reactions. A simplified version of RIOSA obtained by assuming the central atom to be infinitely heavy has been also used. This assumption reduces significantly the required computer work.

At a given value of the scattering angle θ the RIOSA differential state to state cross section for the generic $A + BC(v_i) \rightarrow BC(v_f) + C$ reaction reads as:

$$\frac{d\sigma}{d\Omega} = \frac{1}{8k_{v_i}^2} \sum_{l_i l_i'} (2l_i+1)(2l_i'+1) P_{l_i}(\cos\theta) P_{l_i'}(\cos\theta) \int_{-1}^1 d(\cos\gamma_i) S_{l_i, j_i}^{v_i v_j}(\gamma_i) S_{l_i', j_i'}^{* v_i v_j}(\gamma_i) \quad (1)$$

while the state to state integral cross section reads as

$$\sigma(E|v_i, v_f) = \frac{\pi}{2k_{v_i}^2} \sum_{l_i} (2l_i + 1) \int_{-1}^1 d(\cos \gamma_i) |S_{l_i, j_i}^{v_i, v_f}(\gamma_i)|^2 \quad (2)$$

Here E is the total energy, v_i and v_f are the initial and final vibrational states, k_{v_i} is the initial wave number, l_i and j_i are the orbital and the internal angular momentum quantum numbers in the initial channel, γ_i is the initial orientation angle defined as $\cos^{-1}(\hat{R}_i \hat{r}_i)$ (where \hat{R}_i and \hat{r}_i are the initial translational and vibrational vectors) and $S_{l_i, j_i}^{v_i, v_f}(\gamma_i)$ is the state to state element of the S matrix calculated by integrating the IOS differential equations.

The infinite central mass case, known also as the Light-Heavy-Light (LHL) case artificially imposes that the exchanged atom is much heavier than its reaction partners. Such an assumption is quite natural for the investigated system ($Li + HCl$) because of the heavyness of the Cl atom. An immediate advantage of this assumption is that reactant Jacobi coordinates convert into product ones by exchanging their role ($\vec{R}_i \rightarrow \vec{r}_f$ and $\vec{r}_i \rightarrow \vec{R}_f$) and lead to analytical relationships between entrance and exit wavefunctions.

RIOS cross sections and its LHL version have been calculated for the title reaction on an extended interval of collision energy. Calculated integral reactive cross sections are in poor agreement with experimental findings while more detailed quantities better reproduce measured values.

This work has been partially supported by the CNR within the *Progetto finalizzato: Sistemi Informatici e Calcolo Parallelo*

References

- 1 E. Garcia and A. Laganà, *Mol. Phys.* **56**, 529 (1985).
- 2 P. Palmieri, E. Garcia and A. Laganà, *J. Chem. Phys.* **88**, 4775 (1988).
- 3 M. Baer, *Chem. Phys.* **123**, 365 (1988).
- 4 A. Laganà, E. Garcia and O. Gervasi, *J. Chem. Phys.* **89**, 7238 (1988).

The Oxidation Chemistry of 'Stable'
Electron-Delocalised Radicals

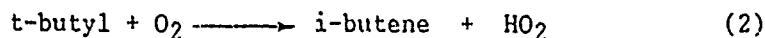
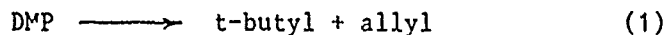
by

R.W. Walker,

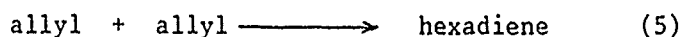
School of Chemistry, Hull University, Hull, N. Humberside, HU6 7RX

Radicals, stabilised by electron delocalisation, play a key role in the oxidation of alkenes, aromatics and cyclo-alkanes, both as major propagation and termination steps. Particularly important examples, include allyl, benzyl and cyclo-pentadienyl radicals. Virtually no kinetic or mechanistic information is available on the oxidation chemistry of electron-delocalised radicals.

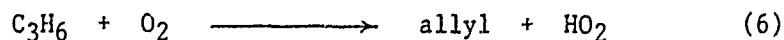
The decomposition of 4,4-dimethylpentene-1 (DMP) in the presence of oxygen between 400 and 500°C has been used as a source of allyl and HO₂ radicals



The presence of relatively high yields of hexadiene in the products confirms the lack of reactivity of allyl radicals with O₂ and hydrocarbons. Rate constants have been obtained for reactions (3) and (4), by use of additional studies of the oxidation of propene, where up to 40% of the allyl radicals recombine to form hexadiene (5).



From measurement of the initial yields of hexadiene, reliable Arrhenius parameters have been obtained for the primary initiation step (6)



No previous determinations have been made of k_3 , k_4 or k_6 or of any closely related rate constants.

The mechanism of oxidation will be discussed together with an outline of the oxidation chemistry of electron-delocalised radicals from aromatic and cyclo-alkane systems.

EXPERIMENTAL INVESTIGATION OF THE AMMONIA CONVERSION TO NO_x IN
A RICH NH_3 SEEDED $\text{H}_2/\text{O}_2/\text{Ar}$ FLAME

Jacques Vandooren

Laboratoire de Physico-chimie de la Combustion. Université
Catholique de Louvain. 1348 Louvain-La-Neuve. Belgium

Using the mass spectrometry analysis coupled with molecular beam sampling (MBMS) the structure of a rich ($\phi = 0.19$) hydrogen-oxygen-argon premixed flat flame seeded by about 3% NH_3 has been established at low pressure (35 torr). Stable compounds such as H_2 , NH_3 , H_2O , N_2 , NO , O_2 , Ar and N_2O as well as radicals such as H , NH , NH_2 , O and OH have been monitored and their concentrations measured throughout the flame.

The aim of this work consists of the determination of the impact of NH and NH_2 reactions with hydrogen atoms on the formation of nitric- and nitrous-oxides at moderate temperatures (500-1200K). The occurrence of high quantities of hydrogen atoms in the reference $\text{H}_2/\text{O}_2/\text{Ar}$ rich flame will allow to obtain important quantitative informations on the NH_3 conversion to NH radicals in such conditions.

On the reaction $\text{CH}_3 + \text{O}_2 \longrightarrow \text{CH}_2\text{O} + \text{OH}$ in problem of modelling methane oxidation.

Institute of Chemical Physics USSR Ac. Sci.

117334, Moscow Kosygin street 4, USSR.

Teitel'boim M.A., Vedeneev V.I., Goldenberg M.Ya., Karnaukh A.A.

The kinetic methane oxidation modelling have been carried out at 870-1070 K. The model include 24 particles and about 100 elementary reactions. Results of the kinetic modelling were compared with some experimental data.

Some new approaches for computer analysis of complicated kinetic scheme were developed. The elementary reactions determining main features of branching, chain propagation, termination and product composition were fixed.

The special attention was payed to analysis of methyl radicals oxidation mechanism, mainly the role of $\text{CH}_3 + \text{O}_2 \longrightarrow \text{CH}_2\text{O} + \text{OH}$ (1) reaction in process of methane oxidation. There are serious contradictions in literature concerning this reaction. Recently the rate constant k_1 was measured ($k_1 = 3 \cdot 10^{11} \exp(-4500/T) \text{ cm}^3/\text{mole s}$ [1,2]). The computer simulation of methane oxidation with and without reaction under question was carried out in temperature range mentioned above. The results of simulation are:

(i) in the absence of reaction (1) the computer simulation is in qualitative agreement with experimental data.

(ii) calculated rates of oxidation always occurred to be much greater experimentally observed when reaction (1) was included in the model with the k_1 mentioned above.

(iii) the best agreement with experimental data is reaching when $k_1 = 3 \cdot 10^{11} \exp(-7500/T) \text{ cm}^3/\text{mole s}$

In the investigated temperature range the most important reaction of methyl oxidation is $\text{CH}_3 + \text{HO}_2 \longrightarrow \text{CH}_3\text{O} + \text{OH}$.

Reference

1. Saito K., Ito R., Kakumoto T., Imamura A. // J. Phys. Chem., 1986, N 90, P. 1422.
2. Zellner R., Ewig F. // J. Phys. Chem., 1988, N 92, P. 2971.

Effect of methane-oxygen mixtures content and of ethane addition on methanol formation.

Moshkina R.I., Polyak S.S., Romanovich L.B., Vedeneev V.I.

Institute of Chemical Physics, USSR Ac.Sci.,

117334, Moscow Kosygin street 4, USSR.

The dependence of methanol formation on the methane-oxygen mixture composition was studied. Experiments were conducted at 723 K, $P_0 = 350$ torr. Two types of mixtures were used.

I. Ratio $\text{CH}_4:\text{O}_2 = 1; 2; 5; 6; 8; 10.5; 12; 14; 16$. The methane content varied from 50 to 94%, of O_2 from 50 to 6%.

II. Ratio $\text{CH}_4:\text{O}_2 = 0.8; 4.5; 6; 8$. The oxygen amount remained constant ($\sim 10\%$), that of methane varied from 8 to 80%. CH_3OH , CH_2O , CO , CO_2 , H_2O were found in reaction products.

The maximal CH_3OH concentration in the type II mixture increased with methane amount. The selectivity (S) of CH_3OH formation calculated from O_2 consumption increased with the amount of added methane, and was higher for the type I mixture. The markedly stronger $S_{\text{CH}_3\text{OH}}$ was due to essentially lowering oxygen content. The same was observed at high pressures. For a mixture $\text{CH}_4:\text{O}_2 = 18$ at 50 atm, $S_{\text{CH}_3\text{OH}}$ was 30%, while at 350 torr $S_{\text{CH}_3\text{OH}} \sim 10\%$ (given paper). Thus $S_{\text{CH}_3\text{OH}}$ grows with increasing pressure and decreasing O_2 concentration.

Two mixtures: $2\text{CH}_4:\text{O}_2$ and $8\text{CH}_4:\text{O}_2$ were used in experiments involving ethane additives. Along with CH_3OH , CH_2O , CO , CO_2 ,

H₂O there appeared also ethylene and ethylene oxide in concentrations increasing with that of ethane. Acetaldehyde was also found. For the 2CH₄:O₂ mixture the selectivity of CH₃OH formation became somewhat greater upon addition of ethane (by a factor of ~1,3).

The kinetic curves for 8CH₄:O₂ oxidation in the presence of 8% C₂H₆ are characteristic of ethane oxidation. The CH₃OH concentration somewhat decreases (from 0.37 % to 0.26 %). The maximal CH₃OH selectivity becomes different in the presence of ethane. While in the absence of ethane $S_{CH_3OH}^{max} \approx 16$, in the presence both of 1.6% and 8% of it, $S_{CH_3OH}^{max} \sim 5-7\%$. At the same time the ethylene oxide selectivity increases. No C₂H₄O is found in the 2CH₄:O₂ mixture. With 1.6% C₂H₆ the C₂H₄O selectivity is 1.5-2%, and with 8% C₂H₆ it is ~ 10%.

The lowering CH₃OH selectivity can be due to competing reactions occurring in the presence of C₂H₆ and yielding C₂H₄ and C₂H₄O:

1. $CH_3O_2 + CH_4 \longrightarrow CH_3OOH + CH_3$
2. $CH_3O_2 + C_2H_6 \longrightarrow CH_3OOH + C_2H_5$
3. $C_2H_5 \longrightarrow C_2H_4 + H$
4. $CH_3O_2 + C_2H_4 \longrightarrow C_2H_4O + CH_3O$
5. $C_2H_5 + O_2 \longrightarrow C_2H_4 + HO_2$

As estimated for the given experimental conditions $w_4/w_1 \sim 1.6-1.7$.

ON HEXANE OXIDATION IN THE OSCILLATION REGIME

Z.A.Mansurov, D.U.Bodikov, S.S.Abilgasinova, G.I.Ksandopulo

Kazakh Kirov State University, Alma-Ata, USSR

This paper presents the oscillation regime of the hexane-air mixture cool flame oxidation under atmosphere pressure. The experiments were carried out in the two-sectional vertically oriented pyrex reactor to be separately heated. The temperature in the first section (T_1) was 450 K, that of the second section (T_2) was being varied from 470 K to 700 K, the hot mixture residence time in the second section (τ_k) being from 5 to 30 s with the components ratio $C_6H_{14}:O_2=1:3, 1:1$.

With respect to the initial temperature in the second section, the other parameters being constant, different oxidation regimes have been stated. At $T_2=450$ K, $\tau_k=20$ s, the components ratio $C_6H_{14}:O_2=1:1$ the following has been stated:

- a) slow oxidation regime with the insignificant increase of the temperature at $T_2 < 480$ K,
- b) stable oscillations at $T_2=480 - 510$ K,
- c) damping oscillations at $T_2= 510 - 540$ K,
- d) stabilized cool flame at $T_2 \geq 540$ K.

While the hexane content in the initial mixture was decreasing, the temperature range extended and stable oscillations were observed, but the latter were available at great residence time. At $\tau_k= 5-10$ s the damping oscillation area was observed to grow.

At $\tau_k=20$ s and $C_6H_{14} : O_2= 1:3, 1:1$ the T_2 increase results in both the decrease of the amplitude magnitude and the stable oscillation period. The further T_2 rise causes the damping oscillations. The growth of the oxygen concentration in the ignition mixture results in the increase of the oscillation

amplitude more than two times. The decrease of the oscillation period is proportional to the increase in τ_k , with the further growth of τ_k oscillations vanish.

As T_1 decreases, the induction time of the oscillations grows, the oscillation amplitude and the limiting temperature differ insignificantly and the oscillation period increases.

The radical oscillations available were registered by the thermocouple probe, which consisted of the differential and ordinary chromel-alumel thermocouples with $d=50$ mkm. One of the joints of the differential thermocouple was covered with the potassium chloride solution.

Our experimental data enabled us to suggest the phenomenological model for the oscillation regime, namely, at first the peroxides pile up to some limiting concentration which induces the reaction of the degenerated chain-branching and the flame front occurrence. As the result of the heat release the flame propagation rate exceeds the oxidation mixture feed rate and the flame propagates in the direction of the fresh mixture. Since the flame front is located in the medium with the lower temperature, the heat dispersion takes place, the gradual flame rate deceleration leads to the failure of the combustion.

Butane Oxidation in a Jet-Stirred Reactor

Per Cederbalk*, Kevin J. Hughes, Michael J. Pilling
and V. Kay Proudler

School of Chemistry, University of Leeds,
Leeds, LS2 9JT, U.K.

The oxidation of n-butane has been studied in an all metal jet-stirred reactor at temperatures and pressures in the range of 590–680 K, 280–500 Torr respectively and at a residence time of 9.4 s and a fuel:O₂ ratio of 1.13:1.

The jet-stirred reactor was based on a design by Bush[1] and contained four jets. The reactants, n-butane and oxygen, were flowed continually through the cell at a constant rate. The temperature was monitored by a very fine Pt–Pt/13%Rh thermocouple and the pressure by a Baratron pressure gauge. A Nd:YAG pumped dye laser was used to investigate formaldehyde variations using the technique of laser induced fluorescence. A GC/MS analysis of the reaction mixture was undertaken.

The system displayed several thermokinetic phenomena, including multiple ignitions and oscillations. The pressure, temperature phase diagram for these phenomena has been mapped out.

In addition, the system has been modelled by adapting a detailed kinetic mechanism developed by Cox and Olsen[2] for n-butane oxidation in a rapid compression machine. In order to reproduce the multiple ignitions, radical wall reactions had to be introduced. Application of principal component analysis[3] enabled the model to be significantly reduced without affecting its ability to reproduce the multiple ignitions.

* Present address: Lund Institute of Technology, Combustion Centre, Box 118, S-22100 Lund, Sweden.

1. S.F. Bush, Trans. Instn Chem. Engrs, 47 T59 (1969)
2. R.A. Cox and G. Olsen, to be published.
3. T. Turányi, T. Bérces and S. Vajda, Int. J. Chem. Kinet., 21 83 (1989)

THE THERMAL DECOMPOSITION OF TOLUENE ISOCYANATES

S Etemad-Rad and E Metcalfe

School of Biological and Chemical Sciences
Thames Polytechnic, London, UK

In recent years there has been a growing recognition of the importance of fire atmospheres in causing injuries and deaths in fires. Irritant and narcotic gases including hydrogen cyanide and carbon monoxide may be produced in large quantities especially in hot, oxygen-deficient regions of a fire.

This study forms part of a programme of work aimed at understanding the kinetics and mechanism of hydrogen cyanide formation in fires involving nitrogen-containing polymers such as polyurethanes. The major features of polyurethane degradation may be summarised:

Polyurethane	--->	{ Aromatic	---	> Organic	---	> HCN
		{ Diisocyanate		Nitrile		
		{ +				
		{ Polyol	---	> Char + CO _x +		
				Hydrocarbons		

The diisocyanates formed in the initial depolymerisation step are commonly MDI (4,4' diphenylmethane diisocyanate) or TDI (toluene diisocyanate). The next stages of the decomposition yield toluene monoisocyanates (TMI), phenyl isocyanate and benzonitrile.

In order to investigate the processes involved, the thermal degradation of the three isomeric toluene isocyanates was studied using a tubular quartz flow reactor at atmospheric pressure and temperatures of 550-600°C. Products were identified and analysed using wide bore capillary gc, and gc-ms. In all three cases the decomposition mechanisms were complex, but hydrogen cyanide is not a major product, while benzonitrile is formed in substantial quantities. Since HCN is a major product of benzonitrile pyrolysis an HCN formation route appears to be

MDI/TDI ---> TMI ---> Benzonitrile ---> HCN

The ortho- and para-isomers pyrolyze at similar rates with similar mechanisms, the initiation step involving the rupture of the ArCH₂---H bond.

The meta-isomer reacts much more slowly than the para- and ortho-isomers, and also exhibits a different range of pyrolysis products consistent with Ar---CH₃ bond rupture. These differences in behaviour can be rationalised in terms of the stabilising influence of the -NCO group for ortho- and para-isomers.

CHEMI-IONIZATION INDUCED BY FLUOROCARBON ADDITIVES IN H₂/CO/O₂ FLAMES

Philippe Rocteur and Pierre J. Van Tiggelen
Laboratoire de Physico-chimie de la Combustion
Université Catholique de Louvain
Louvain-la-Neuve. BELGIUM

Chemi-ionization phenomena in flames have been recognized a long time ago. The elementary steps responsible for the primary ion formation are ascribed to the reaction $\text{CH} + \text{O} \rightarrow \text{CHO}^+ + \text{e}^-$ for hydrocarbon fuels and to $\text{N} + \text{O} \rightarrow \text{NO}^+ + \text{e}^-$ for nitrogen containing compounds. More recently, an increase of the ions in hydrocarbon flames doped with either sulphur- and/or fluorine-containing molecules has been observed. But to the best of our knowledge, no direct production of ions from fluorocarbon has been reported in the literature.

Saturation currents (i_s) have been measured in hydrogen-carbon monoxide-oxygen-argon flames seeded with traces of CF_4 , CF_3H , CF_3Br , CF_3Cl , CF_2Cl_2 , CFCl_3 and CF_2HCl . The ionic yield depends on the nature of the additive and on the equivalence ratio, the dilution, the percentage of hydrogen and the temperature of the reference flame. The reference flame does not produce chemi-ions. Except for CF_2HCl , the ionic yield is lower than the one noticed when CH_4 traces are added.

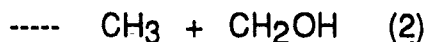
From intercomparison of all the data a mechanism is suggested for ion production when fluorocarbons are added.

THE UNIMOLECULAR DECOMPOSITION OF ETHANOL

Harrauld V. Linnert and Jose M. Riveros*,

Institute of Chemistry, University of Sao Paulo, Sao Paulo, Brazil.

The increasing use of ethanol as an alternative fuel has stimulated considerable interest in the primary processes relevant to its gas phase chemistry and combustion. The decomposition of ethanol promoted by vibrational multiphoton excitation at low pressures suggests that water elimination is the main unimolecular dissociation channel and presumably the lowest activation energy path. However, carbon-carbon bond fission and carbon-oxygen bond fission can also be inferred from some of the final products observed in these experiments. On the other hand, pyrolysis at higher pressures suggests that free radical mechanisms originating from bond fission primary processes are almost exclusively responsible for the gas phase chemistry under these conditions. An RRKM calculation has been performed for this system for the three likely processes,



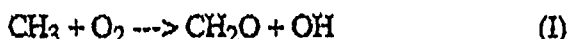
by suitable modelling of the transition states and reasonable assumptions for the activation energies. The calculations reveal two important features: (a) the unimolecular decomposition of ethanol is predicted to proceed primarily by reaction (1) at excitation energies below 100 kcal/mol but bond fission processes become increasingly important at higher levels of excitation; (b) modelling of the reaction at pressures above 100 torr suggest that collisions are effective in the relaxation of the lower tail of excited molecules prior to dissociation, and thus making bond fission processes the most likely chemical reaction.

TWO OLD PROBLEMS REVISITED: CH₃ + O₂ & OH + CO.

Alan B. McEwen and David M. Golden
Department of Chemical Kinetics, Chemistry Laboratory
SRI International, Menlo Park, CA, 94025

The Reaction of CH₃ with O₂

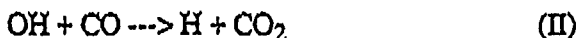
Recent [1,2] work has led to the conclusion that reaction (I) proceeds with the rate constant: $k/\text{cm}^3\text{molec}^{-1}\text{s}^{-1} = 10^{-12.2}\exp(-4500/T)$.



This is in contrast to earlier work from this laboratory [3] in which the lack of an observable process in a VLPP system at 1200K was used to deduce an activation energy of > 25 kcal/mole using an assumed A-factor of $10^{-11.8}\text{cm}^3\text{molec}^{-1}\text{s}^{-1}$. We will report on the re-examination of this process using Laser Pyrolysis [4] with in situ detection of CH₃ via REMPI.

The Reaction of OH with CO

We have recently [5], along with many others [6,7], modeled the pressure and temperature dependence of the reaction:



Data [8,9] on this reaction using OD has convinced us that we and others have deduced a physically untenable potential energy surface. We report here on modifications to the generally accepted treatment that are compatible with the isotopic data.

References:

1. K. Saito, R. Ito, t. Kakumoto and A. Imamura, J. Phys. Chem. **90**,1422(1986)
- 2.a) F. Fwig, D. Rhasa and R. Zellner, Ber. Bunsenges. Phys. Chem. **91**,708(1987)
- 2.b) R. Zellner and F. Ewig, J. Phys. Chem., **92**,2971(1988)
3. A. C. Baldwin and D. M. Golden, Chem. Phys. Lett. **55**,350(1978)
4. S. E. Nigenda, D. F. Mc Millen and D. M. Golden, J. Phys. Chem. **93**,1124(1989)
5. C. W. Larson, P. H. Stewart and D. M. Golden, Int. J. Chem. Kinetics, **20**,27(1988)
6. M. Mozurkewich and S. W. Benson, J. Phys. Chem. **88**,6435(1984)
7. J. Bruning, D. W. Derbyshire, I.W. M. Smith and M. D. Williams, J. Chem. Soc. Faraday Trans. **2**,84,105(1988)
8. G. Paraskevopoulos and R. S. Irwin, Chem. Phys. Lett. **93**,138(1982)
9. G. L. Vaghjiani and A. R. Ravishankara, Personal Communication

DETAILED KINETIC MODELING OF PROPYNE AND ALLENE OXIDATION

Philippe Dagaut, Brahim Aboussi, Michel Cathonnet, Jean-Claude Boettner

C.N.R.S.

*Centre de Recherches sur la Chimie de la Combustion
et des Hautes Températures*

*1C, Avenue de la Recherches Scientifique
45071 Orléans Cedex 2
France*

Propyne and allene oxidation were modeled using a comprehensive kinetic reaction mechanism including the most recent findings concerning the kinetics of the reactions involved in the oxidation of propyne and allene. The proposed mechanism is able to reproduce experimental data obtained in our high-pressure jet stirred reactor (oxidation of propyne and allene) and in shock tube (oxidation of propyne) in the pressure range 1-13 atm, for temperatures extending from 950 to 2000 K and equivalence ratios of 0.5 to 2. The proposed propyne and allene oxidation mechanism is able to correctly reproduce ignition delay times of propyne mixtures, measured in shock tube and molecular species concentrations measured in our jet stirred reactor (JSR) during the oxidation of propyne and allene. The same detailed mechanism was also validated for the pyrolysis and oxydation of ethylene in similar conditions.

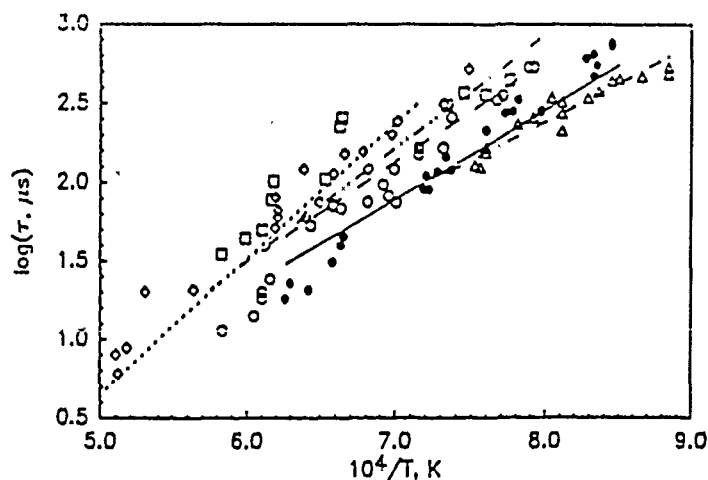


Figure 1. Ignition delay times of propyne. Comparison between experimental data [5] (symbols) and computations (lines): \bigcirc —, Mixture 1; Δ —, Mixture 2; \diamond —, Mixture 3; \bullet —, Mixture 4; \square —, Mixture 11.

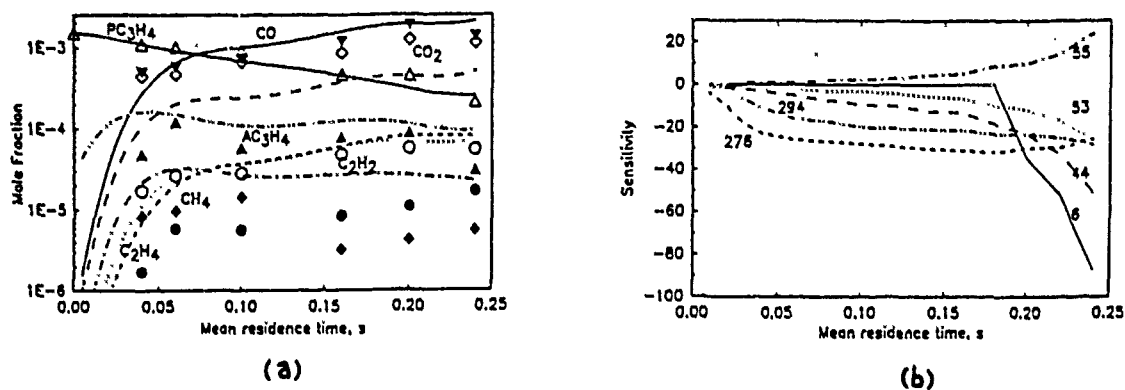


Figure 2. (a) Molecular species concentrations in the jet-stirred reactor during the oxidation of a $\phi=0.5$ propyne mixture. Symbols represent experimental data while curves are the modeling results using the reaction mechanism given in Table I with the initial conditions given in Table II. ∇ —, CO ; \diamond —, CO_2 ; \circ —, C_2H_2 ; \diamond —, CH_4 ; \bullet —, C_2H_4 .
(b) Sensitivity coefficients (in %) for propyne in the conditions of (a).

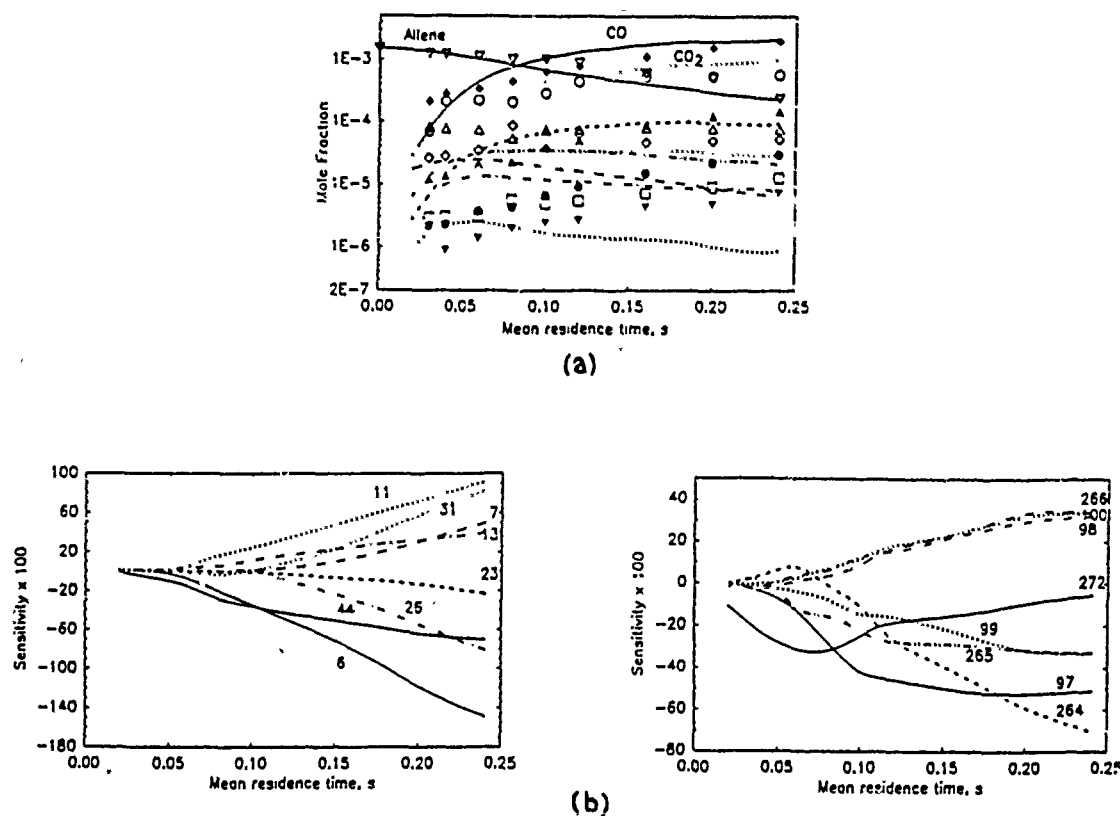


Figure 3. (a) Species concentrations in the jet stirred reactor during allene oxidation (Allene 0.15%, $\phi=0.2$, $T=1030K$). Symbols represents experimental data and lines the results of the computation (\diamond —, CO ; \circ —, CO_2 ; \bullet —, CH_4 ; Δ —, C_2H_2 ; \triangle —, C_2H_4 ; \square —, C_3H_6 ; \diamond —, PC_3H_4 ; ∇ —, AC_3H_4 ; ∇ —, C_6H_6).
(b) Sensitivity analysis results for allene.

OXIDATION OF LARGE HYDROCARBON RADICALS PRODUCED BY UV-LASER PHOTOLYSIS

C.Hao, M.Schneider, and J.Wolfrum

Physikalisch-Chemisches Institut der Universität

Im Neuenheimer Feld 253, D-6900 Heidelberg, F.R.Germany

Although a great deal of experimental study has been addressed to the problem of autoignition^(1,2) and approximate theoretical calculations were developed recently to describe the oxidation of large hydrocarbon radicals⁽³⁾, the chemistry of the system is very complex and not yet sufficiently understood. UV-laser induced oxidation of specific long chain hydrocarbon radicals has been studied in present work, to simplify the mechanistic studies of large hydrocarbon oxidations. Chemical analysis of the products was performed with gas chromatography and coupled gas chromatography/mass spectrometry.

The work shows that, in the temperature range 500-600 K, the short chain (C_1 - C_6) hydrocarbon products were remarkably similar for n-heptane thermal oxidation and 1-chloroheptane photo-induced oxidation. By contrast, long chain (C_7) products were very different. In the case of n-heptane oxidation at lower temperature, (less than 1000 K⁽³⁾), initiation occurs by hydrogen abstraction from the substrate by radicals like O, OH, H, O_2 , which attack the molecule predominantly in the secondary positions giving the products 2-, 3-, 4-heptanone; while in the photo-induced oxidation of 1-chloroheptane, the 1-heptyl radical is the only species leading to oxidation products in the primary position like heptaldehyde. It is also shown that, in the low temperature range (500-600 K and below), the hydroperoxy radicals are relatively unreactive and are likely diffuse to the walls of the reactor to form predominantly ketonic products. Most significantly, further oxidation of the unreactive-hydroperoxide radicals will become possible, due to the rapid internal isomerization by intramolecular H-atom transfer⁽⁴⁾. In particular with the very long hydrocarbon straight-chain of the 1-heptyl radical, which has a large number of secondary H atoms that are relative easily abstracted⁽³⁾, further oxidation will then occur more readily resulting in an enhanced yield of short-chain aldehydic and ketonic products.

REFERENCES

1. K. Brezinsky, and F.L. Dryer, Society of Automotive Engineers Paper SAE-812109 (1987)
2. J.A. Barnard, and B.A. Harwood, Combust. and Flame 21, 345 (1973).
3. C.K. Westbrook, J. Warnatz, and W.J. Pitz, to be published.
4. A. Fish, W.W.Haskell, and I.A.Read, Proc. Roy. Soc. (London) A313, 261 (1969).

THE DETECTION OF THE BUTINYL RADICAL BY MULTIPHOTON IONIZATION/ MASS SPECTROMETRY AND THE APPLICATION TO THE STUDY OF THE REACTIONS WITH DEUTERIUM AND OXYGEN ATOMS

R. Buth, J. Edelbüttel-Einhaus, and K. Hoyerermann

Institut für Physikalische Chemie, Universität Göttingen

Tammannstr. 6, D-3400 Göttingen

The formation and the reactions of butynyl radicals (C_4H_5) were studied at low pressure (around 1 mbar) and room temperature (295 K) in a discharge flow reactor. Samples were withdrawn continuously by a molecular beam sampling device and analyzed mass spectrometrically after laser induced multiphoton ionization (MPI) and conventional electron impact ionization.

The C_4H_5 radicals were formed via the fast reactions of 2-butyne with Cl and F atoms leading to the rate constants of $2 \cdot 10^{14}$ and $1 \cdot 10^{14} \text{ cm}^3/\text{mol} \cdot \text{s}$, respectively. The abstraction route in the $F + C_4H_6$ reaction dominated over the exchange reaction ($CH_3 + C_3H_3F$, below 5%). The wavelength selective multiphoton ionization of the C_4H_5 radical was found at 429.3 nm with a high intensity parent peak ($C_4H_5^+$) and the fragment ions $C_2H_2^+$, C_2^+ , and C^+ . (The precursor molecule 2-butyne was detected by MPI at 448 nm.) The possible CH_3 formation was monitored by the MPI of CH_3 at 450.9 nm. Secondary reactions of C_4H_5 radicals with molecular Cl_2 and F_2 turned out to be fast and were suppressed by a high excess of C_4H_6 .

The reaction $C_4H_5 + D$ is fast, showing negligible isotope exchange reaction ($C_4H_5 + D \rightarrow C_4H_4D + H$, < 10%) and the dissociation ($C_4H_5 + D \rightarrow C_3H_3(C_3H_2D) + CH_2D(CH_3)$, < 10%). This was established by the non-detection of C_4H_4D and CH_3 by MPI.

The reaction $C_4H_5 + O$ is equally fast, exhibiting a complex reaction mechanism ($C_4H_4O + H$; $CH_2O + C_3H_3$; $OH + C_4H_4$).

OH Distribution in Pre-Flame Zone of C_3H_8 /Air Flame.

Konnov A.A., Ksandopulo G.I.

The Kazakh SHS-Interbranch Scientific and Technical Centre,
172, Kirov st., Alma-Ata, 480012, USSR

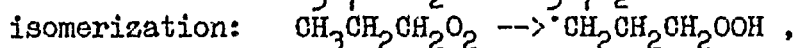
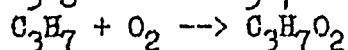
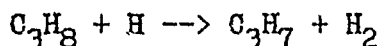
The experimental study of the structure of the hydrocarbon conical atmospheric pressure flames made it possible to find out that in pre flame zone the fuel conversion proceeded with the insignificant mixture heating up. For example, conversion of nearly 50 % of propane and other hydrocarbons to intermediate products among which carbon monoxide and hydrogen being in large quantities, takes place with heating-up not exceeding 100 K [1]. A great number of works on the flame structure study has been carried out with flame stabilized over porous burners which makes difficult to investigate the pre-flame zone due to the unavoidable distortions caused by heat- and mass-transfer to the burner surface.

Thus, the object of the present work was to determine OH radicals distribution in the atmospheric pressure premixed propane-air flame stabilized over Bunsen burner. The experiments were held on the home-built computer equipped laser-induced fluorescence arrangement. OH concentration profiles have been obtained in the torch section of slightly rich propane-air flame with spatial resolution about 70 μm .

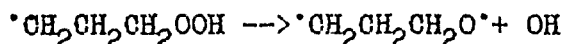
The maximum concentration of OH radicals in the flame front is about $5 \cdot 10^{15} \text{ cm}^{-3}$. The concentration drops to the length of -0.6 mm from the inner boundary of the luminous front exponentially due to diffusion. But at distance -0.6...-0.8 mm the rate of concentration drop appreciably decreases. Hence, it can be supposed that mixture heating up being insignificant, there exists a source of OH radicals connected with the observed decay of fuel molecules into intermediate products. To confirm this experimental results the measurements of OH concentration profiles over burners having diameter equal to 8 mm and 10 mm were held. In all the cases the experimental OH profile is the

same which allows to decline the assumption about possible registration of the signal from the flame neighboring zones.

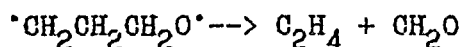
Earlier the similar profile in the low temperature area of the inhibited C_3H_8 /air flame had been found out for H-atoms [1]. There has been suggested the mechanism with peroxide biradicals participation during the decay of which the formation of excited formaldehyde molecules has been presupposed. As soon as only reaction of branching can serve as a source of superequilibrium H and OH concentration then the alternative mechanism of low-temperature oxidation, propane being taken as an example, can include the following reactions:



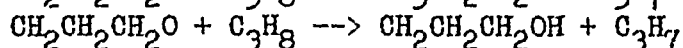
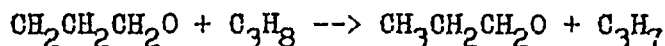
with the consequent quick decay:



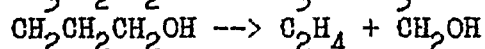
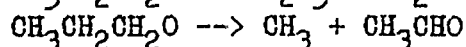
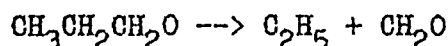
$CH_2CH_2CH_2O$ biradical may be decayed along different channels, for example,



Besides, reacting with saturated molecules biradical leads to the continuation:



with the following decay:



The reaction of RO_2 radicals isomerization by intramolecular transition of H-atom and the following $R'OOH$ decay is the key stage of this mechanism. The probability of the peroxide radical decay into OH and biradical is small but the preliminary estimations show that even insignificant portion of branching acts can lead to the observed effects in the pre-flame zone.

Reference

1. Ksandopulo G.I., Dubinin V.V. Khimiya gazofaznogo gorenija. M.,Chimiya,241 p.

Kinetics of the thermal decomposition of cyclohexane-decane binary mixture at ca 720°C

F. Billaud, K. Elyahyaoui, F. Baronnet

Département de Chimie-Physique des Réactions
URA 328, ENSIC (INPL), 1, rue Grandville BP 451
F 54001 NANCY Cedex (France)

The thermal decomposition of cyclohexane has been the topic of many studies (Tsang (1978), Zimmerman et al. (1985), Arabike and Susu (1988)). Various mechanisms of reactions have been proposed to attempt to explain the formation of the different products of this reaction.

At the Department of the Physical Chemistry of Reactions in Nancy (France), we have undertaken this study in order to understand the thermal decomposition of cyclohexane-decane mixture. We have suggested a free radical scheme mechanism, according to the theory of Rice-Herzfeld-Kossiakoff (1934,1943).

Given that the C₆ cyclanes, and especially the cyclohexane are important elements in industrial and fuel mixtures, a better knowledge of elementary steps and of the resulting closed sequences is thus of importance for the understanding of hydrocarbon cracking and combustion.

In this study, we have worked on the thermal decomposition at low conversion (less < 5 %) of the equimolecular binary mixture : cyclohexane / n-decane. The n-decane is used as a solvent, its mechanism of decomposition has been the subject of a previous study (Billaud and Freund, 1986).

The experimental set-up used in our experimental investigation is a steam cracking micropilot equipped with a tubular reactor (assimilated to an ideal plug flow reactor). We describe the primary decomposition of cyclohexane by three closed sequences which lead to the primary stoichiometries. The concentration of the various reaction products of cyclohexane and their distribution versus residence time are plotted. The extrapolation at zero time of the primary product distribution shows that C₂H₄, H₂, 1-3 C₄H₆ are the main products of this reaction. If we define the selectivity of a product B in relation to reactant A a ratio of the number of moles of product B per mole of A transformed, we can note that the selectivity of the three main products directly depends on the conversion of n decane in a reactional medium.

We have shown in this study that the thermal decomposition of the cyclohexane-decane mixture is interpreted by a long chain radical mechanism, essentially initiated by the n-decane.

By using the compilation of kinetic parameters (preexponential factor and activation energies) proposed by Allara and Shaw (1980) for the pyrolysis of alkanes, we performed a first simulation using the MORSE programme (Côme et al., 1988).

A fitting of the kinetic parameters was done in order to obtain a satisfactory modelling compared with our experimental results.

Literature cited.

- Allara, D.L., and Shaw, R., J. Phys. Chem. Ref. data, 1980, 9, 523.
- Arabike and Susu, Ind. Eng. Chem. Res., 1988, 27, 915.
- Billaud, F. and Freund, E., Ind. Eng. Chem. Fundam. Ref. data, 1986, 25 (3), 433.
- Côme, G.M. ; Scacchi, G. ; Muller, C. and Marquaire, P.M., J. Chim. Phys., 1988, 85 (2), 201.
- Rice, F.O. ; Herzfeld, K.F., J. Am. Chem. Soc., 1934, 56, 284.
- Rice, F.O. ; Kossiakoff, A., J. Am. Chem. Soc., 1943, 65, 590.
- Tsang, W., Int. J. Chem. Kinet., 1978, 10, 599-10, 1119.
- Zimmerman, G.; Zychluiski, W. ; Bach, G. and Rennecke, D., J. Prakt. Chemie, 1985, 327, (1), 10.

Thermal decomposition of cyclohexane at 720°C

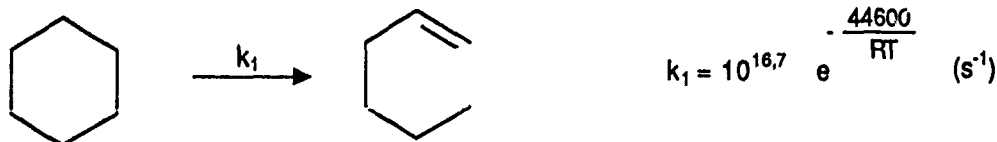
F. Billaud, K. Elyahyaoui, F. Baronnet

Département de Chimie-physique des Réactions
URA 328, ENSIC (INPL), 1, rue Grandville, BP 451
F-54001 Nancy Cedex (France)

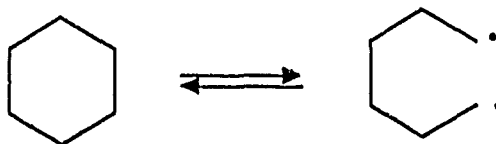
The present work is a part of a more general research project aimed at a better understanding of the reaction mechanism of the production by steam cracking of light olefins from naphthenic feedstocks. The model reactant chosen for the present study, cyclohexane, is representative of the unsubstituted cycloalkanes within the naphta boiling range.

The naphthenes and especially cyclohexane have not received nearly as much attention from the investigations of pyrolytic decomposition as the paraffins. Some attempts have been made at high conversion : Arabike and Susu (1988) investigated the decomposition of cyclohexane using the annular tubular reactor pulse method and demonstrated that in the 730-860°C range the cyclohexane decomposition is a first order reaction.

Tsang (1978 a,b) investigated the decomposition mechanism from single pulse shock tube experiments at 800-850°C and demonstrated that the main initial process is the isomerization of cyclohexane into 1-hexene followed by the decomposition of 1-hexene :



On the contrary Arabike et al. (1981) like Kotzun et al. (1979), Kalinenko et al. (1976) wrote the initiation of chains by the dissociation of cyclohexane but this breaking leads to the formation of a biradical :



At 810°C, in a plug flow reactor heated by high frequency electromagnetic induction, Billaud et al. (1988) proposed the overall results of the yields of characteristic products in a cyclohexane-paraffin mixture.

In fact, it seems to us that the mechanism of cyclohexane decomposition at low conversion is known with insufficient accuracy to allow reliable simulations of the distribution of the main primary products.

The thermal decomposition of cyclohexane is studied at 720°C in a plug-flow reactor at atmospheric pressure and with steam dilution. The heating of the reactor is achieved by means of insulating resistors with an Inconel sheeting (brand name Thermocoax) directly coiled round the stainless steel tube. We present the results of a preliminary investigation on a micropilot (cyclohexane partial pressure of ~ 90 mbar) concerning the effect of residence time on the conversion and selectivity. The main products are H₂, C₂H₄, C₃H₆, C₄H₆. Small amounts of acetylene, benzene and toluene are also found.

We propose a primary mechanism of the decomposition of cyclohexane which enables us to deduce the main primary stoichiometries and accounts for the distribution of reaction products.

References

- Arabike, D.S. ; Susu, A.A. and Ogunge, A.F., *Thermochim. Acta*, 1981, 47, 1.
 Billaud, F. ; Chaverot, P. ; Berthelin, M. and Freund, E., *Ind. Eng. Chem. Research* 1988, 27, 759.
 Kalinenko, R.A. ; Shevel'kova, L.V. ; Titov, V.B. ; Back, G. and Novak, Z., *Neftekhimija*, 1976, 16 (1), 100.
 Korzum, N.V. ; Magaril, R.Z. ; Plynsnina, G.N. and Semukhina, T.I., *Russian Journal of Phys. Chem.*, 1979, 53 (5), 631.
 Tsang, W., *Int. J. Chem. Kinet.*, 1978 a, 10, 599.
 Tsang, W., *Int. J. Chem. Kinet.*, 1978 b, 10, 1119.

Development of methane into higher hydrocarbons

F. Billaud, C. Guéret, F. Baronnet

Département de Chimie-physique des Réactions

URA 328, ENSIC (INPL), 1, rue Grandville, BP 451

F-54001 Nancy Cedex (France)

J. Weill

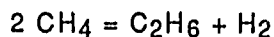
Institut Français du Pétrole, CEDI

BP 3 F-69390 Vernaison (France)

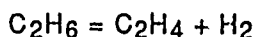
The present work is a part of a more general research project aimed at understanding the reaction mechanism of the production of light olefins from natural gas feedstock. Pyrolysis of methane is the method used in this project.

The first stages (primary reactions) in the decomposition of methane have now been clearly defined, but details of high conversion reactions and especially formation of carbon and C₆-C₁₂ hydrocarbons (Benzene, Toluene, Xylenes and naphthalenic species) have not yet been entirely elucidated. However a survey of the literature published before 1988 on the pyrolysis of methane and related to gaseous product formation has been discussed by Billaud et al. (1989). In this work, there is a particularly valuable paper, (Back and Back, 1983) which brought to light a mechanism which explains the formation of C₁-C₄ hydrocarbons during methane pyrolysis (ethane, ethylene, acetylene, propene, allene, propyne, 1 butene) and is in general agreement with the experiments.

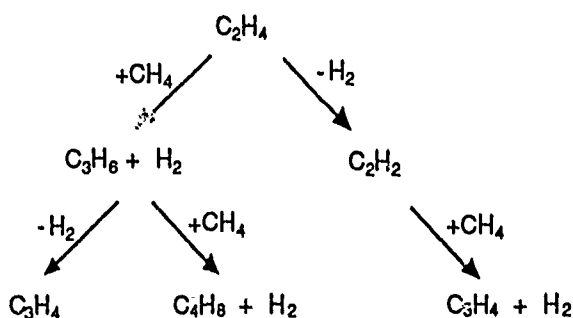
So the primary formation of ethane and H₂ proceeds through a radical mechanism by stages which is compatible with the following stoichiometric equation :



Secondary reactions of ethane by deshydrogenation via a radical chain mechanism account for the formation of secondary hydrogen and ethylene .



The following steps proceed either through a deshydrogenation or a methylation mechanism. Indeed the formation of acetylene, propene, propyne, allene and 1-butene can be interpreted as follows :



Dean (1990) in his kinetic modeling of autocatalysis in methane pyrolysis takes into account the formation of cyclopentadiene and naphthalene which actually appear in pyrolysis. But in all the research projects so far no one has simultaneously studied light and heavy hydrocarbons ranging from C_2 to C_{12} formed in methane pyrolysis (ethane, ethylene, acetylene, propene, allene, propyne, 1 butene, cyclopentadiene, benzene, toluene, xylene, styrene, phenylacetylene, naphthalenic species and coke).

We propose a mechanism which takes into account the whole range of products. For this reason a quantitative research on the thermal decomposition of methane at 1160°C is made on our scale laboratory plug flow reactor.

This reactor is an alumina tube (length = 420 mm, inside diameter = 12 mm, outside diameter = 18 mm) crossed by a 15 l/h flow rate. An electric furnace is used to supply the energy and heat level required for the highly endothermic reaction of thermal methane decomposition.

During the pyrolysis step, hydrogen is determined by GC with an external calibration by a thermal conductivity detector (TCD). Hydrocarbons are analysed by a GC equipped with a capillary column (Hewlett-Packard Pona type, 50 mm). The coke formed in the tube is evaluated after air oxydation at 1000°C . The yield of formed $\text{CO}\text{-CO}_2$ is measured by an infra-red spectrometer. The balance is determined by integrating total flow rate and analyses. For a preliminary study, we have chosen to investigate the influence of hydrogen content as a diluent gas. The influence of the hydrogen is to cause a sharp decrease in coke formation and methane conversion.

References

- Back, M.H. and Back, R.A., Pyrolysis : Theory Ind. Pract. 1983, 1-24, Ed. Albright, L.F., Crynes, B.L. and Corcoran, W.H.
 Billaud, F. ; Baronnet, F. ; Freund, E. ; Busson, C. and Weill, J., Rev. Inst. Fr. Petrole, 1989, 44 (3), 813.
 Dean, A.M., J. Phys. Chem., 1990, 94, 1432.

High Temperature Pyrolysis of Benzyl Radicals

M. Braun-Unkhoff, Th. Just, and P. Frank

DLR, Institut für Physikalische Chemie der Verbrennung
Pfaffenwaldring 38-40, 7000 Stuttgart 80, W. Germany

Benzyl radicals play a key role in the high temperature decay of alkyl-substituted benzene molecules e.g. toluene /1/. However, their decomposition pathways and decay rates are presently not well known. In the present work, it was tried to get more insight into the unimolecular decomposition of benzyl by using very low initial concentrations in order to reduce possible contributions of subsequent reaction steps.

The experiments have been performed behind reflected shock waves at temperatures between 1400 and 1700 K and at total pressures around 2 bar. ARAS was used to monitor simultaneously time-dependent concentrations of H-atoms at $\lambda = 121.5$ nm and of iodine atoms at $\lambda = 164.2$ nm. The test gas mixtures consisted of argon with relative concentrations of 0.3 - 3.7 ppm benzyliodide, C_7H_7I . The radical precursor is completely decomposed into benzyl and iodine atoms at temperatures $T > 1300$ K. The very low initial benzyl concentrations were determined by observing the resonance absorption of iodine atoms originating from the very fast decay of benzyliodide.

The experimental H-profiles clearly reveal that H-atoms are formed in considerable amounts without any detectable induction period. This indicates that, at the begin of the observation time interval, H-atoms must be produced either by an initiation reaction or by subsequent, very fast reaction steps.

All the measured H-profiles can be reproduced by applying a small set of elementary reactions (see table I) as sensitivity studies demonstrated. A series of experiments with initial concentrations of benzyliodide ≤ 1.0 ppm allowed to evaluate the rate coefficient of the H-atom forming reaction R1: $C_7H_7 \rightarrow H + X$ without any appreciable influence of the subsequent reactions R2: $C_7H_7 + H \rightarrow C_7H_8$ and R3: $H + X \rightarrow \text{products}$ (products $\neq C_7H_7$) (see Fig. 1). The data from the low concentration measurements formed the basis for the evaluation of experiments with higher C_7H_7 -concentrations where the H-atom consuming reactions R2 and R3 become important (see Fig. 2). From all these data a least squares fit for reaction R 1 (see Fig. 3) gives a first order rate coefficient of:

$$k_1 = 10^{15.53 \pm 0.3} \times \exp(-(42865 \pm 1800)/T) \text{ s}^{-1}.$$

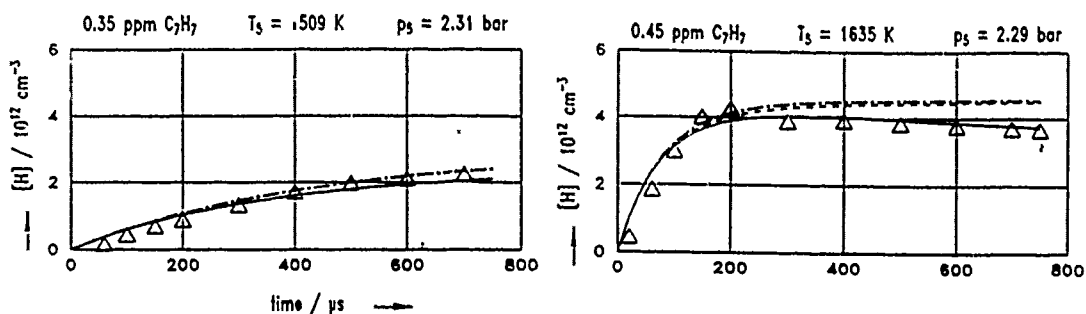
Thermochemistry suggests that the benzyl decay is preceded by an isomerization of benzyl, R1a: $C_7H_7 \rightarrow \text{isomer}$, followed by fast H-abstraction from the isomer, R1b: $\text{isomer} + H \rightarrow X$. The measured H-atom profiles only can be reproduced by model calculations if $k_{1b} > k_{1a}/K_{c,1a}$ is valid. One possible model which may be in accordance with the above mentioned assumption, is the "chain model". the isomer is identified as the open chain C_7H_7 -radical which dissociates immediately to form the stable C_7H_6 -molecule and H-atoms.

/1/ M. Braun-Unkhoff, P. Frank, and Th. Just:
22nd Symp. (Int.) on Combustion, 1053 (1988)

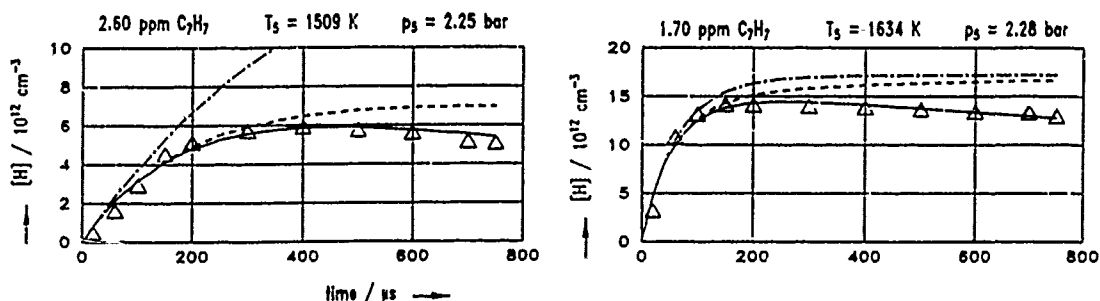
Table I: Mechanism for benzyl pyrolysis

	Reaction	log A	n	E/R	Ref.
R (1)	$C_7H_7 \rightarrow H + X$	15.53	-	42865	a
R (2)	$H + X \rightarrow C_7H_8$	13.93			*, /1/
R (3)	$H + X \rightarrow \text{products (products} \neq C_7H_7)$	13.6 ± 0.2			a

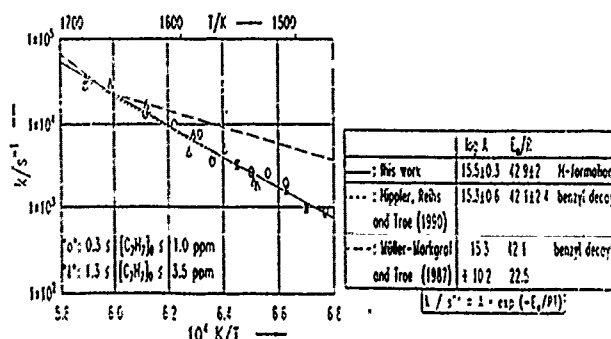
$k = A \times T^n \times \exp(-E_a/RT)$; units: K, cm, mol, s;
 a: this work; *: calculated from K_c and k_r , as given in ref./1/

Fig.1 Experimental (Δ) and computational (curves) results

full line: calculated with the reaction scheme of Table I

dash-dotted line: calculated only with k_1 short-dashed line: calculated with k_1 and k_2 Fig.2 Experimental (Δ) and computational (curves) results

full line: calculated with the reaction scheme of Table I

dash-dotted line: calculated only with k_1 short-dashed line: calculated with k_1 and k_2 Fig.3 Arrhenius diagram for k_1

full line: least squares fit

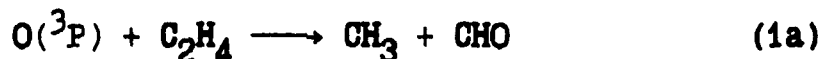
THE REACTION OF O(³P) ATOMS WITH ETHYLENE AT LOW PRESSURES

V.S.Arutunov, V.D.Knyazev and V.I.Vedenev

Institute of Chemical Physics, Acad.Sci., USSR,

117334, Moscow

This work proceeds with our investigation of the mechanism of the title reaction¹. In numerous previous works the two main channels of this reaction



have been established. The mean rate constant of O atoms disappearance $k_1 = (7.8 \pm 0.6) \cdot 10^{-13} \text{ cm}^3 \text{ molecules}^{-1} \text{ s}^{-1}$ ($T = 298\text{K}$) has been determined to be practically unchanged within the accuracy limits in pressure range from 0.35 to 240 Torr. But we have found¹, that in this range increase of pressure causes a decrease of the relative H atoms yield, i.e. the rearrangement of reaction channels takes place. This phenomenon enables to explain discrepancies in various experimental results concerning the relative role of this two reaction channels. On the base of the available theoretical calculations of this system we have presented a tentative qualitative explanation of this rearrangement. It predicts the fall of total reaction rate constant by approximately 3 times at pressures below 0.3 Torr with H atoms yield rising up to 1.

The results reported in this work were obtained by resonance-fluorescence technique under discharge-flow conditions at 298K in the pressure range from 0.08 to 1.5 Torr.

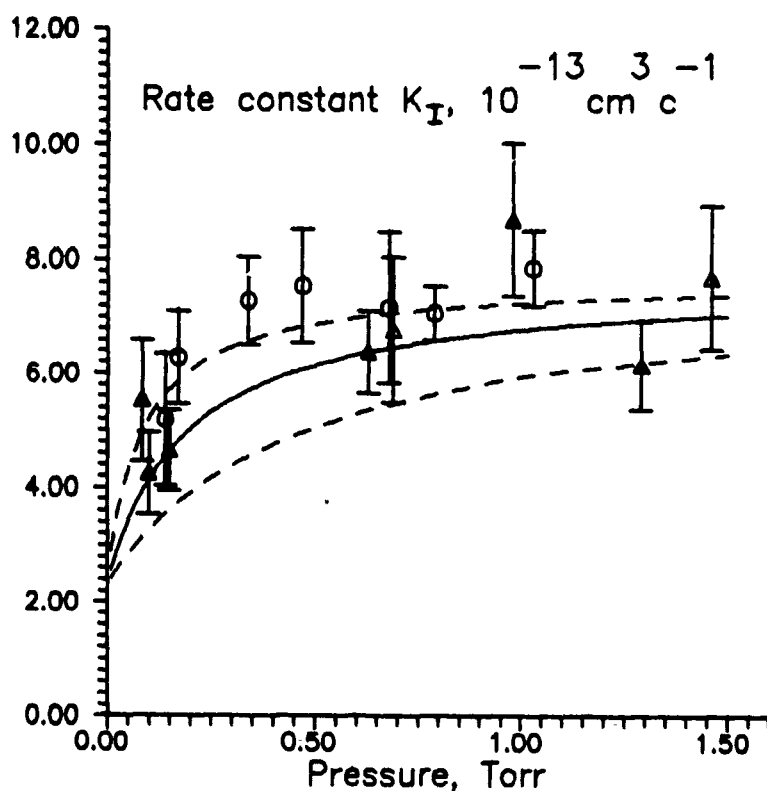


Fig 1. Pressure dependence of rate constant K_I . — reactor tube diameter 20 mm, — 11 mm.

These results let us experimentally reveal the drop in total reaction rate constant predicted by the model. Experimental data are plotted with the results of rate constant calculation completed by RRKM method on the base of the mechanism introduced¹. The heat of formation of $\dot{\text{C}}\text{H}_2\text{CH}_2\text{O}^\bullet$ biradical from reactants — 32.9 (solid line) \pm 4 kcal/mole (dashed lines) was obtained thermochemically.

Reference

1. E.N.Aleksandrov, V.S.Arutunov, V.I.Vedeneev, V.D.Knjazev, S.N.Kozlov, Tenth International Symposium on Gas Kinetics, Swansea, 1988, Abstracts of papers, A.10.

STUDY OF THE $\text{SO}_2 + \text{CO}$ REACTION

V.S.Arutunov, V.Ya.Basevich, A.V.Chernyshova,

V.A.Ushakov and V.I.Vedeneev

Institute of Chemical Physics, Acad.Sci., USSR,

117334, Moscow

The problem of reduction and utilization of sulfur oxides in combustion processes and industry has a great ecology importance. One of possible reduction agents discussed in literature is a synthesis gas with one of its main components - carbon oxide.

In this work the UV and IR spectroscopy has been used for studying kinetics of reaction between SO_2 and CO in the temperature range 1100-1350K. It was found that the velocity of SO_2 disappearance is directly proportional to CO concentration and independent of SO_2 concentration, pressure, and dimensions of reaction vessel. The activation energy of the process was determined to be approximately 46 kcal/mole. The main intermediate in this process revealed by IR analysis was carbon sulfuroxide COS and its kinetics was also investigated.

THE PYROLYSIS OF PERACETIC ACID

by

B. SEYDI, R. RIGNY and K. A. SAHETCHIAN, Laboratoire de Chimie Générale,
Université P. et M. Curie. Tour 54-55, 4 Place Jussieu, 75252 PARIS CEDEX 05
FRANCE

and

I. BATT, Department of Chemistry, University of Aberdeen, Meston Walk. ABERDEEN
AB 9 2UE, SCOTLAND.

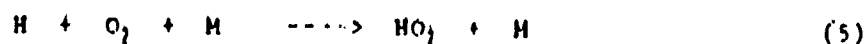
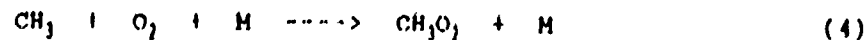
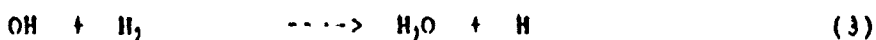
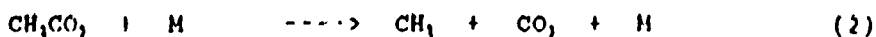
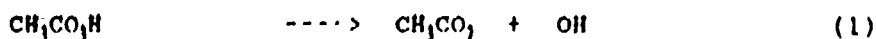
Aldehydes, in particular acetaldehyde, are important intermediates in the oxidation of hydrocarbons [1]. The latter aldehyde is a precursor of peracetic acid which along with alkyl hydroperoxides, are thought to be responsible for cool flame production [2]. Recently we have found evidence for the production of primary and secondary butyl hydroperoxides together with peracetic acid in the oxidation of butane [3]. All three hydroperoxides are formed in the same order of magnitude of concentration. In order to assess their role in these oxidising processes, it is important to determine their rates of decomposition.

Little is known about the decomposition of peracetic acid [4]. In order to study its decomposition, a technique was used to isolate the bond breaking step:



The radicals formed were converted to inert products by equimolar mixtures of hydrogen and oxygen which were part of a nitrogen flow system operating at atmospheric pressure. The quartz reactor was treated by coating with boric acid followed by slow reaction with a hydrogen/oxygen mixture at 530°C to minimise any heterogeneous reaction.

Under the experimental conditions it is easy to show that the consumption of peracetic acid is essentially via reaction (1). The first order rate constant does not vary either as a function of time or different initial concentrations of acid (figure). Although not proven, the results strongly suggest absence of any heterogeneous contribution to the rate of decomposition. This is in keeping with the following mechanism :



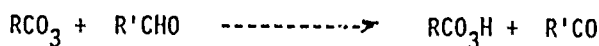
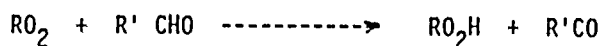
Clearly any reactive radicals or atoms that are produced are converted into inert products. The Arrhenius plot leads to the following result for reaction (1):

$$\text{Log } (k_1/\text{s}^{-1}) = 14.72 \pm 0.4 - (40.10 \pm 0.13 \text{ Kcal mol}^{-1}/2.303 \text{ RT})$$

This leads to a value for $D(\text{CH}_3\text{CO}_2 - \text{OH})$ of $41.6 \text{ kcal mol}^{-1}$. The results are in agreement with that predicted by group additivity rules within experimental error.

The A factor for process (1) has previously been assumed to be 10^{15} s^{-1} . The present value is a factor of two less than that. This either represents a tighter transition state than previously estimated or suggests that the decomposition process (1) is still pressure dependent under our conditions.

Contrary to previous conclusions, peracetic acid decomposes at a rate comparable to alkyl hydroperoxides [5]. This may mean that the supposed accelerating effects of aldehydes is via the reactions :



REFERENCES

- [1] S.W. Benson, Prog. Energy Combust. Sci. 125,17 (1981)
- [2] M. Pilling and I. Smith, "Modern Gas Kinetics "
- [3] K.A. Sahetchian, R. Rigny, N.Blin, A. seydi and M. Murat, Combust. and Flame, in the press.
- [4] C. Schmidt and A.M. Sehon, Canad. J. Chem., 41,1819 (1963)
- [5] K.A. Sahetchian, A. Heiss, R. Rigny and R.J. Ben-Aim, Int. J. Chem. Kinet., 14, 1325 (1982).

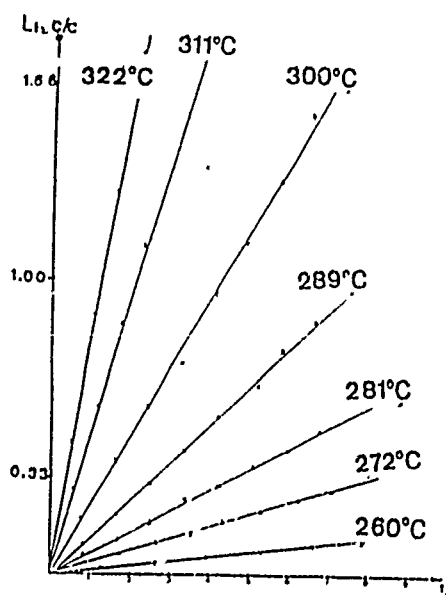


Figure :

Experimental curves of $\text{Ln } C_0/C$ versus residence time;

C: concentration of peracetic acid

Gas phase reactions of 1,4-dioxane with chlorine

Frédérique BATTIN, Paul-Marie MARQUAIRE,
François BARONNET and Guy-Marie CÔME

Département de Chimie Physique des Réactions, CNRS URA 328, INPL-ENSIC,
Université NANCY I, 1, rue Grandville, 54000 NANCY (France)

1,4-dioxane is used as a solvent in the chemical industry in some specific chlorination reactions; explosions between chlorine and dioxane in the gas phase have been observed; therefore a better knowledge of the reactions between chlorine and 1,4-dioxane may lead to an improvement of the safety of operations involving this solvent.

We have first determined the pressure-temperature diagram of the thermal phenomena for mixtures containing 20 to 50 % of dioxane over a temperature range from 80 to 300°C at subatmospheric pressure in a static apparatus.

In this diagram, 2 different regions can be observed, corresponding respectively to slow reaction with no variation of temperature and a small diminution of pressure and to auto ignition characterised by a violent temperature and pressure rise, an induction period, a light emission and an important carbonaceous deposit. The limits between these regions are very sensitive to wall effects.

Auto ignitions are observed for temperature below 100°C with pressure below 200 Torr, this is an evidence of the important reactivity of the mixtures of 1,4-dioxane and chlorine.

This work has been carried on by studying the slow reaction in a continuous dynamic reactor at space times between 0.8 and 1.6 s, at temperatures between 30 and 250°C, at a pressure of 400 Torr and with an equimolar mixture of chlorine and gaseous dioxane, together with nitrogen as an inert gas.

Between 30 to 150°C, the major products of the slow reaction were dioxene, monochlorodioxane and hydrochloric acid and minor products included monochlorodioxene and some dichlorodioxanes. At 150°C, a material balance, at high conversion, has been performed for verifying that all the main reaction products are correctly identified and analysed.

Up to 150°C until about 220°C, the reaction seemed to be completely inhibited: we obtained no more conversion.

Above 220°C, we observed a slow reaction of "high temperature" whose major products are polychloro dioxane.

These phenomena, and the important problems of reproducibility that we could observed, are probably the consequence of a particular sensitivity of reactions involving chlorine to wall effects at low temperaure.

Tentative reaction mechanisms are proposed in order to explain, at least qualitatively, our results.

Aknowledgement: This work has been supported by "Rhône-Poulenc Industrialisation", Environment and Safety Departement, Décines Research Centre.

Kinetic modeling CH₄-O₂-Cl₂ flame reaction

Rémi LE BEC, Paul-Marie MARQUAIRE and Guy-Marie CÔME

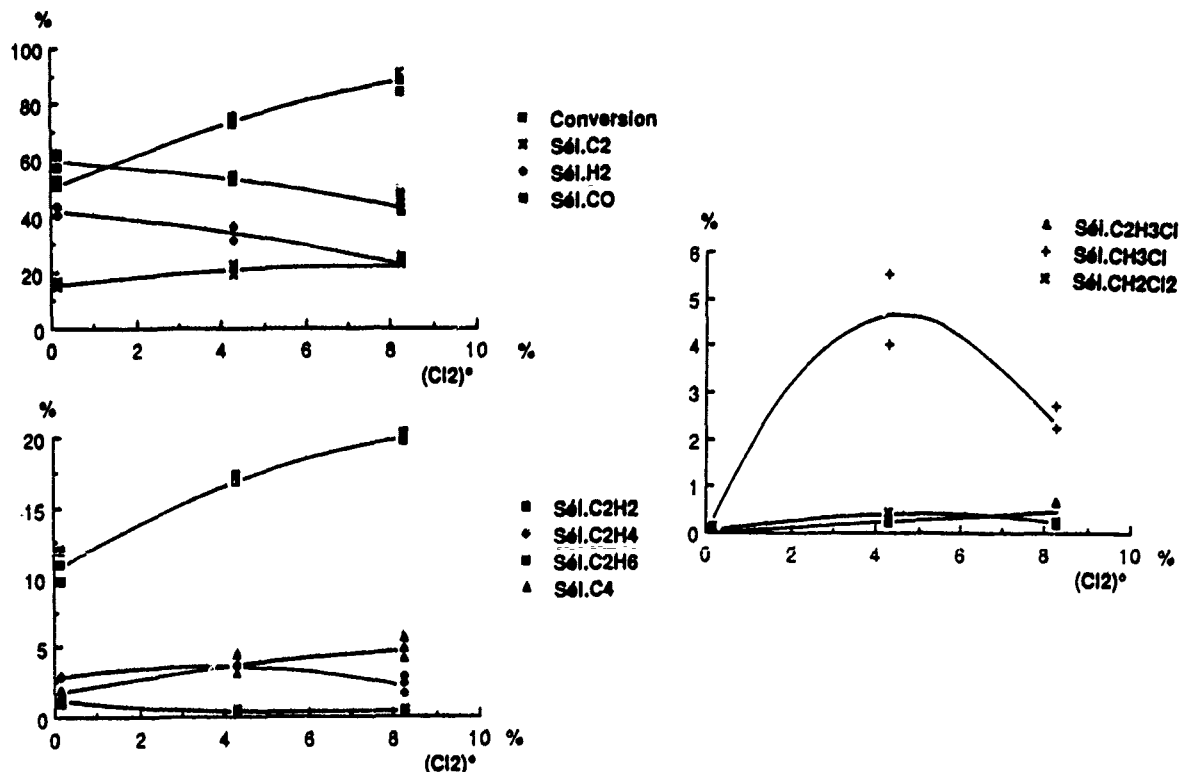
Département de Chimie Physique des Réactions, CNRS URA 328, INPL-ENSIC,
Université NANCY I, 1, rue Grandville, 54000 NANCY (France)

The methane conversion into C₂ hydrocarbons has been studied by a combination of the BASF process (CH₄/O₂ reaction), the BENSON process (CH₄/Cl₂ reaction) and the SENKAN process (CH₃Cl/O₂ reaction).

The reaction is carried out in very short space time diffusion flames quenched by jets of an inert cold gas.

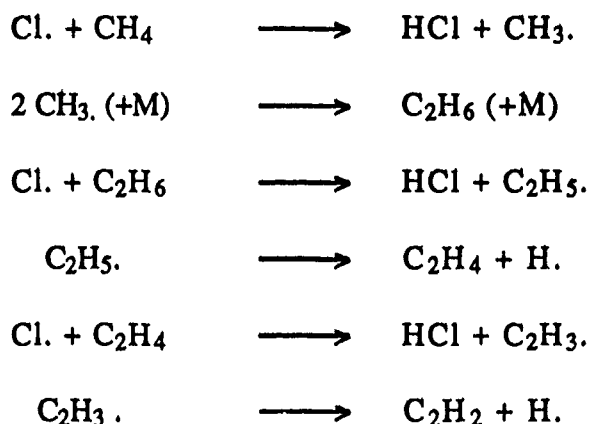
The reaction products include C₂H₂, C₂H₄, C₂H₆, CO, CO₂, CH₃Cl, C₂H₃Cl, CH₂Cl₂, C₄ and soot.

The influence of various parameters on methane conversion, C₂ selectivity and soot formation, has been experimentally studied. Adding Cl₂ to CH₄/O₂ mixtures results in the increase of these three quantities. The soot formation is very sensitive to the conditions of admission of the reactants. For "high" methane space times, the soot formation is drastic, and much less at "low" methane space times.



The modelling of the process has been achieved, using comprehensive free radical mechanisms for the reaction, and sets of connected CFSTR's for the flame reactor. A sensitivity analysis of the reaction mechanism has been done, in order to detect the most determining elementary reactions, allowing a qualitative understanding of the factors governing the reaction

The presence of Cl atoms accelerates both the conversion of methane and the selectivities in C₂ molecules by the reaction path :

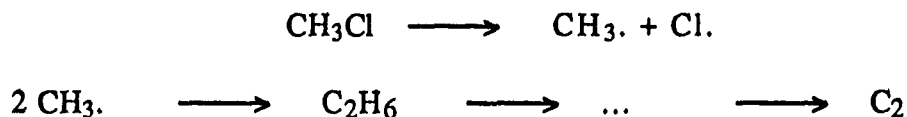


This path produces the undesirable HCl, but also increases the formation of free radicals such as C₂H₃. and C₂H. which are well-known plausible precursors of soot . Consecutive additions such as C₂H₂ + .C₂H₃ → .CH=CH-CH=CH₂, and further cyclization lead to the growth of Polycyclic Aromatic Hydrocarbons (PAH) which are thought to play a central role in the soot formation process. The increase of the selectivity in C₄ molecules and of soot formation with Cl₂ addition in our experimental results partly confirms this point of view.

Methyl chloride is the most important chlorinated hydrocarbon produced in all our experiments. It is formed via the reaction :



followed by its rapid decomposition :



ACKNOWLEDGEMENT

This work has been funded in part by the Commission of The European Communities, through the research programme "Optimization of the production and utilisation of hydrocarbons" (Contract EN3C/0035F/CD).

TEMPERATURE DEPENDENCES OF CH_2 ($\tilde{a}^1\text{A}_1$) REMOVAL RATES

P. Biggs, G. Hancock, M. R. Heal, D. J. McGarvey and A. D. Parr

Physical Chemistry Laboratory, Oxford University,

South Parks Road, Oxford, OX1 3QZ. U.K.

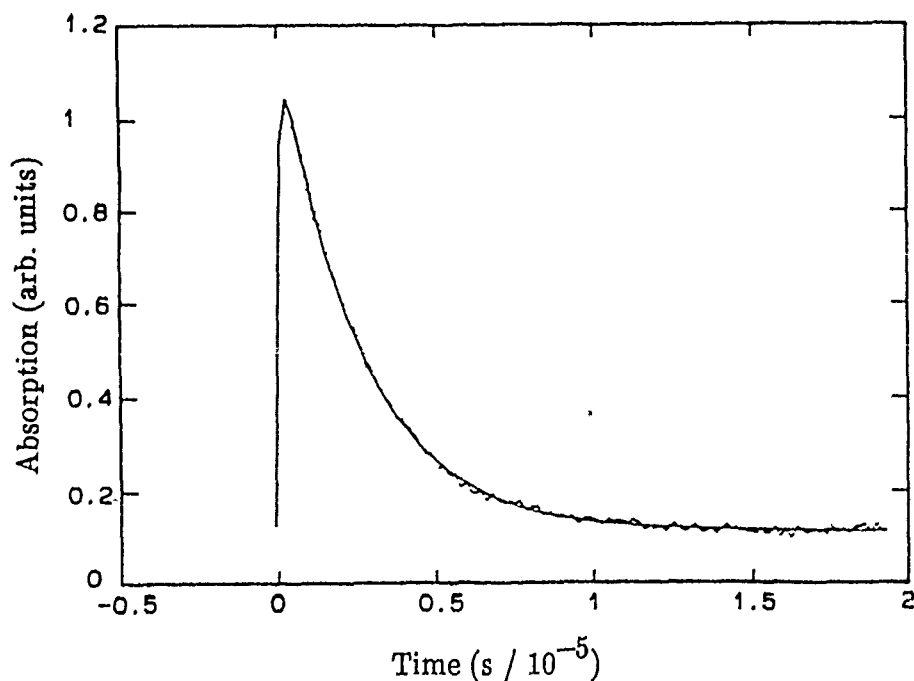
Absolute rate constants for the collisional removal of CH_2 ($\tilde{a}^1\text{A}_1$) have been directly measured as a function of temperature using 308nm UV excimer laser photolysis of ketene (CH_2CO) to prepare the radicals and time resolved cw resonance absorption to observe them. The cw dye laser was used to directly monitor the time evolution of the 4_{14} rotational level of the ground vibrational state via the $4_{04} \leftarrow 4_{14}$ transition near 590.5 nm in the $\tilde{b}^1\text{B}_1 \Sigma(0,14,0) \leftarrow \tilde{a}^1\text{A}_1 \Pi(0,0,0)$ sub-band. For removal by CH_2CO , NO, H_2 and Ar, room temperature (295 K) rate constants of 200, 160, 100 and $5.2 \times 10^{-12} \text{ cm}^3 \text{ molecule}^{-1} \text{ s}^{-1}$ were found respectively. The data are in good agreement with other literature values also obtained by direct observation of the $^1\text{CH}_2$ radical [1,2], although the constants for CH_2CO and Ar removal rates represent a slight decrease from the previously reported measurements using a similar detection technique [2].

The 40 cm length stainless steel multi-pass absorption cell used in these experiments could be maintained at any elevated temperature up to 430 K. For the reaction of $^1\text{CH}_2$ with NO and H_2 there was no significant deviation in removal rate constant at higher temperatures from those measured at ambient. The collisional quenching by Ar appears to rise slightly to a value of $7.6 \times 10^{-12} \text{ cm}^3 \text{ molecule}^{-1} \text{ s}^{-1}$ at 431 K while the rate constant for removal by ketene was observed to decrease to $164 \times 10^{-12} \text{ cm}^3 \text{ molecule}^{-1} \text{ s}^{-1}$ at 428 K. There have been no previously reported temperature dependent data on CH_2 ($\tilde{a}^1\text{A}_1$) removal for comparison.

Recent calculations of the collision induced intersystem crossing rate using the mixed state model [3] show that the observed rate constants should depend upon

a combination of rotational energy transfer rates within the ground state \bar{X}^3B_1 manifold, together with populations of the \bar{a}^1A_1 rotational levels which are most strongly mixed with the triplet levels and act as "doorway" states for the energy transfer process. The present results will be discussed in terms of the expected temperature dependences of both these energy transfer processes and chemical removal steps.

- [1] M. N. R. Ashfold, M. A. Fullstone, G. Hancock and G. W. Ketley,
Chem. Phys. 55, 245 (1981).
- [2] A. O. Langford, H. Petek, and C. B. Moore,
J. Chem. Phys. 78, 6650 (1983).
- [3] U. Bley, M. Koch, F. Temps and H. Gg. Wagner,
Ber. Bunsenges. Phys. Chem. 93, 833 (1989).



An example decay trace after 100 laser shots showing the temporal evolution of the 4_{14} rotational level of CH_2 (\bar{a}^1A_1) in 60 mTorr CH_2CO with 46 mTorr NO at a temperature of 383 K. The solid line corresponds to a least squares fitting of an exponential rise and fall with rates of 3.40×10^6 and $3.92 \times 10^5 \text{ s}^{-1}$ respectively.

Laser-Induced Fluorescence of Silicon and Silicon Monoxide in a Glow Discharge and an Atmospheric Pressure Flame.

Anthony J. Hynes

Molecular Sciences Branch, Georgia Tech Research Institute, Georgia Institute of Technology, Atlanta, GA 30332

Silicon monoxide (SiO) and atomic silicon (Si) are potentially important intermediates in a variety of combustion and plasma environments. Examples include silicon doped flames used in Vapor-phase Axial Deposition for the manufacture of optical waveguides, and a variety of CVD and plasma-enhanced CVD processes for the deposition of silicon and silica in microelectronics fabrication.

We have observed LIF from SiO in low pressure glow discharges in Ar/O₂/SiCl₄ mixtures and in atmospheric pressure CH₄/O₂ flames doped with SiCl₄. Fluorescence was excited via the A¹Π-X¹Σ⁺ transition at ≈230 nm. Spectra were assigned by comparison with simulated spectra computed from previously reported line positions and rotational and vibrational temperatures obtained. Resolved fluorescence measurements using a gated optical multichannel analyzer have been used to measure energy transfer rates in the A¹Π state.

Si atoms have been observed in low pressure discharges and also as a product in the 193 and 251 nm multiphoton dissociation of silanes. Si atoms were monitored via LIF by scanning the laser across the 4s ³P^o -> 3p² ³P transition at ≈250 nm and monitoring the undispersed fluorescence measurements. Production of Si 4s ³P^o in the 193 and 251 nm multiphoton dissociation of silanes has also been observed and the implications for Si atom diagnostics will be discussed.

A Flash Photolysis Study of the Self-Reactions and UV Spectra of the Neopentylperoxy and t-Butylperoxy Radicals

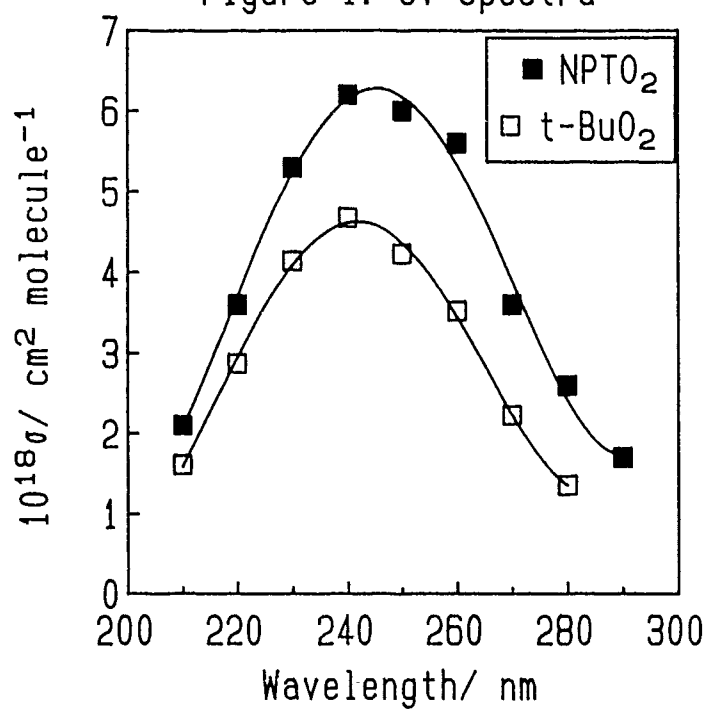
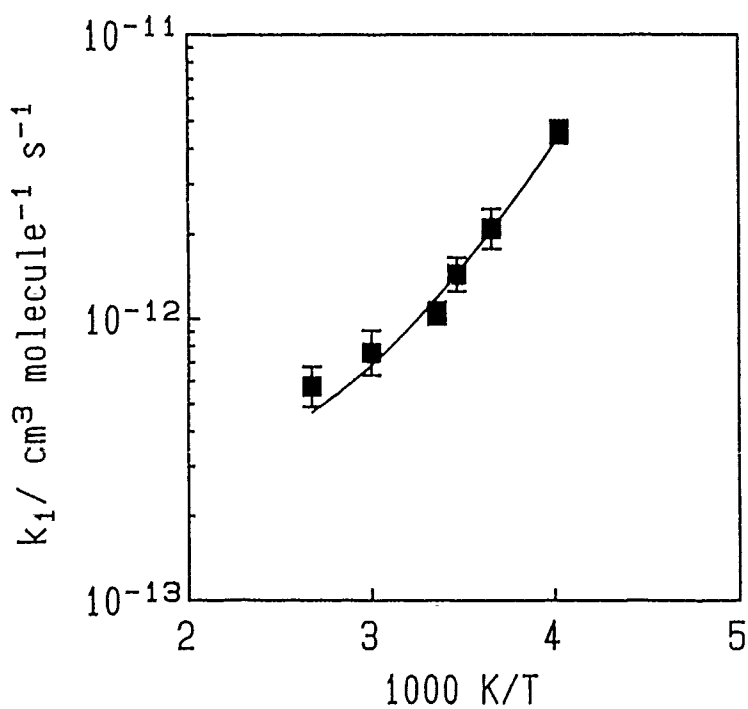
P.D. Lightfoot, P. Roussel, B. Veyret and R. Lesclaux

Laboratoire de Photophysique et Photochimie Moléculaire,
Université de Bordeaux I,
33405 TALENCE Cedex, FRANCE.

The self-reaction of neopentylperoxy radicals, neo-C₅H₁₁O₂ (NPTO₂):
 $\text{NPTO}_2 + \text{NPTO}_2 \rightarrow 2 \text{ t-C}_4\text{H}_9\text{CH}_2\text{O} + \text{O}_2$ (1a); $\rightarrow \text{ t-C}_4\text{H}_9\text{CHO} + \text{ t-C}_4\text{H}_9\text{CH}_2\text{OH} + \text{O}_2$ (1b); $\rightarrow \text{ t-C}_4\text{H}_9\text{CH}_2\text{OOCH}_2\text{C}_4\text{H}_9\text{-t} + \text{O}_2$ (1c), has been studied from 248 to 373 K and from 50 to 760 Torr total pressure. The neopentylperoxy radicals formed via channel (1a) react, under most experimental conditions, by unimolecular decomposition: $\text{t-C}_4\text{H}_9\text{CH}_2\text{O} + \text{M} \rightarrow \text{ t-C}_4\text{H}_9 + \text{HCHO} + \text{M}$ (5). The t-butyl radicals so formed are rapidly converted into t-butylperoxy radicals under our conditions; these radicals are unreactive on the timescale of the NPTO₂ decay and enable the branching ratio for reaction (1) to be determined via their u.v. absorption. The overall rate constant reaction (1) displays a strong negative temperature dependence, being well-described by $k_1/\text{ cm}^3 \text{ molecule}^{-1} \text{ s}^{-1} = 3.02 \times 10^{-19} (T/298)^{9.48} \exp(4260/T)$ over our temperature range. The non-terminating channel (1a) becomes increasingly important with increasing temperature, with $\beta = (197 \pm 67) \exp(-(1658 \pm 98)/T)$, where β is the ratio of those radicals which react via the non-terminating channel (1a) to those which react via the terminating channels (1b) and (1c). By measuring the reduction in the fraction of NPTO₂ radicals converted to t-butylperoxy radicals with increasing oxygen concentration, rate constants for reaction (5) were determined, giving $E_5/\text{ kJ mol}^{-1} = 42.7 \pm 2.1$. The u.v. spectra of NPTO₂ and t-C₄H₉O₂ have been determined relative to that of CH₃O₂^{1,2}; both are similar in shape and magnitude to other alkylperoxy radical spectra, displaying maxima around 240 nm, with $\sigma_{240 \text{ nm}}(\text{NPTO}_2)/\text{ cm}^2 \text{ molecule}^{-1} = (6.2 \pm 1.1) \times 10^{-18}$ and $\sigma_{240 \text{ nm}}(\text{t-C}_4\text{H}_9\text{O}_2)/\text{ cm}^2 \text{ molecule}^{-1} = (4.7 \pm 0.9) \times 10^{-18}$. The self-reaction of t-butylperoxy radicals: $2 \text{ t-C}_4\text{H}_9\text{O}_2 \rightarrow 2 \text{ t-C}_4\text{H}_9\text{O} + \text{O}_2$ (11) was also briefly studied, resulting in $k_{11}/\text{ cm}^3 \text{ molecule}^{-1} \text{ s}^{-1} \approx 1.0 \times 10^{-11} \exp(-3890/T)$. Errors are 1 σ .

1. P.D. Lightfoot, R. Lesclaux and B. Veyret, *J. Phys. Chem.*, **94**, 700 (1990).
2. P.D. Lightfoot, R. Lesclaux and B. Veyret, *J. Phys. Chem.*, **94**, 708 (1990).

Figure 1. UV Spectra

Figure 2. NPTO₂ + NPTO₂ Arrhenius Plot

High Pressure Effects of Water on Combustion Kinetics*

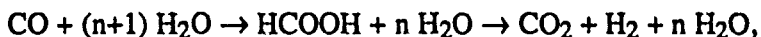
C. F. Melius and N. Bergan
Combustion Research Facility
Sandia National Laboratories
Livermore, California 94551-0969

and

J. E. Shepherd
Rensselaer Polytechnic Institute
Troy, New York 12180-3590

Abstract

The effect of water at high pressure on the water gas shift reaction has been studied theoretically using the quantum chemical BAC-MP4 method coupled with the Peng-Robinson non-ideal-gas equation of state. We consider the effect of water on rate constants both as a solvating agent and as an integral participant in bond forming and breaking. Transition states have been identified for the reaction mechanism occurring via the formic acid intermediate,



as a function of additional water molecules n ($0 \leq n \leq 2$). We present results for the thermodynamic properties (enthalpies, entropies, and free energies) of the reactants, intermediates, products, and transition state structures which are used in transition state theory to determine the rate constants. Results are presented for temperatures and pressures above the critical point of water as well as for liquid water. The change in chemical potentials due to liquid water is found to be large, while above the critical temperature, the change is relatively small, even at 300 atm. pressure. The structures of the transition states indicate that as the hydrogen atoms shift from one bond to another, they acquire a more positive charge (relative to that in water), indicating the initial stages of formation of hydrated protons, even in the gas phase. In conclusion, we find that water can play an important role in the high pressure gas phase chemical kinetics, both explicitly in altering the reaction pathway and implicitly as a solvating agent.

*This work supported by the U. S. Department of Energy.

EXPERIMENTAL AND MODELLING INVESTIGATION OF BUTANE AUTOIGNITION
IN A RAPID COMPRESSION MACHINE

M. CARLIER, R. MINETTI, J.F. PAUVELS, M. RIBAUCCOUR, L.R. SOCHET

Laboratoire de Cinétique et Chimie de la Combustion

UA CNRS 876

Université des Sciences et Techniques de Lille, Flandres Artois

59655 VILLENEUVE D'ASCQ Cedex. France

As part of a work related to knock in spark ignited engines, autoignition of butane has been studied in a rapid compression machine ($p = 10:1$) at different temperatures ($650K < T < 900K$) and under a pressure of 10 bar. Two mixtures including N_2 and/or Ar as a diluent have been investigated for different equivalence ratio ($\phi = 0.8, 1, 1.2$). A negative temperature coefficient for ignition delays was observed with a two-stage autoignition at low temperature.

The experimental results are confronted with the predictions from calculations based on a detailed mechanism (133 species, 689 reversible elementary reactions) including both pyrolysis of alkyl radicals and isomerization of peroxy radicals. A relatively good agreement of the negative temperature coefficient is obtained.

The evolution of autoignition delays is strongly influenced by the rate constants of peroxy radicals isomerization and hydroperoxide formation reactions.

A REDUCED CHEMICAL KINETIC MECHANISM FOR THE SULPHUR INHIBITION IN FLAMES

J.F. PAUWELS, M. CARLIER, P. DEVOLDER, L.R. SOCHET

Laboratoire de Cinétique et Chimie de la Combustion

UA CNRS 876

Université des Sciences et Techniques de Lille, Flandres Artois

59655 VILLENEUVE D'ASCQ Cedex, France

A low-pressure premixed stoichiometric methanol-air flame doped with up to 2.4% H_2S has been analyzed. The experimental data obtained by Sampling Probe / Gas Chromatography / Electron Spin Resonance technique are compared with the predictions from a one-dimensional model. A reduced chemical mechanism including only 5 sulphur species involving in 13 reversible reactions is proposed for the sulphur inhibition and gives a reasonable description of the major features of the experimental data.

The relevant effect of sulphur addition is a significant increase of H_2 and CO mole fractions and a decrease of CO_2 , O and OH shown by both numerical and experimental procedures.

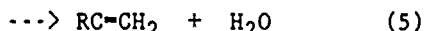
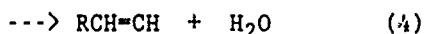
A reaction path analysis, including the calculation of the net reaction rates and the contribution of certain elementary reaction pairs is used to interpret the model. This indicates that (i) hydrogen sulfide disappears principally by the radical abstraction reactions $\text{H}_2\text{S} + \text{H} = \text{SH} + \text{H}_2$ and $\text{H}_2\text{S} + \text{OH} = \text{SH} + \text{H}_2\text{O}$, (ii) SO is rapidly formed, earlier than H, O and OH radicals in the reaction zone, by a competition between $\text{S} + \text{O}_2 = \text{SO} + \text{O}$ and $\text{SO} + \text{OH} = \text{SO}_2 + \text{H}$ reactions, (iii) the SO_2 chemistry is essentially controlled by SO reaction with OH on the whole reaction zone.

Branching Ratio of OH-Alkene ReactionsC Anastasi⁺, C Morley[#], D Muir⁺, J Andarez-Alvarez^{*}⁺ Department of Chemistry, University of York, Heslington, York, YO1 5DD, England^{*} Department of Chemical Engineering, University de Los Andes, Merida, Venezuela[#] Shell Research Ltd., Thornton Research Centre, P.O.Box 1, Chester, EnglandABSTRACT

The reaction of OH radicals with alkenes is of interest in atmospheric chemistry¹, due to its role in photochemical air pollution systems. The reaction is also important in the consideration of combustion chemistry², in particular in autoignition phenomena. The rate constant for the overall reaction (1) has been studied^{3,4}, most recently by flash photolysis/kinetic absorption techniques³.



However, there has been no quantitative study to date of the branching ratio between the possible routes for the reaction (reactions (2), (3), (4) and (5)), particularly in the temperature range from 500-700K where the mechanism of the overall reaction is believed to change.



(Where R=H or an alkyl group, H producing a special case where the products of reactions (2) and (3) are the same and the products of reactions (4) and (5) are also the same)

We have carried out a study of the branching ratio between these reactions for ethene and propene via a pyrolysis/radical trap method using gas chromatography for product analysis. The reactions have been studied over the temperature range 450-650K and in a pressure regime from 50-500 Torr. The effect of the addition of the alkene to the pyrolysis of a hydroperoxide has been used to determine the final products of its reaction with OH and hence the branching ratio of the reaction.

References

1. B.J.Finlayson-Pitts & J.N.Pitts,Jr., "Atmospheric Chemistry", p.431-441, Wiley Interscience, 1986
2. R.R.Baker, R.R.Baldwin & R.W.Walker, Symp.(Int.) Combust.[Proc.], 13th, 291 (1971).
3. F.P.Tully, Chem.Phys.Lett., 96, 148, (1983)
4. A.C.Lloyd et al, J.Phys.Chem., 80, 789, (1976)

TEMPERATURE MEASUREMENT IN A CW CO₂ LASER BEAM BYLASER-INDUCED FLUORESCENCE OF O₂

C. LALO, J. MASANET, J. DESON AND R. BEN-AM

Laboratoire de Chimie Générale, UPMC-CNRS URA 870

Tour 55-54, 4^e Etage, 4 Place Jussieu,

75252 Paris Cedex 05, FRANCE.

and

J. ROSTAS

Laboratoire de Photophysique du CNRS and IPCM

de l'Université Paris-Sud B^t 213, Université Paris-Sud,

91405 Orsay, FRANCE.

We report on the determination, by ArF laser induced fluorescence from O₂(B³Σ_u⁻) of the temperature achieved in a SF₆/O₂ non reactive flow heated by a CW IR laser⁽¹⁾.

A mixture of SF₆ (1 mb) + O₂ (300 mb) is irradiated by an infrared (10.6 μm) CW CO₂ laser. The SF₆ absorbs the infrared energy which is redistributed through collisional energy transfers into both species within a few microsecondes. The thermal equilibrium which is reached in the laser beam strongly depends upon the vibrationally excited species diffusion out of the IR laser beam, upon the laser fluence, the gas pressure and the flow rate.

Radiation from an ArF excimer laser (193.3 nm) which is not absorbed by SF₆, excites O₂ to the B³Σ_u⁻ state, and the dispersed B³Σ_u⁻ - X³Σ_g⁺ emission (Schumann-Runge bands) is recorded. The intensity of the observed emission bands is directly related to the rovibrational population of the O₂ ground-state. The O₂ temperature in the CO₂ laser beam is determined by comparison of the observed fluorescence spectrum with spectra simulated between 220 and 260 nm for various temperatures from 300 to 800 K, assuming a Boltzmann population distribution.

Laser Induced Fluorescence (LIF) spectra were first recorded at low flow rate (1 cm³sec.⁻¹) without IR laser irradiation, in order to have a reference spectrum at 300 K. At 300 K, only the v'' = 0 level of the X³Σ_g⁺ ground state is significantly populated and the ArF laser band excites the v' = 4 level of the B state. The main features of the fluorescence are thus assigned to the B(v' = 4) → X(v'' = 5-8) bands.

The fluorescence spectrum in the IR laser beam consists of blue-shifted bands, the intensity of which is enhanced by a factor of 10 with regard to the LIF spectrum observed at 300 K ; it decreases (50 %) as the gas flow rate is increased by two orders of magnitude (Fig. 1). The fluorescence results from direct excitation by the ArF laser of the B(v' = 4-13) ← X(v'' = 0-2) rovibronic transitions and each feature of the fluorescence spectrum consists of the superposition of the rotational envelope of several vibrational bands.

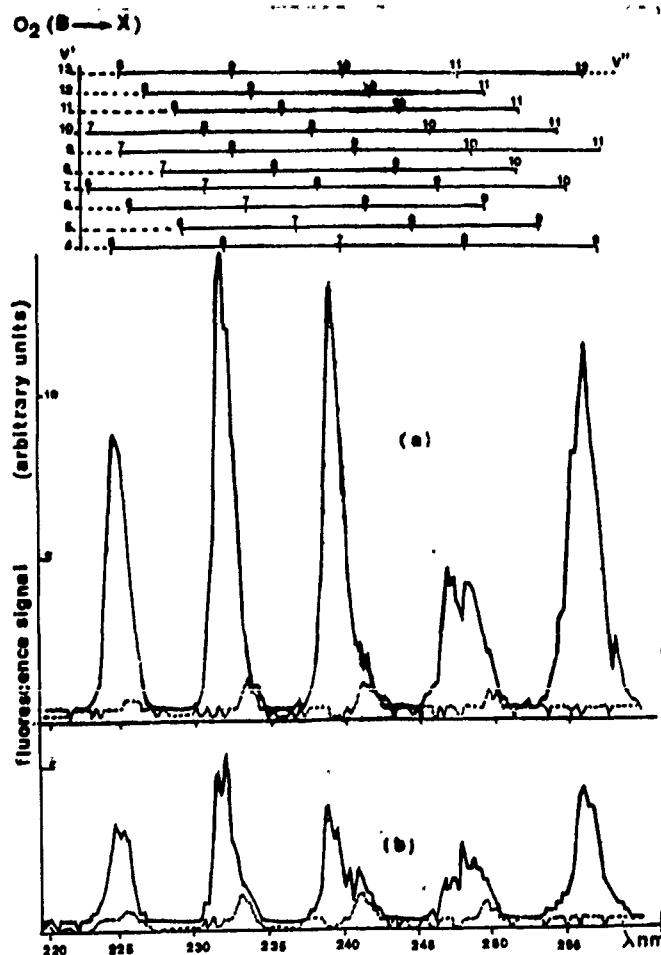
The LIF spectrum was calculated in two steps, using the RLS computer code developed by Albritton et al⁽²⁾ I) calculation of the relevant absorption spectrum in the wavelength range of the ArF laser line II) calculation of the total fluorescence spectrum summed over all emissions wavelength, corrected for the predissociation of the B state for each vibrational level ; fluorescence yield was calculated using recently measured predissociation linewidths⁽³⁾.

Analysis by spectrum simulation was performed for temperatures from 300 to 1500 K between 230 and 260 nm. The shape and relative intensity of the various fluorescence features being strongly temperature dependent, from a comparison of simulated spectra with the observed emission bands, the temperature of hot O_2 in the laser beam is measured.

References

- (1) C. Lalo, J. Masanet, J. Deson, R. Ben-Aim and J. J. Rostas.
Applied Spectroscopy (to be published).
- (2) D.L. Albritton, D.L. Harrop, A.L. Schmeltekopf, R.N. Zare.
J. Mol. Spectrosc. 46 (1973) 103.
- (3) A.S.C. Cheung, K. Yoshino, J.R. Esmond, S.S.L. Chiu.
J. Chem. Phys. sous presse.

Fig. 1 Dispersed ArF laser induced fluorescence spectrum of O_2
(B - X) bands
(resolution 0.5 nm)
---- at room temperature
— heated in a CW laser beam
a : low flow rate
b : high flow rate



A KINETIC STUDY OF THE REACTION BETWEEN MAGNESIUM ATOMS AND NITROUS OXIDE

C. Vinckier and P. Christiaens

Department of Chemistry, K.U. Leuven, Belgium

In this work a kinetic study is made of the reactions between ground state magnesium atoms in the gas phase and nitrous oxide



Thermally generated Mg atoms are carried downstream in a quartz fast flow reactor where they are allowed to react with N_2O . The detection is carried out by atomic absorption spectroscopy in the concentration range from $9.6 \cdot 10^8$ to $2.9 \cdot 10^{10}$ atoms cm^{-3} . By following the decrease of the Mg absorbance as a function of added N_2O the rate constant k_1 can be derived and is equal to $1.2 \pm 0.1 \times 10^{-13}$ $\text{cm}^3 \text{ molec}^{-1} \text{ s}^{-1}$ at 788 K. In the temperature range from 470 to 900 K the Arrhenius expression for k_1 is given by

$$k_1 = (7.72 \pm 1.63) \times 10^{-11} \text{ e}^{\frac{-10.2 \pm 0.67 \text{ kcal mol}^{-1}}{RT}}$$

$\text{cm}^3 \text{ molec}^{-1} \text{ s}^{-1}$. It was verified that the value of k_1 given by the above expression is independent of various experimental parameters such as the reactor pressure, nature of the carrier gas, mixing time and initial Mg concentration. The activation energy of 10.2 kcal for reaction 1 could be the result of a combined effect. The first barrier arises from the repulsive forces when the Mg atom with a closed shell structure interacts with the molecule N_2O . The second barrier is due to the bending energy required to pass from the linear N_2O molecule to the lowest lying N_2O^- ion configuration.

Reaction of HO₂ radical with hydrogen sulfide.

V.P.Bulatov, S.I.Vereshuk, V.N.Khabarov, O.M.Sarcisov.

Institute of Chemical Physics, USSR Academy of Sciences

Three series of experiments were carried out to study reaction (1) at 298K.



In the first series of experiments, kinetics of HO₂ radicals was studied both in the presence of H₂S and without it. HO₂ radicals were formed by flash photolysis of Cl (or NOCl) in the presence of CH₃OH+O₂ (Cl₂+hν → Cl, Cl+CH₃OH → HCOH+HCl, HCOH+O₂ → HO₂+CH₂O). The registration of HO₂ radicals was realized by intracavity laser spectroscopy in the near infrared range (λ 1.3 μm). Without hydrogen sulfide decay profile was characterized only by the reaction HO₂ with HO₂. In the presence of H₂S the rate of HO₂ decay was increased. The rate constant of reaction (1) was obtained as k₁=(4±1)·10⁻¹²cm³s⁻¹. In the second series of experiments the kinetics of HSO radicals was studied in the same gas mixture (Cl₂(or NOCl)+CH₃OH+O₂+H₂S). However these experiments were realized on other setup and gas concentration of mixture was changed. We observed the formation of HSO radicals registered by intracavity laser spectroscopy in visible range. These experimental data may be explained, if we assume that HSO radicals are the products of reaction (1).

In the third series of experiments hydrogen sulfide was photolysed only in the presence of oxygen. In these experiments concentration of radicals was lower in order to exclude radical-radical reaction HO₂+HS→HSO. In these system the observed HSO radicals may be explained by the following steps: H₂S+hν→HS+H, H+O₂+M→HO₂+M, HO₂+H₂S→HSO+H₂O.

The experiments performed enable to assume that the reaction (1) is a limiting stage of photooxidation of hydrogen sulfide in troposphere.

New Notion on the Mechanism of Gas-Phase
Oxidation of Unsaturated Hydrocarbons

A.A.Mantashyan, S.D.Arsentiev, R.R.Grigoryan,
E.A.Arakelyan, A.N.Kocharyan

Institute of Chemical Physics, Armenian
Academy of Sciences, USSR

The mechanism of gas-phase oxidation of unsaturated hydrocarbons, based on the addition reactions of atoms and radicals to the double $C=C$ bond is proposed. New experimental data on radicals behaviour at ethylene, propylene and benzene oxidation processes are the foundation of this mechanism. Using the ESR-spectrometry it was established that at the oxidation of ethylene and propylene as well as in the case of corresponding saturated hydrocarbons-ethane and propane-alkylperoxy and hydroperoxy radicals were formed and accumulated in the highest concentration. At the oxidation of benzene the carbon-containing radicals were detected together with peroxy radicals. The study of kinetic behaviour of molecular products together with radicals in the processes of oxidation of ethylene, propylene and their mixtures with different hydrocarbons shows that alkylperoxy radicals interact with olefins, leading to their epoxidation and forming more active alkoxy radicals responsible for further chain propagation.

The totality of obtained data is the experimental foundation of new notion on the mechanism of gas-phase oxidation of unsaturated hydrocarbons.

Rates and Mechanisms of Gas-Phase Desubstitution of Benzene Derivatives by Hydrogen Atoms near 1000 K.

*Jeffrey A. Manion[‡] and Robert Louw**

Utilizing a competitive technique, rates and mechanisms of desubstitution of C_6H_5X , $X = D, CH_3, CF_3, OH, Cl$, and F , have been examined. Mixtures of C_6D_6 and C_6H_5X were thermolyzed in H_2 in a tubular flow system at atmospheric pressure between 898 and 1039 K. Removal of D or X occurs via hydrogen atom attack and lower deuterated benzenes and C_6H_6 are formed. Mass spectral product analyses for (deutero)benzenes have been used to determine the rates of desubstitution $C_6H_5X + H\bullet \rightarrow C_6H_6$ (1) relative to $H\bullet + C_6D_6 \rightarrow C_6D_5H$ (2). For $X = D, CH_3, CF_3$, and OH , displacement occurs by an addition/elimination sequence. For $X = Cl$ direct abstraction also takes place and for $X = F$, abstraction is the only operative mechanism. Evidence is presented that hydrogen migration around the ring in cyclohexadienyl radicals does not occur under the conditions studied. Based on k_2 , absolute expressions for k_1 have been derived. Results are compared with literature data and the substituent effect is discussed.

[‡]Chemical Kinetics Department, Chemistry Laboratory
SRI International
Menlo Park, CA 94025, USA

*Center for Chemistry and the Environment, CCE
Gorlaeus Laboratories
Leiden University, P.O. Box 9502
Leiden, The Netherlands

COMPARISON OF THE THERMAL AND LASER-INDUCED
DECOMPOSITION OF 1,2-DICHLOROETHANE

by

P.E. Dyer,* K.A. Holbrook, M. Matthews* and G.A. Oldershaw

School of Chemistry, University of Hull, Hull, U.K.

Thermal decomposition of 1,2 dichloroethane is the major industrial route to vinyl chloride and therefore of major importance in the polymer industry. The thermally induced process is a well known example of a free radical chain process subject to complicating heterogeneous processes. Photochemical initiation of the reaction offers many apparent advantages and has therefore been the subject of several recent papers.

The present work describes a direct comparison in the same static reactor between the thermal reaction at 703 K and the pulsed KrF laser-induced process (248 nm). Quantum yields of between 6×10^3 and 12×10^3 were found which showed an inverse square root dependence on the initial chlorine atom concentration. By-product formation was investigated using glc and gc/ms methods. The major by-products were identified as ethene, acetylene and 1,2,3,4-tetrachlorobutane in agreement with other observations.

The photochemical reaction was found to proceed about three times faster than the thermal reaction under the same conditions even at a low repetition rate of 0.5 s^{-1} and to produce far fewer by-products.

Computer modelling of a complete reaction mechanism was used to predict both quantum yields and by-product yields under a range of conditions.

* Department of Applied Physics

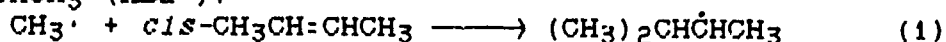
RATE CONSTANTS OF H-ATOM ABSTRACTION BY THE $\text{CH}_3\cdot$ AND $(\text{CH}_3)_2\text{CHCHCH}_3$ RADICALS FROM AND ADDITION OF THE $\text{CH}_3\cdot$ RADICAL TO *cis*- $\text{CH}_3\text{CH}=\text{CHCH}_3$

L. Seres and A. Nacsá

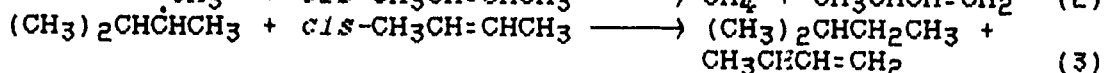
*Institute of General and Physical Chemistry,
Attila József University, Szeged, Hungary*

The di-*t*-butyl peroxide (DTBP)-initiated thermal reaction of *cis*- $\text{CH}_3\text{CH}=\text{CHCH}_3$ (B2) was studied in the temperature range 395-443 K at reactant concentrations of $3.5 \cdot 10^{-3}$; $[\text{B2}]/\text{mol dm}^{-3}$; $6.6 \cdot 10^{-3}$ and $2.9 \cdot 10^{-4}$; $[\text{DTBP}]/\text{mol dm}^{-3}$; $6.8 \cdot 10^{-4}$. End-products were analysed by GC and GC-MS techniques, and the rates of formation of products were determined in the early stages of the reaction.

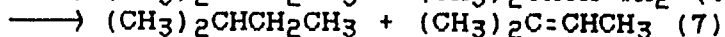
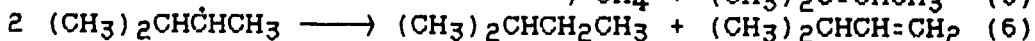
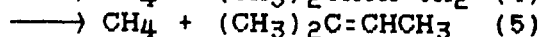
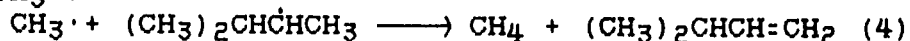
Addition of the $\text{CH}_3\cdot$ radical to B2 yields the radical $(\text{CH}_3)_2\text{CH}\dot{\text{C}}\text{HCH}_3$ (MB2 \cdot):



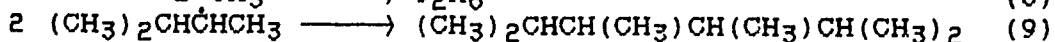
and H-abstraction by the $\text{CH}_3\cdot$ and MB2 \cdot radicals from B2 yields the radical $\text{CH}_3\text{CHCH}=\text{CH}_2$ (MA \cdot), CH_4 and $(\text{CH}_3)_2\text{CHCH}_2\text{CH}_3$ (2MBA):



Disproportionations yield $(\text{CH}_3)_2\text{CHCH}=\text{CH}_2$ and also $(\text{CH}_3)_2\text{C}=\text{CHCH}_3$:

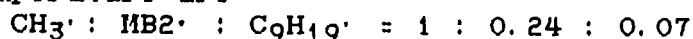


The Arrhenius parameters of the rate constants relative to the combinations



were estimated from the initial rates for reactions (1)-(3).

Some of the $\text{CH}_3\cdot$ radicals yield oligomeric radicals before they are converted into end-products. The ratios of different oligomeric radicals incorporated in the products at medium temperature are



Thus, the reactions of the radicals $>\text{C}_9\text{H}_{19}\cdot$ are of minor kinetic importance and they were not considered further.

Since all the products of the MB2 \cdot radical were measured, and only negligible amounts of $\text{C}_9\text{H}_{19}\cdot$ radicals were formed, the rate constant ratio for $\text{CH}_3\cdot$ addition to B2 relative to its recombination could be evaluated:

$$\frac{k_1}{k_8^{1/2}} = \frac{\sum v_j r_j}{r(\text{C}_2\text{H}_6)}$$

where subscript *j* refers to the rate of formation of all the measured products incorporating the MB2 \cdot and $\text{C}_9\text{H}_{19}\cdot$ radicals.

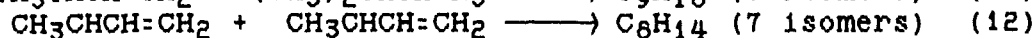
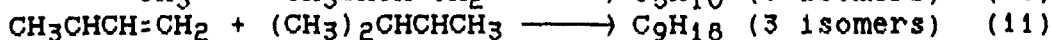
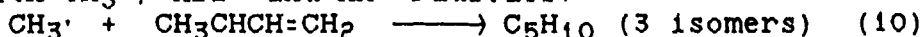
The value obtained is

$$\log(k_1/k_8^{1/2}) = (3.90 \pm 0.40) - (41.93 \pm 1.91)/\theta$$

The units of $k_1/k_2^{1/2}$ and E are $\text{dm}^3/2 \text{ mol}^{-1/2} \text{ s}^{-1/2}$ and kJ mol^{-1} , respectively, and $\Theta = RT \ln 10$.

CH_4 and 2MBA are products of H-abstractions from B2 and $\text{MB2}\cdot$. It is easy to show that the contribution of disproportionation reactions is relatively small and can be easily estimated.

The $\text{MA}\cdot$ radical is converted into end-products via combination with $\text{CH}_3\cdot$, $\text{MB2}\cdot$ and $\text{MA}\cdot$ radicals:



The octadiene isomers formed were measured, while the amounts of $\text{MA}\cdot$ converted into C_5H_{10} and C_9H_{18} isomers were estimated by using the cross-combination rule. The ratio of products incorporating the $\text{MA}\cdot$ radicals to that of paraffins formed in H-abstraction and disproportionation at medium temperature

$$\frac{2\text{EC}_8\text{H}_{14} + (\text{C}_5\text{H}_{10})_{\text{comb}} + (\text{C}_9\text{H}_{18})_{\text{comb}}}{\text{CH}_4 + 2\text{MBA}} = 0.93$$

indicates that most of the CH_4 and 2MBA is produced in H-abstraction from B2.

Since $\Delta(\text{CH}_3\cdot, \text{MB2}\cdot) = 0.144$ and $\Delta(\text{MB2}\cdot, \text{MB2}\cdot) = 1.49$ are known [1,2], the contribution of disproportionation to CH_4 and 2MBA formation could be estimated and the rate constant ratios for H-abstraction from B2 by the $\text{CH}_3\cdot$ and $\text{MB2}\cdot$ radicals relative to their recombinations were evaluated from the equations

$$\frac{k_2}{k_8^{1/2}} = \frac{r(\text{CH}_4)_{\text{abs}}}{r(\text{C}_2\text{H}_6)^{1/2} [\text{B2}]}$$

$$\frac{k_3}{k_9^{1/2}} = \frac{r(2\text{MBA})_{\text{abs}}}{r(\text{C}_{10}\text{H}_{22})^{1/2} [\text{B2}]}$$

The values obtained are

$$\log(k_2/k_8^{1/2}) = (3.32 \pm 0.33) - (35.83 \pm 1.40)/\Theta$$

$$\log(k_3/k_9^{1/2}) = (3.69 \pm 0.52) - (42.91 \pm 2.36)/\Theta$$

Measurement of the self- and cross-combination products of the $\text{CH}_3\cdot$, $\text{MA}\cdot$ and $\text{MB2}\cdot$ radicals allowed evaluation of some cross-combination rate constants:

$$\phi(\text{CH}_3\cdot, 3\text{MB2}\cdot) = 2.15 \pm 0.03$$

$$\phi(\text{CH}_3\cdot, \text{trans-MA}\cdot) = 1.98 \pm 0.03$$

$$\phi(3\text{MB2}\cdot, \text{cis-MA}\cdot) = 2.02 \pm 0.03$$

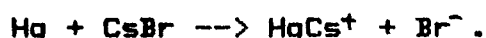
$$\phi(\text{CH}_3\cdot, \text{cis-MA}\cdot) = 1.96 \pm 0.03$$

$$\phi(\text{trans-MA}\cdot, \text{cis-MA}\cdot) = 1.99 \pm 0.03$$

[1] C.W. Larson, S. Rabinovitch and D.C. Tardy, J. Chem. Phys., **47**, 4570 (1967).

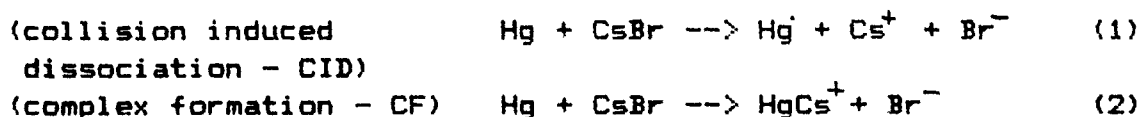
[2] J.H. Georgakakos, B.S. Rabinovitch and C.W. Larson, Int. J. Chem. Kinet., **3**, 535 (1971).

EXCITATION FUNCTION FOR THE COMPLEX FORMATION REACTION



V.M.Akimov, L.V.Lenin, L.Yu.Rusin
 Institute of Energy Problems of Chemical Physics
 Academy of Sciences of the USSR
 USSR, Moscow, Leninsky pr. 38, bld.2

The collisions of atomic mercury with cesium bromide at enough high translation energy result in two reactive channels:



We have already reported the investigations of CID [1]. In this paper are presented the results of crossed molecular beam measurements of the branching ratio of these channels. The supersonic seeded (in H_2 -carrier) beam of mercury atoms and the thermal effusive beam of CsBr were crossed at the right angle. The mass-resolved positive ion flux was measured by a time-of-flight mass-spectrometer. The branching ratio $\text{BR} = I(\text{Cs}^+)/I(\text{HgCs}^+)$ was defined at the relative collision energies E_{rel} from 4.5 eV to 7.0 eV and ranged approximately from 40 to 1500. The dependence of BR on E_{rel} was fitted by $\exp(-1.53 \cdot E_{\text{rel}})$. Expressing the complex intensity in terms of the intensity of cesium cations defined in [1] and BR ($I(\text{HgCs}^+) = I(\text{Cs}^+)/\text{BR}$), one can obtain the usual shape of the excitation function of CF [2]. It has the pronounced threshold near the reaction endoergicity and the maximum near 6 eV. Thus, one can interpret the excitation functions for CF observed in [2] in terms of the "association probability", i.e. the CF channel is the part of the CID channel with the probability exponentially decreasing when the energy increases.

We performed also the 2D impulsive calculations of the CF process. The complex was assumed to be formed if the kinetic energy of the relative motion of Hg and Cs^+ was less than the definite value (about 0.1 eV). The excitation function simulated has the like form with the pronounced threshold and the maximum near 6 eV. This curve corresponds to the encounter with Br-end of the molecule. The interesting result is the existence of another peak with the threshold near 8 eV and the maximum near 10.5 eV. It corresponds to the encounter with Cs-end of the molecule and is even more intensive than the first peak. Unfortunately, neither Parks et al. nor we worked in the enough high energy range to be able to observe the second peak.

1. L.V.Lenin, L.Yu.Rusin, Chem.Phys.Lett., in press
2. E.K.Parks, L.G.Pobo, S.Wexler, J.Chem.Phys. 80 (1984) 5003.

**KINETICS OF $\text{CH}_3\text{O}_x + \text{HO}_x$ INTERACTIONS:
A COMBINED PHOTOFRAGMENT EMISSION/LIF STUDY.**

R. Zellner

Institut für Physikalische Chemie und Elektrochemie,
Universität Hannover, 3000 Hannover, FRG

J. Karthäuser, D. Hartmann

Institut für Physikalische Chemie,
Universität Göttingen, 3400 Göttingen, FRG

Reactions between CH_3O_x and HO_x ($x=1,2$) radicals provide an interesting kinetic analogy to the mutual reactions of HO_x and an extension of radical-radical interactions via bound intermediates to include partially oxidized hydrocarbon species. Except for (1) $\text{CH}_3\text{O}_2 + \text{HO}_2$ these reactions have to our knowledge not previously been studied.

In our experiments the individual reagent were generated using laser co-photolysis techniques with the following precursors: $\text{CH}_3\text{ONO} + h\nu$ (193, 248 nm) for CH_3O , $\text{HNO}_3 + h\nu$ (193, 248 nm) for OH ; $(\text{CH}_3)_2\text{N}_2/\text{O}_2 + h\nu$ (193 nm) for CH_3O_2 and $\text{CCl}_4/\text{CH}_3\text{OH}/\text{O}_2 + h\nu$ (193 nm) for HO_2 . By means of a suitable choice of initial precursor concentrations the initial radical concentrations can be varied such that pseudo-first order kinetic conditions pre-

vail. For the time resolved detection we have used LIF (for OH and CH₃O) and a novel photofragment emission technique [1] (for CH₃O₂). The following results were obtained (all at 298 K):

Reaction	k/cm ³ molecule ⁻¹ s ⁻¹
(1) CH ₃ O ₂ + HO ₂	(4.8 ± 1.5) 10 ⁻¹²
(2) CH ₃ O ₂ + OH	(4.0 ± 1.0) 10 ⁻¹¹
(3) CH ₃ O + HO ₂	(1.2 ± 0.4) 10 ⁻¹²
(4) CH ₃ O + OH	(1.2 ± 0.3) 10 ⁻¹¹

For identical CH₃O_x, the rate coefficient is found to decrease upon exchange of OH by HO₂ by an order of magnitude. For identical HO_x on the other hand, the rate coefficient decreases by a factor of ~ 4 upon replacement of CH₃O₂ by CH₃O.

The products of the individual reactions have as yet not been fully analyzed. We assume, however, that they are initiated by radical-radical recombination followed by fragmentation or stabilization of the intermediate adducts. Of particular kinetic interest are reactions (2) and (3) which may be expected to yield an identical but differently energized adduct (CH₃OOOH[‡]). Attempts to quantify the different reactivities using empirical energy correlation diagrams and RRKM modelling will be presented.

[1] D. Hartmann, J. Karthäuser, R. Zellner, J.Phys. Chem, in press, 1990

THE KINETICS OF REACTION OF CH_3 WITH PROPENE

Maureen J. MacDonald and John M. Roscoe
Department of Chemistry, Acadia University
Wolfville, Nova Scotia, Canada

Photolysis of acetone is one of the most thoroughly studied photochemical systems. This, combined with the good thermal stability of acetone and its ease of handling makes acetone photolysis an attractive source of CH_3 radicals for kinetic measurements. Photolysis of acetone at 193.3 nm has been shown to be a clean source of CH_3 suitable for kinetic measurements (1). However, a number of compounds whose reactions one might wish to study also absorb strongly at that wavelength. We are investigating the utility of photolysis of acetone with an excimer laser using the XeCl transition at 308 nm as a source of CH_3 for kinetic measurements.

The use of an excimer laser precludes a steady-state analysis of the reaction since the photochemical events span a comparatively short (approximately 20 ns) portion of the time between laser pulses (approximately .1 to .3 seconds). The experimental results were analysed by numerical integration with a computer program we have used elsewhere (2) modified to permit variable light intensity during the early part of the reaction period. The laser pulse shape was approximated as a double exponential for this purpose but the pulse characteristics used in the model could cover a rather wide range without affecting the ability of the model to describe the experimental results.

The experiments covered acetone pressures ranging from 10 to 130 Torr at temperatures from 298 K to approximately 600 K. Propylene pressures were less than about 15% of the acetone pressure and conversions of acetone, based on product yields measured by gas chromatography, were less than 0.5%. Product yields varied linearly with the number of laser pulses and were independent of the laser pulse rate within the range of conditions used in the experiments. The yield of CO in the absence of propylene at temperatures above 430 K was slightly greater than $\text{C}_2\text{H}_6 + 0.5 \text{CH}_4$ but the difference was within the uncertainty of the analytical data. As the temperature decreased from 430 K the yields of CO decreased and became correspondingly less accurate. Addition of propylene reduced the yields of all products. This could be accounted for by a combination of quenching of triplet acetone (3) and reaction of CH_3 with propylene. Reaction of the acetyl radical with propylene has a significant effect on the yields of CH_4 and C_2H_6 under those conditions in which the rate of decomposition of acetyl is sufficiently rapid to contribute to the production of CH_3 but sufficiently slow that its reactions with propylene occur at rates which are comparable to the rate of decomposition.

The model used in the calculations was based on the mechanism developed by Nicholson (3). The incident light intensity used in the calculation was adjusted to give the experimentally observed amount of reaction per laser pulse. At the higher temperatures, where decomposition of the acetyl radical

is rapid, the yield of CO was used for this purpose. When this was not practical, the yields of CH_4 and C_2H_6 were used to indicate the extent of decomposition of acetone. The rate constants for the reactions of propylene with CH_3 and with acetyl radicals were then adjusted to provide agreement with the yields of CH_4 and C_2H_6 observed experimentally. As the temperature increased, the decomposition of acetyl to CH_3 and CO became the dominant loss route for that radical and its importance in determining the ratio of C_2H_6 to CH_4 decreased. The details of the photochemical steps in the mechanism were less important than the part of the mechanism describing the reaction after the laser pulse had died away since the short duration of the pulse corresponds to only a very small proportion of the total reaction time provided the laser pulse width is small relative to the "chemical" half life of the radicals produced in the laser pulse.

1. P. D. Lightfoot, S. P. Kirwan and M. J. Pilling. *J. Phys. Chem.*, **92**, 4938-4946 (1988); Irene R. Slagle, David Gutman, Joanne W. Davies and Michael J. Pilling, *J. Phys. Chem.*, **92**, 2455-2462 (1988).
2. J. M. Roscoe and M. J. Thompson. *Int. J. Chem. Kinet.*, **17**, 967-990 (1985).
3. R. E. Rebbert and P. Ausloos. *J. Amer. Chem. Soc.*, **87**, 5569-5572 (1965).
4. A. J. C. Nicholson. *Can. J. Chem.*, **61**, 1831-1837 (1983).

THE EFFECT OF INTERPARTICLE INTERACTIONS ON GAS KINETICS

Pytel Z., *Institute of Physics, Polish Academy of Sciences,*
Al. Lotnikow 32/46, 02-668 Warsaw, Poland.

Korneta W., *Technical University, Department of Physics,*
Malczewskiego 29, 26-600 Radom, Poland.

The aim of this paper is to describe the effect of interactions between gas particles on transport coefficients. We consider gas described by the following kinetic equation:

$$\frac{\partial f(\vec{r}, \vec{v}, t)}{\partial t} = \left[\hat{R}_{HC} + \hat{R}_V + \vec{v} \cdot \nabla_{\vec{r}} \right] f(\vec{r}, \vec{v}, t) \quad (1)$$

where $f(\vec{r}, \vec{v}, t)$ is one particle distribution function, whereas operators \hat{R}_{HC} and \hat{R}_V denote respectively hard core interactions and weak two-particle long-range attractive interactions described by the potential $V(\vec{r})$. Performing the Fourier transform with respect to space variables and the Laplace transformation with respect to time variable, one may determine all allowed energies of the gas. These energies we obtained using perturbation calculation to the second order in k^2 . The eigenvalues of the equation (1) can be compared with general expressions for eigenvalues of hydrodynamic equations, what allows one to obtain expressions for the velocity of acoustic waves in the gas and different transport coefficients. We obtained analytical expressions for the following transport coefficients: the coefficient κ describing heat conductivity and coefficients η and ζ describing respectively kinematic viscosity and volume viscosity. These coefficients can be written in the form

$$\kappa = \frac{2}{3} \frac{C_v}{a^2} \left[\frac{k_B T}{m} \right]^{0.5} * \left[\frac{75}{64} \frac{1}{\sqrt{\pi}} \frac{(1 + 0.4 * \pi * g(a) * n_0 * a^3)^2}{g(a)} + \frac{2}{3} \pi * g(a) * n_0^2 * a^6 \right] ,$$

(2)

$$\eta = \left(\frac{mk_B T}{a} \right)^{0.5} * \left(\frac{15}{16} \frac{1}{\sqrt{\pi}} \frac{(1 + 0.3 * \pi * g(a) * n_0 * a^3)^2}{g(a)} + \frac{4}{15} \sqrt{\pi} * g(a) * n_0^2 * a^6 \right) \quad (3)$$

and

$$\zeta = \left(\frac{mk_B T}{a} \right)^{0.5} * \frac{4}{15} \sqrt{\pi} * g(a) * n_0^2 * a^6 \quad (4)$$

where n_0 is the gas density and $g(a)$ is the two-particle correlation function in the absence of long-range interactions. The distance a and C_v are to be determined from the following equations:

$$C_v = \frac{3}{2} k_B T + 2\pi n_0 * \int_0^{\infty} d\bar{r} V(r) g(r) \quad (5)$$

$$n_0 a^3 g(a) = \frac{3}{2\pi} \frac{1}{\sqrt{k_B}} * \left(\frac{3}{2} \frac{T}{C_v} \frac{\partial P / \partial T}{n_0} \right)^{0.5}$$

The above expressions show that transport coefficients increase when the range of interparticle attractive interactions increases. Knowing these expressions we studied the effect of different forms of the potential $V(r)$ on transport coefficients.

This work was supported by the Ministry of Education in Poland under Grant CPBP-01.08.

Reactions of Ca (3P) with halomethanes at $T = 600-1000$ K.

F. Castaño, F. Beitia and M.N. Sanchez Rayo

Departamento de Química Física. Universidad del País Vasco. Apart. 644.
E48080. Bilbao. Spain.

Summary

A study of the reactions between $\text{Ca}(^3P)$ and CH_4 , CH_3F , CH_2F_2 , CHF_3 , CF_4 , CClF_3 , etc at temperatures ranging from 600 to 1000 K has been performed. The reactions are monitored by following the resonant emission at 657.3 nm used in the preparation of $\text{Ca}(^3P)$, with a gated photomultiplier. Kinetic constants and chemiluminescence products will be presented

**Reactions of radical CHF(X) with unsaturated hydrocarbons
at room temperature.**

F. Castaño, A. Ortiz de Zárate and M.N. Sanchez Rayo

Departamento de Química Física. Universidad del País Vasco. Apart. 644.
E48080. Bilbao. Spain.

Summary

Reactions of ground state CHF radical, prepared by infrared multiple photon dissociation of precursor CH_2F_2 , with selected unsaturated hydrocarbons, $\text{CH}_2=\text{CH}_2$, $\text{CH}_2=\text{CH}-\text{CH}_3$, $\text{CH}_2=\text{C}-(\text{CH}_3)_2$, etc were monitored by cw LIF of the A-X transition of CHF. Kinetic constants vary from $5.4 \cdot 10^{-12} \text{ cm}^3 \text{ molecule}^{-1} \text{ s}^{-1}$ for $\text{CH}_2=\text{CH}_2$ to $2.2 \cdot 10^{-11} \text{ cm}^3 \text{ molecule}^{-1} \text{ s}^{-1}$ for 1,2 butadiene. A discussion of the relationship of the observed kinetic constant with the number of double bonds, the hydrocarbon structure, the laser fluence and the luminescence produced by IRMPD of the hydrocarbon is presented.

KINETICS OF REACTIVE D₂-F₂-O₂-CO₂ MIXTURES*

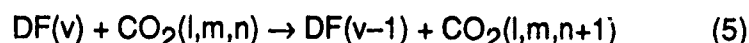
W. D. Breshears, H. A. Fry and C. W. Wilson

Chemical and Laser Sciences Division

Los Alamos National Laboratory

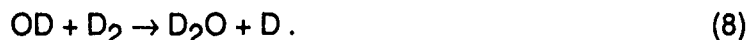
Los Alamos, NM 87545, U. S. A.

We are studying the kinetics of various reactive and energy transfer processes in mixtures of D₂-F₂-O₂-CO₂ dilute in Ar. The following reaction sequence is initiated by pulsed irradiation with a XeCl laser at 308 nm:



Experimental conditions are chosen such that (i) $k_2(\text{D}_2)$, $k_3(\text{F}_2)$, $k_5(\text{CO}_2) \gg K_4 = k_4(\text{O}_2)(\text{M})$, $K_6 = k_6(\text{M})$; and (ii) the total DF formed per laser shot is sufficiently small that (D_2) , (F_2) and the temperature remain essentially constant. The resulting time-dependent infrared emission in the region $2000\text{-}3000 \text{ cm}^{-1}$ is recorded. Broad ($50\text{-}100 \text{ cm}^{-1}$) spectral resolution indicates that, under the above conditions, the emission originates almost entirely from the ν_3 vibrational mode of CO₂. The time dependence of the signal takes the form, after an initial very rapid transient, $S = A \cdot \exp(-K_4 t) + B \cdot \exp(-K_6 t)$, with $B \approx -A$. The process governing the signal decay is determined by the ratio K_4/K_6 , and thus by the O₂ partial pressure. At sufficiently low values the decay constant is K_4 ; at high values it is K_6 . Values of k_{6-M} determined for $M = \text{Ar}$, CO₂, D₂, O₂ and F₂ at $\sim 300 \text{ K}$ and at high O₂ partial pressures ($\geq 20 \text{ Torr}$) agree well with literature reports. Values of k_{4-M} for $M = \text{Ar}$, CO₂, D₂ and F₂ were determined at $\sim 300 \text{ K}$ and at low O₂ partial pressures

(≤ 2 Torr). Experimental measurements and detailed computational modeling both indicate a small but significant contribution to the observed signal decay from the reactions



A nonlinear least-squares procedure, incorporating a recently reported value for k_8 ¹ and treating k_7 as an adjustable parameter, was employed to provide a first-order correction for the effects of reactions (7) and (8) to the measured decay constants. The results for k_{4-M} are:

M	k_4 ($\text{cm}^6 \text{s}^{-1} \times 10^{32}$)
Ar	1.7 ± 0.1
CO_2	16.3 ± 1.1
D_2	8.8 ± 1.2
F_2	32.1 ± 4.3

The least-squares result, $k_7 = (4 \pm 2) \times 10^{-11} \text{ cm}^3\text{s}^{-1}$, which should be considered only as an order-of-magnitude estimate, agrees well with literature values for the hydrogen analog of reaction (7).² The result reported in the only previous study of reaction (4),³ $k_{4-\text{Ar}} = (3.1 \pm 0.9) \times 10^{-32} \text{ cm}^6\text{s}^{-1}$, appears to be significantly above the present value.

* Work supported by the U. S. Department of Energy

1. G. L. Vaghjiani, A. R. Ravishankara and N. Cohen, J. Phys. Chem. **93**, 7833 (1989).
2. U. C. Sridharan, L. C. Qui and F. Kaufman, J. Phys. Chem. **86**, 4569 (1982); L. F. Keyser, J. Phys. Chem. **90**, 2994 (1986).
3. M. A. A. Clyne and B. A. Thrush, Proc. Roy. Soc. A **275**, 559 (1963).

Temperature Dependence of the Rate Constant
for the reaction $\text{HCO} + \text{O}_2 \rightarrow \text{HO}_2 + \text{CO}$

L. J. Stief, F. L. Nesbitt, and J. F. Gleason

Laboratory for Extraterrestrial Physics,
NASA/Goddard Space Flight Center
Greenbelt, MD 20771, U.S. A.

The absolute rate constant for the reaction $\text{HCO} + \text{O}_2 \rightarrow \text{HO}_2 + \text{CO}$ (1) has been measured over the temperature interval 200 to 398 K. This study represents the first measurements of this rate constant below 298 K. The measurements were made in a discharge flow system and the decay of the HCO radical was monitored, in excess O_2 , by collision-free sampling to a photoionization (10.2 eV) mass spectrometer. The HCO radical was generated in the back of the flow tube via the rapid reaction $\text{Cl} + \text{H}_2\text{CO} \rightarrow \text{HCO} + \text{HCl}$ (2). O_2 was added through a movable injector. Rate data for the reaction of HCO with O_2 at five temperatures is summarized in the table. Despite slight curvature in the Arrhenius plot with a possible minimum near 300 K, our data for $200 \leq T \leq 398$ K can be fit by the expression $k_1 = 3.2 \times 10^{-12} \exp(87/T) \text{ cm}^3 \text{ s}^{-1}$.

A review of this and all previous determinations reveals larger than expected discrepancies for what appears to be a relatively simple and well studied reaction. Our data is not consistent with an extrapolation of the Veyret and Lesclaux¹ data (298 - 503 K) which exhibits a slight negative temperature dependence nor an extrapolation of the Timonen et al.² data (298-713K) which shows a slight positive temperature dependence. The trend of our data is not fully consistent with a calculation by Langford and Moore³ which suggests a decrease in k for the region 300 to 200 K. Although all available data (with the exception of that at 713 K) can be accommodated by a single temperature independent value of $k_1 = (5.3 \pm 2.4) \times 10^{-12} \text{ cm}^3 \text{ s}^{-1} (\pm 2\sigma)$ for $200 \leq T \leq 610$ K, this range of values seem unusually large and simple averaging may disguise real differences. An understanding of the origins of these differences could lead to a better understanding of the $\text{HCO} + \text{O}_2$ reaction itself as well as of subsequent chemistry occurring in the various complex systems used to arrive at a measure of the rate constant.

We also performed a limited number of experiments on the related reaction $\text{HCO} + \text{NO} \rightarrow \text{HNO} + \text{CO}$ (3) at 298 K. The result is $k_3 = (1.3 \pm 0.2) \times 10^{-11} \text{ cm}^3 \text{ s}^{-1}$. The studies on this reaction at 298 K, although fewer in number, do not show nearly so large a range of values for k_3 as noted above for k_1 .

Table. Summary of rate data for the reaction



T	[O ₂]	Number of	k
K	10 ¹³ cm ⁻³	experiments	10 ⁻¹² cm ³ s ⁻¹
200	0.5 - 7.6	27	5.27 ± 0.80
222	0.5 - 8.2	18	4.83 ± 0.72
250	0.6 - 7.7	21	4.35 ± 0.65
298	0.5 - 8.8	29	4.00 ± 0.60
398	0.8 - 9.9	16	4.46 ± 0.67

a. typical $[\text{HCO}] = 2 \times 10^{11} \text{ cm}^{-3}$.

b. uncertainty in k is an estimate of the precision based on a propagation of error analysis.

References

1. B. Veyret and R. Lesclaux, J. Phys. Chem. 85, 1918 (1981).
2. R. S. Timonen, E. Ratajczak and D. Gutman, J. Phys. Chem. 92, 651 (1988).
3. A. O. Langford and C. B. Moore, J. Chem. Phys. 80, 4211 (1984).

Direct Measurement of Methylene Removal Rates by Species Containing the OH Functional Group

WARREN S. STAKER and KEITH D. KING

*Department of Chemical Engineering,
University of Adelaide,
Adelaide, S.A. 5001*

GREG J. GUTSCHE and WARREN D. LAWRENCE

*School of Physical Sciences,
Flinders University,
Bedford Park, S.A. 5042*

The industrially important processes of silicon and germanium chemical vapour deposition (CVD) intimately involve the kinetics of silicon and germanium radical species respectively. The ability to understand and control the reactions of the chemical intermediates is an important element for the improving of existing technologies for the production of microelectronics components. It is planned to study the gas phase reactions of the diradical hydrides silylene and germylene (the key intermediates in thin film growth by CVD from gaseous silanes and germanes). As a preliminary exercise the bimolecular reactions involving the first excited singlet state of methylene, $^1\text{CH}_2$, are being studied to test the experimental technique being used. $^1\text{CH}_2$ is also of considerable interest as it plays significant roles in organic synthesis and combustion processes.

Although $^1\text{CH}_2$ has been the subject of some investigation, very little has been done to determine $^1\text{CH}_2$ bimolecular reaction rate constants using direct methods. In our investigations the technique of laser flash photolysis/laser absorption has been used to study bimolecular reactions involving $^1\text{CH}_2$ and various molecules containing the hydroxyl group. $^1\text{CH}_2$ is prepared by photodissociation of the stable precursor, ketene (CH_2CO), using an excimer laser at 337 nm. A frequency stabilized CW ring dye laser is used to monitor the $^1\text{CH}_2$ absorption. The decay of the $^1\text{CH}_2$ population provides a measurement of the bimolecular reaction rate of the $^1\text{CH}_2$ with the substrate reactant gas. The bimolecular rate constant for the reactions of $^1\text{CH}_2$ with H_2O , CH_3OH , $\text{C}_2\text{H}_5\text{OH}$, and $\text{C}_3\text{H}_7\text{OH}$ were found to be 1.00, 1.41, 1.49, and $2.10 \times 10^{14} \text{ mol}^{-1} \text{ cm}^3 \text{ s}^{-1}$, respectively. A comparison is made with the rate constants obtained for the corresponding alkanes.

Elementary Reactions of Electronically Excited
Radicals and Molecules.

W. Hack, Max-Planck-Institut für Strömungsforschung
3400 Göttingen

Reactions of electronically excited species are of significant importance in various photolytic systems. The electronic structure and thus the reactivity of a radical or molecule can be altered, in a specific way, by electronic excitation. The excitation energy enables energy transfer processes. This study is concerned with molecules which have a singulett electronic ground state (N_2) and radicals (NH , CH_2) with a triplett electronic ground state.

The reaction products of energy transfer and/or chemical reactions of $N_2(A\ ^3\Sigma_u^+)$, which is metastable and has an excitation energy of 595 kJ/mol were studied in a fast flow reactor. For the reaction $N_2(A) + O_3$, for which $NO(X)$ was detected as a product, it was the first time that $N_2(A)$ was found to take part in a chemical reaction to a significant amount.

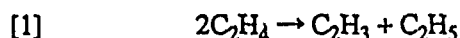
NH , which is isoelectronic with O and CH_2 has a metastable ($a^1\Delta$) – state with an excitation energy of 151 kJ/mol. The reactivity of NH in this electronic state is of special importance in comparison to the other electronic species mentioned above, since these three particles are isoelectronic on one hand and on the other hand differ significantly in the excitation energy. Thus the influence of the electronic structure and excitation energy can be concluded from the observed reactivities. The rates and products of the reactions of $NH(a)$ $CH_2(\tilde{a})$ and $O(^1D)$ with molecules like HF , HCN and H_2O will be presented.

THE HOMOGENEOUS THERMAL CONVERSION OF METHANE TO HIGHER HYDROCARBONS IN THE PRESENCE OF ETHYLENE

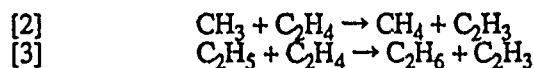
Alain R. Bossard and Margaret H. Back

Ottawa-Carleton Chemistry Institute
Department of Chemistry, University of Ottawa
Ottawa, Canada K1N 6N5

The pyrolysis of mixtures of methane and ethylene has been studied over the temperature range 774-1023 K at total pressures below atmospheric to explore the effectiveness of ethylene as a catalyst for conversion of methane to higher hydrocarbons. At temperatures in the neighbourhood of 800 K ethylene undergoes decomposition and polymerisation by a chain reaction mechanism, initiated by the bimolecular reaction of ethylene,

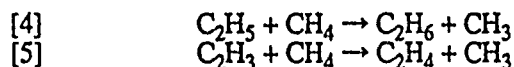


and followed by addition, abstraction, decomposition and isomerization reactions of the ethyl, vinyl and other radicals. The four major products, methane, ethane, propylene and 1-butene constitute about 80% of the products volatile at room temperature. Methane and ethane, the only saturated products, are formed by hydrogen-abstraction by the corresponding radical,

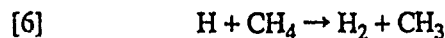


Propylene and butene-1 are formed by addition of radicals to ethylene followed by isomerization and decomposition reactions.

When methane is added to the system at the lower temperatures (dissociation of methane is negligible in these experiments) the two new reactions of most importance are



Thus methane enters the propagation reactions and is converted to ethane. The effect of methane on the rate of formation of ethane at 774 K is shown in Figure 1. As the ratio of methane to ethylene is increased the ethyl and vinyl radicals are replaced by methyl radicals and the product distribution shifts in favour of propylene rather than ethane. This shift is very noticeable in the higher temperature range where hydrogen atoms, formed by dissociation of radicals, are also converted to methyl radicals.



The distribution of products as a function of time at 1023 K, for a high ratio of methane to ethylene, is shown in Figure 2.

Thus methane is converted to ethane or propylene depending on the temperature range and the ratio $\text{CH}_4/\text{C}_2\text{H}_4$. Although the rate of conversion of methane is less than in a catalytic reaction, the homogeneous system has the advantage that no methane is lost to the formation of carbon monoxide or carbon dioxide.

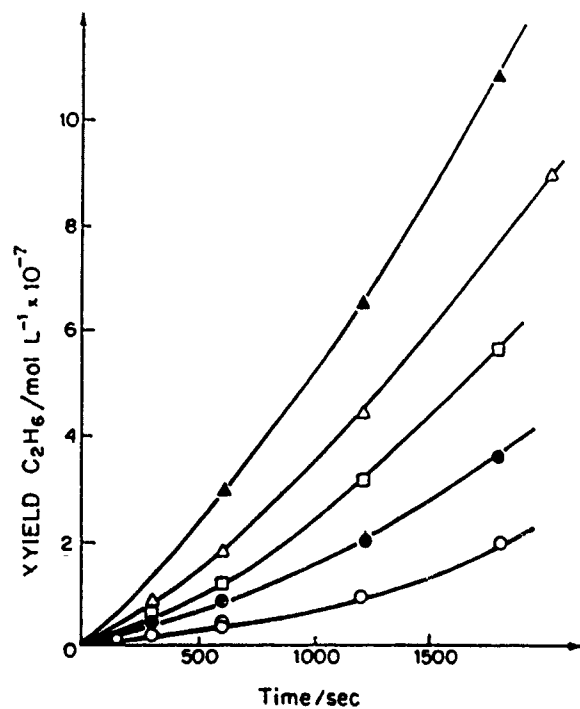


Figure 1. Yield of ethane as a function of time at 774 K in the presence and absence of methane with an initial pressure of ethylene of 50 Torr.

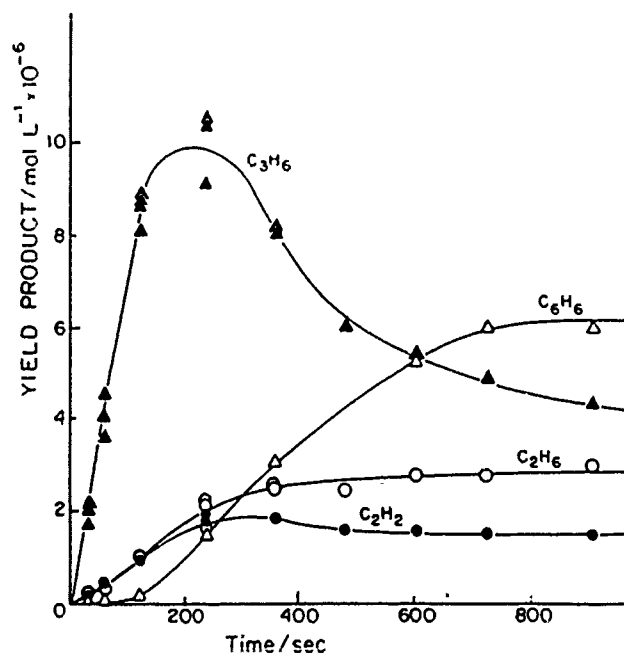


Figure 2. Yield of product as a function of time at 1023 K. Initial pressure of ethylene 6.5 Torr. Initial pressure of methane 356 Torr.

THERMAL DECOMPOSITION OF AZOISOPROPANE IN THE PRESENCE
OF 2,3-DIMETHYL-2-BUTENE

T. Körtvélyesi, A. Tóth and L. Seres

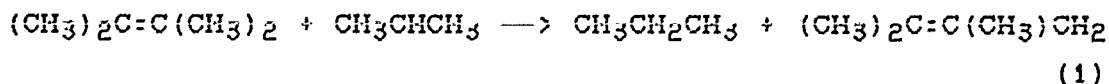
*Institute of Physical Chemistry,
Attila József University, Szeged, Hungary*

By the thermal decomposition of azoisopropane (AIP), the CH_3CHCH_3 (P^\cdot) radical-initiated homogeneous gas-phase thermal reaction of 2,3-dimethyl-2-butene (DMB) yielded $(\text{CH}_3)_2\text{CHC}(\text{CH}_3)_2\text{C}(\text{CH}_3)_2$ (TMP^\cdot) and $(\text{CH}_3)_2\text{C}=\text{C}(\text{CH}_3)\text{CH}_2$ (A^\cdot) radicals. The reaction was studied at 480-540 K in the concentration ranges $1.05 \leq [\text{DMB}]_0/10^{-3} \text{ M} \leq 2.9$ and $1.06 \leq [\text{AIP}]_0/10^{-4} \text{ M} \leq 3.05$. The products were identified by means of GC and GC-MS. A reaction mechanism was suggested on the basis of the product formation. The reaction mechanism was supported by computer simulation. The mechanism and the initial rates of product formation were utilized to determine some preliminary data on the elementary radical reactions.

The rate constant of the decomposition of AIP is

$$\log (k_0/\text{s}^{-1}) = (16.6 \pm 0.3) - (194.6 \pm 2.0)/\theta$$

Radical A^\cdot is formed in the H-abstraction reaction:



The rate constant ratio is

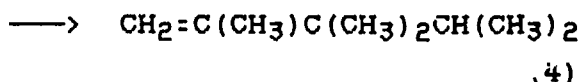
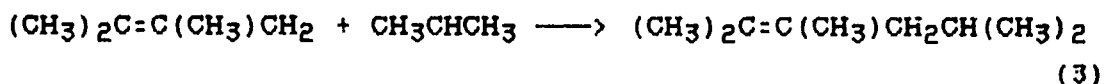
$$\log (k_1/k_2^{1/2}) = (4.9 \pm 0.3) - (53.2 \pm 1.6)/\theta$$

where k_2 refers to the combination



The units of $k_1/k_j^{1/2}$ and E are $\text{dm}^{3/2} \text{mol}^{-1/2} \text{s}^{-1/2}$ and kJ mol^{-1} , respectively, and $\Theta = RT \ln 10$.

Radical A^\cdot combines with P^\cdot in two ways:



The ratio of the rate constants is independent of temperature within the limits of experimental error:

$$k_3/k_4 = 2.86 \pm 0.13$$

The cross-combination ratios calculated for radicals A^\cdot and P^\cdot are

$$\phi(P^\cdot, A^\cdot) = 2.15 \pm 0.11$$

$$\phi(P^\cdot, \Sigma A^\cdot) = 2.35 \pm 0.20$$

Radical P^\cdot disproportionates with both radicals P^\cdot and A^\cdot . The disproportionation-combination ratios were determined to be

$$\Delta(P^\cdot, P^\cdot) = 0.66 \pm 0.12 \text{ and}$$

$$\Delta(P^\cdot, A^\cdot) = 0.041 \pm 0.019$$

Cope rearrangement of methyl-substituted 1,5-hexadienes was observed at our reaction conditions (around 500 K) [1]. Thus, some isomerization of the combination products of radical A^\cdot occurs under the experimental conditions of the present work.

Reference:

- [1] W. von Doering and W. R. Roth, *Tetrahedron*, **18**, 67 (1982).

THE THERMAL DECOMPOSITION OF AZOISOPROPANE IN THE
PRESENCE OF *trans*-CH₃CH=CHCH₃

M. Görgényi¹, R. Fischer² and L. Seres¹

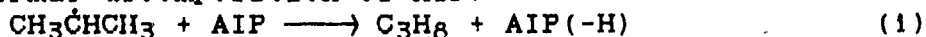
¹Institute of Physical Chemistry,
Attila József University, Szeged, Hungary

²Technische Hochschule, Section Chemie,
Leuna-Merseburg, GDR

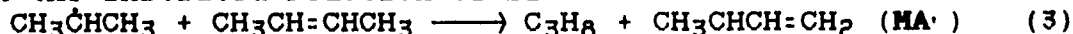
The thermal reaction of *trans*-CH₃CH=CHCH₃ (B2), initiated by azoisopropane (AIP), was investigated at 489.5-542 K. The amount of AIP was 4.2, 6.6 or 10% of the total pressure. The thermal decomposition of clean AIP was also studied at 466-540 K, at a concentration of $8 \cdot 10^{-4}$ mol dm⁻³. Preliminary results of these studies are reported here.

The kinetics of the following elementary reactions was studied:

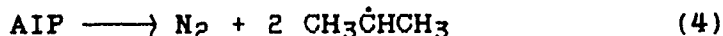
In the thermal decomposition of AIP:



In the initiated reaction of B2:



In both systems:



The concentration of the CH₃ĊHCH₃ (P·) radical was eliminated from the rate equations by means of the combination reaction



Rate constant ratios were obtained from the rate of accumulation of products. Relative rate constants of H-abstraction by P· from AIP were calculated from the expression

$$k_1/k_5^{1/2} = \frac{r_{\text{C}_3\text{H}_8} - r_{\text{C}_3\text{H}_6}}{r_{\text{DMBA}}^{1/2} \cdot [\text{AIP}]}$$

$$\log(k_1/k_5^{1/2}) = (4.3 \pm 0.1) - (45.7 \pm 1.2)/\theta$$

The units of $k_1/k_5^{1/2}$ and E are dm^{3/2} mol^{-1/2} s^{-1/2} and kJ mol⁻¹, respectively, and $\theta = RT \ln 10$.

The $k_3/k_5^{1/2}$ ratio was calculated from the rates of formation of propane corrected by the contribution of self- and cross-disproportionation reactions of P· and P· + 3,4-dimethylpentyl-2 radicals [1] and that of the H-abstraction from AIP

$$\frac{k_3}{k_5^{1/2}} = \frac{r_{\text{C}_3\text{H}_8} - 0.62 r_{\text{DMBA}} - 0.54 r_{\text{TMHA}} - r_1}{r_{\text{DMBA}}^{1/2} \cdot [\text{B2}]}$$

$$\log(k_3/k_5^{1/2}) = (3.5 \pm 0.2) - (45.5 \pm 2.0)/\theta$$

where TMHA denotes 2,3,4,5-tetramethylhexane and

$$r_1 = k_1/k_5^{1/2} r_{\text{DMBA}}^{1/2} [\text{AIP}]$$

In the temperature range 482-540 K, the self-disproportionation-combination ratio of P· radicals is

$$\Delta(\text{P}^\cdot, \text{P}^\cdot) = k_2/k_5 = \frac{r_{\text{C3H6}}}{r_{\text{DMBA}}} = 0.62 \pm 0.04$$

The rate constant k_4 in the AIP-B2 system was calculated from the expression

$$k_4 = \frac{0.5(r_{\text{C3H8}} + r_{\text{C3H6}} + r_{\text{34DMP1}} + r_{\text{c+t5MH2}}) + r_{\text{DMBA}} + r_{\text{TMHA}}}{[\text{AIP}]}$$

where the abbreviations are: 3,4-dimethyl-1-pentene (34DMP1), *cis*- and *trans*-5-methyl-2-hexene (c+t5MH2):

$$\log(k_4/\text{s}^{-1}) = (16.7 \pm 0.1) - (204.9 \pm 1.3)/\theta$$

In the thermal decomposition of clean AIP:

$$k_4 = \frac{r_{\text{DMBA}} + 0.5 \cdot (r_{\text{C3H8}} + r_{\text{C3H6}})}{[\text{AIP}]}$$

$$\log(k_4/\text{s}^{-1}) = (17.0 \pm 0.1) - (206.9 \pm 1.7)/\theta$$

Doering et al. [2] observed the Cope rearrangement of *meso*-3,4-dimethyl-1,5-hexadiene (mDMHD) at 225 °C and of *rac*-3,4-dimethyl-1,5-hexadiene (rDMHD) at 180 °C. Thus, some isomerization occurs in our system, too. The isomer composition of the MA· combination products is known from studies carried out at lower temperatures, where no Cope rearrangement is expected. Since the composition was found to be independent of temperature, we assume that the stereoselectivity is the same in our temperature range, and the concentrations of the octadiene isomers were estimated from Er_{octadienes} by using the product distribution measured in our laboratory in the methyl radical-initiated reaction of *cis*-CH₃CH=CHCH₃ at 395-445 K. The calculated cross-combination ratios are

$$\phi(\text{P}^\cdot, \text{MA}^\cdot) = \frac{r_{\text{c5MH2}}}{r_{\text{DMBA}}^{1/2} \cdot r_{\text{ccOd}}^{1/2}} = 2.15 \pm 0.11$$

$$\phi(\text{CMA}^\cdot, \text{tMA}^\cdot) = \frac{r_{\text{c+t3MHd}}}{r_{\text{m+rDMHD}}^{1/2} \cdot r_{\text{cc+ct+ttOd}}^{1/2}} = 2.04 \pm 0.13$$

where the abbreviations are: *cis*- and *trans*-3-methyl-1,5-heptadiene (c and t3MHd), *trans,trans*- (ttOd), *cis,trans*- (ctOd) and *cis, cis*-2,6-octadiene (ccOd).

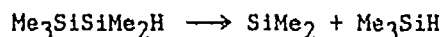
[1] C.W. Larson and E.S. Rabinovitch, J. Chem. Phys., 50, 871 (1969).

[2] W. von Doering and W.R. Roth, Tetrahedron, 18, 67 (1962).

THE THERMAL DECOMPOSITION REACTION OF PENTAMETHYLDISILANE
AND ITS REVERSE INSERTION REACTION

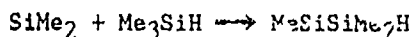
by J S Bertram, R Becerra, R Walsh and I M Watts,
Department of Chemistry, University of Reading, Whiteknights
Reading RG6 2AD, U. K.

A controversy has recently arisen concerning the nature of the transition state of the title reaction. Recent kinetic remeasurements of the reaction



have yielded $\log(k_1/\text{s}^{-1}) = 12.83 - 196 \text{ kJ mol}^{-1}/RT \ln 10$.

The Arrhenius parameters are in close agreement with earlier measurements of Davidson et al. The measured A factor confirms the tight nature of the transition state of this reaction. This apparently contrasts with the moderately fast reverse reaction,



for which $k = 4.5 \times 10^{-12} \text{ cm}^3 \text{ molecule}^{-1} \text{ s}^{-1}$ has been obtained in our laboratory (collision efficiency ca 0.01).

This issue is resolved by the proposition of a complex mechanism which will be discussed in detail at the meeting.

FREE RADICAL PROCESSES IN ACETYLENE CHEMISTRY

by

Dr. Sidney W. Benson and Dr. Chellappah Channugathas

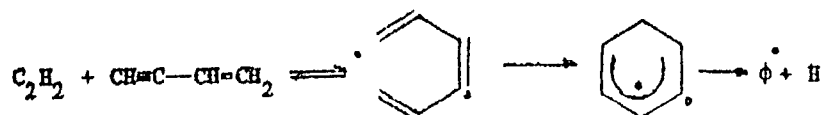
Donald P. and Katherine B. Loker Hydrocarbon Research Institute
 Department of Chemistry
 University of Southern California
 University Park
 Los Angeles, California 90089-1661

Past investigations have demonstrated that the chemistry of acetylene is dominated by a radical chain and an induction period. Criticisms of radical processes center about the fact that the obvious source of radicals:



is not fast enough to account for observed rates (800-1200°K). In addition no one has proposed the autocatalytic agent responsible for the induction period.

We shall show that this precursor is vinyl acetylene which replaces the above initiation by:



with an overall activation energy of only 32 kcal/mole.

We can assign Arrhenius parameters to the various initiation steps and derive explicit expressions for the induction period in C_2H_2 pyrolysis in excellent agreement with experimental observations. Acetylene pyrolysis will be shown to be a simple polymerization reaction with vinyl radical the most important propagating species.

STUDY OF ELEMENTARY REACTIONS OF FO RADICALS.

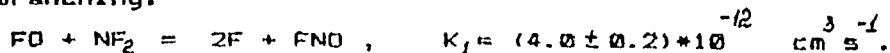
V.B.Rozenshtein, Yu.R.Badjanian, E.M.Markin, Yu.M.Gershenson.

Moscow, USSR.

In our previous work [1] we have found a new branch chain reaction $\text{NF}_2 + \text{O}_3$. Here we give the results of independent investigations of the main elementary steps. The experiments were carried out at room temperature under flow conditions using EPR/LMR spectrometer. The FO radicals were produced either in microwave discharge of CF_4 (with He) or by means of fast reaction $\text{F} + \text{O}_3 = \text{FO} + \text{O}_2$. The FO radicals were registered by LMR technique with sensitivity better than 10^{10} cm^{-3} .

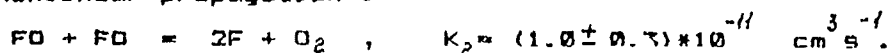
The following results were obtained.

(1) Branching.



Our preliminary communication [1] had a misprint related to value of K_1 rate constant (instead of $6 \cdot 10^{-16}$ one ought to read $6 \cdot 10^{-12}$).

(2) Nonlinear propagation.



(3) Termination on quartz surface.

$$K_3 = (3 \div 6) \text{ s}^{-1}, \quad \gamma_{\text{FO}} = (1.7 \div 3.4) \cdot 10^{-4}.$$

The reactions (1,3) have not been studied previously. The value of K_2 is in good agreement with that obtained earlier [2].

1. Gershenson Yu.M. and Rozenshtein V.B. Tenth International Symposium on Gas Kinetics 24-29 July 1988, Swansea, UK.

2. Clyne M.A.A. and Watson R.T., J.Chem.Soc.Faraday Trans.1., 70, 1109 (1974).

The Photolysis of Acetaldehyde

by Rosa Becerra¹ and H Monty Frey²

¹Instituto de Quimica Fisica 'Rocasolano'
C.S.I.C. Madrid, Spain

²Chemistry Department, Reading University, U.K.

Despite many studies going back nearly 50 years there are still uncertainties about the detailed photochemistry of acetaldehyde, the simplest typical aldehyde. We report some quantitative studies in the gas phase using 313, 288 and 248 nm radiation. As expected the major products are methane and ethane (plus carbon monoxide) but there are also significant yields of acetone, ethanol, 2-propanol and biacetyl.

We have produced a quantitative kinetic model to obtain relative quantum yields of the primary processes. By using literature values of rate constants (or our estimates where they are not available) in our model we have been able to account for product yields from both continuous and pulsed light sources. Our model also fits the product yield dependence on pressure and temperature.

THE KINETICS OF HYDROXYL RADICAL REACTIONS WITH CYCLOPROPANE AND CYCLOBUTANE

S.Dóbbé, T.Turányi, T.Bérces and F.Márta

Central Research Institute for Chemistry
Hungarian Academy of Sciences
Budapest, Hungary

The temperature dependences of the rate coefficients of hydroxyl radical reactions with cyclopropane and cyclobutane have been investigated for which no direct studies are available in the literature. The reactions were investigated by the laser flash photolysis-resonance fluorescence technique. The OH radicals were produced by photolyzing nitric acid with the 193 nm flash from an excimer laser. The OH radical decay was monitored by its resonance fluorescence under pseudo first order conditions in the presence of cycloalkane excess and the bimolecular rate coefficients were obtained from plots against cycloalkane concentration.

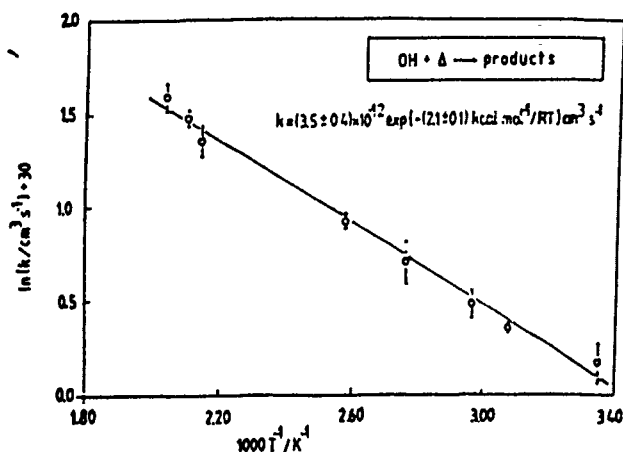


Fig.1. Arrhenius plot
of the kinetic
results for reaction
OH + cyclopropane

The rate coefficients were determined as a function of temperature in the range of 300–500 K. An Arrhenius plot for the reaction between OH radical and cyclopropane is shown in Fig. 1. The results can be described in an Arrhenius form although small deviations

from the Arrhenius law are apparent which suggests that a $k = Bf^{\frac{1}{2}} \exp (-H/RT)$ type representation would fit better the experimental results. Similar observations have been made also with cyclobutane.

Table I. Summary of kinetic data

	DH^0 (C-H) kcal mol ⁻¹	$k \times 10^{13}$ cm ³ molec ⁻¹ s ⁻¹	$A \times 10^{12}$ cm ³ molec ⁻¹ s ⁻¹	E kcal mol ⁻¹
Cyclopropane	106.3	1.1 (0.7)	3.5 (3.1)	2.1 (2.8)
Cyclobutane	96.5	12 (12)	3.9 (4.1)	1.2 (1.3)
Cyclopentane	94.5	52 (56)	14 (14)	0.6 (0.4)
Cyclohexane	95.5	75 (83)	18 (17)	0.5 (0.4)

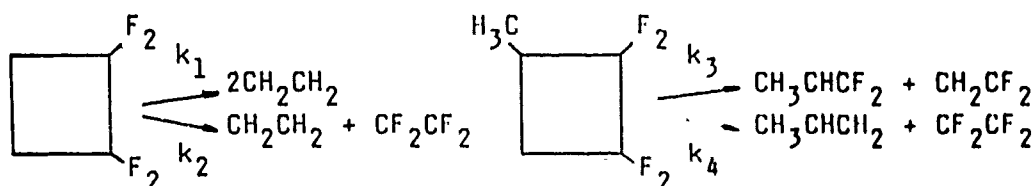
Some of the kinetic results are summarized in Table I. The Arrhenius parameters are given for simplicity and literature data are indicated for cyclopentane and cyclohexane. The reactivities increase with increasing ring size which reflects the tendency of the C-H bond strengths. The experimental results are very well reproduced by the results of calculations made by Atkinson's empirical scheme (see results given in brackets).

DECOMPOSITION OF TETRAFLUOROCYCLOBUTANES
GAS/GAS AND GAS/WALL ACTIVATION

L.Zalotai, T.Iurányi, I.Bérces and F.Márta

Central Research Institute for Chemistry
Hungarian Academy of Sciences
Budapest, Hungary

The two channel thermal decomposition of 1,1,2,2-tetrafluorocyclobutane (TFCB) and 1-methyl-2,2,3,3-tetrafluorocyclobutane (MTFCB) have been studied using homogeneous and heterogeneous activation. The decomposition of TFCB and MTFCB could be represented by the following stoichiometry



where all pathways were first order processes.

The homogeneous thermal decomposition of TFCB and MTFCB were studied between 730 and 805 K at pressures ≥ 1.4 kPa where the first-order rate coefficients were found to be pressure independent. Least squares fit to the data yielded the following Arrhenius parameters:

Channel	1	2	3	4
$\log(A/s^{-1})$	15.5 ± 0.1	15.4 ± 0.1	15.2 ± 0.1	15.3 ± 0.1
$E_A/kJ \text{ mol}^{-1}$	294 ± 1	310 ± 1	294 ± 1	310 ± 1

The pressure dependence of the homogeneous decomposition rate and the efficiency of the gas phase collisional energy transfer have been studied at three temperatures between 0.001 to 4.6 kPa and $\langle \Delta E \rangle_{\text{down}}$ values were extracted from the investigation of the

two-channel decomposition of 1FCB and MFCB. Experimental results and calculated fall-off curves for the rate coefficient ratios for MFCB are plotted vs. collision frequency in fig.1.

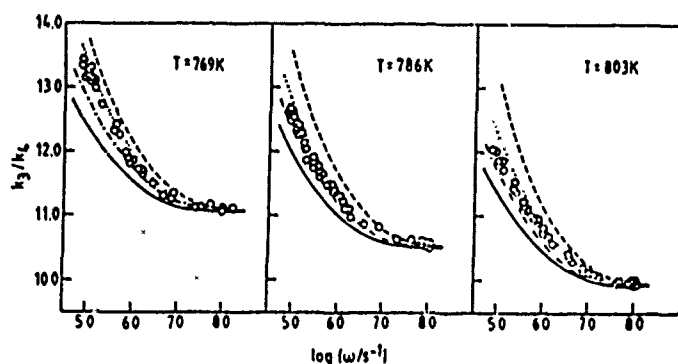


Fig.1. Pressure dependent ratio of the two reaction channels for MFCB decomposition at 769, 786 and 803 K. o, Experimental; —, RRKM strong collision hypothesis; ---, RRKM stepladder model with $\langle \Delta E \rangle_d = 1200 \text{ cm}^{-1}$; ..., with $\langle \Delta E \rangle_d = 1500 \text{ cm}^{-1}$ and -.-, with $\langle \Delta E \rangle_d = 1800 \text{ cm}^{-1}$.

The efficiency of the surface-gas energy transfer has been studied by the "variable encounter method" in the range of 750-1100 K. The average probability of reaction per collision, $P_c(m)$ for a given reactor was calculated from the data and was compared with the theoretical stochastic calculations based on Gaussian and exponential energy transfer probability models. The results obtained for the temperature dependence of the ratios of decomposition probabilities are presented for the MFCB in fig.2.

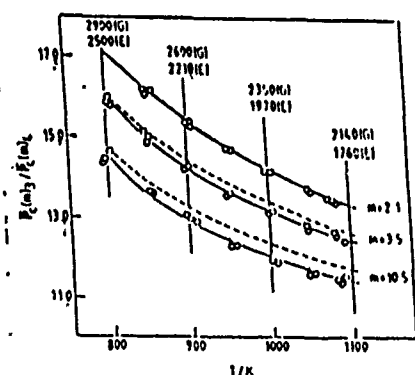


Fig.2. Temperature dependence of reaction probabilities for the two reaction channels in MFCB decomposition. Transition probability models were Gaussian (—) and exponential (---) functions. $\langle \Delta E' \rangle$ values are given at four different temperatures.

The results on gas/gas and gas/wall collision efficiencies are discussed and compared with literature data for related molecules.

**Kinetic Study of the Reaction $\text{OD} + \text{DNO}_3 \rightarrow \text{D}_2\text{O} + \text{NO}_3$
Temperature and Pressure Dependence of the Rate Constant.**

D.L. Singleton, G. Paraskevopoulos, and R.S. Irwin

Division of Chemistry, National Research Council of Canada
Ottawa, Ontario, Canada, K1A 0R6

Abstract

Absolute rate constants for the reaction of OD radicals with DNO_3 have been determined in the gas phase, in the temperature range 269-446K, by a flash photolysis-resonance absorption technique. OD radicals were generated by pulsed laser photolysis of DNO_3 vapor at 222 nm with a KrCl excimer laser and were monitored by time resolved resonance absorption at 307.6 nm. The Arrhenius plot of the low pressure rate constant has a shallow minimum at 323K. The rate constant in $\text{cm}^3/\text{mol s}$ can be represented by the following Arrhenius expressions: for $263\text{K} < T < 446\text{K}$, by $k = (3.18 \pm 0.77) \times 10^9 \exp [(241 \pm 70)/T]$, and for $323\text{K} < T < 446\text{K}$, by $(1.86 \pm 0.11) \times 10^{10} \exp [(-322 \pm 21)/T]$. The rate constant was found to increase in the presence of 107 torr SF_6 at 269 and 296K but not at 443K. A two channel-mechanism is consistent with the data, one channel, dominant at low temperatures, involves formation of a complex intermediate, and the other, direct hydrogen abstraction.

REACTIONS OF O (³P) WITH AROMATIC HYDROCARBONS IN THE GAS PHASE

H.Frerichs, R.Koch and M.Tappe

Institut für Physikalische Chemie der Universität Göttingen

Tammannstraße 6, D-3400 Göttingen, Western Germany

H.Thiesemann

MPI für Strömungsforschung

Bunsenstraße 10, D-3400 Göttingen, Western Germany

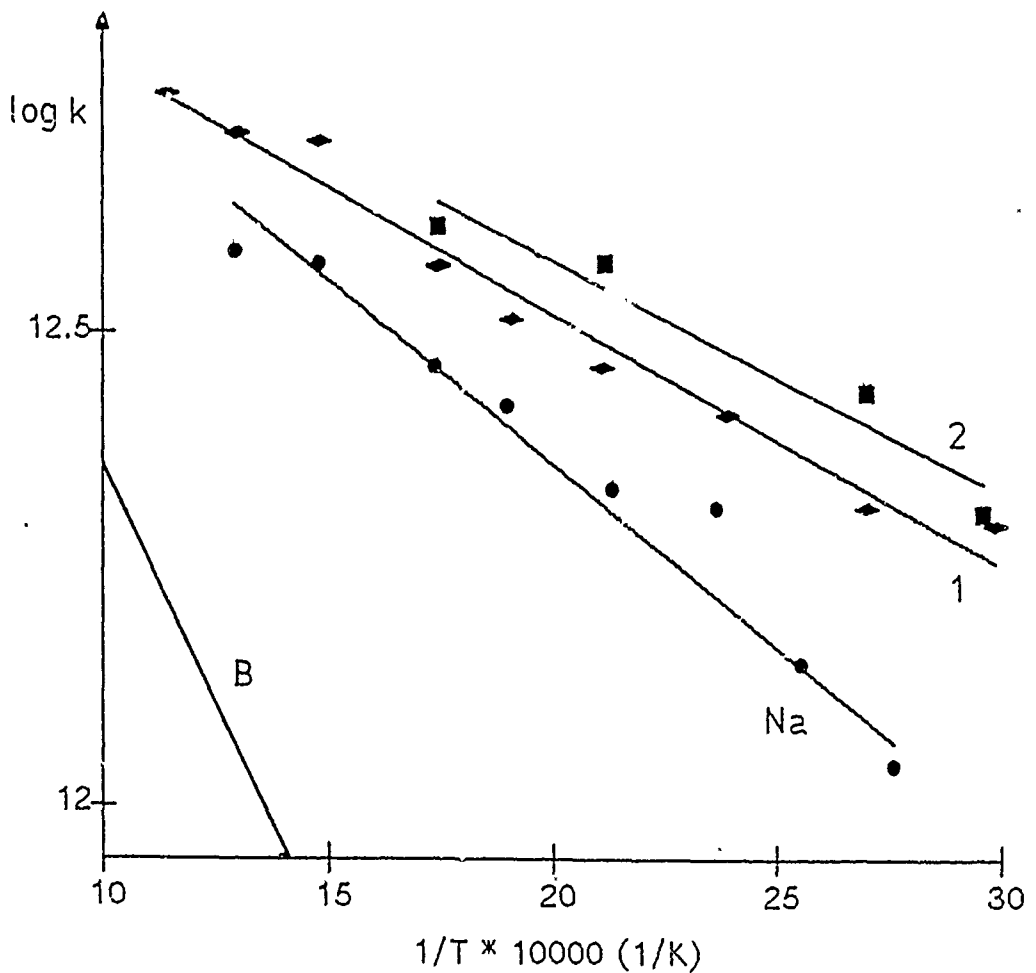
Oxidation processes of aromatic hydrocarbons play an important role in combustion as well as in atmospheric chemistry. The reaction rates of atomic oxygen in the electronic ground state with monocyclic aromatic hydrocarbons are relatively well known, whereas the reactions with polycyclic aromatics were not investigated in the past.

We studied the reactions of O (³P) with biphenyl, naphthalene and methylnaphthalenes, and phenanthrene in an isothermal low pressure discharge flow system with mass spectrometric detection. The investigations were carried out in the temperature range 298 K to 870 K. The oxygen atoms were produced by microwave discharge in O₂/He mixtures and the measurements took place under O atom excess over hydrocarbon, thus reducing significantly the possibility of formation of tar-like by-products.

The obtained Arrhenius expressions fit well into the framework of aromatic hydrocarbon + O (³P) reaction rate data and support the

proposed mechanism of addition of the electrophilic ω atom to the aromatic ring, with activation energies depending on the size and structure of the molecule.

For monocyclic aromatics with alkyl side-chains the ratio of OH formation to overall reaction was investigated using a similar flow system with LIF for detection of the OH radical.



Arrhenius plot for benzene (B), naphthalene (Na), 1-methylnaphthalene (1) und 2-methylnaphthalene (2)

The High Temperature Decomposition of $(\text{CH}_3)_2\text{N}_2$, CH_4 and
 CH_3 -radicals Reactions in Shock Waves.

A.V.Bulgakov, A.G.Zborovsky, D.V.Muratov, Yu.P.Petrov,
 S.A.Smirnov, S.V.Turetsky.

N.N.Semenov Institute of Chemical Physics Acad.Sci.USSR.
 Moscow, USSR.

The thermal decomposition of $(\text{CH}_3)_2\text{N}_2$, CH_4 and the high temperature recombination and disproportionation of CH_3 -radicals have been studied in shock waves using UV absorbtion of CH_3 -radicals near 2160 Å and absorbtion of $(\text{CH}_3)_2\text{N}_2$ near 2000 Å.

For $(\text{CH}_3)_2\text{N}_2$ decomposition at $T=800-1000^\circ\text{K}$ and $M \approx 5 \cdot 10^{-6} \text{ mol/cm}^3$ $k_{\text{diss}} \sim 10^{13.7} \exp(-43.5/RT) \text{ sec}^{-1}$ in good agreement with thermodynamics of reaction. The T and p dependence of the initial rate constants of CH_4 decomposition was measured at $T = 1800 - 2400^\circ\text{K}$ and $p = 2-60 \text{ atm}$. Values of k_{diss} have been obtained are one order higher than earlier recommended ones. This higher values agree with recent data. CH_3 -radicals recombination rate constants were measured at $T = 1150-1560^\circ\text{K}$ and $p=0.3-10 \text{ atm}$. k_{rec} slightly decrease with temperature and demonstrate unimolecular falloff behavior; k_{obs} of CH_3 radicals disproportionation was measured at $T = 1700-2700^\circ\text{K}$. ($k_{\text{obs}} \sim 10^{13.8} \exp(-14.7/RT) \text{ cm}^3/\text{mol} \cdot \text{sec}$).

The numerical simulation of all investigated processes was performed.

The High Temperature Reduction of SO_2 in Shock Waves.

A.V.Bulgakov, A.G.Zborovsky, D.V.Muratov, Yu.P.Petrov,

S.A.Smirnov, S.V.Turetsky.

N.N.Semenov Institute of Chemical Physics Acad.Sci.USSR.

Moscow, USSR.

The kinetics of high temperature reduction of SO_2 is closely connected with combustion chemistry and ecochemistry. However, it is unsufficiently studied, in particular because of complication by heterogeneous processes.

In the present work the kinetics of interaction $\text{SO}_2 + \text{H}_2$ (1) and $\text{SO}_2 + \text{CH}_4$ (2) was studied in homogeneous conditions in shock waves using UV absorbtion of SO_2 and the products of reaction in spectral range 1950 - 3070 Å. With 5-25 times variation of the initial concentrations of SO_2 and H_2 the observed rate constant of reaction (1) was directly measured at $T = 1300 - 3000^\circ\text{K}$ and $p = 1\text{atm.}$ ($E_{\text{act}} \approx 46 \text{ kcal/mol, } A \approx 10^{14.7} \text{ cm}^3/\text{mol}\cdot\text{sec}$). The spectral features of reaction (2) were investigated, and SO_2 with some hydrocarbons interaction rate constants were estimated.

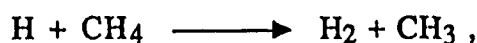
The mechanism of $\text{SO}_2 + \text{H}_2$ interaction was obtained and the numerical simulation was performed.

The reaction of hydrogen atoms with methane

Paul-Marie MARQUAIRE* and Philip D. PACEY

Department of Chemistry, Dalhousie University,
Halifax, Nova Scotia, Canada B3H 4J3

Previous measurements of the rate constant for the reaction,



are not in agreement with the accepted thermochemistry and kinetics of the reverse reaction. At the lowest temperature studied, 372 K, the discrepancy is a factor of 5.

We are studying the rate of this reaction in a flow system. Hydrogen atoms are generated in a microwave discharge and monitored by electron spin resonance spectroscopy. Measurements of the decay rate at temperatures close to 372 K are in agreement with previous measurements.

We are therefore studying the rates of product formation by gas chromatography to attempt to gain an understanding of other reactions which may remove hydrogen atoms in this system. Experimental reactant concentrations, total pressures, reactor geometries, and the identity of the gas used in blank runs are all being changed. The experimental temperature range has been extended down to 313 K.

Computer models incorporating these other reactions are being compared with experimental results.

* Present address : DCPR-ENSIC, 1, rue Grandville 54000 NANCY, FRANCE.

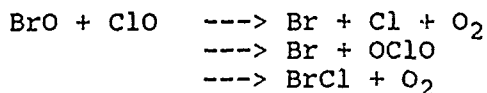
KINETICS AND PRODUCTS OF SELF AND CROSS COMBINATION REACTIONS OF HALOGEN OXIDE RADICALS

I.T. Lancar, G. Laverdet, G. Le Bras and G. Poulet
Centre de Recherches sur la Chimie de la Combustion et des
Hautes Températures - C.N.R.S. -45071 ORLEANS Cedex2 (France)

The gas phase recombination reactions of XO radicals (X = F, Cl, Br, I) possess a complex behaviour leading to the simultaneous formation of several products such as X, X₂, OXO, X₂O₂. The temperature and pressure dependence of the various channels involved needs to be precisely known since most of these reactions play a significant role in atmospheric processes.

Using the discharge-flow technique and the direct monitoring of the XO radicals and of the products by mass spectrometry, the rate constants and branching ratios have been measured at 298 K for the BrO + BrO and BrO + ClO reactions. For example, the branching ratios for the channels forming Br₂ (in the BrO + BrO reaction) and BrCl (in the BrO + ClO reaction) have been found to be 0.15 and 0.12, respectively, at 298 K.

The data obtained for the temperature dependence of the rate constants for the different channels of the BrO + ClO reaction will be discussed, in relation with their impact on the stratospheric polar ozone chemistry:



The self reactions of ClO and IO, which are under study, will be also presented.

EXPERIMENTAL STUDIES AND THEORETICAL MODELLING OF THE
DYNAMICS OF SiMe_2 INSERTION REACTIONS

by R Walsh, Department of Chemistry, University of Reading,
Whiteknights, Reading, RG6 2AD, U.K.

Recent time-resolved kinetic studies (mostly unpublished) using Laser Flash Photolysis have shown that the reactive species SiMe_2 undergoes rapid insertion and addition reactions with negative activation energies. In some cases, rate decreases of a factor of 10 between 300 and 600 K (corresponding to $E_a = -12 \text{ kJ mol}^{-1}$) have been observed. Pressure dependences have also been detected for some reactions. These processes involve coupled electrophilic and nucleophilic interactions during the course of reaction. An analysis of these effects suggests the involvement of intermediate complexes (of the donor-acceptor type). We have carried out calculations of the RRKM type on the two channel behaviour of such a complex in order to find out its relative propensity for dissociation, isomerisation and stabilisation (via collisions). The results of these calculations depend on the energy-well depth of the complex. Such complexes are an unusual case for such modelling in that thermal population distributions, even at room temperature, extend well above the threshold for reaction. Theoretical results can be made to fit experimental findings provided the energy-well depth of the complex is within well-defined limits. Details of these calculations will be presented at the meeting.

Non-Equilibrium Kinetics of the $\text{OH} + \text{Cl} \rightleftharpoons \text{HCl} + \text{O}$ Reaction

Heshel Teitelbaum
Department of Chemistry
University of Ottawa
Ottawa, Canada K1N 6N5

As part of our continuing programme for assessing the importance of non-equilibrium phenomena to chemical kinetics, we have examined the reaction $\text{OH} + \text{Cl} \rightleftharpoons \text{HCl} + \text{O}$ (1). We have solved the master equation describing the rates of change of the vibrational level populations of OH in the steady-state limit. The reaction itself depletes the vibrational level population which in turn reduces the reaction rate. However, to date, it is not known how severe the depletion is.

Our study makes use of measured¹ microscopic state-selected rate constants for (1) as well as measured² V-T and V-V energy transfer rate constants involving O:H in order to estimate the depletion. The effect is manifested as a reduction of the thermal rate-coefficient and of the Arrhenius activation energy and depends on the identity and quantity of the species which can vibrationally relax OH. It is a small effect at low temperatures, but becomes more important at intermediate temperatures and finally less important again at high temperatures. The effect is stronger than what we observed previously in studies of the H/H_2 , O/H_2 , OH/H_2 systems, but not as strong as observed in the Br/HCl system.³⁻⁵

Our study shows that theoretical calculations of thermal rate coefficients should account for these effects before comparison is made with corresponding experimental data.

1. A. Blackwell, J.C. Polanyi, J.J. Sloan, Chem. Phys. 24, 25 (1977).
2. H. Teitelbaum, P. Aker, J.J. Sloan, Chem. Phys. 119, 79 (1988).
3. C. Bowes, N. Mina, H. Teitelbaum, J. Chem. Soc. Faraday Trans., submitted.
4. H. Teitelbaum, J. Phys. Chem (in press).
5. H. Teitelbaum, J. Chem. Soc. Faraday Trans. 2, 84, 1889 (1988).

Rates of Vibrational Energy Transfer in Collisions between HCN, DCN and Light Gases

I.W.M. Smith and J.F. Warr

School of Chemistry
University of Birmingham
Edgbaston
Birmingham B15 2TT, U.K.

We shall report the results of three types of experiment designed to provide a complete quantitative picture of the transfer of vibrational energy between H_2 , D_2 , HD and, for comparison, ^3He and ^4He . First, we have studied the rates of relaxation from the (101), (011) and (001) states of HCN induced by these light gases. Molecules are excited using pulsed infrared radiation from an optical parametric oscillator (OPO), and time-resolved IR fluorescence is observed from gas mixtures of different composition. A cold gas filter is used to discriminate between emissions from different excited levels.

In our second series of experiments, H_2 and D_2 have been excited to $v=1$ by Raman pumping and the rates at which these molecules transfer energy by V-V exchange to HCN and DCN have been measured by monitoring the IR fluorescence from the IR-active molecules. The excitation of H_2 or D_2 is achieved by focussing two beams of radiation into the sample gas: one is the frequency-doubled output of a Nd:YAG laser at 532 nm, the other is the radiation obtained by frequency-shifting the laser output to 683 nm (or 633 nm) using the stimulated Raman effect in high pressure H_2 (or D_2).

Finally, we expect to report preliminary results from double resonance experiments in which single rovibrational levels of HCN are excited with radiation from the OPO and the subsequent (rotational and vibrational) energy transfer processes are observed using laser-induced fluorescence in the ultraviolet at ca. 200 nm.

We shall discuss the implications of results for the operation of chemical and energy transfer lasers operating on rovibrational transitions in HCN.

Rate Constants for the Reactions of Methoxy and Ethoxy Radicals with NO_2
and with NO over a Range of Temperature and Total Pressure

M.J. Frost and I.W.M. Smith

School of Chemistry
University of Birmingham
Edgbaston
Birmingham B15 2TT, U.K.

The kinetics of the reactions of RO ($\text{R} = \text{CH}_3, \text{C}_2\text{H}_5$) with NO_2 have been studied using pulsed laser photolysis to generate RO radicals from RONO and time-resolved LIF to observe the decay of $[\text{RO}]$. With NO_2 , association to RONO_2 appears to dominate. The $\text{C}_2\text{H}_5\text{O} + \text{NO}_2$ reaction is in its high pressure limit at the total pressure (> 15 Torr) of our experiments at 295 K. The fall-off behaviour for $\text{CH}_3\text{O} + \text{NO}_2$ has been analysed and rate constants at 295 K in the limit of low pressure ($\text{M} = \text{He, Ar, CF}_4$) and high pressure will be presented, along with some results at higher temperature.

Extensive data ($296 < T/\text{K} < 573$; $3 < P/\text{Torr} < 125$) will also be reported for the reaction of CH_3O with NO . In this case, detailed analysis of the experimental results, as well as comparison with theoretical estimates of the rate constants for association, strongly suggest that reaction occurs by two competing channels: association to CH_3ONO and reaction to $\text{H}_2\text{CO} + \text{HNO}$. This analysis yields rate constants in the limits of low and high pressure for these reactions.

Our study indicates that a re-evaluation of the kinetics and mechanism of $\text{CH}_3\text{O} + \text{NO}$ is required. Our results will also be compared with data for the related reactions of NO_2 and NO with OH , SH , RS and other RO radicals.

Alkyl Radical Heats of Formation

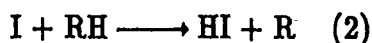
P.W. Seakins¹ and M.J. Pilling²

A controversy has existed for some time regarding alkyl radical heats of formation. [1,2]. Recent time resolved studies [3,4,5] have confirmed Tsang's proposed higher values for $\Delta H_f^\circ(298)$ C_2H_5 and $i-C_3H_7$ radicals, which are significantly higher than recommended by earlier halogenation studies of the equilibrium E(1) [1].



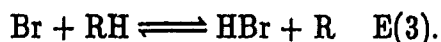
The discrepancies between the various determinations are attributable to the negative activation energies measured by Gutman et al [1,7] for reaction (-1) and assumed by the earlier studies [1].

However, debate still exists as to the mechanism of alkyl radical + HX reactions [5,6]. Muller-Markgraf et al [6] studied $t-C_4H_9$ in a Very Low Pressure Photolysis system, and measured a rate constant 50 times less than Gutman et al [2], and with an positive activation energy. Whilst conceding that the activation barrier in reaction (-1) may be lower than originally assumed, Benson has argued [5] that errors in the activation energies for the abstraction reaction:



are large enough to encompass the new radical heats of formation, without having to invoke a complex mechanism, with a negative temperature dependence for the reverse reaction.

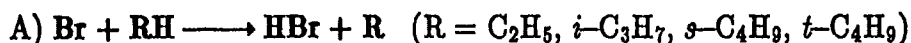
Results will be presented on several aspects (A-C) of the equilibrium E(3):



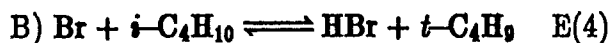
All studies were performed using a conventional Laser Flash Photolysis/Resonance Fluorescence apparatus, monitoring Br atom fluorescence in real time experiments.

¹Physical Chemistry Laboratory, South Parks Rd, Oxford, OX1 3QZ, UK.

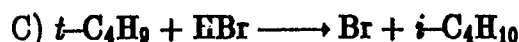
²School of Chemistry, Leeds University, Leeds, LS2 9JT, UK.



Temperature dependent studies have been carried out on the above reactions. In combination with the direct measurements of Gutman et al [7], second and third law calculations yield radical heats of formation in excellent agreement with recent determinations.



Br atom signal was monitored in the presence of both isobutane and hydrogen bromide. Analysis of the resultant decay traces, as the system relaxes to equilibrium, yielded a direct determination of the equilibrium constant for E(4). Third law calculations produced a value of $\Delta H_f^0(298) t\text{-C}_4\text{H}_9 = 48.3 \pm 4.0 \text{ kJmol}^{-1}$ in good agreement with the studies of Gutman et al [2].



Br atom fluorescence was monitored following the photolytic production of $t\text{-C}_4\text{H}_9$ radicals in the presence of HBr. Numerical analysis of the atom traces yielded a room temperature rate constant of $(3.2 \pm 1.0) \times 10^{-11} \text{ cm}^3 \text{ molecule}^{-1} \text{ s}^{-1}$, higher by factors of 3.0 and 1.9 than two recent determinations [2,8], and a factor of 150 above that reported in ref[6]. A value of $\Delta H_f^0(298) t\text{-C}_4\text{H}_9 = 50.0 \pm 3.5 \text{ kJmol}^{-1}$ is calculated from this determination.

References

- [1] D.F. McMillan and D.M. Golden, *Ann.Rev.Phys.Chem.*, **33** (1982) p493.
- [2] J.J. Russell, J.A. Seetula, R.S. Timonen, D. Gutman and D.F. Nava, *J.Am.Chem.Soc.* **110** (1988) p3084.
- [3] M.Brouard, P.D. Lightfoot and M.J. Pilling, *J.Phys.Chem.*, **90** (1986) p445.
- [4] W. Tsang, *J.Am.Chem.Soc.* **107** (1985) p2872.
- [5] S.S. Parmar and S.W. Benson *J.Am.Chem.Soc.* **111** (1989) p57.
- [6] W. Muller-Markgraf, M.J. Rossi and D.M. Golden, *J.Am.Chem.Soc.* **111** (1989) p956
- [7] J.J. Russell, J.A. Seetula and D. Gutman, *J.Am.Chem.Soc.* **110** (1988) p3092.
- [8] P.Richards, R. Ryther, and E. Weitz, *Chem.Phys.Lett.* submitted.

Mechanism of ions Ti^+ formation in vacuum arc in presence of argon

L.Y. Rusin, A.A. Sidorenko

Electrical arcs in metal vapors (vacuum arcs) play a very important role in modern technologies, but the physical and chemical processes determining arc nature are but poorly studied. The vacuum arcs are used as source of chemically active particles for synthesis of wear resistant coats and compounds with improved tribological and anticorrosion properties [1]. These arcs may be useful as source of ionic and neutral beams of refractory metal atoms over a wide range of translation energy.

It is found in [2] that the ion flux intensity generated by a titanium vacuum arc can be increased (more than by an order) with addition to the arc region of small quantities of nitrogen or rare gases. It was suggested that the mechanism of this phenomenon includes ionisation of neutral Ti atoms in plasma by collisions with metastable particles produced under interaction of ground state atoms with electrons in adjacent space-charge region.

To ascertain the kinetics of the ionic products yield increase in vacuum arc plasma we studied the energy distribution of Ti^+ ions, generated by an arc in titanium vapors in the presence of argon atoms. The experimental set up is shown in fig. 1. It consists of four differentially pumped chambers. The first chamber contains a vacuum arc generator. The plasma flux is collimated by skimmers and is passed through an energy analyser with retarding field into a monopolar mass-spectrometer. The experimental set up is controlled by CAMAC interfaces.

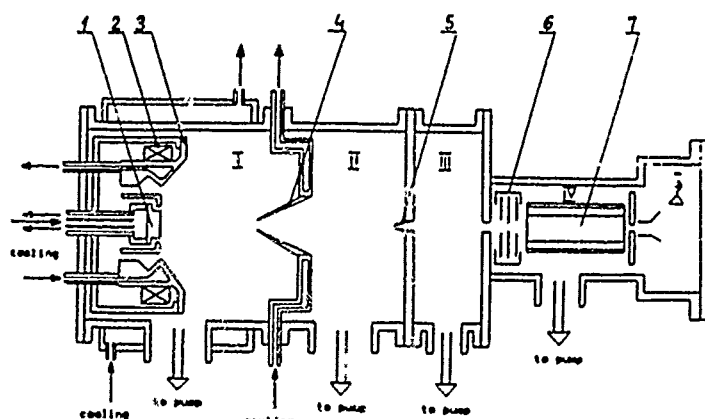


Fig. 1. Schematic view of the apparatus. I-IV - differentially pumped chambers. 1 - cathode; 2 - magnetic coil; 3 - anode; 4,5 - skimmers; 6 - energy analyser; 7 - mass-spectrometer

Typical energy distributions are shown in fig. 2 where 1 stand for the energy spectrum of Ti^+ ions at $5 \cdot 10^{-6}$ Torr (without Ar) and 2 for the energy distribution under the same conditions at $8 \cdot 10^{-5}$ Torr (with Ar additions). The difference between distributions is a new small energy peak showing the appearance of a second channel of ion generation. The first channel represents ionisation by electrons in the adjacent space-charge region and the energy distribution shows two 30 eV and 60 eV maxima. The energy distribution reflects the structure and magnitude of the space-charge barrier. The addition of argon atoms not only increases the total ion flux in the detector direction but also essentially changes the energy distribution shape. This results from the change in the ion formation mechanism. The latter involves along with electron ionisation processes of metastable atoms formation also the reaction

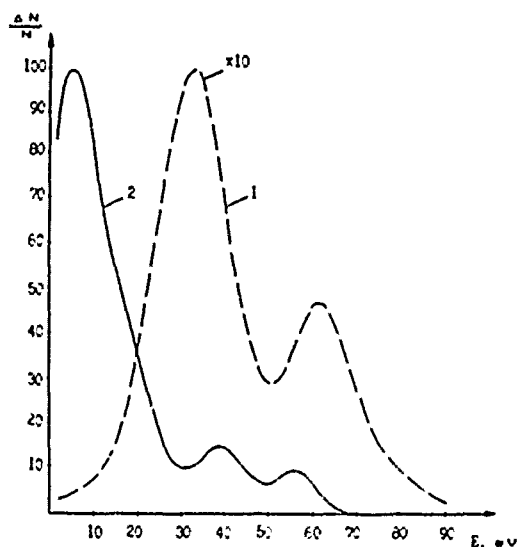


Fig. 2. Energy distribution of Ti^+ ions. 1 - without Ar additions ($p = 5 \cdot 10^{-6}$ Torr); 2 - with Ar additions ($p = 8 \cdot 10^{-5}$ Torr)

In general this mechanism is realised near the energy barrier bottom. Probably it is the reaction for appearance of the strongest distribution maximum at 10 eV. Further studies of kinetic ionisation in the adjacent space-charge region by the molecular beam diagnostic will help to understand one of the most fundamental problems of the vacuum arc nature.

References

1. "Vacuum Arcs. Theory and Application", edited by J.M.Lafferty, Wiley & Sons, New York, 1982.
2. A.F.Ragosin, L.Yu.Rusin, Soviet "Chemical Physics", 1987, 6, 45.

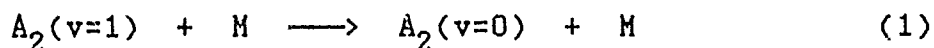
APPLICATION OF THE THERMOMETRIC SYSTEM FOR INVESTIGATION OF VIBRATION RELAXATION PROCESSES AND REACTIONS IN GASES.

Orkin V.L.

Institute of Energy Problems of Chemical Physics,
Academy of Sciences of the USSR, Moscow.

Flow technique with a high-sensitive thermocouple detection system was used successfully for investigation of the set of gas processes.

The sensitivity as high as 10^{10} - 10^{11} particles/cm³ was achieved in the case of detection of vibrationally excited molecules of H₂, D₂, N₂. For the relaxation of these vibrationally excited molecules in the process of collisions with molecules M



rate constants were measured at room temperature (units are 10^{-14} cm³/s):

A ₂ \ M:	H ₂ O	D ₂ O	CO ₂	NO ₂	O ₃	CH ₃ COCH ₃
N ₂	0.54	1.4	50	0.035	0.08	3.1
H ₂	21	2.2	1.5			
D ₂	1.8	19	32			

Moreover the rate constants of relaxation processes of these vibrationally excited molecules due to collisions with surfaces of some materials were determined.

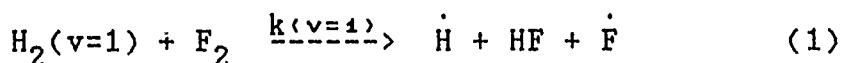
High-sensitive technique for detection of hydrogen (fluorine) atoms was made on the base of thermometric system using the "chemical amplification" of heating due to the fast chain reaction between hydrogen and fluorine. The sensitivity as high as 10^7 - 10^8 atoms/cm³ was achieved. Some reactions of molecular fluorine which produce atoms of fluorine were investigated. For example the rate constants of atom production due to reaction between molecular fluorine and NO, C₂H₄, C₂F₄ are: $1.0 \cdot 10^{-14}$, $6.1 \cdot 10^{-17}$, $3.1 \cdot 10^{-16}$ (units are cm³/s) respectively, T= 315 K. This technique allow one determine rate constants of atoms generating reactions when their values are in the range from 10^{-19} cm³/s to 10^{-13} cm³/s.

ATOMS PRODUCTION IN REACTION OF VIBRATIONALLY EXCITED HYDROGEN WITH MOLECULAR FLUORINE AND KINETIC INVESTIGATION OF $H_2 + F_2 + O_2$.

Orkin V.L.

Institute of Energy Problems of Chemical Physics,
Academy of Sciences of the USSR, Moscow

An elementary reaction



was studied by a flow technique with a thermometric detection system. A sensitivity of the detection system to hydrogen (fluorine) atoms was $10^7 - 10^8$ particles/cm³; to vibrationally excited hydrogen molecules (VEHM) - $10^{10} - 10^{11}$ particles/cm³. A special thermal source of VEHM which permitted to determine there absolute concentrations was used.

Under mixing VEHM with molecular fluorine in the flow a production of atoms was detected and the rate constant of (1) was determined:

$$k(v=1) = (1.6 \pm 0.6) \cdot 10^{-19}, \text{ cm}^3/\text{s} \quad (T = 315 \text{ K})$$

$$k(v=2)/k(v=1) < 300.$$

The method of $k(v=1)$ determination is in need of none external data.

The kinetic investigations of " $H_2 + F_2 + O_2 + He$ " system were carried out in the quartz flow reactor. Reaction (1) was shown to be the chain branching process. A substantial enlargement of kinetic chains due to heterogeneous atom regeneration from HO_2 - radicals with a participation of fluorine was shown to take place. A probability of the process



per collision of HO_2 with surface was determined as

$$\varepsilon = (0.4 \div 1.6) \cdot 10^{-3} + (1 \div 2) \cdot 10^{-18} \cdot [F_2]$$

Specific kinetic relationships, that should take place due to heterogeneous process of regeneration of the active radicals from the relatively less active ones were analyzed.

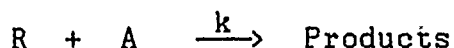
IN SITU DETERMINATION OF HETEROGENEOUS PROCESSES CONTRIBUTION IN FLOW TECHNIQUE INVESTIGATIONS OF HOMOGENEOUS REACTIONS.

Orkin V.L., Khamaganov V.G.

Institute of Energy Problems of Chemical Physics,
Academy of Sciences of the USSR, Moscow

Flow technique is of current usage to measure precisely rate constants of different types of gas reactions. However, this method does not allow one to distinguish unambiguously homogeneous reactions from heterogeneous ones.

Along with the homogeneous reaction of active particles R with A



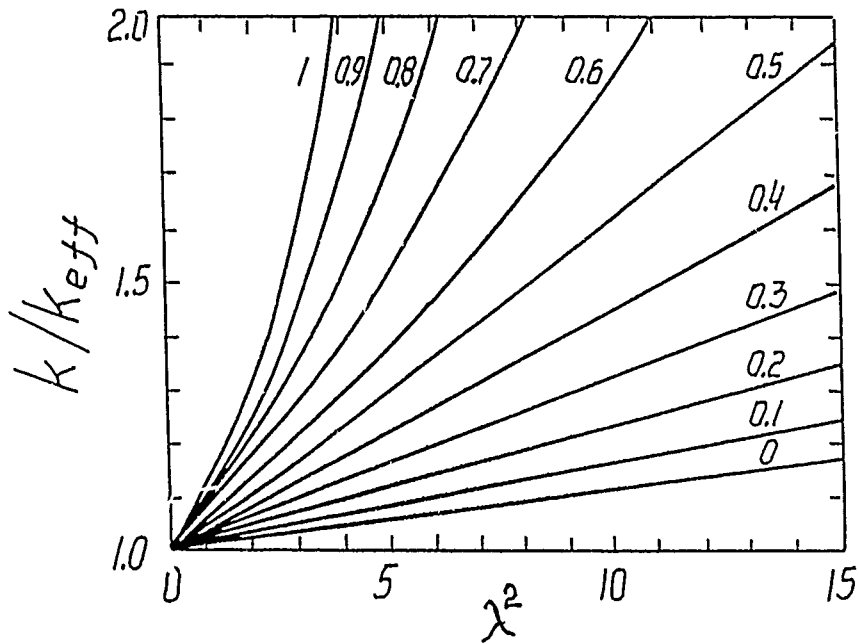
the heterogeneous process with participation either R or A can take place. In order to determine nature of the reaction, measurements are sometimes carried out in tubular reactors of different radius or with different sort of surface of the tube. Nevertheless, these experiments can not be considered as an unambiguous proof. As a rule the reaction under investigation is believed to be homogeneous *a priori*.

Quantitative analysis of the influence of the diffusion on the flow experiment data allowed us to propose a method of determination of the reaction nature.

In flow experiments under conditions of $[R]_0 \ll [A]$, lifetime of active particles τ_{eff}^{-1} is determined to get the value of k_{eff} .

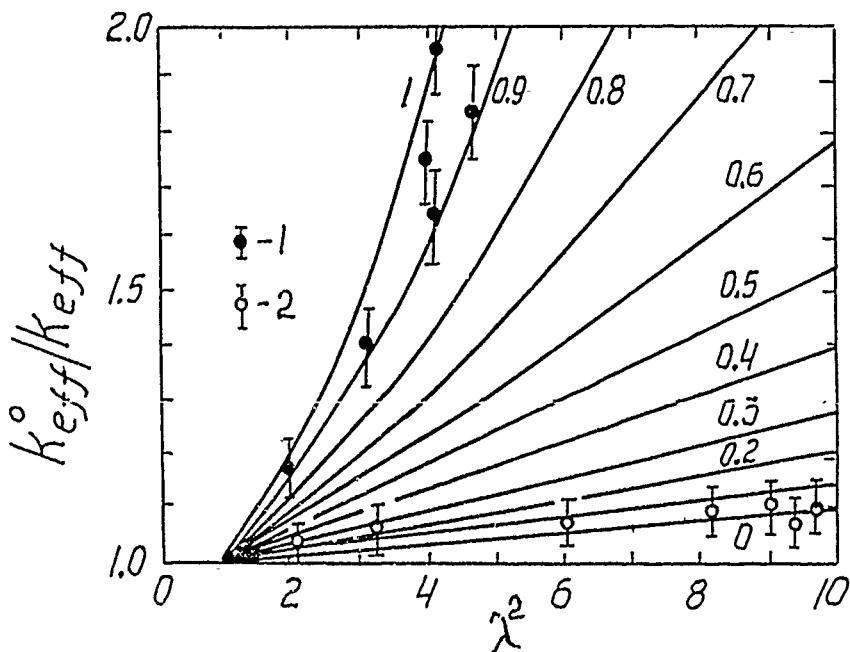
$$-k_{\text{eff}}[A] = v \frac{d \ln[R]}{dz} \Big|_{[A]} - v \frac{d \ln[R]}{dz} \Big|_{[A]=0} = \tau_{\text{eff}}^{-1} - (\tau_{\text{eff}}^{\text{het}})^{-1}$$

The value obtained coincides with the rate constant of reaction under study ($k_{\text{eff}} = k$) only in the case of either fast radial diffusion ($\lambda^2 = 2\tau_{\text{eff}}^{-1}r^2/D \ll 1$, r is the radius of tube, D is the diffusion coefficient) or high flow velocity ($v^2 \gg \tau_{\text{eff}}^{-1}D$). On the other hand for slow radial diffusion ($\lambda^2 > 1$) one always has $k/k_{\text{eff}} > 1$, and dependencies k/k_{eff} on λ^2 differ essentially for homogeneous and heterogeneous reactions. Analysis of this dependencies allows one to distinguish a part of the heterogeneous channel of reaction. Fig.1 shows such dependence.



Numbers at the curves indicate the fraction of the total rate of transformation of the substance occurring at the reactor surface when $\lambda^2 \ll 1$. (There is no heterogeneous nonreactive active particle removal).

Fig.2 show the result of the method using for investigation of either heterogeneous (1) or homogeneous (2) reactions of OH-radicals with HCl in the reactors covered with different substances. The reaction nature has been known *a priori* in this case.



MECHANISM AND KINETICS OF THE XeCl* FORMATION IN Xe-RCI SYSTEMS.

A.Jowko, M.Forys and E.Bartkiewicz

Institut of Chemistry, Agricultural and Teachers University
08-110 Siedlce, Poland.

Excitation energy transfer processes were investigated in Xe-RCI (RCI = CCL₄, S₂Cl₂, HCl) systems by observation of the time resolved fluorescence of XeCl excimers.

Linear electron accelerator ELU-6, which can produce 8MeV electron pulses of 7ns. FWHM was used as the irradiation source.

The primary results seems to suggest that very fast ($k \approx 5 \times 10^{-28} \text{ cm}^6 \text{ s}^{-1}$) third order reaction



can contribute to the formation of XeCl excimers.

K. Scherzer, J. Gebhardt, M. Olzmann

Sektion Chemie der Technischen Hochschule "Carl Schorlemmer"
Leuna-Merseburg, GDR

Chemical activation of cycloalkenes by hydrogen atoms

The reactions of hydrogen atoms with the cycloalkenes C_5 to C_8 and the *n* alkenes C_2 to C_8 have been studied at room temperature and 150 Pa in an isothermal flow system. In contrast to investigations known from the literature an excess of H atoms was used. The ratio of the concentrations hydrocarbon/H atoms has been varied between 0.002 and 2.6. Under such conditions multiple activation steps are possible, that means the primerly formed activated radicals can recombine with H atoms yielding highly vibrational excited alkane molecules. Via such processes degradations up to methane occur. The ratio decomposition/collisional stabilization (D/S) decreases with increasing ratio $c_{\text{hydrocarbon}}/c_{\text{H}}$ and with increasing size of the reactant.

To calculate the ratios D/S for the first and the second activation step the classical formalism for chemically activated systems is extended. A method based on the coupling of two conventional steady-state master equations is presented to evaluate the contribution of either of the two reaction paths. The treatment proposed is demonstrated for the exemples cyclopentene and cis but-2-ene within molecular hydrogen as a bath gas. It turns out that the second way, via activated alkanes, is not negligible under these conditions.

The $B(^2P) + H_2O (X^1A_1)$ reaction: Potential energy surface and quasiclassical 3D trajectory calculation

M. Albertí, R. Sayós, A. Solé and A. Aguilar

Departament de Química Física, Universitat de Barcelona

Martí i Franquès 1, 08028 Barcelona (Spain)

Reactions between atomic boron and R-OH molecules (being R H or organic radicals) have been a fruitful research area due to the importance of the oxidation processes involved in combustion reactions[1]. Atomic boron reacts with H_2O , H_2O_2 , alcohols and ethers to give several oxidation products[2]. Due to the large B-O bond energy, all of these reactions have more than one exoergic channel, thus easing their relative reactivity determination at energies not far away of the threshold. For the reaction of boron with water molecules, both theoretical [3-6] and experimental [7] information is available.

In order to perform a quasiclassical 3D trajectory study of the $B(^2P) + H_2O(X^1A_1)$ we have carried out an analytical fit of the H_2BO doublet ground state PES using a single-valued Sorbie-Murrell-like representation[8,9]. The function obtained, which has been fitted to the ab initio results at MP3/6-31G**//HF/6-31G** level, does reproduce the main characteristics of the PES[3,5,6].

The quasiclassical four-center trajectory calculation shows the formation of several boron oxidation products: HOB, HBO and BO, the relative reactivity being that predicted from PES characteristics[5]. Neither BH_2+O nor $BH+OH$ formation was observed although these endoergic channels are still accesible at the higher collision energy values studied.

From the selection of rotational energy at 300 K, with the H_2O molecule in its ground vibrational level (0,0,0), the overall reaction cross section (S_r) increases with collision energy. This is in accord with the PES topology as it presents a barrier in the reactants channel.

Reactants vibrational energy capability to enhance reactivity depends on which vibrational mode gets excited. Thus, giving vibrational energy to the stretching symmetric mode $(0,0,0) \longrightarrow (1,0,0)$ almost does not modify the cross section value, while the excitation of both bending, $(0,0,0) \longrightarrow (0,1,0)$, and stretching antisymmetric $(0,0,0) \longrightarrow (0,0,1)$ vibrational modes, enhances overall reactivity.

At the investigated conditions, we have found that reactivity is diminished by increasing rotational energy. This can be justified by considering that such an increase disrupts the particularly preferred orientation for the reaction (for the $B+H_2O$ system, the minimum energy reaction path lies to a transition state with C_{2v} symmetry).

In respect to the energetic distribution into the products we have found, for all of the investigated initial conditions, that the PES tends to channelize a high content of energy as products internal energy.

A more detailed discussion of the results obtained will be reported at the Symposium.

References

- [1] A.W Hanner and J.L. Gole. J. Chem. Phys., 73 (1980) 5025.
- [2] T.G. DiGiuseppe, R. Estes and P. Davidovits. J. Chem. Phys., 86 (1982) 260.
- [3] S. Sakai and K.D. Jordan. J. Phys. Chem., 87 (1983) 2293.
- [4] S. Sakai and K.D. Jordan. Chem. Phys. Lett., 136 (1986) 103
- [5] M. Albertí, R. Sayós, M. González, J. Bofill and A. Aguilar. J. Mol. Struct. (Theochem) 166 (1988) 301.
- [6] M. Albertí. Ph.D. Thesis. Dept. Química Física. Universitat de Barcelona 1990.
- [7] J.L. Gole and S.A. Pace. J. Phys. Chem., 85 (1981) 2651.
- [8] J.N. Murrell and S. Carter. J. Phys. Chem. 88 (1984) 4887.

HIGH RESOLUTION CROSSED BEAM STUDIES OF INTERMOLECULAR FORCES:
POTENTIAL ENERGY SURFACES FOR O_2 , N_2 , NO, Cl_2 - RARE GASES

L. Beneventi, P. Casavecchia, and G.G. Volpi
Dipartimento di Chimica, Università di Perugia,
06100 Perugia, Italy.

In our laboratory we have recently exploited the very detailed information content of diffraction scattering for the determination of interaction potentials for isotropic¹ and anisotropic²⁻⁴ van der Waals systems. It has been shown that precise total differential cross section (DCS) measurements, carried out in high-resolution conditions and presenting well resolved diffraction oscillations, coupled to absolute total integral cross sections, second virial, diffusion and viscosity coefficients, and semiempirical long-range coefficients from literature, permit deriving within the IOS approximation reliable PES for systems as He and Ne interacting with simple diatomic molecules (O_2 , N_2 , and NO).^{2,3} The reliability of the IOS decoupling scheme in deriving a fully anisotropic PES from the measured scattering dynamics for He-containing systems^{2,5} and also for relatively heavy systems, as Ne- N_2 ,³ has been examined and demonstrated by performing exact close-coupling calculations.

Here we report experimental results on total DCS for Ne- O_2 and NO, Ar- O_2 and N_2 , and He, Ne, Ar- Cl_2 , which represent an extension of previous work on He- N_2 , O_2 , and NO,² Ne- N_2 ,³ Ar and Kr-NO,⁶ and He- CO_2 .⁴ The experiments were performed on a high resolution universal crossed molecular beam apparatus which has been described elsewhere.^{1,2,6}

As example of the data quality, in Fig.1 we report the total DCS data, multiplied by $\Theta^{7/3}$, for Ne- O_2 measured at positive and negative angles. Data analysis has been carried out along the lines followed for the He-containing systems² and Ne- N_2 ,³ that is by simultaneously fitting all other available experimental properties. For Ne- O_2 these properties are: absolute total integral cross sections, diffusion and viscosity coefficients, and the Zeeman spectrum.⁷

For Ne-NO the results are compared with the PES previously proposed⁸ from the analysis of integral cross section measurements with state selected NO.

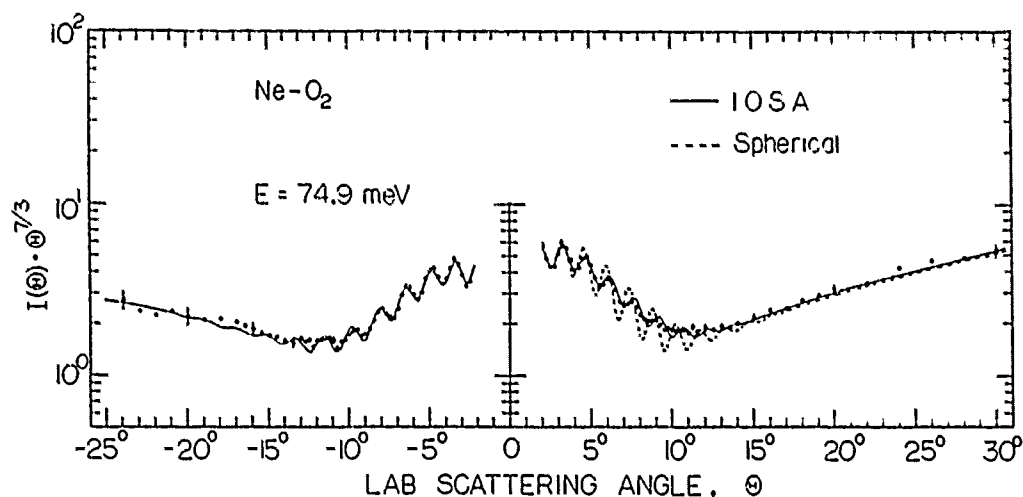


Fig. 1. Total differential cross section data for Ne-O₂. Continuous line: IOS calculations with best-fit potential₂ surface. Dashed line: calculation with the spherical limit potential.

relaxation phenomena, which should lead to a significant improvement of the presently available PESs.

The rare gas-chlorine systems have recently attracted much interest in relation to vibrational predissociation studies⁹. Total DCSs at two collision energies with well resolved diffraction oscillations have been measured for He-Cl₂. The diffraction structure superimposed on the main rainbow oscillation has also been resolved for Ne-Cl₂. The main rainbow and two supernumerary rainbows have been observed for Ar-Cl₂. Data analysis to derive fully anisotropic PESs is currently under way.

REFERENCES

1. L.Beneventi, P.Casavecchia, and G.G.Volpi, *J.Chem.Phys.* **84**, 4828 (1986); in *Structure and Dynamics of Weakly Bound Molecular Complexes*, ed. by A.Weber, NATO ASI Ser.C (Reidel, Dordrecht, 1987), Vol. 212, p. 441.
2. L.Beneventi, P.Casavecchia, and G.G.Volpi, *J.Chem.Phys.* **85**, 7011 (1986).
3. L.Beneventi, P.Casavecchia, F.Vecchiocattivi, G.G.Volpi, D.Lemoine, and M.H.Alexander, *J.Chem.Phys.* **89**, 3505 (1988).
4. L.Beneventi, P.Casavecchia, F.Vecchiocattivi, G.G.Volpi, U.Buck, Ch.Lauenstein, and R.Schinke, *J.Chem.Phys.* **89**, 4671 (1988).
5. L.Beneventi, P.Casavecchia, G.G.Volpi, D.Lemoine, and G.Corey, to be published.
6. P.Casavecchia, A.Lagana', and G.G.Volpi, *Chem.Phys.Lett.* **112**, 445 (1984).
7. L.Beneventi, P.Casavecchia, F.Pirani, F.Vecchiocattivi, G.G.Volpi, and J.Reuss, to be published.
8. H.Thuis, S.Stolte, and J.Reuss, *Chem.Phys.* **43**, 351 (1979).
9. N.Halberstadt, J.A.Beswick, and K.C.Janda, *J.Chem.Phys.* **87**, 3966 (1987), and references therein.

CROSSED BEAM STUDY OF THE IONIZATION PROCESSES IN THERMAL ENERGY COLLISIONS
BETWEEN $\text{Ne}^*(^3P_{2,0})$ AND HCl

A.Aguilar, B.Brunetti, M.Gonzalez, F.Vecchiocattivi, and G.G.Volpi,
Dipartimento di Chimica, Università di Perugia, 06100 Perugia, Italy

The ionization processes in collisions of rare gas metastable atoms with atomic or molecular targets have been extensively studied in the last years (1). Nevertheless only a small number of detailed studies have been devoted to the dynamics of those processes which lead not only to Penning and associative but also to rearrangement ionization. In these cases a chemical reaction occurs between the collision partners, after the electron ejection (2).

This work is devoted to the study of the thermal energy ionization in collisions of neon metastable atoms with HCl , whose mass spectrum, as measured in our laboratory, indicates the formation of HCl^+ , NeH^+ and NeHCl^+ in a ratio $\sim 1:0.1:0.02$. The energy dependence of the cross section for each ionization channel have been measured in the 0.03-0.5 eV energy range. The goal is to give a dynamical picture of the collision before and after the ionization event.

Beyond the fundamental interest of understanding the ionization dynamics, the study of the ionization of HCl by neon metastable atoms appears to be interesting because this reaction plays an important role in some laser sources, e.g. in the XeCl laser, where the excimer molecule is produced in a discharge of a Xe/HCl mixture in a bath of neon.

The experiment has been carried out in a crossed beam apparatus previously used for other studies and described elsewhere.

The total ionization cross section and the partial ionization cross section for each one of the ions produced as a function of the collision energy will be presented at the conference.

In these collisions HCl^+ ions are formed in the fundamental ($X\ ^2\Pi$) and first excited ($A\ ^2\Sigma^+$) state with a ratio $A/X \approx 0.64$ (4). Energetic considerations indicate that NeH^+ can be formed through an atom-molecular ion

reaction, within the collision complex, involving HCl^+ ($A^2\Sigma^+$). A simple mechanism based on these considerations and on a modification of the tp-L (turning point-Langevin) model, originally proposed by Siska and coworkers (2), appears to give satisfactorily account of the experimental results.

-
- 1) H.Morgner, Comments At.Mol.Phys. 21, 195 (1988) and references therein.
 - 2) D.W.Martin, D.Bernfeld and P.E.Siska, Chem.Phys.Lett. 110, 298 (1984);
D.W.Martin, C.Weiser, R.F.Sperlein, D.Bernfeld and P.E.Siska, J.Chem. Phys. 90, 1564 (1989); A.Munzer and A.Niehaus, J.Electr.Spectrosc.Relat. Phenomena 23, 367 (1981).
 - 3) L.Appolloni, B.Brunetti, F.Vecchiocattivi and G.G.Volpi, J.Phys.Chem. 92, 918 (1988).
 - 4) A.J.Yencha, J.Ganz, M.W.Ruf and H.Hotop, Z.Phys. D-Atoms, Molecules and Clusters (1989).

MOLECULAR BEAM STUDIES OF COLLISIONAL PROCESSES
OF METASTABLE HYDROGEN ATOMS

G.Vassilev, F.Perales, Ch.Miniatura, J.Robert,
J.Reinhardt, F.Vecchiocattivi*, and J.Baudon
Laboratoire de Physique des Lasers
Université de Paris-Nord
Villetaneuse, France

The integral and differential elastic cross sections for the collision between the excited $H^*(2s)$ atom and the ground state H_2 molecule have been measured in beam-gas and in crossed beam experiments respectively, for the thermal collision energy range.

The excited H^* atom beam is produced by electron bombardment of a ground state H atom beam obtained by a radiofrequency discharge beam source. The velocity distribution of the H^* atoms is measured by time-of-flight technique. The H^* atoms are detected by looking at the Lyman- α photons emitted when these excited atoms are quenched by an electric field.

The target H_2 molecules are contained in a scattering box for the integral cross sections experiment, and in a secondary thermal beam for the differential cross section experiments. Cross sections have been measured also for D^*-H_2 collisions.

The experimental results have been analyzed by using a simple phenomenological optical potential, whose real part, a LJ(8,6) potential, gives account of the elastic channel, while the imaginary part, a simple exponential potential, gives account of all the non-elastic channels (quenching, exchange-reaction, H_3^+ production, etc.).

* Dipartimento di Chimica, Università di Perugia,
06100 Perugia, Italy.

OPTICAL POTENTIAL FOR $\text{Ne}^*(^3\text{P}_{2,0})\text{-Ar,N}_2$ SYSTEMS

J.Baudon, P.Feron, C.Miniatura,
F.Perales, J.Reinhardt, and J.Robert
Laboratoire de Physique des Lasers,
Université de Paris-Nord
Villetaneuse, France

H.Haberland
Institut für Physik, Universität Freiburg,
Freiburg im Breisgau, FRG

B.Brunetti and F.Vecchiocattivi
Dipartimento di Chimica, Università di Perugia,
Perugia, Italy

The optical model for particle scattering is based essentially on the assumption that the interaction between two colliding partners is described by a complex potential. This model has been formerly introduced for the description of nuclear reacting collisions, but has been also largely used for atomic and molecular collisions. The presence of an imaginary part in the potential produces an "opacity" in the scattering characteristics which gives account of the non-elastic part of the collision. As known this model does not allow to discriminate among the possible non-elastic channels and therefore has to be simply considered as a phenomenological model useful to describe in a rational and unified way the general elastic and non-elastic scattering features. However the optical model resulted to be successful in understanding details of the collision dynamics for some processes such as Penning ionization. In this case different observables, namely elastic scattering cross sections, electron energy

spectra, and ionization cross sections, can be satisfactorily reproduced by a suitable optical model used in a semiclassical treatment of the collision.

For systems involving metastable helium atoms a large body of experimental data is available and rather accurate optical potentials have been obtained. Also for systems involving metastable neon atoms large experimental information has been obtained, but optical potentials able to reproduce univocally different observables of the same system are not still available. Moreover in the metastable neon atom case the interaction is complicated by the anisotropic nature of the interaction due to the P-state nature of these excited atoms. Recent experiments have provided J-selected results for elastic scattering, ionization cross sections and electron energy spectra. However a complete analysis of these so detailed data appears a difficult task also because the lack of a reliable spherical average optical potential.

We have measured differential elastic cross sections for the scattering of metastable neon atoms by argon atoms and by nitrogen molecules in a crossed beam apparatus at different collision energies. These data are therefore analyzed, together with the integral cross sections and the total ionization cross sections previously measured in other laboratories and in Perugia. The final product of this analysis is an accurate complex potential for the average interaction of metastable neon atoms with Ar and N_2 .

The determination of accurate intermolecular potentials from a simultaneous analysis of several different experimental properties has become recently a relatively common practice for systems involving atoms or molecules in their ground state. This work represents an attempt to apply a multiproperty analysis also to the more complicate systems which involve excited atoms.

The NIST Gas-Phase Chemical Kinetics Database: Progress and Plans

W.G. Mallard and J.T.Herron, Chemical Kinetics Division,
National Institute of Standards and Technology, Gaithersburg, MD 20899 USA

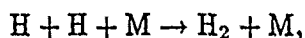
The NIST Chemical Kinetics Database for gas phase reactions was released in 1989. It is one of a series of databases that allow for rapid access to thermodynamic, ion energetic and reaction rate data on personal computers. The reaction rate database allows for rapid access to the chemical data. Searching is rapid in all of the databases due to the use of fully indexed files. Worst case searches for a given datum typically take about a second. Since the original release, the contents of the database have been augmented by the addition of over 4000 new rate constants (a 50% increase) and a doubling (4000-8000) of the number of chemical species for which there are data. In addition, the database software has been modified to provide the user with a broader range of features. Data may now be plotted in either 2 or 3 parameter Arrhenius form and the Arrhenius parameters derived. Bibliographic files and numerical data sets may be abstracted from the database for user application.

Theoretical studies of three-body hydrogen recombination

David W. Schwenke
NASA Ames Research Center, MS 230-3, Moffett Field, CA, 94035

Abstract:

We are involved in the theoretical study of the three body recombination process



for various M. Results have been obtained at 1000, 3000 and 5000 K for the third bodies $\text{M}=\text{H}$ and H_2 by means of an analysis of the numerical solution of the master equation governing the concentrations of the internal vib-rotational levels of H_2 . A total of 348 bound and quasi-bound levels of H_2 were included and the state-to-state rate constants were obtained using the quasi-classical trajectory method with a realistic potential. The agreement with experiment for $\text{M}=\text{H}_2$ is very good for all three temperatures.

In order to extend our results to other temperatures and other systems, we have begun the development of approximations to the full solution of the master equation. The accurate results which we have previously obtained will provide very useful guide-lines in the formulation of reliable approximations. Preliminary indications are that significant savings are possible without loss of accuracy. The most promising methods will be applied to lower temperatures for $\text{M}=\text{H}_2$ and also to the third bodies $\text{M}=\text{Ar}$ and $\text{M}=\text{H}_2\text{O}$.

**An Investigation of Temperature and Pressure Dependence of the
Reaction of CF_2ClO_2 Radicals with Nitrogen Dioxide by Flash
Photolysis and Time Resolved Mass Spectrometry**

Fuxiang Wu and Robert W. Carr

Department of Chemical Engineering and Materials Science
University of Minnesota
Minneapolis, Minnesota 55455, U.S.A.

Rate coefficients of the termolecular reaction



were determined over the temperature range of 248 - 324 K and at pressures from 1 to 10 torr by time resolved mass spectrometry. CF_2ClO_2 radicals were generated by flash photolysis of CF_2ClBr in the presence of oxygen. Their rate of decay was measured by following CF_2O_2 fragment ions formed in the ion source. With 2 to 40 mtorr of NO_2 present the dominant removal pathway is addition to form the peroxyxynitrate. The third order rate coefficients are wholly within the falloff over the experimental pressure range, and have a negative temperature coefficient. Extrapolation to lower and higher pressures, and estimates of low and high pressure limiting rate coefficients, k_0 and k_∞ were done by nonlinear least squares fit of the experimental data, using the empirical F_c equations developed by Troe.

LOW ENERGY STATE SELECTED ION MOLECULE REACTIONS

P-M Guyon, J B Ozenne

Laboratoire des collisions atomiques et moléculaires (Orsay France)

O Dutuit, C Metayer, T Weng, G Bellec

Laboratoire de Physicochimie des rayonnements (Orsay France)

D Gerlich, M Schweiser

University of Freiburg (Freiburg RFA)

J Hepburn,

University of Waterloo (Ontario Canada)

LURE Université Paris XI 91400 (Orsay France)

A new experiment CERISES (collision et réaction d'ions sélectionnées par les électrons de seuil), was developed in Orsay to study ion molecule reactions at near thermal energy i.e. 0.02 to 10 eV cm, where the reactant ions are prepared in selected vibronic states over a wide range of vibronic levels.

1: The experimental method

The reactant ions are prepared by photoionization with monochromatized light from Super ACO the newly constructed 800 MeV positron synchrotron radiation storage ring. Detection of threshold electrons allows state selectivity of the reactant ions. The latter are accelerated at the nominal laboratory energy and collide with the target gas at room temperature in a 5 cm long reaction cell. The unreacted parent ions as well as the reaction product ions drift in an octopole ion guide towards a quadrupole mass spectrometer. The ions are detected in delayed coincidence with the threshold electrons.

This experiment allows the determination of absolute cross sections for charge transfer, reactive collisions and collision induced dissociations. Information on the final state energy distributions is obtained from the analysis of the product ions time of flight peak shapes.

2: The $[\text{Ar O}_2]^+$ systema) $\text{Ar}^+ + \text{O}_2$

We measured the absolute cross section for the charge transfer reaction $\text{Ar}(^2\Pi_g)^+ + \text{O}_2$ for both $j = 1/2$ and $3/2$ at center of mass energies from 0.1 to 5 eV. This cross section was previously measured by Scherbarth and Gerlich (1) for a mixture of the two states. Both states behave differently and the ratio $\sigma_{1/2}/\sigma_{3/2}$ shows a maximum of

= 3 at 0.8 eV cm. These results quite different from those recently obtained by Ng et al. using a different technique (2). They can be interpreted qualitatively as the sum of two processes, the first one, very exothermic, leads to the formation of O_2^+ in its electronic ground state $X^2\Pi_g$. Its cross section decreases rapidly with collision energy. And a quasi resonant, slightly endothermic process (i.e. $\Delta E = 0.07$ and 0.3 eV for $Ar^+ j = 1/2$ and $j = 3/2$ respectively), leading to the formation of excited metastable $O_2^+ a^4\Pi$ ions with a cross section which rises above threshold.

b) $O_2^+ + Ar$

We also measured the cross section for the reverse reaction in which O_2^+ was prepared either in its excited $a^4\Pi_u$ state ($v = 0$ to 6) or in the electronic ground state $X^2\Pi_g$ with vibrational levels from $v = 17$ to $v = 24$ at 0.5 , 1 , and 5 eV lab. collision energies. Electron transfer from Ar to $O_2^+ a^4\Pi_u$ is quasisresonant and the cross section is large. We observed a strong variation with v which may indicate changes in the energy gaps between the closest vibronic diabatic Charge Transfer states. The somewhat smaller cross sections observed for O_2^+ vibrationally excited X states are not yet understood since the Franck-Condon factors are very unfavourable.

- 1) S.Scherbarth and D.Gerlich J. Chem. Phys. 99, 1610, 1989
- 2) G.D.Flech, S.Nourbaksh, and C.Y.Ng submitted to J. Chem.Phys.

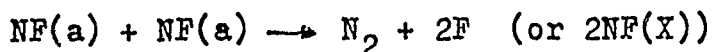
THE GENERATION OF $\text{NF}(a)$ RADICALS

Jan Habdas (Department of Chemistry, Silesian University,
40006 Katowice, Poland)

Donald W. Setser (Department of Chemistry, Kansas State
University, Manhattan, Kansas 66506, U.S.A.)

The chemical source for generation of the $\text{NF}(a^1\Delta)$ radicals was investigated. Among a few ways to chemically produce the $\text{NF}(a)$ metastable states we have found that the one of more useful is the $\text{F} + \text{HN}_3$ system with an excess of the F atoms. Also the $\text{F} + \text{HN}_3$ system has fewer kinetic complications than $\text{H} + \text{NF}_2$, since H atoms react with $\text{NF}(a)$ to give N atoms. A comparison of the $\text{NF}(a)$ concentration from the $\text{F} + \text{N}_3$ reaction with that obtained from $\text{H} + \text{NF}_2$ for a known NF_2 concentration shows that HN_3 can be converted to $\text{NF}(a)$ with high efficiency ($\geq 85\%$). Formation of the $\text{NF}(b)$ states was also observed from collisions between $\text{HF}(v \geq 2)$ and $\text{NF}(a)$, and the $\text{NF}(b)$ concentration was about 10^{-4} times smaller than that of $\text{NF}(a)$.

Concentration of the F atoms was determined using two titration reactions ($\text{H}_2 + \text{F} \rightarrow \text{HF} + \text{H}$, and $\text{Cl}_2 + \text{F} \rightarrow \text{ClF} + \text{Cl}$) and it was monitored at the end of the flow reactor by the $\text{HF}(3-0)$ emission intensity from the $\text{F} + \text{C}_2\text{H}_6$ reaction. Formation of $\text{NF}(a)$ in the concentration range of 10^{12} to 10^{13} molecule $\cdot\text{cm}^{-3}$ HN_3 shows self-destruction or quenching by HF or some products from the CF_4 discharge, as shown below:



From our experiments we deduced that the primary $\text{F} + \text{HN}_3$ reaction is largely an abstraction reaction. The secondary $\text{F} + \text{N}_3$ reaction has a rate constant equal to $(5 \pm 2) \cdot 10^{-11}$ $\text{cm}^3 \cdot \text{molecule}^{-1} \cdot \text{s}^{-1}$.

KINETICS OF HYDROGEN SULPHIDE DISSOCIATION
IN ELECTRIC DISCHARGES.

B. V. Potapkin, M. I. Strelkova, V. D. Rusanov, A. A. Fridman

The plasmochemical process of hydrogen sulphide dissociation is the object of steady great interest at the present time, because natural H_2S is the rich potential source of hydrogen and sulphur.

This work presents experimental and theoretical investigations of H_2S dissociation plasmochemical processes of pure H_2S and mixtures with CO_2 and O_2 in plasma of microwave and high-frequency moderate pressure discharges.

The mathematical modeling of H_2S dissociation plasmochemical processes in gas mixtures was carried out, in which dissociation mechanism, chemical composition of after discharge gas as function of the specific energy expense, pressure, initial composition of gas mixture, temperature of discharge area, quenching rate were determined. The processes were optimized for the given products (sulphur, hydrogen) and energetics.

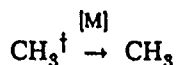
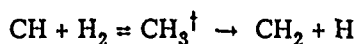
The experimental investigations were carried out in both microwave and high-frequency pressure ($P=10-100$ kPa) discharges over the range of the power input into the plasma of 1-30 kW. The experimental results have shown that highly efficient H_2S dissociation can be realized in fast-rotation spatially-nonuniform microwave discharge. It is shown, that the selective outflow of sulphur clusters in centrifugal force field determines a non-equilibrium character of H_2S dissociation process. Also it is the main reason for an experimentally observed considerable reduction of energy expenses, compared with quasi-equilibrium systems.

Generally, the results indicate the high potentialities of the plasma-chemical method of hydrogen and sulphur production from H_2S .

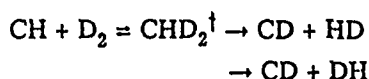
Temperature Dependence of the Reaction of CH (CD) + D₂C.T. Stanton[†] and Nancy L. Garland

Chemistry Division, Naval Research Laboratory, Washington, D.C. 20375-5000

The methylidyne radical CH is an important participant in diverse chemical processes.^{1,2} Lin and coworkers¹ have studied the reactions CH + H₂ and CD + D₂ from 150-670 K and proposed the following mechanism



The CH₃[‡] formation rate is not easily extracted from the disappearance rate of CH at pressures attainable in the laboratory. We can obtain the association rate with isotopic substitution which opens new product pathways for dissociation of the complex.



This paper presents the results of reaction rate measurements of CH + D₂ from 298-1260 K in 20 Torr of bath gas. We also present measured reaction rates of CD + D₂ from 560-1120 K at 100 Torr. For the reaction CH + D₂, we show that the complex stabilization and endothermic abstraction channels are negligible under our experimental conditions. Therefore, an estimate of the complex formation rate is obtained by assuming each decay channel of the complex contributes 1/3 to the total loss. The rate of loss of CH is then approximately 2/3 the formation rate of the complex.

All measurements have been made in a high temperature reactor³ based on a design by A. Fontijn. The CH (CD) radical is produced from laser photolysis of CHBr₂Cl (CDBr₃) at 248 nm and detected using laser-induced fluorescence on the B²Σ⁺-X²Π transition. Rotational temperatures are used for the data analysis.

Room temperature measurements of the rate for CH + D₂ between 10-100 Torr show the reaction is pressure independent over this range. A fit of our temperature data to the Arrhenius expression $k(T) = A \exp[-E_a/RT]$ yields a value for A of $(4.3 \pm 0.3) \times 10^{-11} \text{ cm}^3 \text{ s}^{-1}$ and for E_a of $-0.45 \pm 0.05 \text{ kcal mol}^{-1}$.

For the reaction CD + D₂, we derived a temperature dependent abstraction rate coefficient by subtracting the collisional stabilization contribution estimated from the work of Lin and coworkers¹ from our measured CD disappearance rate measurements. A fit of the data yields $k_{\text{abs}}(T) = (6 \pm 3) \times 10^{-11} \text{ cm}^3 \text{ s}^{-1} \exp[(-2.8 \pm 0.9 \text{ kcal mol}^{-1})/RT]$.

The activation energy obtained from this fit is close to the abstraction reaction enthalpy of $2.6 \text{ kcal mol}^{-1}$. Our results are consistent with recent calculations of the potential energy surface of the $\text{CH}_2 + \text{H}$ reaction indicating no barrier to complex formation.⁴ Assuming threshold energies for abstraction are approximated by reaction enthalpies in these systems, the dominant reaction channel above 2100 K is expected to be abstraction.

[†]ONT/NRL Postdoctoral Research Associate

- 1) Sanders, W.A. and Lin, M.C. in *Chemical Kinetics of Small Organic Radicals*, Alfassi, Z., ed.; CRC; Boca Raton, FL, 1986, 103.
- 2) Strobel, D.F. *Planet. Space Sci.* 1982, 30, 839.
- 3) Garland, N.L.; Stanton, C.T.; Fleming, J.W.; Baronavski, A.; Nelson, H.H. *J. Phys. Chem.*, in press.
- 4) Aoyagi, M.; Shepard, R.; Wagner, A.F.; Dunning, T.H.; Brown, F.B. *J. Phys. Chem.* 1990, 94, 3236.

Molecular Beam Measurement of the Interatomic Forces Between Chlorine Atoms and Rare Gases

V. Aquilanti, R. Candori, D. Cappelletti, V. Lorent, E. Luzzatti, and F. Pirani*
Dipartimento di Chimica
Università di Perugia
Italy

The characterization of the interactions between open shell atoms, in particular the halogen atoms with rare gases and simple molecules is motivated by the peculiar nature of the bonding involved, by the use of their molecular bands to obtain UV laser action and by the need of understanding the role of the spin-orbit interaction on the features of the long range part of potential energy surfaces [1]. Furthermore it is of interest to understand the role which these interactions play in inelastic effects when electronically excited species are involved. The production of an intense and stable halogen atom beam and the control of the involved magnetic sublevels are described. An inhomogeneous magnetic field is used to differentially defocus from the beam direction those atoms which show a non zero effective magnetic moment. Analysis of polarization states as a function of pressure and temperature of the discharge is accomplished by Stern-Gerlach magnetic selection of substates. For atoms such as the halogens, showing besides orbital and spin angular momenta also nuclear spin, an angular coupling scheme analysis is developed and used in connection with the experimental results. In this paper we report recent measurements of the absolute integral cross sections, as a function of the beam velocity, for scattering of

*Permanent address: Dépt. de Physique, Univ. Cathol. Louvain, B1348 Louvain-La-Neuve, Belgium.

chlorine atoms by rare gases. Some previous papers can be consulted for further details [1, 2, 3, 4, 5], only some features relevant for the present experiments are described. The chlorine atom beam is produced in a microwave discharge source. Integral cross section data, at different distributions of magnetic sublevels of chlorine atoms, are measured in the beam velocity range 0.5-2.5 Km/s for the chlorine atom-rare gas systems. In the case of Cl-Kr and Cl-Xe, collision of an atomic chlorine beam almost completely in the $^2P_{1/2}$ state was performed. For the analysis of these scattering data we use the adiabatic approach [6, 7, 8] suggested by the large spin-orbit interaction in the chlorine atom. For all the Cl-rare gas systems it is possible to characterize the ground and the lowest excited electronic states and also to obtain the nonadiabatic coupling matrix elements. The interactions are represented as a spherical part and an anisotropic component. Features of the spherical part of the potentials confirm what is presently known on general trends in van der Waals forces [8, 9].

References

- [1] V.Aquilanti, E.Luzzatti, F.Pirani, and G.G.Volpi, *J.Chem.Phys.*, **89**(1988)6165.
- [2] V.Aquilanti, E.Luzzatti, F.Pirani, and G.G.Volpi, *Chem.Phys.Lett.*, **90**(1982)382.
- [3] V.Aquilanti, R.Candori, and F.Pirani *J.Chem.Phys.*, **89**(1988)6157.
- [4] V.Aquilanti, R.Candori, L.Mariani, F.Pirani and G.Liuti, *J.Phys.Chem.*, **93**(1989)130.
- [5] V.Aquilanti, R.Candori, D.Cappelletti, E.Luzzatti, and F.Pirani; *Chem.Phys.*, in press.
- [6] V.Aquilanti and G.Grossi, *J.Chem.Phys.*, **73**(1980)1165.
- [7] V.Aquilanti, P.Casavecchia, G.Grossi, and A.Laganà, *J.Chem.Phys.*, **73**(1980)1173.
- [8] V.Aquilanti, G.Liuti, F.Pirani, and F.Vecchiocattivi, *J.Chem.Soc.Farad.Trans.*, **85**(1989)2.
- [9] G.Liuti and F.Pirani, *Chem.Phys.Lett.*, **122**(1985)245.

Alignment Effects in Beam-Gas Dynamics ExperimentsJ.D. Kettleborough and K.G. McKendrick,

Department of Chemistry, Edinburgh University, U.K.

Model calculations have been performed to investigate the potential magnitude of experimentally observable effects of spatial alignment of target molecules in effusive atomic beam-thermal target gas ("beam-gas") experiments. The target gas is assumed to be a diatomic molecule prepared in a specific rovibrationally excited state with an anisotropic spatial distribution of molecular axes by pumping with a polarised i.r. laser. The calculations correctly include the averaging effects of the Maxwellian velocity distribution of the atomic beam and of the isotropic thermal velocity distribution of the target gas.

The magnitudes of observable signals are predicted for various model forms of the dependence of the probability of reaction on the direction of approach of the attacking atom with respect to the diatom axis. These predictions are compared with the available experimental results for the reactions $M + HF \rightarrow MF + H$ ($M=Ca, Sr$). Conclusions are drawn about the possibility of determining information on preferred geometries for reaction in such experiments.

LASER INDUCED FLUORESCENCE STUDY OF Se_2

E. Martínez*, P. Puyuelo⁺ and B. Cabañas*.

(*) Facultad de Químicas. U. Castilla-La Mancha. C. Real (SPAIN)

(+) Dpto. Química Física. U. País Vasco. Apdo 644. Bilbao (SPAIN).

Time resolved fluorescence decay studies of selenium dimers, and enriched $^{80}\text{Se}_2$ have been carried out. Excitation spectra were obtained by using a Lambda Physik excimer laser, (220 mJ at 308 nm). Temperatures around 775 \pm K, were maintained at the quartz cell, while the selenium finger was maintained near 550 \pm K, giving vapor pressures in the 50 - 100 m Torr interval. Rovibrational lines of several transitions of the A-X and B-X systems, have been assigned, in the strongly overlapped region between 380 - 390 nm. Fluorescence lifetimes have been measured, for vibrational levels $V'= 3-6$ of the B state and $V'= 12-15$ of the A state, giving collision free values of ~ 50 ns and ~ 600 ns respectively.

"KINETICS OF THE PREDISSOCIATED LEVELS $V' > 12$ OF THE $B^1\Pi(O_u^+)$ STATE OF Cl_2 USING LASER INDUCED FLUORESCENCE"

E. Martínez*, F. Basterrechea⁺, F. Castaño⁺ and J. Albaladejo*

(*) Facultad de Químicas. Universidad de Castilla-La Mancha.
Paseo de la Universidad, 4. 13071 CIUDAD REAL. SPAIN.

(+) Departamento de Química Física. Universidad del País Vasco.
Apartado 644. BILBAO. SPAIN.

Narrow band tunable dye lasers pumped by a Nd-YAG or excimer laser, have been used to excite fluorescence from specific rovibrational levels of the Cl_2 $B^1\Pi(O_u^+)$ state. For predissociated levels, collision free lifetimes, fit quite well with the expression: $\tau_{v'v''}^{-1} = \tau_R^{-1} + K_{v'} \cdot J(J+1)$, and $K_{v'}$ values have been measured, for several levels $12 < V' < 25$. Results will be discussed in terms of which state (A or $^1\Pi(A_u)$) is responsible in causing predissociation. The nature of the predissociating state has been established and a potential energy curve with an equilibrium internuclear distance R_e around 2.48 Å is proposed.

OH VIBRATIONAL ENERGY DISTRIBUTION
IN REACTIONS OF $O(^1D)$ ATOMS.

S.G.Cheskis, A.A.Iogansen, P.V.Kulakov, I.Yu.Razuvaev,
O.M.Sarkisov and A.A.Titov.
Institute of Chemical Physics, USSR Academy of Sciences,
Moscow, USSR.

1. Direct time-resolved measurements of $OH(v)$ vibrational relaxation kinetics are demonstrated to be a powerful means of determining nascent vibrational energy distribution (VED) of OH radicals in reactions of $O(^1D)$ atoms with H-containing molecules.

For a number of interesting systems this "kinetic approach" enables to obtain almost total OH VED by monitoring only three states of OH in relative units (one rovibronic state for each vibrational level $v=0,1,2$). The experimental procedure¹ is much more easier than those used in analogous studies.

2. OH VED in $O(^1D) + H_2$, CH_4 , NH_3 reactions were obtained (see Table 1). The surprisal plots for all three are reasonably linear. For $O(^1D) + H_2$ reaction the measured OH VED is in good agreement with the results of trajectory calculations².

Using kinetic approach for O_3/CH_4 system, we have determined the role of chain reactions, in which the vibrationally excited OH radicals do participate³.

Comparison with VED data reported in literature shows that the results, obtained by various fixed-time-delay methods, are probably somewhat distorted either by fast relaxation processes⁴ (in case of NH_3) or by subsequent chain reactions with $OH(v)$ participation^{5,6}.

3. Alongside with distributions, the rate constants of vibrational relaxation of OH($v=1,2,3$) and OD($v=1,2,3$) in collisions with ammonia and methane were measured (see Table 2).

Table 1. OH(v) disposal in O(1D)+RH reactions.

v	Population (%)			
	NH ₃	CH ₄	H ₂	D ₂
0	20	18	28	16
1	32	29	30	29
2	34	37	24	26
3	14	15	14	11
4	0	1	4	11
5	-	-	-	7

Table 2. OH (OD) quenching rate constants (cm³/s).

Radical	Quencher	
	NH ₃	CH ₄
OH(1)	$2.1 \cdot 10^{-11}$	$5.2 \cdot 10^{-13}$
OD(1)	$1.6 \cdot 10^{-11}$	$1.6 \cdot 10^{-13}$
OH(2)	$1.0 \cdot 10^{-10}$	$1.5 \cdot 10^{-12}$
OD(2)	$0.5 \cdot 10^{-10}$	$3.3 \cdot 10^{-13}$
OH(3)	$3.0 \cdot 10^{-10}$	$7.0 \cdot 10^{-12}$
OD(3)	$1.5 \cdot 10^{-10}$	$5.1 \cdot 10^{-13}$

REFERENCES

1. S.G. Cheskis, A.A. Iogansen, P.V. Kulakov, O.M. Sarkisov, A.A. Titov, Chem. Phys. Lett., 143, 348 (1988).
2. M.S. Fitscharles, G.C. Schatz, J. Phys. Chem., 90, 36 (1986).
3. S.G. Cheskis, A.A. Iogansen, P.V. Kulakov, O.M. Sarkisov, A.A. Titov, Khim. Fizika (in Russian) (1988, in press).
4. P.M. Aker, J.A. O'Brien, J.M. Parsons, J.J. Sloan, Can. J. Chem., 64, 2315 (1986).
5. P.M. Aker, J.J. Sloan, J. Chem. Phys., 85, 1412 (1986).
6. P.M. Aker, J.J. Sloan, J. Chem. Phys., 84, 745 (1986).

Variational Transition State Theory: a Simple Model for
Dissociation and Recombination Reactions of Small Species

Meredith Jordan, Sean C Smith and Robert G Gilbert
School of Chemistry, Sydney University, NSW 2006, Australia

A simple interaction potential will be presented for reactions such as $\text{CH}_3\text{OH} \rightarrow \text{CH}_3 + \text{OH}$ (and their reverse recombination reactions). This is based on the Gorin notion of two independent moieties (CH_3 and OH in this case) plus an interaction made up of a Morse potential and sinusoidally-hindered rotors whose parameters can be found from "benchmark" quantum calculations for other systems such as $\text{H} + \text{CH}_3$. Together with new extensions to the Beyer-Swinehart algorithm appropriate for these potentials, variational transition state theory can then be applied to calculate $k(E, J)$ with trivial computational effort. Together with the biased random walk model for finding the collisional energy transfer rate, this model leads to a new, easily-applied method of calculating rate coefficients for such reactions in the high-pressure and falloff regimes which leads to results that compare very favourably with experiment, and which therefore should be able to be used reliably for predictive purposes.

EMISSION OF THE C_2N_2 MOLECULE AND A NEW VALUE FOR THE HEAT OF FORMATION OF CN

SAMUEL A. BARTS, KAREN V. PINNEX AND JOSHUA B. HALPERN

Howard University
Dept. of Chemistry
Washington, DC 20059, USA

ABSTRACT

Simple nitriles play important roles in the photochemistry of nitrogen-methane planetary atmospheres. Cyanogen (C_2N_2) is also an extremely simple tetra-atomic system in which to study predissociation. Calculated potential surfaces are available for cyanogen so it can be used to evaluate theories of dissociation.

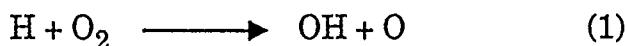
We have discovered that this molecule has a strong and distinctive emission spectrum. The lowest vibrational bands of the $A^1\Sigma^-$ state are bound and fluoresce. The absorption, emission and photodissociation yield spectra of C_2N_2 have been measured between 224 and 210 nm, between the 4_1^0 and $1_0^1 4_0^1$ bands of the $A^1\Sigma^- \leftarrow X^1\Sigma^+$ system. Radiative lifetimes range from 1.4 μs in the 4_0^1 band to 0.6 μs for the $1_0^1 4_0^1$ band. Self quenching rates range from gas kinetic ($4.3 \times 10^{-10} \text{ cm}^3/\text{molecule-s}$) for the 4_0^1 band to $13.0 \times 10^{-10} \text{ cm}^3/\text{molecule-s}$ for the $1_0^1 4_0^1$ band. Foreign gas quenching rates have been measured against He, Ar, N_2 and CH_4 .

Strong fluorescence is observed from all vibrational bands up to and including $1_0^1 4_0^1$. This establishes a lower limit for the bond energy of $47,756 \text{ cm}^{-1}$, which implies a lower limit of 439.5 kJ/mole for the heat of formation of the CN radical. This should be compared with the accepted value of 422 kJ/mole.

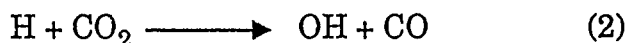
ABSOLUTE REACTIVE CROSS SECTIONS
AND PRODUCT STATE DISTRIBUTIONS FOR
REACTIONS OF HOT H-ATOMS

A. Jacobs, F. M. Schuler, H. R. Volpp, M. Wahl and J. Wolfrum
Physikalisch-Chemisches Institut der Universität Heidelberg
Im Neuenheimer Feld 253, D-6900-Heidelberg, F.R. Germany

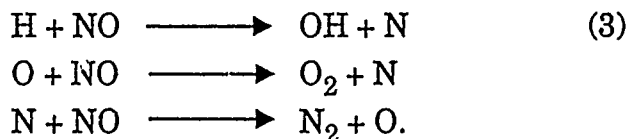
The reactions



and



are of great importance in the combustion of hydrocarbons, in chemical processes in the upper atmosphere, and in the production of photochemical smog, as well as the formation and decomposition of thermal NO, which is usually well described by the extended Zeldovich mechanism



For a more detailed understanding of the exact temperature behavior of chemical reaction rates, information on the role of internal degrees of freedom of the reacting molecules as well as on the accurate dependence of the reactive cross section on the relative translational energy of the reactants is required.

Photolysis of HCl and HBr with an ArF excimer laser at 193 nm was used to generate hot H atoms with well-defined translational energies, which react with CO₂, O₂ and NO to form OH. The product OH radicals were detected by laser-induced fluorescence (LIF). From the LIF spectra, the nascent OH vibrational and rotational fine-structure distributions were determined. Also, absolute reactive cross sections for the reactions (1 to 3) were measured and will be presented. The results are compared to previous experimental and theoretical work at different collision energies.

KINETIC STUDIES OF ROVIBRATIONAL LEVELS OF CO A¹Π BY VUV LASER INDUCED FLUORESCENCE

M. Castillejo, A. Costela, J.M. Figuera and J.M. Muñoz

Instituto Rocasolano CSIC, Serrano 119, 28006 Madrid, Spain.

In recent years coherent tunable narrow bandwidth light sources have become available in the vacuum ultraviolet (VUV) region below 200 nm. Thus a lot of spectroscopic and kinetic studies can be performed in a group of small molecules of primary interest in the chemistry of atmospheric processes and astrophysical phenomena.

VUV coherent light generated by third harmonic conversion of dye laser radiation in Xenon was used to study the kinetics of selected rovibrational levels of CO A¹Π using the Laser Induced Fluorescence technique.

Spectra of the CO A¹Π (v'=4) ---- X¹Σ⁺ (v''=0) band was obtained, its rotational transitions assigned, and quenching measurements by several atomic and molecular species performed. In this way it was possible to extract information on the mechanisms of the perturbation of the selected rovibrational levels wich will allow to establish comparisons with theoretical models.

Similar measurements in other vibrational levels of the A¹Π state are under way.

Parametric Representation of Unimolecular Reaction Falloff Behavior

W. Gardiner and I. Oref

*Israel Institute of Technology — Technion, Haifa, Israel
and University of Texas, Austin, Texas, U.S.A.*

The transition between the high and low pressure limits of unimolecular reaction rate constants is regarded today as a problem that has been solved in principle: whatever model is adopted for the limiting rate constants, numerical evaluation of the RRKM weak collision master equation provides the rate constant at any temperature and density of interest. In large scale modeling efforts, however, such master equation calculations can not be used. Unimolecular reaction rate constants have to be recomputed whenever the temperature or the pressure changes, and master equation recomputations are too demanding of computer resources for such applications. Accordingly, the common practice in modeling has been to adjust unimolecular rate constant expressions on an ad hoc basis, ignoring temperature, pressure and weak collision corrections to the falloff.

An approach to solving this problem systematically was developed by Troe,¹ who derived a correction expression F to the Lindemann formula that accounted for the greater spreading of the falloff curve found experimentally

$$k = k_{\infty} \frac{x}{1+x} F$$

where $x = P/P_{3/2}$ is the ratio of the pressure to the pressure at which the high and low pressure rate constant expressions are equal and the order of reaction is 3/2. An alternative to Troe's approach is the Minkowski metric formula²

$$k = [(k_0 P)^a + k_{\infty}^a]^{1/a}$$

Another is the equation³

$$k = \frac{-(k_{\infty} + k_0 P) + [(k_{\infty} + k_0 P)^2 + 4(J-1)k_{\infty}k_0 P]^{1/2}}{2(J-1)}$$

It is appropriate to evaluate the parameters a and J of these equations at $P = P_{3/2}$. Using

$$a_{3/2} = \log(k_{3/2}/k_{\infty})/\log 2 \quad \text{and} \quad J_{3/2} = (k_{\infty}/k_{3/2} - 1)^2$$

in these equations provides parametric representations of the entire falloff behavior, exact at both limits and at $P = P_{3/2}$, once k_0 , k_∞ and $k_{3/2}$ are known.

In order to test the accuracy of these representations we carried out strong-collision and weak-collision master equation RRKM calculations for representative unimolecular reactions over wide ranges of temperature and pressure. The reactions considered were cyclobutane decomposition to ethylene, cyclobutene isomerization to 1,4-butadiene, quadricyclane isomerization to norbornadiene, HCl and DCl loss from $\text{CH}_2\text{DCH}_2\text{Cl}$, cyclopropene isomerization to allene and methylacetylene, and HBr loss from $\text{C}_2\text{H}_5\text{Br}$. The temperature range in each case was extended up to where the ratio of critical to average energy was about 0.5. The pressure ranged several orders of magnitude on either side of $P_{3/2}$ at each temperature. It was found that the performance of the three parametric representations is more or less the same for these reactions, the maximum deviations between computed and formula results ranging from 2% in the best cases to 40% in the worst.

For use in modeling it is necessary to be able to represent the temperature variation of a or J analytically. The Arrhenius-like behavior of k_0 and k_∞ suggests that $a_{3/2}$ and $J_{3/2}$ should be representable as $A + B/T + C \ln T$, which proved to be appropriate for the strong collision case. For weak colliders the quadratic form $1/a_{3/2} = AT^2 + BT + C$ proved to be suitable. The use of fitting formulas rather than directly computed $a_{3/2}$ or $J_{3/2}$ values did not degrade the quality of the representations significantly.

Weak collision (WC) effects on the falloff curve were evaluated as corrections to the strong collision (SC) values of $a_{3/2}$ and $J_{3/2}$ as functions of temperature and average energy α transferred per down collision

$$\frac{a_{3/2}^{WC}}{a_{3/2}^{SC}} \quad \text{or} \quad \frac{J_{3/2}^{WC}}{J_{3/2}^{SC}} = A(\alpha) \left(\frac{1000}{T} \right)^2 + B(\alpha)$$

where A and B are polynomial functions of α .

¹ Troe, J.: J. Phys. Chem. 1979, 83, 114; Troe, J.: Ber. Bunsenges. Phys. Chem. 1983, 87, 161; Gilbert, R.G., Luther, K., & Troe, J.: Ber. Bunsenges. Phys. Chem. 1983, 87, 169.

² Gardiner, W.: Proceedings of the 12th IMACS World Congress on Scientific Computation, Paris, 1988, p. 582.

³ Oref, I.: J. Phys. Chem. 1989, 93, 3645; Pawlowska, Z., & Oref, I.: J. Phys. Chem. 1990, 94, 567.

CHEMILUMINESCENCE AND ENERGY TRANSFER IN COLLISIONS OF Mn ATOMS
WITH D₂ AND HYDROCARBONS

Martin R Levy

Department of Chemical and Life Sciences

Newcastle upon Tyne Polytechnic

Newcastle upon Tyne NE1 8ST, UK.

Laser ablation of a solid metal target has been used to generate a pulsed Mn beam of wide velocity range and consisting of both ground-state (6S) and metastable-state (6D_J , 2P_J , 4D_J , ...) atoms. $MnH^*(A^7\Pi \rightarrow X^7\Sigma^+)$ chemiluminescence and $Mn^*(^2P_J \rightarrow ^6S)$ collision-induced emission have been observed on passing the beam through low pressures of the gases CH₄, C₂H₄, C₂H₆, n-C₃H₈, 1-C₄H₈, C(CH₃)₄; but, with D₂, only the energy transfer channel has been detected. In contrast to the reactions of Mn with oxygen-containing molecules [1,2], the chemiluminescence channel is much *weaker* than that for collision-induced emission.

Translational excitation functions $\sigma(E_T)$ for the two processes have been determined by comparing the time profiles of the luminescence with that of the long-lived $Mn^*(^2P_J \rightarrow ^6S)$ emission from the beam. Converting these results to yield functions $Y(E_T)$ ($= E_T \cdot \sigma(E_T)$) then allows the contributions of different atomic states and dynamical processes to the overall signal to be determined. For chemiluminescence, analysis is complicated by the lack of a reliable value for the MnH dissociation energy. However, starting from the known very approximate upper limit [3], $D_0 < 134 \text{ kJ mol}^{-1}$, it is possible not only to establish which atomic states are involved, but to obtain a more precise lower limit for D_0 .

For CH₄, the chemiluminescence results are consistent with reaction of the Mn^* 6D_J , 4D_J and 6D_J states; C₂H₄ and C₂H₆ appear to involve only 4D_J and 6D_J atoms; whereas, for the higher hydrocarbons, the 6D_J and 6S states seem to be responsible. The change in reacting state can be ascribed to the

changing importance of competing channels as molecular size increases. $D_0(\text{MnH})$ is determined to be $134 \pm 7 \text{ kJ mol}^{-1}$; but, whatever its value, a number of the reactions seem to involve excess barriers over the endothermicity. The contributions from quartet states show a clear violation of spin conservation, implying that the reaction may proceed via insertion, producing an intermediate which lives long enough for the spin-flip to occur. Further evidence for insertion is given by the increasing tendency of the yield function to show 'concave-up' character as the molecular size increases - implying the participation of several vibrational and rotational modes in the transition state [4].

All species show low thresholds for collision-induced $\text{Mn}^*(^2\text{P}_j)$ production. Normally such behaviour is associated with ionic-covalent curve crossing [5]; and, certainly, the observation of $^2\text{P}_j$ excitation from $^4\text{D}_j$ atoms, for C_2H_4 , and from both $^4\text{D}_j$ and ^4S atoms, for C_4H_8 , is consistent with the relatively high electron affinities of the alkenes. The low thresholds which are observed for $^4\text{D}_j \rightarrow ^2\text{P}_j$ excitation on collision with the saturated hydrocarbons are therefore quite surprising in this context. Both D_2 and CH_4 show the slightly endothermic excitation $^4\text{D}_j \rightarrow ^2\text{P}_j$, in the former case exclusively. For D_2 , involvement of an ionic surface is ruled out, as the D_2^- ion is dissociative: a covalent chemical interaction is thus implied, in which the intermediate lives long enough for the spin change to occur.

References

1. M R Levy, *J Phys Chem* 93, 5195 (1989).
2. M R Levy, *J Phys Chem*, submitted for publication.
3. A Kant & K A Moon, *High Temp Sci* 14, 23 (1981).
4. A González Ureña, *Mol Phys* 52, 1145 (1984).
5. V Kempter, *Adv Chem Phys* 30, 417 (1975).

QUENCHING OF DIFFERENT METHYLENE 1B_1 ROVIBRATIONAL
OVERTONES BY SEVERAL GASES AND VAPOURS.

M. Castillejo, J.M. Figuera, I. García-Moreno, J.C.
Rodríguez and H.A. Zeaiter.

Instituto Química-Física "Rocasolano", C.S.I.C.,
Serrano 119, 28006 Madrid, Spain.

Rate constants for quenching of methylene $^1B_{1n}(0,13,0)$, $^1B_{1\pi}(0,14,0)$, $^1B_{1\pi}(0,16,0)$ and overtone $(0,18,0)$ in a non previously assigned band have been measured with several gases and vapours. Methylene 1B_1 was prepared by a two-step process. In the first, ketene was photodissociated by a XeCl home made excimer laser yielding $CH_2(^1A_1)(0,0,0)$. Subsequently $CH_2(^1B_1)$ in the desired rovibrational state was populated by dye laser absorption from the previously prepared 1A_1 state. Time resolved fluorescence from the prepared 1B_1 was followed and the quenching rate constants with different gases and vapours measured.

With the rare gases, the quenching rate constants found show a significative dependence on the K_a values of the studied state (see table). The differences between constants can be qualitatively explained considering Renner-Teller and spin-orbital couplings, as well as Fermi resonances of the energy levels.

QUENCHING RATE CONSTANTS k_Q FOR CH_2 (1^3B_1) IN
THE SELECTED OVERTONES

$k_Q \times 10^{10}$ $\text{cm}^3 \times \text{molec}^{-1} \times \text{s}^{-1}$				
GAS	(0,13,0) $K_a=1$	(0,14,0) $K_a=0$	(0,16,0) $K_a=0$	(0,18,0) $K_a=?$
He	0.95	0.53	0.31	1.0
Ne	0.91	0.65*	0.56	0.8
Ar	1.9	1.5*	1.1	2.5
Kr	2.0	2.0*	1.5	2.7
Xe	3.2	2.3*	3.4	4.0

(*) Rate constants taken from M.N.R. Ashfold
et al., Chem. Phys. 55 (1981) 245

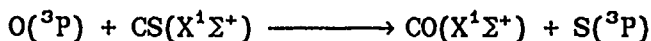
Product Rotational Distributions and Alignment for the Reaction

G. Hancock and A.J. Orr-Ewing

Physical Chemistry Laboratory, Oxford University,

South Parks Road, Oxford OX1 3QZ, UK.

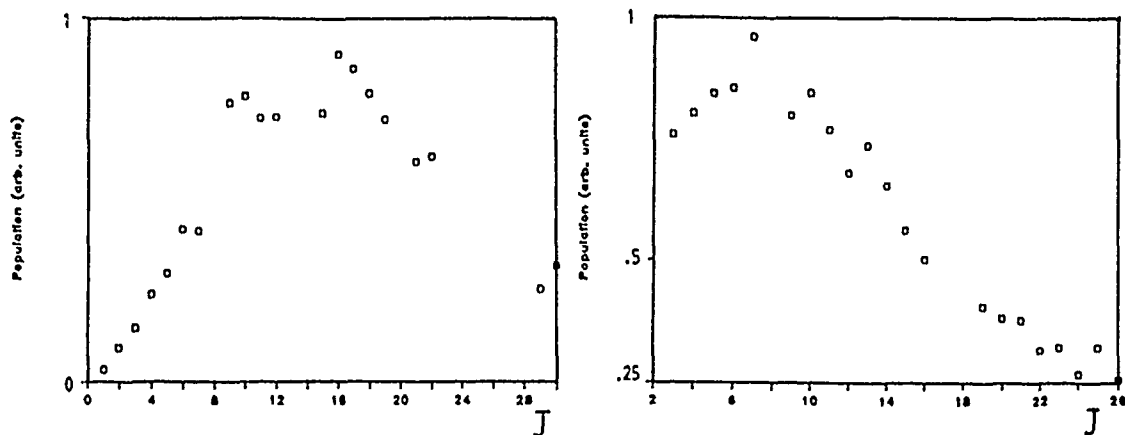
The reaction



has been studied by Laser Induced Fluorescence using the $\text{A}^1\Pi - \text{X}^1\Sigma^+$ system of CO. The nascent CO is vibrationally excited, with a population distribution that peaks at $v=14$. This enabled UV excitation of the $\text{CO}(\text{X}^1\Sigma^+)$ to the $\text{A}^1\Pi$ state, followed by VUV fluorescence. Two experimental arrangements were employed:

- (1) The reagents were generated by microwave discharge of O_2/Ar and CS_2/Ar gas mixtures, and injected into a high vacuum cell through inlet pinholes, giving intersecting sprays of radicals. The reaction was monitored at the intersection region by a frequency doubled tunable excimer pumped dye laser at wavelengths in the region of 220 nm.
- (2) NO_2 was injected into the reaction cell through a pinhole, and crossed with a CS effusive spray. Photolysis of the NO_2 by horizontally polarised 355nm radiation from a Nd^{3+} YAG laser was used to generate $\text{O}(^3\text{P})$ atoms with a known recoil velocity distribution. The product $\text{CO}(\text{X}^1\Sigma^+)$ was probed by the excimer pumped dye laser, which propagated coaxially to the photolysis beam.

Rotationally resolved LIF spectra of several bands of the CO ($\text{A}^1\Pi - \text{X}^1\Sigma^+$) system were recorded, and the line intensities analysed to obtain the populations of the rotational states. Nascent rotational distributions for the $\text{CO}(\text{X}^1\Sigma^+)$ $v=12$ and $v=14$ vibrational levels determined by the first experimental method are plotted in the diagram.



Nascent rotational distributions for $\text{CO}(\text{X}^1\Sigma^+)$ $v=12$ and $v=14$

The fraction of available energy channelled into rotation, $\langle f_r \rangle$, is low, being of the order of 5% for $\text{CO}(v=12)$. Measurements of these rotational distributions with oxygen atoms from NO_2 photolysis showed that much of the additional translational energy of the $\text{O}(^3\text{P})$ was converted into rotation of the $\text{CO}(\text{X}^1\Sigma^+)$.

Investigations of the nascent product rotational angular momentum (J) disposal suggested that the $\text{CO}(\text{X}^1\Sigma^+)$ was formed with non-zero alignment moments, d_q^k . A polarisation switching KD^*P crystal was used to compare spectra taken with both horizontally and vertically polarised probe laser light under identical conditions. The polarised laser photolysis of NO_2 generated an anisotropic distribution of $\text{O}(^3\text{P})$ recoil velocities, characterised by an anisotropy parameter $\beta=0.74$. Laboratory frame alignment parameters (referenced to the electric vector of the photolysis laser, \underline{e}) were transformed to centre-of-mass alignments (referenced to the relative velocity vector for the reactive collision, \underline{k}). Results for both thermal and translationally hot $\text{O}(^3\text{P})$ atoms will be discussed in terms of features on the potential energy surface for the $\text{O}(^3\text{P}) + \text{CS}(\text{X}^1\Sigma^+)$ reaction.

DETERMINATION OF STATE-TO-STATE ROTATIONAL ENERGY

TRANSFER COEFFICIENTS FOR OH ($A^2\Sigma^+$, $v'=0$)

T. Griffin, A. Jörg, U. Meier, K. Kohse-Höinghaus
DLR-Institut für Physikalische Chemie der Verbrennung,
D-7000 Stuttgart 80, West Germany

The quantitative measurement of concentrations and temperatures using laser-induced fluorescence (LIF) requires information about various collisional energy transfer processes. For the hydroxyl radical, which is important in combustion and atmospheric chemistry, little information concerning rotational energy transfer (RET) processes is available. Our goal is the construction of a numerical model of the energy transfer of the hydroxyl radical, which would help to determine the applicability of OH LIF techniques in various combustion environments. Such a model would be based upon a nearly complete set of state-specific energy transfer coefficients as a function of collision partner and temperature. Since it is not feasible to measure all of this information, one must develop strategies for data extrapolation. Thus, our experimental program has been focussed not only on the measurement of RET coefficients with combustion-relevant gases, but also on the understanding of the RET process itself.

We have employed a direct experimental method to determine state-to-state RET coefficients; namely, we measure, with a transient digitizer or a gated boxcar integrator, time-dependent fluorescence signals from a laser-excited state and a collisionally populated state'. By extrapolation to short times after the laser pulse, or employing a short, prompt boxcar gate, the method allows the measurement of individual RET coefficients, independent of any assumptions concerning the values of other coefficients, or the adherence of the RET coefficients to any particular fitting law.

We have measured downward RET coefficients from the $F_2(4)$ and $F_2(5)$ states of OH ($A^2\Sigma^+$) at 300 K for He and Ar as well as for the combustion-relevant gases N_2 , CO_2 and H_2O . The RET coefficients obtained range in value from $1.1 \times 10^{-12} \text{ cm}^3\text{s}^{-1}$ (for

He, $F_2(4) \rightarrow F_1(5)$) to $4.0 \times 10^{10} \text{ cm}^3\text{s}^{-1}$ (for H_2O , $F_2(4) \rightarrow F_2(3)$) and follow different trends for the various collision partners. Interestingly, the values found for Ar and CO_2 are quite similar in magnitude and display the same behavior: a preference for transitions with $\Delta J=1$ and $\Delta K=0$ and no propensity to conserve spin parity. For RET collisions with N_2 there is also no propensity for spin conservation. In contrast, coefficients obtained for water exhibit a strong propensity for spin conservation and transitions with $\Delta J=\Delta K=1$ are most favored. For He there is also a preference for spin conservation; however, the transitions with $\Delta K = 2$ are strongest.

Upward RET from the $F_1(0)$ state has been measured for Ar and He. Such measurements are relevant because of the importance of the lowest-energy initial state for some dynamically-based scaling laws². For He, the propensity for spin conservation and $\Delta K=2$ transitions is also exhibited in the $F_1(0)$ upward RET coefficients. However, the greater disparity in the magnitude of these coefficients leads to a larger influence of multiple collisions in the data analysis than found in the case of downward RET from $F_2(4)$ or $F_2(5)$. All of the measured coefficients for Ar and He can be compared to recent quantum-scattering calculations^{3,4}, yielding excellent agreement both in observed trends and quantitative values.

Various scaling and fitting laws will be tested for their ability to represent our measured RET coefficients. Interpretation of all the above, disparate trends in terms of simple exponential fitting laws is highly improbable. In the case of He and Ar, the results of the quantum-scattering calculations mentioned above may also be employed as a data base for the testing of the selected scaling laws.

1. A. Jörg, U. Meier, and K. Kohse-Höinghaus, submitted to J. Chem. Phys.
2. T. A. Brunner and D. Pritchard, Adv. Chem. Phys. 50, 589 (1982).
3. A. Degli Esposti and H.-J. Werner, submitted to J. Chem. Phys.
4. A. Jörg, A. Degli Esposti and H.-J. Werner, to be published.

Inelastic Collisions of State Selected $\text{NH}(\text{A}^3\Pi)$

Steven Aragon and Roger Anderson
Department of Chemistry
University of California, Santa Cruz, CA 95064

State selected $\text{NH}(\text{A}^3\Pi)$ molecules are produced in a two laser experiment. Two 193 nm photons photodissociate ammonia to form electronically excited NH with much rotational energy. After a several microsecond delay (to allow decay to the ground state and to achieve some rotational relaxation) a frequency doubled excimer pumped dye laser tuned to specific $\text{X}(\Sigma^-)-\text{A}(\text{A}^3\Pi)$ transitions produce the selected states. The inelastic processes are observed by measuring the time evolution of emission from the optically pumped and collisionally excited $\text{NH}(\text{A})$ states. Cross sections are determined for rotational energy level, spin level, and lambda doublet level changing collisions. Matching the experimental results with the results obtained from integration of coupled rate equations provide a self-consistent fit.

The Internal State Distribution of NCO formed in the Radical-Radical
Reaction: $\text{CN} + \text{O}_2 \rightarrow \text{CO} (\text{X}^2\Pi, v', j') + \text{O}$

L.F. Phillips,* I.W.M. Smith, R.P. Tuckett and C. Whitham

School of Chemistry
University of Birmingham
Edgbaston
Birmingham B15 2TT, U.K.

Radical-radical reactions generally occur across strongly attractive potential energy surfaces and the existence of a deep minimum on the surface may exert a dominating influence on the dynamics. This can be investigated by observing how far the product internal state distribution differs from statistical expectation, but the dynamics of radical-radical reactions are not easy to study experimentally.

Taking account of a number of favourable factors in the system, we are studying the internal state distribution of NCO formed in the reaction:



$$\Delta H^\circ_{298} \approx -27 \text{ kJ mol}^{-1}$$

CN radicals are produced in the presence of excess O_2 by pulsed photolysis of NCNO using the frequency-doubled output ($\lambda = 532 \text{ nm}$) of a Nd:YAG laser. The NCO formed in the reaction can then be observed by laser excitation spectroscopy using an excimer-pumped scanning dye laser. The time delay between the photolysis and probe pulses can be varied to estimate how the nascent internal state distribution is relaxed in subsequent collisions.

Preliminary results indicate substantial excitation of the ν_2 bending mode vibrational progression (up to $\nu_2 \approx 6$), and we shall present results on the initial distributions of NCO over these vibrational states. These data will be compared with what would be expected for simple models of reaction.

COLLISION DYNAMICS OF AKALI ATOMS WITH ORGANIC MOLECULES. ABSOLUTE DETERMINATION OF THE REACTION CROSS-SECTION.

by

L. Bañares, G. Muga and A. González Ureña

Departamento de Química Física
Facultad de Química
Universidad Complutense de Madrid
28040 MADRID
SPAIN

Differential reaction cross-sections for the $\text{Cs} + \text{ICH}_3 \rightarrow \text{CsI} + \text{CH}_3$ system have been measured as a function of the collision energy using a simple molecular beam apparatus. The analysis of the centre-of-mass angular and recoil velocity distributions of the product indicated (a) a backward peak corresponding to a direct, rebound mechanism, (b) and increasing forward scattering as the collision energy increases, (c) that the average translational energy of the products, \overline{E}_T' , increases approximately linearly with increasing collision energy, \overline{E}_T , as follows

$$\overline{E}_T' / \text{kJ} \cdot \text{mol}^{-1} = 0.64 \cdot \overline{E}_T / \text{kJ} \cdot \text{mol}^{-1} + 77.2$$

The backward to sideways scattering evolution with increasing \overline{E}_T is discussed in the light of a possible insertion mechanism in addition to the (low collision energy) abstraction one.

In addition an absolute determination of the reaction cross-section was carried out using the $\text{K} + \text{CH}_3\text{I}$ reaction as standard. Furthermore the attacking atom effect in the reaction dynamics of the following sequence $\text{K}, \text{Rb}, \text{Cs} + \text{CH}_3\text{I}$ was also studied.

A semiempirical potential energy surface was built on which extensive trajectory calculations were carried out to obtain the total and differential reaction cross-section to compare with the experimental molecular beam results

Unimolecular Dissociation of Diethylnitramine

Yannis G. Lazarou, Keith D. King * and Panos Papagiannakopoulos

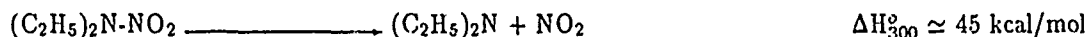
Department of Chemistry, University of Crete

Institute of Electronic Structure and Laser, Research Center of Crete

P.O. Box 1470, Heraklion 714 09, Crete, Greece

* Department of Chemical Engineering, The University of Adelaide,
Adelaide, South Australia 5001.

The infrared multiphoton dissociation of diethylnitramine in the gas phase by a pulsed CO₂ Laser has been studied in order to determine the decomposition dynamics of diethylnitramine from its ground state. The steady-state rate coefficient for its unimolecular decomposition was found to be $k_{st} = 10^{5.2 \pm 0.2} \text{ (I/MW cm}^{-2}\text{) s}^{-1}$ for laser intensities 2-10 MW cm⁻², that corresponds to unimolecular dissociation rate constants $k_{uni} = 10^{5.5} \cdot 10^{6.2} \text{ s}^{-1}$ respectively. Scavenging experiments with Cl₂, NO, NO₂ and (CD₃)₂NNO₂ molecules have shown that the photodissociation mechanism of diethylnitramine includes mainly the scission of the N-NO₂ bond :



Diethylnitrosamine was the major final product which is mainly produced through the oxidation reaction :



in a similar manner as in dimethylnitramine decomposition [1]. Our results are in agreement with thermal decomposition experiments [2] although the obtained activation energy (41.6 kcal/mol) for the N-NO₂ scission channel is rather small, indicating the complex reaction mechanism that is involved in the overall thermal decomposition of diethylnitramine.

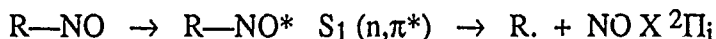
1. Y. Lazarou and P. Papagiannakopoulos, J. Phys. Chem., accepted (1990)
2. B.L. Korsunskii, F.I. Dubovitskii and E.A. Shurygin, Izv. Akad. Nauk. SSSR, 7, 1452 (1967)

State-selected Predissociation Dynamics of Perhalogen Nitrosomethanes

A.W. Simpson, J.A. Dyet, M.R.S. McCoustra and J. Pfab
Heriot-Watt University, Edinburgh, EH14 4AS

Previous studies by Houston, Reisler and Wittig have indicated the potential of simple C-nitroso compounds to serve as testbeds for state-selected photochemistry.^{1,2} CF₃NO and t-nitrosobutane (t-BuNO) in particular are model compounds for elucidating the non-radiative decay and unimolecular dissociation behaviour of larger state-selected polyatomic molecules.^{2,3} Other C-nitroso compounds also offer the opportunity to achieve vibronic state-selection in the convenient red spectral region where excitation by a narrow bandwidth dye laser can be combined with the jet-cooling technique.⁴ The photodissociation of these compounds from their S₁ (n,π*) states is unique in permitting one to probe both the entrance channel by fluorescence decay and the exit channel by means of product state distributions for the NO fragment.

The S₁ (n,π*) ← S₀ electronic transition of C-nitroso alkanes in the 500 to 750 nm range frequently supports structured spectra. Quantum yields for fluorescence are often adequate for recording excitation spectra and fluorescence decay times. Photodissociation produces an alkyl and a ground state NO radical:



Detailed product state distributions for the NO fragment are now available from LIF measurements for the near-threshold dissociation of CF₃NO, CClF₂NO and CCl₂FNO.³⁻⁵ In all these cases deviations from statistical distributions are very minor except for the NO spin-orbit ratios, F₁/F₂ which favour strongly the lower F₁ (²Π_{1/2}) component.

Changes in the F₁/F₂ ratios with excess energy above threshold are slight for CF₃NO and CClF₂NO, in contrast to CCl₂FNO where they remain non-statistical but approach the statistical limit. For CCl₃NO the visible absorption spectrum reveals a weakly structured continuum. Here the disposal of excess energy into NO rotation favours non-statistical Gaussian-type rotational distributions. NO is formed promptly and without selectivity in the population of the spin-orbit states.

Fluorescence excitation spectra of the molecular parents have been recorded for the fluorine containing nitroso methanes. The time-resolved fluorescence decay curves following excitation of single vibronic levels do not reflect simple first-order decay and show complex characteristics. They can be simulated, however, by the super-position of a fast (τ_1) and slow (τ_2) decay component. The calculated radiative lifetime of 15 μ s is typical for an $^1A'' \leftarrow ^1A'$ (n, π^*) transition. The observed lifetimes are much shorter due to higher rates of dissociation and inter-system crossing. Fluorescence yields decrease with increasing substitution of F by Cl in the series of nitrosomethanes. No luminescence can be detected for CCl_3NO for which the upper state does not appear to be bound.

Table: Comparison of electronic origins of $\tilde{A} \leftarrow \tilde{X}$ spectra, fluorescence lifetimes* and spin-orbit ratios of NO photolysis products of jet-cooled nitrosomethanes

	CF_3NO	$CClF_2NO$	CCl_2FNO	CCl_3NO
$\bar{\nu}_{00}/cm^{-1}$	13929	14190	14522	16000 ⁺
τ_1/ns	147	150	315	-
F_1/F_2	5.0	1.5	7.0	1.0

* for excitation on 12_0^3 transitions except for CCl_3NO

+ uncertainty ± 200 , absorption spectrum continuous

References

1. R.D. Bower, R.W. Jones and P.L. Houston, J. Chem. Phys., **79**, 279 (1983).
2. M. Noble, C.X.W. Qian, H. Reisler and C. Wittig, J. Chem. Phys., **85**, 5763 (1986).
3. J.A. Dyet, M.R.S. McCoustra and J. Pfab, J.C.S. Faraday II, **84**, 463 (1988).
4. J.A. Dyet, M.R.S. McCoustra and J. Pfab, J.C.S. Faraday Trans., **86**, 2049 (1990).

ENERGY FLOW AND ENERGY POOLING IN NO FOLLOWING NO₂ PHOTODISSOCIATION

G. E. Gadd and T. G. Slanger
Molecular Physics Laboratory
SRI International
Menlo Park, CA 94025
USA

ABSTRACT

There is insufficient energy at 157 nm to produce the NO(A) and NO(B) states from photodissociation of NO₂. They are, nevertheless, produced, and from the temporal behavior of the emission, it is evident that energy pooling is involved. The very broad vibrational distribution of NO in its ground electronic state is presumably the source of the energy for A and B state excitation, although to generate NO(A) in its v=0 level requires the pooling of two ground state molecules in v=13. The generation of NO(a⁴Π) in v=0 is barely possible at 157 nm, so we cannot yet exclude the idea that pooling of the energy of NO(a) and NO(X) in lower vibrational levels is taking place.

Direct NO(A) and NO(B) production at 157 nm occurs when the NO₂ is dissociated out of a prepared excited state. Photoexcitation of NO₂ in the 540-550 nm region followed by photodissociation produces a range of A and B state levels, the yields tracking the NO₂ absorption cross section for the visible photon. When the first photon is capable of photodissociating the NO₂, at wavelengths below 400 nm, then excitation of the product NO can occur. This is shown by photodissociation of NO₂ at 355 nm, producing NO in v = 0,1, followed by broadband 193 nm excitation. The v=1 level is photoexcited, resulting in intense emission from the D²Σ⁺(v=0) and A²Σ⁺(v=4) levels.

MULTIPHOTON IONIZATION STUDIES OF THE COMPETING C-C AND C-H
BOND FISSIONS IN HIGHLY VIBRATIONALLY EXCITED ALKYL BENZENES

K. Luther, T. Rech, A. Schmoltner, K.-M. Weitzel and J. Troe
Institut für Physikalische Chemie der Universität
Göttingen, Tammannstraße 6, D-3400 Göttingen, West Germany

The unimolecular dissociation of highly vibrationally excited alkyl benzenes in competing channels is studied under collisionless conditions. Specific rate constants and branching ratios between C-H and C-CH₃ bond fissions are obtained from time resolved direct product detection.

The aromatic molecules are excited by 193 nm Excimer Laser radiation and subsequently undergo rapid internal conversion into the highly vibrationally excited ground state. The CH₃ radicals formed in the dissociation process are detected using (2+1)-REMPI and TOF mass spectrometry. Specific rate constants for the dissociation reactions are obtained by measuring the time dependence of the CH₃⁺ signal. For ethylbenzene, dissociation into benzyl and methyl radical constitutes the only major channel.

Comparison of the CH₃ yields from toluene, xylenes, and related compounds with those from ethylbenzene allows the determination of the branching ratio between the channels producing CH₃ and H for these molecules. In the case of toluene, 17% of the molecules dissociate through the C-C channel [1]. Analysis of the results by unimolecular rate theory determines the variation of thermal branching ratios for C-C bond fission with temperature.

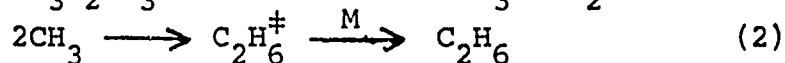
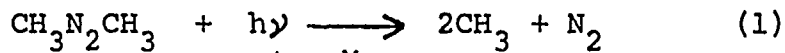
- [1] K. Luther, J. Troe, and K.-M. Weitzel, J. Phys. Chem. 1990, in print.

MINOR PRODUCTS IN THE PHOTOLYSIS OF AZOMETHANE AT
LOW PRESSURE: ALTERNATIVE DECOMPOSITION CHANNELS OF
VIBRATIONALLY EXCITED ETHANE.

R.A. BACK, Chemistry Division, National Research Council
of Canada, 100 Sussex Drive, OTTAWA, Canada, K1A 0R6
and

J.M. ROSCOE, Chemistry Department, Acadia University,
Wolfville, Nova Scotia, Canada, B0P 1X0

The photolysis of azomethane at ~ 365 nm has been studied
at room temperature and pressures from 10 mTorr to 10 Torr.
More than 99% of the reaction can be described by the
reactions



but there are also small but measurable yields of propane,
ethylene, methane and hydrogen. The presence of ethyl
radicals is implied, and the mechanism of their formation
by reactions of CH_3 with azomethane is discussed. The
alternative decomposition channels of $\text{C}_2\text{H}_6^{\ddagger}$, formed in
reaction 2, to give $\text{C}_2\text{H}_5 + \text{H}$ and $\text{C}_2\text{H}_4 + \text{H}_2$, are
considered. At low pressure, there is tentative evidence
for the latter molecular dissociation, based on quantum
yields of H_2 of 4×10^{-5} and 2×10^{-5} at 0.1 and 1.0 Torr
of azomethane respectively. These values at least define
upper limits for the extent of the molecular dissociation,
and possible reasons for this rather low efficiency are
discussed.

THE IR MULTIPHOTON DISSOCIATION OF CF_3I . EFFECT OF PRESSURE AND OF VISIBLE LIGHT

C.Rinaldi, S.I.Lane, E.V.Oexler, J.C.Ferrero and E.H.Staricco

Departamento de Físico Química, Facultad de Ciencias Químicas, Universidad Nacional de Córdoba, Ciudad Universitaria, 5016 Córdoba.

The IR laser photolysis of CF_3I has drawn the attention of many investigators and is known to yield CF_3 radicals and iodine atoms in the ground electronic state. The CF_3 radicals recombine to yield C_2F_6 or react with iodine to regenerate CF_3I .

In this work we have studied the IR multiphoton dissociation of CF_3I in the presence of Isobutane. The excitation of the CF_3I molecule was made with the radiation of a pulsed TEA CO_2 laser, at a frequency of $1074,65 \text{ cm}^{-1}$.

The products observed are CHF_3 , C_2F_6 and I_2 . The ratio $\text{CHF}_3/\text{C}_2\text{F}_6$ is independent of the number of pulses and increases with the pressure of Isobutane. The total reaction yield decreases sharply with the increment of pressure. A model calculation of these results allowed obtainment of information about the transference of energy from vibrationally excited CF_3I by collisions with Isobutane.

All of the above experiments were performed in the dark. Simultaneous irradiation with continuous visible light of different wavelengths, resulted in an increment of the dissociation yield, at least by a factor of two. This process is due to an electronic transition taking place from vibrational excited CF_3I .

DYNAMICS OF ANISOLE PHOTODISSOCIATION

A. M. Schmoltner^{*}, D. S. Anex, and Y. T. Lee
Department of Chemistry, University of California, Berkeley,
CA 94720, USA

^{*} Present Address: Institut für Physikalische Chemie,
Tammannstrasse 6, D-3400 Göttingen, Fed. Rep. Germany

The photodissociation dynamics of anisole was studied using the crossed laser/molecular beam technique. A skimmed supersonic molecular beam of anisole (methyl-phenyl-ether) in a carrier gas was crossed with the focussed output of either a pulsed CO₂ laser operating at 9.6 μ m or an excimer laser at 193 nm or 248 nm. The molecular beam source was rotatable about the intersection point of the molecular and the laser beam, allowing variation of the angle between molecular beam and detector axis. The dissociation products were detected using electron impact ionization, a quadrupole mass filter and a single ion counting detector. The translational energy release for a dissociation channel was determined from the analysis of the TOF spectra.

The intense CO₂ laser radiation induced IRMPD (infrared multiphoton dissociation), a process which yields information about the lowest energy dissociation channels of hot ground state molecules, similar to thermal dissociation. In the case of anisole, the only primary channel observed was O-CH₃ rupture resulting in phenoxy and methyl radicals. At conditions of higher laser fluence, secondary decomposition of the phenoxy radicals into carbon monoxide and cyclopentadienyl radical took place.

Absorption of a UV photon was found to lead to a number of different primary and secondary dissociation channels. Rapid internal conversion into highly vibrationally excited ground state (which is known to occur for many aromatic compounds) apparently plays only a minor role for anisole. Most dissociation channels therefore originate in an electronically excited state. Major product channels were tentatively assigned to the formation of methyl and phenoxy radicals, methanol and benzyne, and methoxy and phenyl radicals. The phenoxy radical dissociation products CO and C₅H₅ were detected as well. In the case of photodissociation by 248 nm radiation, multiphoton absorption precedes certain channels.

PHOTOCHEMICAL DYNAMICS OF HOCl

Andrew J. Bell, Patrick E. Pardon

Chris Hickman, and Jeremy G. Frey

Department of Chemistry, Southampton University

Southampton SO9 5NH, UK

The dynamics of the photodissociation of HOCl at 248 nm have been investigated by observing the laser induced fluorescence (LIF) spectrum of the OH product formed in a collision free molecular beam environment.

The energy released in the reaction is predominantly disposed into relative translational energy. The OH product is found only in its vibrational ground state and with rotational populations extending up only as far as $N=10$. A preference is seen for the lower energy spin-orbit state and for the $\Pi(A')$ lambda doubled components.

The use of a molecular beam, supersonic expansion allowed us to investigate the influence of the parent rotational state on the OH product rotational distribution.

RESONANCE RAMAN SPECTRA OF NOCl: PHOTOCHEMICAL DYNAMICS

Andrew J. Bell and Jeremy G. Frey

Department of Chemistry, Southampton University

Southampton SO9 5NH, UK

The very small yield of photons following the excitation of a molecule to a repulsive electronic state can provide useful information on both the vibrational levels of the ground state and the dynamics of the upper state. The observation of a Resonance Raman spectrum from molecules undergoing direct dissociation was first demonstrated by Kinsey and Imre for methyl iodide and ozone and subsequently for a number of other molecules. However not all the molecules investigated show the expected long vibrational progressions. We will present work on NOCl showing the expected vibrational progression following excitation at 266 nm but in the rest of the extensive absorption band of the molecule we have studied we only observed a simple Raman spectrum.

Photodecomposition of Group III and V Organometallic Compounds at 193 nm

W. Braun, R. Klein, A. Fahr, H. Okabe
 Chemical Kinetics Division
 National Institute of Standards and Technology
 Gaithersburg, Md 20899
 &
 A. Mele
 Department of Chemistry
 University of Rome
 Ple. A. Moro 5, Rome, Italy

Chemical vapor deposition may be achieved by the pyrolysis or photodecomposition of appropriate organometallic compounds. In this investigation the goal is to evaluate the photodecomposition mechanism of trimethyl gallium (TMG) and trimethyl arsine (TMA) in the vacuum ultraviolet, specifically at 193 nm, the ArF laser line.

The sharp absorption peak of CH_3 at 216.4 nm furnishes a convenient analytical approach for the quantitative assessment of the temporal methyl concentration subsequent to the laser pulse. Chromatography of the end products is used to confirm the optical results. A comparison with an actinometric standard such as acetone, with known quantum yield from methyl production of 2 should, by comparison with the organometallic compound, lead to the appropriate quantum yield for the organometallic. In the case of TMG, a discrepancy was found between the ethane found chromatographically and that expected on the basis of the optical methyl analysis. The latter was considerably higher. This result was attributed to a radical containing gallium moiety from the photolysis that absorbed where methyl does, at 216.4 nm.

A method based on isotope distribution was devised to evaluate the photochemical decomposition mechanism for TMG¹. This involved the photolysis of a mixture of completely deuterated acetone with TMG. The CD_3 and CH_3 produced in the decomposition recombine to give completely deuterated, half deuterated, and nondeuterated ethanes. The ratio $(\text{CH}_3\text{CD}_3)^2/(\text{C}_2\text{H}_6)(\text{C}_2\text{D}_6)$ must equal 4 if no source of ethane extraneous to methyl recombination is present. For the acetone- d_6 and TMG system it was found, however, that the above expression did not yield 4. It was concluded that in the TMG photolysis at 193 nm there is an intramolecular ethane elimination channel.

If we define P_D , ϵ_D , P_H and ϵ_H as the pressures and the absorption coefficients of the acetone- d_6 and TMG respectively and define Q as the quantum yield of 'total' methyl, F as the fraction of 'total' methyl that is free, $(1-F)$ the fraction produced intramolecularly, then the following two equations can be derived:

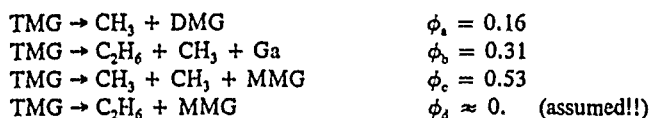
$$X = QF = \frac{[\text{CH}_3\text{CD}_3] \epsilon_D P_D}{[\text{C}_2\text{D}_6] \epsilon_H P_H}; \quad Y = \frac{4 \epsilon_D P_D [\text{C}_2\text{H}_6]}{\epsilon_H P_H [\text{CH}_3\text{CD}_3]} = Q + \frac{2(1-F) \epsilon_D P_D}{F \epsilon_H P_H}$$

By constraining QF to the value given by the first of these equations, the second results in an expression for F given by,

$$F = \frac{(QF)\epsilon_H P_H / \epsilon_D P_D + 2}{4[\text{C}_2\text{H}_6]/[\text{CH}_3\text{CD}_3] + 2}$$

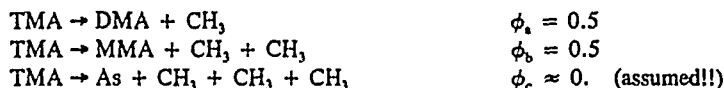
If CD_3 reacted with TMG, if F and Q were functions of pressure, or if there were different production rates for CH_3 and CD_3 , the above model would be invalid. However, there is strong evidence that none of these effects occur.

From the measurements and use of the above equations it is concluded that $Q=2.15$ and $F=0.71$ from which the following quantum yields can be derived (DMG=dimethyl gallium, MMG=monomethyl gallium),



The absorption at 216.4 nm attributed to a methyl gallium type radical was found to have an absorption peak at 220 nm as well. This intermediate, postulated to be the dimethyl gallium radical, is most probably a precursor to gallium metal formation.

The photodecomposition of TMA is simpler than that of TMG. Trimethyl arsine was photodecomposed at 193 nm, the course of the reaction being monitored by the observation of methyl formation and decay. The quantum yield for methyl formation was found to be 1.5. The only product found with gas chromatography was ethane. This correlated well with the CH_3 as determined by optical absorption. The methyl decay, determined optically, shows the initial formation and second order decay but even after a period of milliseconds the signal does not revert to the base line. This suggests the formation of relatively stable species such as $\text{As}(\text{CH}_3)_2$ and $\text{As}(\text{CH}_3)$. There is no indication of any intramolecular elimination processes as in the case of TMG. On this basis the following quantum yields are derived.



Further experiments on TMA involving isotopic analysis are in progress. Results of these will be more sensitive for the detection of very small amounts of intramolecular ethane formation.

Present protocols are capable of determining quantum yields for dissociation of a large number of organometallic compounds. Such data provide the necessary first step for unravelling the total reaction kinetics in these potentially complex kinetic systems and hence the complete understanding of the gas phase CVD (photochemical as well as thermal) processes.

REFERENCE:

1. W. Braun, R. Klein, A. Fahr, H. Okabe, and A. Mele, Laser Photolysis of Trimethyl Gallium at 193 nm: Quantum Yields for Methyl Radical and Ethane Production, Chem. Phys. Lett., 166, 397 (1990)

INVESTIGATION OF NOVEL SOURCES OF VINYLIC RADICALS

by S Bish and R Walsh, Department of Chemistry,
University of Reading, Whiteknights, Reading, RG6 2AD, U.K.

A series of azo-compounds of the type $R-N=N-CR'CH_2$ (R = Alkyl, R' = H or Me) has been synthesized and their photochemical decomposition pathways investigated. The bulk of photolyses have been carried out at 206 nm (steady state experiments) and at temperatures of 298 K. Complete gas chromatographic analyses of the hydrocarbon products have been carried out over a range of different times and gas pressures. Experiments with and without added oxygen indicate that, for several precursors, radical pathways are non-existent and products come mostly via unusual molecule isomerisation routes. The compound $t-Bu-N=N-CH=CH_2$, however, gives products suggestive of vinyl radical production. Experiments are currently underway to exploit this source to give abstraction and addition rate constants for vinyl radicals, for which little direct information exists. Results will be reported at the meeting.

C.A.R.S. DIAGNOSTICS OF SMALL HYDROCARBON DECOMPOSITION
IN A RADIOFREQUENCY PLASMA REACTOR FOR CARBON FILM
DEPOSITION

R. FANTONI, M. GIORGI, W.C.M. BERDEN (*),

V. BARBAROSSA (+), S. MERCURI (+), R. TOMACIELLO (+)

ENEA, CRE Frascati, Dip.TIB, C.P.65, 00044 Frascati (RM) Italy

The low-temperature deposition of amorphous diamond-like and crystalline diamond films from hydrocarbon plasma is presently the subject of several works [1-3]. However, the gas-phase chemical processes, involving reactant decomposition, formation of intermediates at the surface or in volume and presence of ionic species, are not yet completely characterized. With the aim of understanding the plasma reactions involved, a space-resolved C.A.R.S. investigation of CH_4/H_2 mixtures excited by R.F. discharge has been undertaken.

The glow discharge reactor is constituted by a stainless-steel vacuum chamber containing a small area RF powered plate, surrounded by a large area grounded mesh. The electrode asymmetry ratio is about 0.09 and the maximum self-bias voltage at the powered electrode is about -500 V. Four optical windows are available to perform space-resolved C.A.R.S. measurements both in the plasma bulk and in the dark sheath region, optical emission spectroscopy of the glow region, optical monitoring of the growing thin film. Measurements are performed both operating the reactor in flow and at steady-state.

Set-ups for broad-band and narrow band C.A.R.S. diagnostics are employed in order to monitor on-line during the R.F. pulse the concentration and the temperature of the reactants and to investigate the presence of reaction intermediates, such as C_2 , whose spectra may be resonantly enhanced by the occurrence of real laser induced electronic transitions. The pump beam for C.A.R.S. is a frequency doubled Nd:YAG laser, which is partially used also to excite either the broadband dye laser (SOPRA) or a commercial grating tunable narrowband dye laser. After space overlap and synchronization the pump and the Stokes

(*) ENEA Guest

(+) ENI Ricerche, Monterotondo Scalo (RM) Italy

are propagated in collinear geometry and focussed in the chosen point of the reactor, the C.A.R.S. signal generated is transmitted out, filtered by dichroics mirrors and by a small monochromator, and detected by an intensified photodiode array (OMA III EG & G). A phototube replace the array in the case of narrow-band C.A.R.S. where the dye laser frequency is slowly scanned and the signal is fed to a BOXCAR averag.r. The main advantage of our C.A.R.S. diagnostic systems is the possibility of single shot measurements either at a fixed frequency or on a large region of Antistokes shifts. This permits a real time monitoring of the turbulent environment generated by the plasma discharge. Furthermore bright and dark regions can be studied by the same technique, giving a complete information on occurring gas-phase reactions.

References

1. A. Bubenzer et al., J.Appl.Phys., 54 (8) (1983) 4590.
2. P. Couderc, Y. Catherine, Thin Solid Films, 146 (1987) 93.
3. K. Kobayashi et al., Thin Solid Films, 158 (1988) 233.

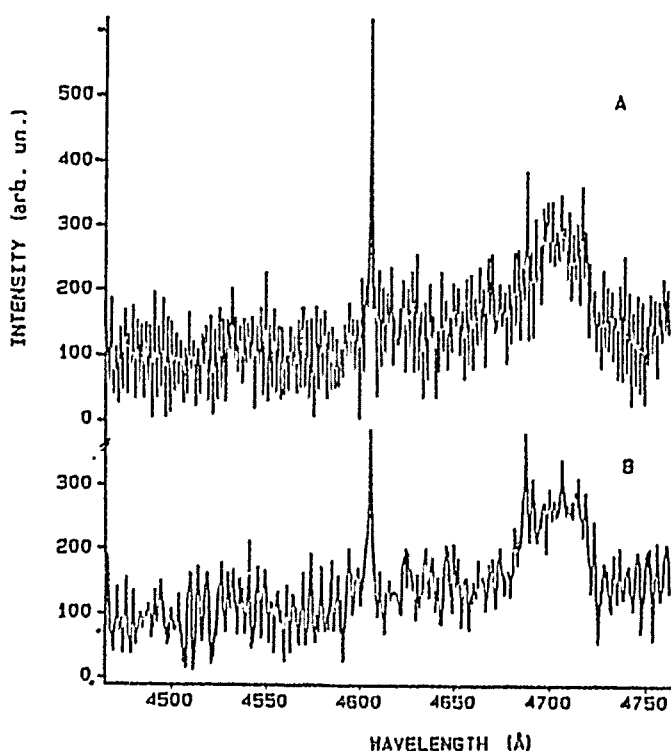


Fig.1 CARS spectra of methane measured in a non-discharge methane/hydrogen flow (A) and in a discharge flow (B). The methane and hydrogen flowrates are both 5.0 sccm, and the total pressure is 920 mTorr (N_2 equivalent). The C_2 Swan system around 470 nm (emission) is a result of laser induced dissociation of methane.

Photooxidation of halogenated anaesthetic agents

Hande, M, McLoughlin, P and Shanahan, I.

School of Chemical Sciences, Dublin City University

Glasnevin, Dublin 9. Ireland

The volatile anaesthetic agents halothane (CF_3CHClBr), enflurane ($\text{CHClFCF}_2\text{OCF}_2\text{H}$) and isoflurane ($\text{CF}_3\text{CHClOCF}_2\text{H}$) are the most widely used general anaesthetic agents in the Western industrialised countries. They are administered to patients in such a way that at least 98% of the volume of anaesthetic used in the hospital is released into the atmosphere. Accurate figures for production and use of these species are not readily available, but calculations in this laboratory place emission rates conservatively in the range $5 \times 10^6\text{g}$ per annum. While the rates of emission are very low relative to those of other halogenated species such as methyl chloroform, these species were only introduced into clinical practice in the 1960's, and emission rates have increased dramatically since then. It is possible that their impact could become significant if rates of emission continue to grow at present rates.

The oxidation products of these three species under simulated atmospheric conditions have been identified using gas chromatography-coupled mass spectrometry. Quantitative measurements of the relative yields of oxidation products from a given compound were made by gas chromatography.

**Direct Observation of Preferential Bond Fission by Excitation of a Vibrational
Fundamental: Photodissociation of HOD (0,0,1)**

I. Bar, Y. Cohen, D. David and S. Rosenwaks
Department of Physics, Ben-Gurion University of the Negev
Beer-Sheva 84015 Israel

and
James J. Valentini
Department of Chemistry, University of California, Irvine, California 92717

The 193 nm photodissociation of individual rotational levels of HOD molecules excited with one quantum of O-H stretching vibrational energy is described. Stimulated Raman excitation and coherent anti-Stokes Raman scattering are used to prepare and detect, respectively, the (0,0,1) vibrationally excited HOD. The OD and OH fragments are detected by laser induced fluorescence. The photodissociation of the HOD (0,0,1) molecules yields at least three times more OD than OH.

This research is supported by a grant from the United States-Israel Binational Science Foundation (BSF), Jerusalem, Israel.

LASER PHOTODISSOCIATION OF $F_2S_2O_4$ AT 193 nm: COLLISIONAL DEACTIVATION OF HIGHLY EXCITED FSO_3 RADICALS

A. E. Croce de Cobos, C. J. Cobos and E. Castellano
Instituto de Investigaciones Fisicoquímicas Teóricas y
Aplicadas (INIFTA), Facultad de Ciencias Exactas,
Universidad Nacional de La Plata, C. C. 16, Suc. 4,
(1900) La Plata, Argentina.

Collisional deactivation of excited FSO_3 radicals generated by 193-nm laser photodissociation of $F_2S_2O_4$ was studied by examining absorption decay times for the He, N_2 , O_2 , and $F_2S_2O_4$ collision partners. Mixtures of $F_2S_2O_4$ were photolysed using an ArF excimer laser in the presence of the above quenchers. The time-resolved absorption profiles were monitored at 450 nm. For all experiments double exponential decays were observed which were attributed to FSO_3 radicals in different states of excitation. The following quenching rate constants for the short-lived component were measured at 295 K for the He and N_2 quenchers: $(5.8 \pm 0.8) \times 10^{-15}$ and $(9.7 \pm 1.4) \times 10^{-15} \text{ cm}^3 \text{ molecule}^{-1} \text{ s}^{-1}$ respectively. For the long-lived component the values $(1.5 \pm 0.2) \times 10^{-15}$, $(3.2 \pm 0.3) \times 10^{-15}$, $(2.6 \pm 0.4) \times 10^{-14}$, and $(1.6 \pm 0.2) \times 10^{-13} \text{ cm}^3 \text{ molecule}^{-1} \text{ s}^{-1}$ were determined for He, N_2 , O_2 , and $F_2S_2O_4$ respectively.

Arguments are presented which suggest that the present quenching data correspond to the vibrational relaxation of highly excited FSO_3 radicals.

A NUCLEOPHILIC SUBSTITUTION REALIZED IN SOLUTION BY MEANS OF A GASEOUS PLASMA TREATMENT : THE SYNTHESIS OF $[\text{Fe}(\text{CN})_5\text{CO}]^{3-}$.

Jean-Louis BRISSET, Avely DOUBLA, Jacques AMOUROUX
Laboratoire des Réacteurs chimiques en Phase Plasma
E.N.S.C.P., 11 rue P. & M. Curie 75005 Paris

INTRODUCTION

The plasma treatments of surfaces leading to new compounds or to materials with improved properties are now developed on the industrial scale although the underlying relevant chemical reactions are not always well understood. For our chemical investigation of the plasma/surface interactions, we first considered aqueous solutions as the targets exposed to the plasma (provided by a point-to-plane air corona discharge (1)). The acidifying effect of the chargeless species could then be quantified (2,3), in connection with the pitting corrosion of metals such as Aluminum (4) on exposure to the corona discharge.

In this study we go on with the acid-base reactions and focus on the Lewis acidity: we tested whether the exchange of a ligand bounded to a complex in solution could be realized under plasma conditions. A good example is provided by the pentacyano(ligand)ferrate(II) for which ligand or electron exchanges are described in aqueous solutions (5,6) and which thus appears as a convenient model molecule. The literature reports numerous studies performed with nitrogen-containing bases as the leaving or entering ligands. We selected the N.methylpyrazinium moiety (referred to as mpz) and substituted pyridines as the leaving ligand, and carbon monoxide as the attacking ligand. The exchange reaction leads to the pentacyano(carbonyl)ferrate(II) which has received a limited attention up to now.

EXPERIMENTAL

The plasma reactor described elsewhere (7) is fitted with 2 stainless electrodes: the hollow point electrode allows the CO inlet ($P_{\text{CO}} = 1 \text{ atm.}$) and is raised to the d.c. HV; the plane electrode is earthed and paralleled to the rod (gap: about 15 mm). This particular device enables the ion and the neutral fluxes to be separated since the electric wind which carries the neutral species roughly blows along the axis of the rod. The liquid target is perpendicular to the point and exposed only to the activated neutrals.

The starting complexes involving N.methylpyrazinium or substituted pyridines were prepared according to known procedures (5) and dissolved in distilled water.

In addition, optical fibers connected to a monochromator and a photomultiplier make easy to follow in situ the absorbance of the solution.

RESULTS AND DISCUSSION

The stirred aqueous solutions of ferrates were then exposed to the flux of the chargeless activated species of the plasma and the resulting absorbance changes were followed spectrophotometrically.

The corona treatment of a blue solution of $\text{Fe}(\text{CN})_5\text{mpz}$ by the flux of the activated neutrals in standard experimental conditions (i.e., positive discharge, $U = 18 \text{ kV}$, $I = 14 \text{ }\mu\text{A}$, discharge duration 600 s, electrode gap 16 mm) leads to the fading of the colour and yields the carbonyl complex while the color change takes several hours to occur in the absence of discharge.

A double set of inferences can be drawn from the ligand exchange:

- due to the drastic increase in its kinetics, the ligand exchange reaction may be considered as a test reaction to characterize the occurrence of excited CO molecules and their relevant concentration, provided the starting complex be in large excess. This is backed up by the fact that exchange reactions with other leaving

ligands (e.g., substituted pyridines) were successful.

- the study of the kinetics also provides valuable informations on the discharge itself and on the plasma-surface interactions.

By following the absorbance A decrease at the absorption peak of $\text{Fe}(\text{CN})_5\text{mpz}$ after controlled exposures to the plasma in given discharge conditions, we could plot the function $\ln |A_\infty - A|$ vs. the treatment time t . The resulting linear plot shows that the mechanism is reduced to a pseudo-1st order kinetic in the considered treatment conditions, while in homogeneous solutions the ligand exchange mechanism is found more complex (5). The following equations are consistent with our experimental results:

$$\text{CO}_{\text{gas}} = \text{CO}_{\text{solution}} ; K = (\text{CO})_{\text{solution}} / p_{\text{CO}} \quad (\text{Henry's law})$$



which leads to the pseudo 1st. order kinetics:

$$v = -d(\text{Fe}(\text{CN})_5\text{mpz})/dt = k'(\text{CO})_{\text{solution}} \cdot (\text{Fe}(\text{CN})_5\text{mpz}) = k \cdot (\text{Fe}(\text{CN})_5\text{mpz})$$

since $(\text{CO})_{\text{solution}}$ is taken constant as the poor saturation solubility of the gas in water.

Complementary experiments performed with various discharge intensities gave evidence that the reaction becomes more rapid as the intensity I increases. It can then be concluded that the kinetic constant k depends on I , and further is a linear function of I (i.e., $k = a + bI$). Hence the kinetic law

$$\ln |A_\infty - A| = k_0(1 + \beta I) \cdot t + \text{constant}$$

(with $\beta = 1.25 \cdot 10^5 \text{ A}^{-1}$) includes the constant $k_0 = 0.5 \cdot 10^{-4} \text{ s}^{-1}$ relevant to the exchange under a mere CO bubbling and without discharge. The high value of β underlines the determining influence of the current intensity on the exchange kinetics and gives evidence of the prominent role of the activated CO^* provided by the discharge. It also suggests that the number of CO^* molecules yielded by the discharge depends both on the relevant intensity and the discharge duration, i.e. on the associated quantity of electricity. In other words, it is related to the number of ions created in the discharge according to the electrolysis laws.

CONCLUSIONS

The mpz exchange by CO on $\text{Fe}(\text{CN})_5\text{mpz}$ is among the first examples of nucleophilic substitutions performed in solution under exposure to a plasma: the activated species of the CO discharge drastically favor the kinetics. The apparent 1st order constant is found to be a linear function of the current intensity from which it can be inferred that the formation of CO^* is governed by the relevant quantity of electricity. The general character of the selected example is backed up by similar substitutions performed on pentacyano(pyridine)ferrates.

ACKNOWLEDGEMENTS:

We are grateful to CNRS-PIRSEM and EDF for financial support.

LITERATURE CITED.

- 1 - R.S. Sigmond, M. Goldman- Electric Breakdown and Discharges in Gases; NATO ASI Series, E.E. Kunhardt & L.T. Luessen Ed., Plenum Press London (1981) Vol. B 89b, pp 1-65
- 2 - J.L.Brisset, A. Doubla, J. Lelièvre, J. Amouroux- Bull. Soc. chim. Fr.(1989), 615-619.
- 3 - J.L.Brisset, A. Doubla, J. Lelièvre, J. Amouroux- Analysis (1990) to be published.
- 4 - A. Goldman, R.S. Sigmond- J. Electrochem. Soc. (1985) 132, 2842-2853.
- 5 - H.E.Toma, J.M. Malin- Inorg. chem. (1973) 12, 1039-1044
- 6 - J.L. Brisset, M. Biquard- Inorg. Chem. Acta (1981) 53, L125-L128
- 7 - A. Doubla- Thesis; University P.&M. Curie, Paris (1989).

He SCATTERING FROM ORDERED STRUCTURES OF ADSORBATES ON SURFACE

G. Petrella - Department of Chemistry, University of Bari,
Bari, Italy.

Calculations are reported on He scattering from clusters of different numbers of CO molecules adsorbed in an ordered way on flat Pt(111) surfaces. The Sudden approximation is used to obtain both the integral cross sections for scattering by adsorbates and the angular intensity distribution of the scattered atoms.

The cross section values have been discussed on the basis of the Comusa and Poelsema overlap approach that, already successfully tested for clusters of vacancies, has been found to hold good even in the case of molecular adsorbates as surface defects.

The angular intensity distribution curves show Fraunhofer interferences and rainbow maxima, as in the case of isolated adsorbates, and periodic diffraction peaks caused by the ordered structure of CO molecules on the Pt. Basically it has been demonstrated that from these peaks it is possible to obtain information on the geometric structure of the adlayer if the adsorbates form a 2-dimensional crystal on the surface.

THE OXIDATION OF SOOT PARTICULATES IN SHOCK WAVES

P. Cadman and R. J. Denning

Department of Biochemistry

Edward Davies Chemical Laboratories

University College of Wales, Aberystwyth, Dyfed SY23 1NE

Soot particulates are often the unwanted emission products from the combustion of carbon containing fuels in burners, engines etc. In some burners, the efficient extraction of heat from the combustion zone is dependent on the presence of these particulates yet their emission into the atmosphere as a final product is undesirable. The modelling of burners, engines etc. therefore needs to include the burnout rate of soot particulates in order to take account of these constraints and ensure that the emissions of exhaust gases is controlled.

The reduction of nitric oxides by carbonaceous particles is recognized as a potential means of controlling NO emissions from combustion systems. The mechanism and kinetic parameters for the reduction of NO by carbon particles, however, is not well understood.

In this study the reaction rates of soot/oxidising gas aerosols have been studied over the temperature range 1200-3800K at pressures up to 14 atmospheres in reflected shock waves using laser absorption measurements to monitor the particulate reaction.

The rate of consumption of soot particulates by oxygen was studied over the range 1-40% oxygen in argon and found to be half order in oxygen and have an activation energy of 110 ± 20 kJ/mol. At temperatures above 2200K maxima appeared in the Arrhenius plots of this rate.

The oxidation of soot by nitric oxide was found to be first order in nitric oxide between 2000-3200K with a surface oxidation rate, w given by $w = 4.9 P_{\text{NO}} \exp(-126 \text{ kJ/mol}/RT) \text{ gcm}^{-2} \text{ s}^{-1}$. The rate is considerably slower than in oxygen at temperatures ~~above~~ ^{below} about 3000K.

THE ROLE OF THE SURFACE IN THE CHAIN OXIDATION PROCESS

I.A. VARDANYAN, R.H. BAKICHADJYAN

Institute of Chemical Physics Armenian Academy of
Sciences, P.Sevak st. 5/2, 375044 Yerevan, USSR

The kinetic peculiarities of the low temperature heterogeneous-homogeneous acetaldehyde and propionaldehyde oxidation depending on the value of surface area (S) has been investigated. The reactions of the leading active centres - RCO_3 radicals in the gas phase and on the solid surface has been studied by EPR method.

It has been shown that the formation by the reaction $\text{RCO}_3 + \text{RCHO} \rightarrow \text{RCO}_3\text{H} + \text{RCO}$ of peroxyacid responsible for degenerate branching of the chains proceeds on the surface too. The experimental evidences of that are: 1. the autocatalytic behaviour of the process, the increasing of the maximum rate in spite of constancy of $[\text{RCO}_3]$ in the gas phase and the rise of the yield of peroxyacid with the increasing of S , 2. the initiation of the process by the peroxy radicals under the conditions of experiments excluding the homogeneous reaction, 3. the establishment of the possibility of the heterogeneous interaction of CH_3CO_3^- and CH_3O_2^- radicals with aldehydes.

The conclusion was made that the solid surface participates not only in the initiation and degenerate-branching, but also in the chain propagation stage.

Effect of Lateral Interactions Beyond Nearest-Neighbors on Size and Shape of Nonequilibrium Island on Surfaces

Shyi-Long Lee^{*}, Feng-Yin Li

Institute of Chemistry, Academia Sinica, Taipei, Taiwan, ROC

Abstract

Monte Carlo simulations were performed to investigate the island formation of adsorbates on surfaces. The surface is modeled by a $N \times N$ square lattice. The adsorbates are initially randomly distributed over the lattice. The movement of each adsorbate is then monitored by a random walk algorithm. Lateral interactions containing contributions from up to the fourth coordination shell are considered. Inclusion of interactions among diagonal neighbors is found to play a key role for the formation of nonequilibrium island. The effect of the interactions contributed from the third and fourth coordination shell on the island shape is discussed.

[*] To whom all the correspondence should be addressed.

Reaction modelling for oxidative coupling of methane over metal oxides

Pascal BARBE, Paul-Marie-MARQUAIRE,
Guy-Marie CÔME and François BARONNET

Département de Chimie Physique des Réactions, CNRS URA 328, INPL-ENSIC,
Université NANCY I, 1, rue Grandville, 54000 NANCY (France)

The high temperature reaction between methane and oxygen over metal oxides leads to the formation of ethylene with a good selectivity. This catalytic heterogeneous reaction clearly involves both homogeneous gas phase free radical processes and heterogeneous molecule-catalyst and radical-catalyst reactions. The modelling of these two types of processes has been done, in order to be able to account for the gas phase and the heterogeneous parts of the reaction, as well as for their irreducible interactions.

Our gas phase reaction mechanism is rather comprehensive including both "high" and "low" temperature elementary steps. The kinetic parameters have been taken from the literature.

Our primary heterogeneous mechanism is written in a formal way, since the real nature of the catalytic active centres is not definitely established. It includes mainly three categories of elementary steps . - Production of free radicals - Primary heterogeneous formation of CO₂ - Regeneration of the catalyst by O₂.

Simulations have been carried out for operating conditions taken from the literature, with no fitting adjustment of the gas phase kinetic parameters, and fitting of the heterogeneous determining rate constants.

The numerical computations lead to a satisfactory agreement with experimental results, even for a very crude reactor model, giving some credit to the mechanism.

However, one cannot conclude from this study that there are inherent limitations to the selectivity and yield of the catalytic coupling, since the critical parameters are adjusted and not deduced from independent experiments.

In order to have a better understanding of the mechanism, a new type of reactor has been designed, which will help in the decoupling of the gas phase reactions and heterogeneous reactions.

This reactor completely made of quartz is composed of two parts :

- * a well-stirred volum (100 cm³) created by four nozzles which are at the extremities of a swastika injector at the center of the reactor. The inside diameters of the nozzles to 0.3 mm to ensure that the reactor is quite well stirred for space times between 0.5 s and 5 s.

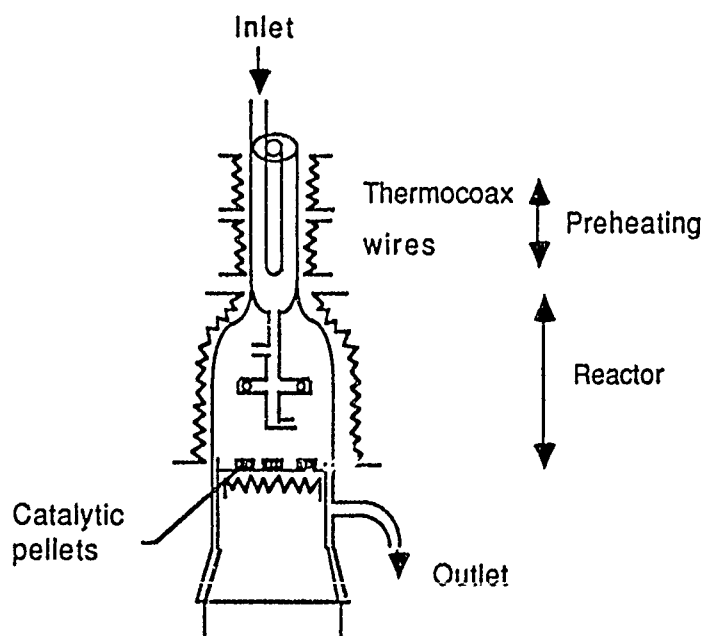
- * a cylinder at the lower part, where catalysts can be placed at the bottom with an apparent surface up to twenty square centimeters.

The heating of the reactor is obtained by Thermocoax wires.

A scheme of the reactor is presented below.

By varying the surface of the catalyst, the temperature of the catalytic support and the temperature of the gas phase in addition of conventionnal parameters, it will be possible to favour the gas phase part or the heterogeneous part of the coupling reaction of methane. Such experiments will help us to elaborate the heterogeneous scheme and to estimate kinetic heterogeneous constants with the support of numerical computations.

The modelling of the catalytic coupling of methane remains also an experimental and theoretical open question.



Scheme of the well-stirred catalytic reactor

ACKNOWLEDGEMENT

This work has been funded in part by the ACTANE CONSORTIUM

MECHANISMS OF BREAKAWAY ZIRCONIUM OXIDATION
AT HIGH TEMPERATURES AND UNDER IRRADIATION CONDITIONS

I. A. Kirillov, V. D. Rusanov, A. A. Fridman

The breakaway regime of interaction of high temperature gases with metal surface in many practically essential cases determines structural materials efficiency in the present-day chemical industry, metallurgy and nuclear power. This work presents experimental and theoretical investigations of mechanisms of breakaway zirconium oxidation.

The new theoretical approach to description of mechano-chemical interaction in oxide layer was proposed. It was shown that one of mechanisms providing the self-similar propagation of the reaction front is the diffusional movement of oxidation wave autocatalysed by the protective scale fracture. Within the framework of the macroscopic model of quasi-brittle fracture of oxide the analytical dependence of breakaway oxidation rate constant, barrier layer thickness and characteristic sizes of cracks in oxide on temperature, mechano-chemical parameters of oxide have been obtained.

The experimental investigations were carried out at 273-800°C temperature interval. It is shown that the irradiation speeding up the breakaway oxidation process due to embrittlement of the oxide film and reduces incubation period of parabolic/linear transition.

AUTHOR INDEX

S.S.Abilgasinova	C5	E.V.Belousova	A27
B.Aboussi	C11	R.Ben-Aim	C31
A.Aguilar	D43, D45	L.Beneventi	01, D44
R.W.S.Aird	A13	T.Ben-Porat	019
V.M.Akimov	D7	S.W.Benson	030, D21
J.Albaladejo	E3	A.Ben-Tov	019
M.Albertí	D43	T.Bércecs	038, D24, D25
M.Alexander	I4	W.C.M.Berden	F12
J.M.Alvariño	B9	N.Bergan	C27
J.Amouroux	G1	J.S.Bertram	D20
C.Anastasi	015, A25, C30	N.N.Bezuglov	B15, B16
J.Andarez-Alvarez	C30	P.Biggs	A11, C24
R.Anderson	047, E14	F.Billaud	C15, C16, C17
D.S.Anex	F7	S.Bish	F11
E.V.Antzupov	046	H.Black	A8
M.Aoyagi	024	J.F.Black	048
V.Aquilanti	026, D55	D.U.Bodikov	C5
S.Aragon	E14	A.E.Bodrov	B12
J.Arey	A7	J.C.Boettner	016, C11
E.A.Arkelyan	D3	F.Boldo	033
S.D.Arsentiev	D3	A.R.Bossard	D17
V.S.Arutuyunov	C19, C20	J.M.Bowman	025
R.I.Asadullina	B15, B16	A.A.Boyd	A11
S.M.Aschmann	012, A7	W.Braun	A28, F10
R.Atkinson	012, A7	M.Braun-Unkhouff	C18
R.A.Bach	F5	W.D.Breshears	D13
M.H.Back	D17	J.L.Brisset	G1
R.H.Bakhchadjyan	G4	M.Broomfield	A25
N.Balakrishnan	B11	A.C.Brown	A12
N.Balucani	01	C.E.Brown	039
L.Bañares	06, E16	B.Brunetti	D45, D47
I.Bar	019, F14	S.N.Buben	A22
V.Barbarossa	F12	V.P.Bulatov	A5, D2
P.Barbe	G6	A.V.Bulgakov	D28, D29
F.Baronnet	C15, C16, C17, C22, G6	J.P.Burrows	07, A1, A30
E.Bartkiewicz	D41	R.Buth	C13
S.A.Barts	E6	B.Cabañas	E2
V.Ya.Basevich	C20	P.Cadman	G3
D.Bassi	033	J.G.Calvert	08, A10
F.Basterrechea	E3	R.Candori	D55
L.Batt	C21	C.E.Canosa-Mas	A11, A12, A13
F.Battin	C22	C.A.Cantrell	08, A10
J.Baudon	D46, D47	D.Cappelletti	D55
D.L.Baulch	A8	F.Caralp	035, A20
I.N.Bebelin	B15, B16	M.Carlier	C28, C29
R.Becerra	D20, D23	R.W.Carr	D50
K.H.Becker	034	P.Casavecchia	01, D44
Yu.R.Bedjanian	D22	F.Castaño	D11, D12, E3
F.Beitia	D11	E.Castellano	F15
A.J.Bell	F8, F9	M.Castillejo	E8, E11
G.Bellec	D51	M.Cathonnet	016, C11
M.Bellimam	016	V.Catoire	035

Author Index - 2

S. Cavalli	026	A. Fahr	A28, F10
P. Cederbalk	C6	R. Fantoni	F12
S. T. Ceyer	I7	P. Feron	D47
C. Chachaty	A24	J. C. Ferrero	F6
A. Chakir	016	J. M. Figuera	E8, E11
J. Chamboux-Crosnier	A24	M. Filippi	033
D. W. Chandler	049	R. Fischer	D19
C. Chanmugatas	D21	J. R. Fisher	025
A. V. Chernyshova	C20	W. Forst	B7
S. G. Chestis	E4	R. Forster	A15
C. Chevalier	018	M. Forys	D41
O. P. Chilova-Lusina	042	P. Frank	C18
M. Chin	A21	H. Frerichs	D27
P. Christiaens	D1	H. M. Frey	032, D23
C. J. Cobos	F15	J. G. Frey	F8, F9
N. Cohen	B5	A. A. Fridman	B17, D53, G7
Y. Cohen	F14	R. Fröchtenicht	031
G. M. Côme	C22, C23, G6	M. J. Frost	03, D35
D. J. Cook	A13	H. A. Fry	D13
L. Copeland	04	G. E. Gadd	F3
A. Costela	E8	F. Gaillard	016
A. E. Croce de Cobos	F15	E. Garcia	B9, B18
J. N. Crowley	07	I. Garcia-Moreno	E11
Ph. Dagaut	C11	W. Gardiner	E9
F. I. Dalidchik	B12	N. L. Garland	D54
M. Damm	031	J. Gebhardt	D42
F. Danis	A20	A. Ge	052
D. David	F14	D. G	D51
P. Davidovits	044	Yu. M. Gershenson	046, D22
E. P. Daykin	A21	R. G. Gilbert	E5
K. Dehe	05	X. Gimenez	B19
A. R. de A. Pereira	017	M. Giorgi	F12
F. Deckert	031	J. F. Gleason	09, D14
A. Degli Esposti	022	C. Godoy	B1
R. J. Denning	G3	D. M. Golden	045, C10
J. Deson	C31	M. Ya. Goldenberg	C3
P. Devolder	A17, C29	M. Gonzalez	D45
S. Dóbé	038, D24	A. González Ureña	06, E16
O. Dobis	030	M. Görgényi	D19
M. Donlon	A2	A. Goumri	A17
R. J. Donovan	050	N. J. B. Green	017
A. Doubla	G1	T. Griffin	E13
I. A. Dubinsky	A5	A. A. Grigorian	D49, D50
B. Duguay	023	R. R. Grigoryan	D3
E. L. Duman	B15, B16	G. Grossi	026
O. Dutuit	D51	Y. Gu	03
P. E. Dyer	D5	C. Guéret	C17
J. A. Dyei	F2	D. Gutman	029
F. Eccher	033	G. J. Gutsche	D15
J. Edelbüttel-Einhaus	C13	P. M. Guyon	D51
T. Ellermann	015	J. Habdas	D52
K. Elyahyaoui	C15, C16	H. Haberland	D47
B. Engelhardt	034	W. Hack	D16
S. Etemad-Rad	C7	P. A. Hackett	039

Author Index - 3

J.B.Halpern	E6	C.E.Klots	B3
G.Hancock	027, C24, E12	A.N.Klucharev	B15, B16
M.Hande	F13	V.D.Knyazev	C19
C.Hao	C12	R.Koch	D27
L.B.Harding	B8	R.Koch	A26
R.J.Harrison	B8	K.Kohse-Höinghaus	E13
D.Hartmann	014, D8	C.E.Kolb	044
D.Hasegawa	012	A.A.Konnov	C14
G.D.Hayman	010, A6	A.N.Korcharyan	D3
M.R.Heal	C24	W.Korneta	D10
D.E.Heard	027	T.Körtvélyesi	B4, D18
D.Heflinger	019	A.M.Kosmas	B6
A.Heiss	A16	K.D.Kreutter	A21
J.Hepburn	D51	G.I.Ksandopulo	C5, C14
J.T.Herron	D48	P.V.Kulakov	E4
H.Heydtmann	05	A.Yu.Kulikov	042
Ch.Hickman	F8	R.Kurtenbach	034
M.Hippler	A29	A.Kvaran	050
H.Hippler	031, A14, A15	A.Laganà	B9, B18, B19
K.A.Holbrook	D5	C.Lalo	C31
U.Hold	036	I.T.Lancar	D31
A.Hopkirk	050	S.I.Lane	F6
P.L.Houston	I8	I.K.Larin	A22
K.Hoyermann	C13	A.Laufer	A28
M.-B.Huang	A24	G.Lavardet	D31
K.J.Hughes	C6	W.D.Lawrance	D15
A.J.Hynes	037, C25	Y.Lazarou	F1
A.A.Iogansen	E4	R.Le Bec	C23
I.P.Ipatova	042	G.LeBras	07, D31
R.S.Irwin	D26	S.L.Lee	G5
S.M.Japar	A4	Y.T.Lee	F7
W.M.Jackson	04	L.V.Lenin	D7
A.Jacobs	E7	R.Lesclaux	035, A20, C26
M.H.M.Janssen	049	M.T.Leu	043
M.E.Jenkin	010, A6	M.R.Levy	E10
F.Jorand	A24	F.Y.Li	G5
M.Jordan	E5	G.Libuda	A3
A.Jörg	E13	P.D.Lightfood	C26, D37
A.Jowko	D41	H.V.Linnert	C9
Th.Just	C18	G.Liuti	I6
J.Kappert	052	E.L.Ljungström	A13
A.A.Karnaukh	C3	V.Lorent	D55
J.Karthäuser	014, D8	V.A.Losovsky	A5
E.E.Kasimovskaya	A23	P.K.Louie	A8
Y.Kaufman	019	R.Louw	D4
D.K.Kela	050	S.Lunell	A24
J.D.Kettleborough	E1	K.Luther	036, F4
L.F.Keyser	043	E.Luzzatti	D55
V.N.Khabarov	A5, D2	U.Maas	018
V.G.Khamaganov	A23, D40	M.J.MacDonald	D9
K.D.King	D15, F1	Yu.N.Makarov	042
F.Kirchner	A3	W.G.Mallard	D48
I.A.Kirillov	G7	J.A.Manion	D4
R.Klein	A28, F10	Z.A.Mansurov	C5

Author Index - 4

A.A.Manthashyan	D3	M.Olzman	D42
D.Maric	A30	I.Oref	E9
E.M.Markin	D22	V.L.Orkin	A23, D38, D39, D40
P.M.Marquaire	C22, C23, D30, G6	J.J.Orlando	08, A10
F.Márta	D24, D25	A.J.Orr-Ewing	E12
E.Martínez	E2, E3	A.Ortiz de Zárate	D12
J.Masanet	A20, C31	J.B.Ozenne	D51
B.Mason	032	Ph.D.Pacey	D30
J.Mateos	B18	P.Pagsberg	015, A25
M.Matthews	D5	A.Palma	B10
M.R.S.McCoustra	F2	P.Palmieri	B9
A.B.McEwen	C10	P.Papagiannakopoulos	F1
D.J.McGarvey	C24	Th.Papenbrock	A19
K.G.McKendrick	E1	G.Paraskevopoulos	D26
P.McLoughlin	F13	P.R.Pardon	F8
U.Meier	E13	D.H.Parker	049
L.Mele	F10	J.M.Parnis	039
C.F.Melius	C27	A.D.Parr	010, A12, C24
L.Mellouki	07	J.-F.Pauwels	A17, C28, C29
S.Mercuri	F12	A.Pearson	047
C.Metayer	D51	J.Peeters	028
E.Metcalfe	C7	V.Pellizzari	026
J.V.Michael	025	F.Perales	D46, D47
A.M.Middlebrook	045	G.Petrella	G2
B.F.Minaev	A28, D51	Yu.P.Petrov	D28, D29
R.Minetti	C28	J.Pfab	A29, F2
Ch.Miniatura	D46, D47	L.F.Phillips	A9, E15
G.Miron	019	M.J.Pilling	017, C6, D36
N.A.Missineva	A22	K.V.Pinnex	E6
S.A.Mitchell	039	F.Pirani	D55
F.Mohammad	04	I.G.Pitt	A16
P.S.Monks	A13	J.M.C.Plane	013
S.B.Moore	043	S.Pollak	015
G.K.Mocitgat	07, A1, A30	S.S.Polyak	C4
C.Morley	C30	A.V.Polyakova	A27
R.I.Moshkina	C4	B.V.Potapkin	B17, D53
G.Muga	E16	G.Poulet	07, D31
D.Muir	C30	V.K.Proudlar	C6
W.Müller-Markgraf	041	A.P.Purmäl	A27
J.M.Muñoz	E8	P.Puyuelo	E2
D.V.Muratov	D28, D29	Z.Pytel	D10
T.P.Murrells	A6	R.Rahn	A14
A.Nacsa	D6	A.R.Ravishankara	011
F.L.Nesbitt	09, D14	J.C.Rayez	023
J.M.Nicovich	A21	I.Yu.Razuvaev	E4
O.J.Nielsen	A2, A25	T.Rech	F4
C.-F.Nien	013	C.M.Reihs	045
E.E.Nikitin	021	J.Reinhardt	D46, D47
E.V.Nosov	B15, B16	M.Ribaucour	C28
C.Nyeland	020	R.Rigny	C21
V.E.Oexler	F6	C.Rinaldi	F6
E.A.Ogryzlo	040	J.M.Riveros	C9
H.Okabe	F10	J.Robert	D46, D47
G.A.Oldershaw	D5	S.H.Robertson	017

Author Index - 5

Ph. Rocteur	C8	T.G. Slinger	F3
J.C. Rodriguez	E11	J.J. Sloan	02
L.B. Romanovich	C4	S.A. Smirnov	D28, D29
J.M. Roscoe	D9, F5	I.W.M. Smith	I5, 03, D34, D35, E15
S. Rosenwaks	019, F14	R.H. Smith	043
M. Rosi	026	S.C. Smith	E5
M.J. Rossi	041	S.P. Smyshlyaev	046
J. Rostas	C31	L.R. Sochet	C28, C29
K. Rothwell	A12	A. Solé	D43
P. Roussel	035, C26	R. Spencer-Smith	03
F.S. Rowland	I2	W.S. Staker	D15
V.B. Rozenshtein	046, D22	C.T. Stanton	D54
V.D. Rusanov	B17, D53, G7	E.H. Staricco	F6
L.Yu. Rusin	D7, D37	F. Stefani	B10
K.A. Sahetchian	A16, A24, C21	L.J. Stief	09, D14
M.N. Sanchez Rayo	D11, D12	W. Stiller	B2
M. Sapir	019	T. Stoecklin	023
O.M. Sarkisov	A5, E4, D2	S. Stolte	049
N. Sathyamurthy	B11	D. Stranges	01
J.P. Sawerysyn	014, A17	M.I. Strelkova	F12
R. Sayós	D43	F. Stuhl	051, A19
K. Scherzer	D42	Q. Sun	025
A. Schmoltner	F4	A. Symonds	036
A.M. Schmoltner	F7	I. Szilágyi	038
M. Schneider	C12	V.L. Talrose	I9
W. Schneider	A1	M. Tappe	D27
F.M. Schuler	E7	F. Tarantelli	026
U. Schwanke	05	J. Tardieu de Maleissye	A16
M. Schweiser	D51	H. Teitelbaum	D33
D.W. Schwenke	D49	M.A. Teitel'boim	C3
P.W. Seakins	D36	F. Temps	052
J. Seetula	029	H. Thiesemann	D27
E. Semprini	B10	J.W. Thoman, Jr.	049
I. Seres	A18	R. Timonen	029
L. Seres	A18, B4, D6, D18, D19	A.A. Titov	E4
D.W. Setser	D52	P.J. Toennies	031
A. Seydi	C21	M.A. Tolbert	045
A. Sgamellotti	026	R. Tomacello	F12
D.V. Shalashilin	B14	P. Tosi	033
I. Shanahan	F13	A. Tóth	D18
R. Shepard	024	S.O. Travin	A27
J.E. Shepherd	C27	J. Treacy	A2
R.E. Shetter	08, A10	J. Troe	021, A14, A15, F4
V.A. Sheverev	B15, B16	E.M. Trophimova	A22
I.P. Shmatov	B15, B16	R.P. Tuckett	E15
A.P. Shvedchikov	A27	T. Turányi	D24, D25
H.W. Sidebottom	A2	S.V. Turetsky	D28, D29
A.A. Sidorenko	D37	G.S. Tyndall	08, A10
M. Siese	A26	Y. Tzuk	019
F.-G. Simon	A1	S. Ya. Umanskii	B14
A.W. Simpson	F2	V.A. Ushakov	C20
I.R. Sims	03	J.J. Valentini	I1, F14
D.L. Singleton	D26	J. Vandooren	C2
G.O. Sitz	049	J.M. Van Doren	044

Author Index - 6

S.Vanhaelemeersch	028
J.Van Hoeymissen	028
P.J.Van Tiggelen	C8
I.A.Vardanyan	G4
G.Vassilev	D46
G.J.Vazquez	B1
F.Vecchiocattivi	D45, D46, D47
V.I.Vedeneev	C3, C4, C19, C20
S.I.Vereshuk	D2
B.Veyret	C26
C.Vinckier	D1
V.Viossat	A24
P.F.Vohralik	I4
G.G.Volpi	01, D44, D45
H.R.Volpp	E7
A.F.Wagner	024
M.Wahl	E7
J.R.Waldeck	048
R.W.Walker	C1
Z.H.Walker	040
T.J.Wallington	A4
R.Walsh	032, D20, D32, F11
J.Warnaz	018
J.F.Warr	D34
L.R.Watson	044
I.M.Watts	032, D20
R.P.Wayne	A11, A12, A13
J.Weill	C17
K.-M.Weitzel	F4
T.Weng	D51
H.J.Werner	022
C.Whithman	E15
J.W.Wiebrecht	052
P.Wiesen	034
C.W.Wilson	D13
M.R.Wilson	A11
P.H.Wine	037, A21
J.Wolfrum	I3, C12, E7
D.R.Worsnop	044
F.Wu	F12
A.J.Yates	A29
A.J.Yencha	050
F.Zabel	A3, A24
M.Zahedi	04
M.S.Zahniser	044
L.Zalotai	D25
R.N.Zare	048
H.A.Zeaiter	E11
A.G.Zborovsky	D28, D29
R.Zellner	014, D8
A.A.Zembekov	B13
C.Zetzsch	A26
Yu.V.Zhiljaev	042
S.G.Zvenigorodsky	046